NATIONAL AERONAUTICS AND SPACE ADMINISTRATION

Technical Memorandum 33-447

Proceedings of the Second Workshop on Voltage Breakdown in Electronic Equipment at Low Air Pressure

held at the Jet Propulsion Laboratory, March 5-7, 1969

Edited by
E. R. Bunker, Jr.

JET PROPULSION LABORATORY
CALIFORNIA INSTITUTE OF TECHNOLOGY
PASADENA, CALIFORNIA

June 30, 1970

Prepared Under Contract No. NAS 7-100
National Aeronautics and Space Administration

PRECEDING PAGE BLANK NOT FILMED.

Foreword

The Second Workshop on Voltage Breakdown in Electronic Equipment at Low Air Pressure was sponored by the Jet Propulsion Laboratory, Pasadena, California.

It has been three and one-half years since the convening of the first workshop on voltage breakdown. In this interval, gains are evidenced in the progress and sophistication in solving voltage breakdown problems affecting electronic equipment operating at high altitudes or other low air pressure environments. Although space applications predominate the area of concern, other projects such as the SST are becoming increasingly involved with voltage breakdown.

High-voltage breakdown in spacecraft continues; however, the incidences of occurrence appear to have decreased in spite of an increase in the number of missions flown. This, it is felt, is due to many project managers now requiring all equipment with voltage in excess of 270-V peak to be designed to operate in the critical pressure region without damage, even though its normal functional environment is sea level pressure and the hard vacuum of space. In addition, designers are becoming more aware of the principle of good high-voltage design by selecting void-free components, proper spacing of conductors, isolating high-voltage circuitry from lower voltage areas, etc. The consensus seems to be that the slight increase in cost to achieve a provable corona-free design is more than offset by the increase in confidence that the equipment will survive accidental loss of vacuum during high-vacuum tests, inadvertent turnon while passing through the critical air-pressure region of earth after launch, or outgassing in flight pressurizing the enclosure into the critical pressure region.

As in the first workshop, to minimize work for the authors and perhaps obtain the latest information, formal papers were not required. It was hoped that this would encourage some to participate who did not have time to prepare a formal paper. To preserve the information presented and produce an accurate record, a tape recording and stenographic transcript were made of each paper. A word-for-word comparison was made of the transcripts and recordings to pick up any omissions or errors, as well as to correct any technical inconsistencies. A manuscript was prepared with grammatical corrections and a consistent style without, we trust, losing the spontaneity of the author's presentation. Each author was given an opportunity to review and approve his manuscript and the question period following, including proper labeling of his illustrations. Frequently, authors would point out regions of interest on their slides; attempts were made, where possible, to include such information in the illustrations or text.

It is hoped that the reader will not be critical of the wording and syntax of the papers, because an orally given presentation loses something when it is written down and read by others who did not hear it initially. However, some authors submitted prepared papers with a request that they be used in place of the transcripts, which was done.

The 23 papers were presented within a 2½-day period, with the last afternoon devoted to a round table discussion, providing an opportunity for all attendees to speak informally on their activities, make comments on the presentations, etc. Unfortunately, the stenographer was not retained and the tape recordings were not clear enough to make a usable transcript; thus, a record of this round table discussion does not appear in these proceedings.

Foreword (contd)

Comparisons were made of the two workshops and the conditions under which they were held to see if any significant trends could be detected. Prior to the first workshop there was no mailing list available of individuals interested in voltage breakdown at low air pressures; press releases were published by some trade journals in addition to official information released through NASA and governmental channels. This resulted in 135 attendees with 36 papers submitted. Following the workshop, many individuals stated they would have attended had they received notification in time.

Proceedings of the first workshop were published (*Proceedings of the Workshop on Voltage Breakdown in Electronic Equipment at Low Air Pressures.* Technical Memorandum 33-280. Edited by E. R. Bunker, Jr. Jet Propulsion Laboratory, Pasadena, Calif., Dec. 15, 1966.) and distributed to all attendees and governmental agencies. A card was enclosed requesting that the recipient sign the card and indicate if he wished additional information on the subject, including information on any future workshops. To date, over 400 copies of the proceedings have been mailed.

The recipients of the proceedings constituted a basis for the mailing list for the second workshop; official governmental channels were also used. Even with this greater spread of information, the second workshop list of attendees only included 107 individuals; 23 papers were submitted. It is felt, however, that the decreased figures reflect recent travel restrictions rather than a lessening of interest.

The consensus of opinions among the attendees was that the three and one-half years interval between the first and second workshops was excessive; a two-year separation was considered more nearly optimal.

A contributor to the present document provided a terse statement describing the ultimate objective of this and succeeding workshops: "Eventually, by learning through these experiences and their analyses, and by an exchange of information such as at this workshop, we hope, and I am sure everybody else does, that the handling of high voltage at orbital low pressures will become a relatively routine matter."

Earle R. Bunker, Jr.

Contents

Welcoming Remarks 1

C. E. Pontius

A Study of Voltage Breakdown in Spacecraft Systems from Test and Flight Experience 3

J. E. Stern and K. R. Mercy

Some Observations of Corona Breakdown on Various Antenna Types in Simulated Planetary Atmospheres 9

C. H. Brockmeyer

VHF Breakdown on a *Nike-Cajun* Rocket 19

J. B. Chown, J. E. Nanevicz, and E. F. Vance

Development of Packaging Techniques for an Amplitron and Power Supply 29

P. Felsenthal, D. Grieco, and J. Fridman

Development of Electronographic Image Converters for Far-Ultraviolet Space Astronomy Applications 41

G. C. Carruthers

Low-Voltage Breakdown in Electronic Equipment When Exposed to a Partial-Pressure Nitrogen Environment Containing Water Vapor . . . 49

R. F. Sharp, E. L. Meyer, and D. E. Collins

The Bendix OAO Star Tracker High-Voltage System and its Design Considerations 59

W. Mitchell

A Vented High-Voltage System for Satellite Applications 73

D. Laffert

Open Construction Magnetic Components for the *SERT II* Power Conditioner 77

D. S. Yorksie and J. Lagadinos

Design Considerations for Corona-Free High-Voltage Transformers . . . 91

H. C. Byers

High-Voltage Packaging Investigations in the Advanced Technology Group 99

E. Bunker, Jr.

Corona Evaluation of Spacecraft Wires and Connectors 109

W. G. Dunbar

Contents (contd)

Low-Level Corona Detectors 117
P. H. Reynolds and C. J. Saile

DC Voltage Breakdown Processes and External Detection Techniques 123
R. E. Heuser

Testing of High-Voltage Spacecraft Systems in a Simulated Ionosphere Plasma 131
D. R. Burrowbridge

Rocket-Exhaust Initiation of Conduction in Connectors at Altitude . . . 139
R. W. Ellison

High-Voltage Breakdown in an OSO-IV Pointed Experiment 155
N. L. Hazen, M. C. E. Huber, and E. M. Reeves

The Prevention of Electrical Breakdown in Spacecraft 169
F. W. Paul and D. R. Burrowbridge

The Influence of Gas Velocity on the Breakdown Potential of Argon, Helium, and Nitrogen 177
J. A. Gardner

Breakdown Studies for Possible Atmospheres on Mars and Venus . . . 183
J. A. Gardner

RF Voltage Breakdown in Coaxial Transmission Lines 189
R. Woo

Reduction of Gas-Discharge Breakdown Thresholds in the Ionosphere Due to Multipacting 193
G. August and J. B. Chown

The Effects of Outgassing Materials on Voltage Breakdown 203
J. F. Scannapieco

LIST OF PARTICIPANTS

ADAMS, R.
Jet Propulsion Laboratory
*AUGUST, G.
Stanford Research Institute

BAEUCHLER, R.
International Telephone and Telegraph Corp.
BENDEN, W. J.
Bellcomm, Inc.
BERNSEN, B.
Aerojet-General Corp.
BIESS, J.
TRW, Inc.
BOUNDY, R. A.
Jet Propulsion Laboratory
*BROCKMEYER, C.
Martin Marietta Corp.
BROWN, K.
International Telephone and Telegraph Corp.
BRYNER, J. C.
North American Rockwell Corp.
*BUNKER, E. R.
Jet Propulsion Laboratory
*BURROWBRIDGE, D. R.
NASA/Goddard Space Flight Center
*BYERS, H. C.
Transformer Electronics Co.
BYRNE, F.
National Aeronautics and Space Administration

CAMERZELL, P. L.
McDonnell Douglas Corp.
CARDWELL, G.
Hughes Aircraft Co.
CARO, E. R.
Giannini-Voltex
*CARRUTHERS, G. R.
Naval Research Laboratory
CHEVRIER, E.
Harvard College Observatory
*CHOWN, J. B.
Stanford Research Institute
*COLLINS, D. E.
Radio Corporation of America
COOPER, H. W.
Naval Research Laboratory
COSTOGUE, E.
Jet Propulsion Laboratory
COTA, L.
Aerojet-General Corp.

DAVIS, B. W.
Battelle Memorial Institute
DAWE, R. H.
Jet Propulsion Laboratory
DEWOLF, K.
Jet Propulsion Laboratory
DIAMOND, S.
Harvard College Observatory
DIETZ, W. R.
National Aeronautics and Space Administration
*DUNBAR, W. G.
The Boeing Co.

EDWARDS, M. D.
National Aeronautics and Space Administration
*ELLISON, R. W.
Martin Marietta Corp.

FAIN, L. T.
National Aeronautics and Space Administration
*FELSENTHAL, P.
A. D. Little, Inc.
FIALA, J.
NASA/Lewis Research Center
FITAK, A. G.
Jet Propulsion Laboratory
FORSBERG, C. A.
Ball Brothers Research Corp.
FORSBERG, K. E.
Transformer Electronics Co.
*FRIDMAN, J.
Raytheon Space and Information Systems Div.

*GARDNER, J. A.
Jet Propulsion Laboratory
GOLDFARE, G.
Aerospace Corp.
GOLDLUST, J. A.
Boston Insulated Wire & Cable Co.
*GRIECO, D.
Raytheon Space and Information Systems Div.

HAFFNER, J. W.
North American Rockwell Corp.
HARPER, J. D.
NASA/Manned Spacecraft Center
HARRISON, R. J.
Ion Physics Corp.
HATHEWAY, A. E.
Electro-Optical Systems, Inc.
HAUGHEY, J. W.
National Aeronautics and Space Administration
HAUSER, R. E.
NASA/Goddard Space Flight Center
*HAZEN, N. L.
Harvard College Observatory
*HEUSER, R. E.
NASA/Goddard Space Flight Center
HILLER, R.
Jet Propulsion Laboratory
HOLBROOK, R. J.
Hughes Aircraft Co.
*HUBER, M.
Harvard College Observatory
HUMMEL, W. M.
Hughes Aircraft Co.
HUNKLE, L. T.
International Telephone and Telegraph Corp.

JAMES, E. L.
Electro-Optical Systems, Inc.
JAN, L.
Electro-Optical Systems, Inc.
JIRARD, F.
Hughes Aircraft Co.
JONES, W. H.
McDonnell Douglas Corp.

KAMBOURIS, G.
NASA/Goddard Space Flight Center
KAPELL, G. F.
Jet Propulsion Laboratory
KERRISK, D. J.
Jet Propulsion Laboratory
KINSINGLE, I.
Aerojet-General Corp.
KLINE, H. C.
McDonnell Douglas Corp.
KRUPINSKI, R. F.
Naval Research Laboratory
KUHLMAN, E. A.
McDonnell Douglas Corp.

*LAFFERT, P. W.
Sylvania Electric Products, Inc.
*LAGADINOS, J.
Raytheon Company
LANBACH, B.
Hughes Aircraft Co.
LAVAMAKI, M.
Time-Zero
LEWTER, B. J.
NASA/Manned Spacecraft Center

MACIE, T.
Jet Propulsion Laboratory
MCCOY, W. K.
Sandia Corp.
MERSCHEL, R. P.
TRW, Inc.

---

*Presented paper at the Workshop.

LIST OF PARTICIPANTS (contd)

*Meyer, E. L.
Radio Corporation of America
Michaels, P. A.
The Bendix Corp.
Mitchell, M.
Representing Self
Mitchell, W.
The Bendix Corp.
Moore, M. L.
Jet Propulsion Laboratory

*Nanevicz, J. E.
Stanford Research Institute

*Paul, F. W.
NASA/Goddard Space Flight Center
Pawlik, E.
Jet Propulsion Laboratory
Pearlston, C.
Aerospace Corp.
Perkins, J. R.
E. I. duPONT de NEMOURS & Co., Inc.
Piemersma, H.
Westinghouse Electric Corp.
*Pontious, C. E.
National Aeronautics and Space Administration
Pryga, S. A.
North American Rockwell Corp.

Rait, J. C.
Hughes Aircraft Co.
Read, W. S.
Jet Propulsion Laboratory
*Reeves, E. M.
Harvard College Observatory
*Reynolds, P. H.
James G. Biddle Co.
Robillard, G.
Jet Propulsion Laboratory
Rook, C. W.
Motorola, Inc.
Rutstein, I.
General Electric Co.

*Saile, C. J.
James G. Biddle Co.
*Scannapieco, J. F.
General Electric Co.
Schaefer, W.
Jet Propulsion Laboratory
Schraut, E. H.
Electro-Optical Systems, Inc.
Schult, R. W.
Aerospace Corp.
Seright, J. E.
Aerospace Corp.
*Sharp, R. F.
Radio Corporation of America
Smith, A. H.
McDonnell Douglas Corp.
Smith, J. K.
Naval Research Laboratory
Smith, W. A.
Rice University
Stelzried, J. E.
Giannini-Voltex
*Stern, J. F.
NASA/Goddard Space Flight Center
Stevens, J. K.
NASA/Manned Spacecraft Center
Street, H. W.
NASA/Goddard Space Flight Center
Swanson, J. T.
Jet Propulsion Laboratory

Tsacoumis, T. P.
National Aeronautics and Space Center
Tu, Kwei
Rice University

*Vance, E. F.
Stanford Research Institute
Vescelus, G.
Jet Propulsion Laboratory

White, W. F.
McDonnell Douglas Corp.
Williams, D. E.
National Aeronautics and Space Administration
*Woo, R.
Jet Propulsion Laboratory

York, L. M.
Collins Radio Co.
*Yorksie, D. S.
Westinghouse Electric Corp.
Young, E. A.
Aerojet-General Corp.
Young, T. V.
Hughes Aircraft Co.

Zaiden, C. E.
American Science and Engineering

Welcoming Remarks

Charles E. Pontious
Chief, Electronic Techniques and Components
National Aeronautics and Space Administration
Washington, D.C.

The first workshop on voltage breakdown in electronic equipment at low air pressures was held at the Jet Propulsion Laboratory in August 1965. The motivation for that first meeting was a series of unexpected problems arising in the development and testing of *Mariner IV*, and the knowledge that Martian surface pressure is essentially centered in the critical corona region. It was felt that a forum was needed to permit engineers and scientists involved in such problems to discuss the tasks associated with voltage breakdown and the potential solutions to these difficulties.

The objective for this second workshop is, once again, to bring together those of you who are working on voltage breakdown problems so as to assess the progress of this work, identify new or continuing problems, and provide a useful interchange of ideas and experiences. Since we are contemplating exploration and operation on and near the Martian surface, it is essential that spacecraft electronic systems operate efficiently and reliably, both in and out of the critical low-pressure regions.

The need for practical engineering solutions to these problems is even more acute today than in 1965.

This workshop has been organized to emphasize informality. Obviously, there are too many attendees to conduct a round-table discussion; however, each of you are urged to express yourselves on any of the topics considered during the period of this workshop.

PRECEDING PAGE BLANK NOT FILMED.

N70-32287

A Study of Voltage Breakdown in Spacecraft Systems from Test and Flight Experience

J. E. Stern and K. R. Mercy
National Aeronautics and Space Administration
Goddard Space Flight Center
Greenbelt, Maryland

I. Introduction

Voltage breakdown at low gas pressures in electrical flight systems was recognized as a problem in high altitude aircraft during World War II. With the advent of ballistic missiles and manned and scientific spacecraft with their complex flight systems and experiments, the problems of voltage breakdown increased in number and variety.

Breakdowns have contributed to the degradation of flight systems and experiments with a resultant decrease in flight mission efficiency. If more reliable spacecraft are to be designed, it will be necessary to eliminate voltage breakdown or at least minimize its effects on spacecraft performance. The problem areas of breakdown must be identified if this is to be accomplished. Therefore, two surveys were conducted to provide a comprehensive understanding of breakdown problems occurring in spacecraft systems and to determine the major factors contributing to these problems.

II. First Survey

A. Background

The first survey of breakdown problems was an in-house effort at the National Aeronautics and Space Administration's (NASA) Goddard Space Flight Center (GSFC). The scope of the survey encompassed spacecraft administered by NASA during the period from 1961 to early 1968. The information was obtained from (1) GSFC sources, e.g., Director's Weekly Reports, Project Reports, Failure Reports, and Test and Evaluation Division Reports, (2) Contractor Test Reports, and (3) Proceedings of the First Workshop on Voltage Breakdown (Ref. 1). Other sources were probed but these yielded little pertinent information. In all, 74 cases were found. It is likely

Preceding page blank

that additional breakdowns had occurred but were either not recorded or were overlooked in the documents reviewed.

Of particular interest to the survey was information on the following:

(1) The nature of breakdown phenomena; e.g., gas ionization, including glow, corona, or arc discharges, and secondary emission, including multipactor discharges.

(2) Systems affected by voltage breakdown.

(3) Known or suspected causes of breakdown phenomena.

(4) Conditions under which breakdowns occur.

B. Results

A summary of test and flight voltage breakdowns given for each year, from 1961 through 1967, is presented in Fig. 1. Considering the relative number of tests and flights, there is not a significant change in the number of occurrences with respect to time. Except for 1966, the number of problems continue at an average rate of about 13 per year, beginning with 1963.

Classification of the breakdown occurrences according to the nature of the phenomena is shown in Fig. 2. Based upon the descriptions provided in the documents surveyed, it was possible to classify the phenomena only as corona, arc-over and multipactor.

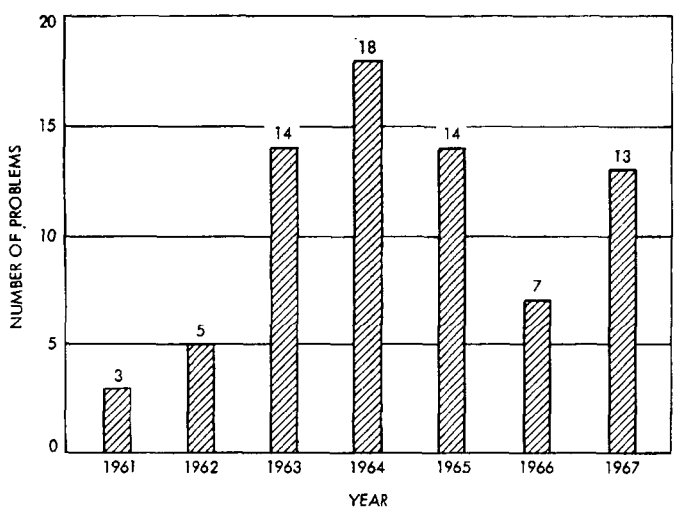

Fig. 1. Minimal annually-reported voltage problems

The term corona is used where a glow was observed. This included any low-current ac or dc gas ionization process. The term arc-over is used to indicate a part or system failure generally accompanied by some visible changes in the neighborhood of the discharge; e.g., a discoloration of parts, tracking marks, etc. Corona was considered a temporary failure mode, and arc-over a catastrophic failure mode. Since arc-over is also an ionization process, then, according to Fig. 2, about 90% of the breakdowns were gas phenomena.

The voltages at which the discharges had occurred are shown in Fig. 3. These ranged from 28 to 5000 V. The breakdown at 28 V occurred in 400-Hz regulators and pyro-power supplies on an Agena vehicle at separation from the booster. The plasma from the rocket plume was believed to be responsible for generating a voltage breakdown environment. The majority of discharges occurred in a range 1000 to 3000 V.

For those cases where data were available, a temperature-pressure relationship was examined and is shown in Fig. 4. It would seem that the pressures around the discharge may have been higher than the pressures at the gages. This can happen if there is outgassing or if there are trapped gases in the neighborhood of the discharge. Temperatures do not appear to be a significant factor except where they may effect outgassing and gas pressures.

Classification of the known or suspected causes of breakdown is shown in Fig. 5 for 37 cases having an identifiable cause. Of these occurrences, more than 50% are due to gas problems and about 40% are due to insulation problems.

Of the 74 cases studied, 22% showed damage to the high-voltage circuit in which the breakdown occurred; 20% showed damage induced by voltage breakdown in adjacent, non-related circuits; 22% were undamaged, and the balance were unidentifiable.

The assignment of responsibility for breakdown problems is shown in Fig. 6. It is evident that the largest burden of responsibility falls upon design and indicates where the effort should be concentrated if the problems of voltage breakdown are to be reduced.

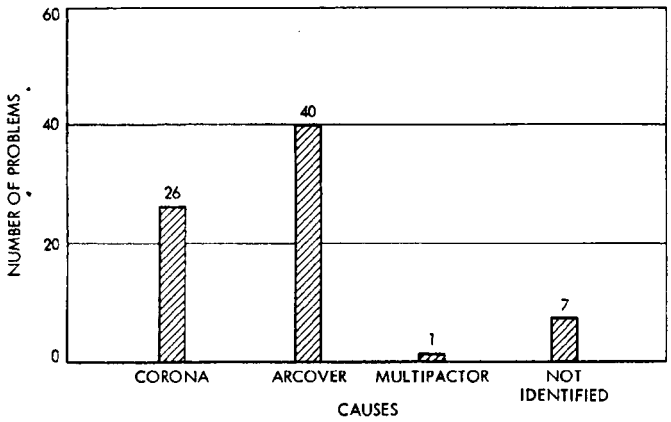

Fig. 2. Voltage discharge problems as identified

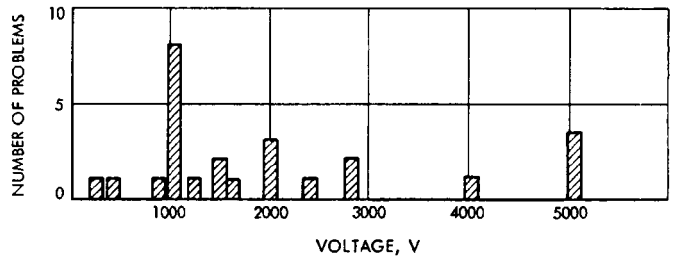

Fig. 3. Voltage levels at which breakdown occurred

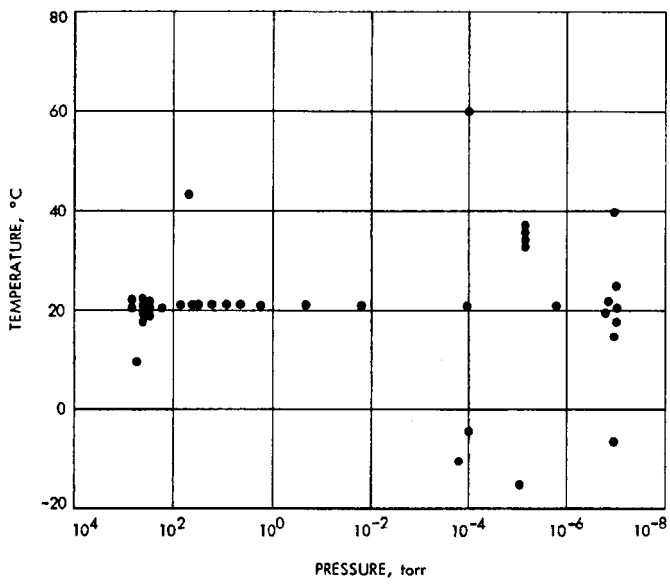

Fig. 4. Voltage discharge problems vs environmental test temperature and vacuum

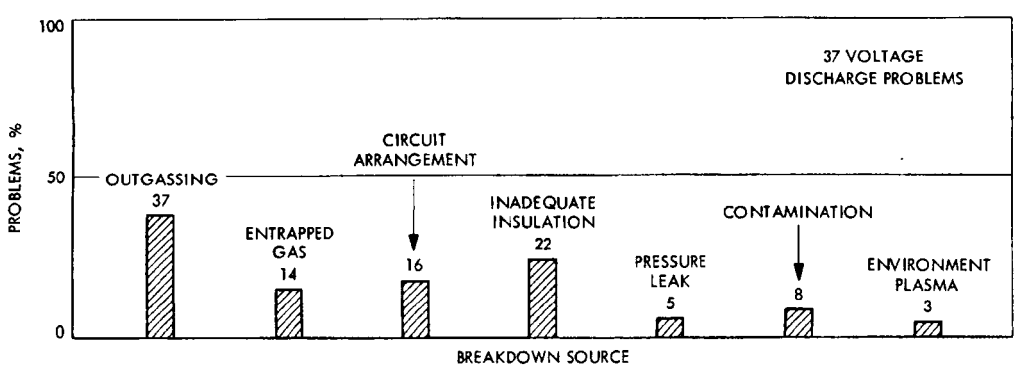

Fig. 5. Voltage discharge problem sources

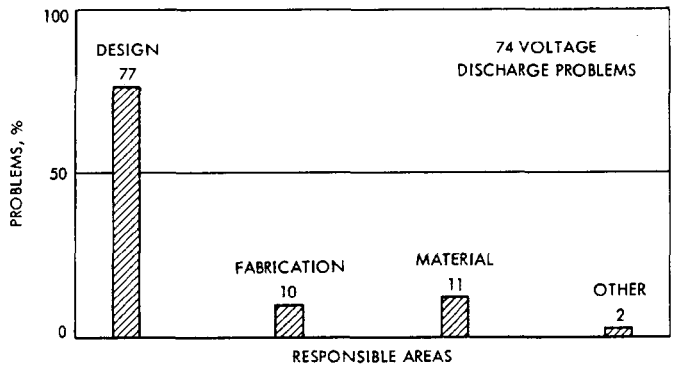

Fig. 6. Areas of responsibility for voltage discharge problems

III. Second Survey

A. Background

The results of the first survey indicated a need for more detailed information on voltage breakdowns in spacecraft systems. A second survey in late 1968 was performed in which the efforts were concentrated on experiments from three GSFC administered spacecraft: *OSO-D, OGO-F,* and *ISIS-A*. Information was obtained directly from scientists and engineers associated with spacecraft systems that might experience breakdown. Personal interviews and mailed questionnaires yielded much data. The following information was requested:

(1) Descriptions of affected systems.

(2) Operating voltage levels.

(3) Determination of voltage breakdown.

(4) Operating and environmental conditions surrounding breakdown occurrence.

(5) Preventive techniques to ensure against and detect breakdown.

(6) Nature of breakdown.

(7) Effects of breakdown of spacecraft systems.

(8) Corrective action taken.

B. Results

There were 36 informative responses to interviews and questionnaires. Of these, 9 described voltage breakdowns consisting of 2 corona, 4 arc, and 3 multipactor discharges. Design inadequacies, e.g., choice of materials and components, and circuit arrangements, explained 7 of the breakdowns; the remaining 2 were attributed to fabrication faults, e.g., poor encapsulation, and improper wire assembly. These findings are consistent with the first survey which indicated that the number of breakdown occurrences were significant, that the nature of the breakdowns were primarily gas ionization, and that the major area of responsibility was design.

IV. Prevention of Breakdowns

The most significant aspects of this survey were determinations of the techniques employed by the respondents to avoid breakdown. These fell into two general classes: (1) control of the electric fields, and (2) elimination of cavities and voids.

Electric fields were controlled by using shielded conductors, minimizing the length of high-voltage conductors, avoiding sharp points and soldering balls at terminals, point-to-point wiring and avoiding connectors, providing adequately insulated conductors and conformal coating, separating high- and low-potential areas, and isolating high-voltage circuits from adjacent circuitry.

Voids were eliminated by encapsulation and potting, and avoidance of components with cavities; e.g., hollow resistors, hollow terminal posts, etc. Some of the polymers used were room temperature curing silicone elastomers (RTV11, Sylgard-182, -184, and -186), hard and foamed epoxies, and polyurethane foams with unicellular or communicating cellular construction. In one case where encapsulation was undesirable, cavities were filled with polystyrene balls to prevent multipaction. Problems encountered in encapsulation were due to (1) poor bond between the polymer and the parts being potted, (2) incomplete polymer cure, (3) entrapment of voids and (4) damage to components or changes in circuit characteristics from stresses arising during the polymer curing process. Careful cleaning of all parts was stressed by all respondents who practiced encapsulation. It was interesting to note that the survey revealed an ambivalence about encapsulation, i.e., some designers avoid it while others welcome it.

A. Protection

Although breakdown prevention was practiced, additional reliability was provided by protecting the circuits

from the consequences of an unforeseen discharge. The design techniques used included:

(1) Current limiting resistors in the output of the high-voltage power supplies to reduce the dissipated and radiated energy of the discharge.

(2) Diodes in the input to the preamplifiers to prevent damage from voltage transients.

(3) Grounded shields on conductors to eliminate or minimize coupling with adjacent circuits.

(4) A gas-discharge tube across the high-voltage output limiting the maximum output voltage.

B. Detection

The general methods for detecting breakdown included monitoring the input or output currents of the high-voltage supply, detector output signals, and RF power output.

V. Summary

The following pertinent information was disclosed by the two surveys:

(1) The frequency of voltage breakdowns has not diminished in the past several years.

(2) Design is the area most responsible for breakdown problems.

(3) Most breakdowns are dc gas discharges; however, multipactor discharges have appeared more frequently of late.

(4) Major factors affecting gas discharges are outgassing, entrapped gases, insulation, geometry, and circuit arrangements.

The technical problems of voltage breakdown were treated by controlling the electrical environment; i.e., circuit arrangement, elimination of high-electrical stress areas, shielded conductors, use of insulation of suitable material and quantity, controlling the gaseous environment, encapsulation of voids and cavities, pressurization or venting where cavities are unavoidable, and controlling operations, such as turning high-voltage systems on when environmental conditions will not support breakdown.

There is no apparent explanation of why the design area is responsible for the high percentage of breakdown problems, except that preventative techniques were not applied to space flight systems because designers were not aware of their existence or were not schooled in their application. This is not an unreasonable assessment when one considers that most electrical systems are designed for use in ground environment conditions. Unless the designer is experienced in flight system designs and has been cautioned about the uniqueness of the space environment and its effects on flight systems, or has been provided with specialized flight design information, it can be expected that design problems will occur.

The following methods are proposed to overcome this general design problem:

(1) Provide electrical flight systems designers with comprehensive explanations of breakdown processes, and with readily available and easily applied design information.

(2) Ensure rapid dissemination of state-of-the-art developments in high-voltage techniques; e.g., insulation, encapsulation, circuitry arrangement, etc.

(3) Initiate step-by-step design and test programs to develop trouble-free systems.

(4) Require several design reviews at various design stages.

(5) Provide explicit instructions to manufacturers to ensure design goals.

(6) Improve methods for functional and environmental breakdown tests of systems and subsystems.

To facilitate part of these proposed solutions, GSFC has prepared and disseminated a design manual and design criteria.

Discussion

Perkins: What I wonder, in your survey, is if you were able to distinguish any difference in the frequency of problems as distinguished by dc versus ac?

Stern: In general, no. Most of the problems we had been able to identify were of a dc nature. Occasionally you might run across a problem around an antenna, but we haven't observed any significant problems in the ac breakdown area.

Discussion (contd)

Perkins: Second, were the corona problems that you observed primarily ones that involved interference with other portions of the circuitry, or ones which could lead to degradation and failure of the circuit?

Stern: Some of the cases were hard to identify because the literature was old, and simply consisted of a report; not a detailed report. I can't honestly answer whether or not the interference, when there was a corona, was of a coupled nature or of a direct nature in the circuit in which the breakdowns occurred. I have no way of identifying that, at least not now.

Perkins: Well, lastly, a rather nasty question, if you would excuse it. You had a distinction between corona and breakdown; how often do you suppose that corona was the cause of the breakdown?

Stern: I will put it this way: when you ask me what is corona and what is breakdown, we bandy this around. I think sometimes we mean one, and sometimes we mean—we mean it to mean anything. Corona can be a breakdown and breakdown can be identified as corona, so forgive me if I have given you the impression that there is a real significant difference at this time. The corona, as I indicated, was basically a glow phenomenon, and that is all. I will not extend it beyond that. It is a glow phenomena, and it is a form of breakdown, if you wish.

Bunker: I might add a comment. We had this problem, too, so we called voltage breakdown either corona or arcing. A corona is a voltage breakdown, high impedance; an arc, of course, is a low impedance.

August: No question, but a comment on your slide of breakdown problems versus voltage. I think that might be more usefully plotted either versus electric field directly or versus electric field divided by pressure.

Stern: It is hard to look at a system and determine what the electric field is. This might be fine in a laboratory in which you are running some controlled experiments, but if you are having a problem within a circuit, I am afraid it is difficult to define what the electric field is like.

Burrowbridge: I think your problem really is that it is even more difficult to define the electric field from looking at a report, which is where this information came from.

Bunker: How do you tell multipacting breakdown? Is multipacting a corona?

Stern: Let us say this: If you have a very-high frequency, up in the high megahertz regions, and you are down in pressure 10^{-6} region, the probabilities are that you are not running into a simple dc gas breakdown.

Lagadinos: I wonder if, in your investigation and the ac excitation, you detected corona starting voltages as a function of frequency?

Stern: No, we have not made any investigation with respect to ac breakdown. Incidentally, there will be a paper a little later given on some of the work that we have been doing in the corona detection area. We have not used ac for stimulating our breakdown. All of it was done with dc in the laboratory under ideal conditions, and some of the breakdown was stimulated by having a UV lamp in the chamber to make certain we could get constant, or reasonably constant, breakdown.

Lagadinos: Is there any simulation between the ac and dc, if, for instance, you are equipped with an ac corona setup and you want a simulated dc test, is there any direct relationship between the two fields or the nature of these two fields?

Stern: I would rather not comment on that. I don't know.

Bunker: I have a comment. The answer is no, at least in my experience. We are doing some work in higher frequencies. We will report on that later.

Reference

1. *Proceedings of the Workshop on Voltage Breakdown in Electronic Equipment at Low Air Pressures,* Edited by E. R. Bunker, Jr., Technical Memorandum 33-280. Jet Propulsion Laboratory, Pasadena, Calif., Dec. 15, 1966.

N70-32288

Some Observations of Corona Breakdown on Various Antenna Types in Simulated Planetary Atmospheres

C. H. Brockmeyer
Electronics Research and Development Dept.
Martin Marietta Corporation
Denver, Colorado

An antenna connected to a transmitter in a laboratory will probably look much the same as it would connected to a transmitter at some field location. Because of the similarity in the environments in terms of atmospheric pressures the fact is often overlooked that an antenna is not an independent component or subsystem whose behavior is totally dependent on design characteristics. It is in reality an interface between two RF transmission media.

An antenna whose performance in terms of power and voltage standing wave ratio may be entirely satisfactory in the laboratory or at an earth based station may perform poorly or not at all in the environment of near space, deep space or a non-earth planetary atmosphere.

The change in behavior of the antenna in these environments is caused primarily by the difference in the interface with the atmospheric or space RF transmission medium.

The interface changes as a result of the way in which the gases which make up the atmosphere vary in their reaction to the application of electrical voltages. For example, at earth sea level, air has a dielectric strength of about 3 KV/mm and is not easily ionized. As the air pressure decreases, its dielectric strength drops and it is more easily ionized. If the pressure is reduced to about 20% of the sea level pressure, in the presence of an electrical potential, the air may ionize with the partial breakdown called corona. Further reduction in pressure causes the dielectric strength to increase again and extinction of the corona.

The breakdown phenomena is well documented in the literature (Ref. 1–9). Briefly, what happens is as follows:

When a radio frequency transmitting antenna is subjected to a continually decreasing pressure, a pressure region will be encountered where the RF energy radiated from the antenna will cause the gas surrounding the antenna to break down or ionize with the characteristic corona. Ionization takes place due to electron motion. Under the influence of an RF field, an electron is accelerated by the field until it collides with a gas molecule. During collision most of the kinetic energy is kept by the molecule because of the large difference in mass ratio between electron and molecule. On the average, the free electrons in a gas will gain energy with each collision until they attain sufficient energy to have an ionizing collision. When the gain in electron density due to ionization of the gas becomes equal to the loss of electrons by diffusion, recombination and attachment, a gas discharge occurs.

The energy transferred to the electrons is a function of E/P, where E is the electrical field strength and P is the pressure. This quantity determines the gain in energy between collisions. At about 50 torr pressure, 60,000 ft altitude in earth atmosphere, the dielectric strength of the atmosphere begins to drop. The mean free time of the electron is small compared to the RF period. There are many electron-gas molecule collisions per oscillation. The energy gain per collision is small, so the breakdown potential in this region varies directly with pressure.

At pressure below 0.001 torr (300,000 ft in earth atmosphere) the dielectric strength of the atmosphere approaches that of a vacuum. The mean free time of the electron is large compared to the RF period and the electrons make many oscillations per collision. Since collisions are necessary for the electrons to gain energy and there are insufficient molecules to support ionization, the breakdown potential varies inversely with pressure.

In the pressure region from about 50 to 0.001 torr (the region from about 60,000 to 300,000 ft altitude in earth atmosphere, called the "critical" region) a transition is made from many electron-gas molecule collisions per oscillation to many oscillations per collision. It is in this region that corona breakdown normally occurs. A typical plot of breakdown power vs pressure is shown in Fig. 1.

It is thought that the breakdown behavior of the gases which constitute the atmospheres of the other planets will be much as it is in an Earth atmosphere at the same temperature and pressure.

A comparison of "present best estimates" of the composition of the atmospheres of our nearest neighbors, Mars and Venus, with our earth atmosphere in terms of volume is shown below:

Atmosphere	Gas content, %				
	N_2	CO_2	O_2	A	Water vapor
Earth	78	0.03	21	1	0–2
Mars	84	16	—	0.6–6	0–1
Venus	90	10	—	—	0–3

Tests were conducted on antennas immersed in gases of nitrogen, carbon dioxide, argon, and air to determine the breakdown behavior of these gases. A monopole antenna undergoing tests is shown in Fig. 2, and Fig. 3 shows the composite graph of the breakdown profile for the gases tested in the high altitude chamber at the Antenna Laboratory.

The left side of both legs of the curve is formed of CO_2, and the mixtures with high percentages of CO_2 lie close to the left side. Air forms the right boundary of the curve with the 20% CO_2 and 80% N_2 lying just within the boundary of that curve. The 30% CO_2, 30% N_2, 40% A breakdown holds about midway on the composite curve. As a result of these tests, it is felt that over a wide

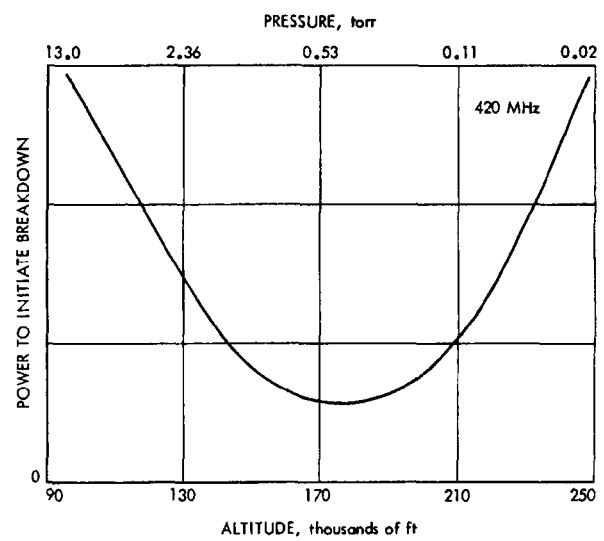

Fig. 1. Power to initiate breakdown vs pressure and altitude

Fig. 2. Monopole undergoing corona breakdown test

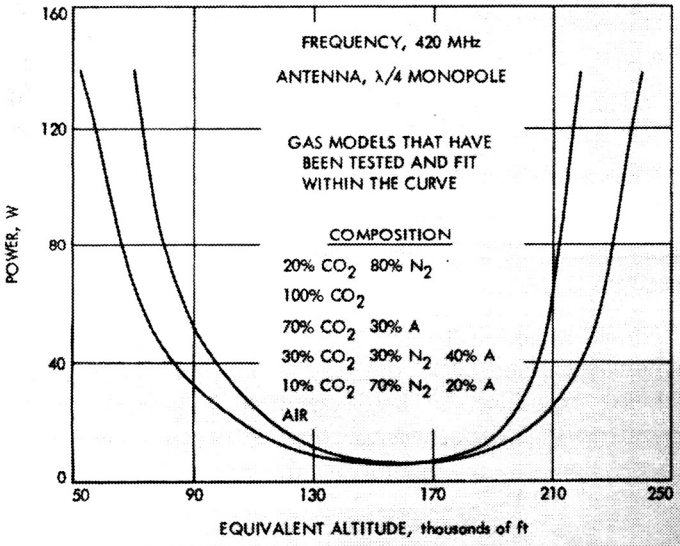

Fig. 3. Composite power breakdown curve of gas mixtures

range of gas pressures, the composition of the gas has little effect on the breakdown level of an antenna immersed in that gas, but the pressures themselves have a major effect.

When the gas surrounding an antenna breaks down, a number of things happen that modify the antenna performance radically. The ionized gas forms a plasma that causes an increase in the RF losses, the impedance and the VSWR will probably change, and the radiation pattern may be affected.

A series of photographs taken of the corona effect in air as the gas pressure was increased from 0.073 to 3.5 torr simulating an antenna entering the atmosphere from outer space, is shown in Figs. 4 through 9.

A corona at the very tip of a 233 MHz quarter wave antenna at a pressure of 0.073 torr and an equivalent

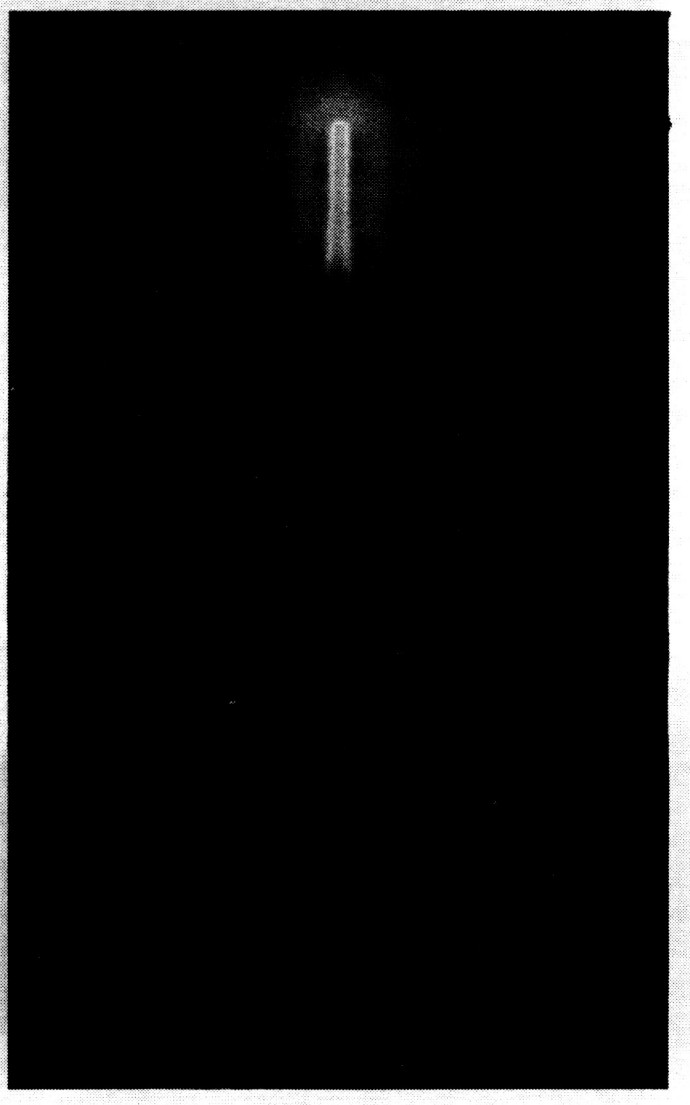

Fig. 4. A 223-MHz quarter-wave monopole antenna breakdown at 0.073 torr (220,000 ft) with 200-W input

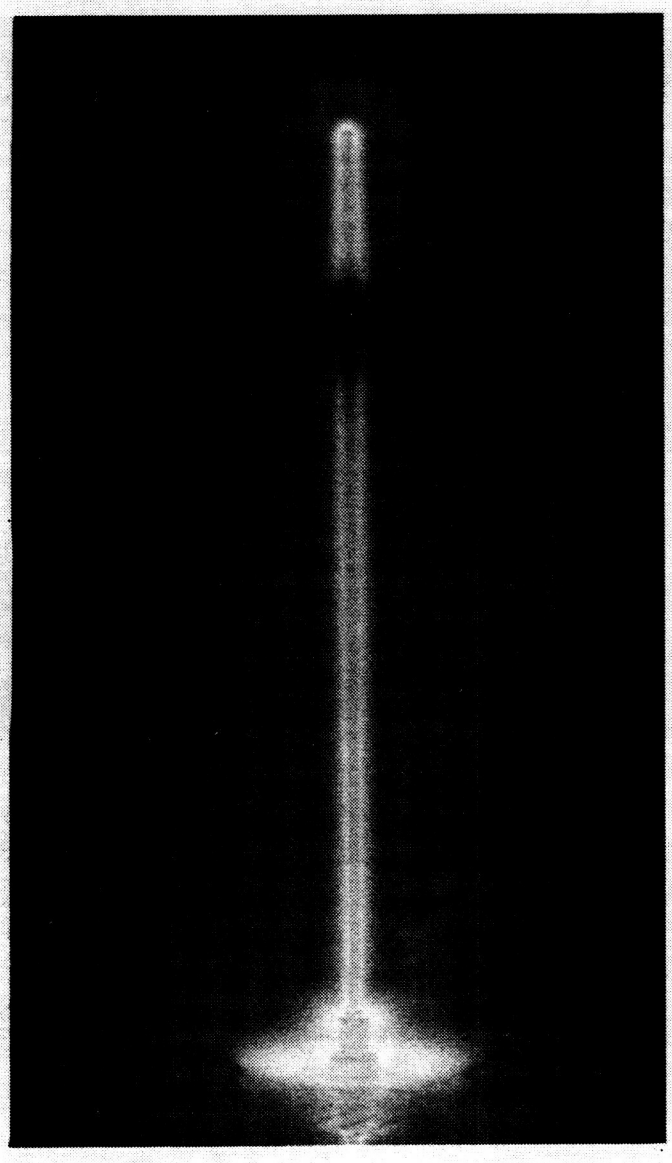

Fig. 5. Breakdown at 0.17 torr (200,000 ft) with 170-W input

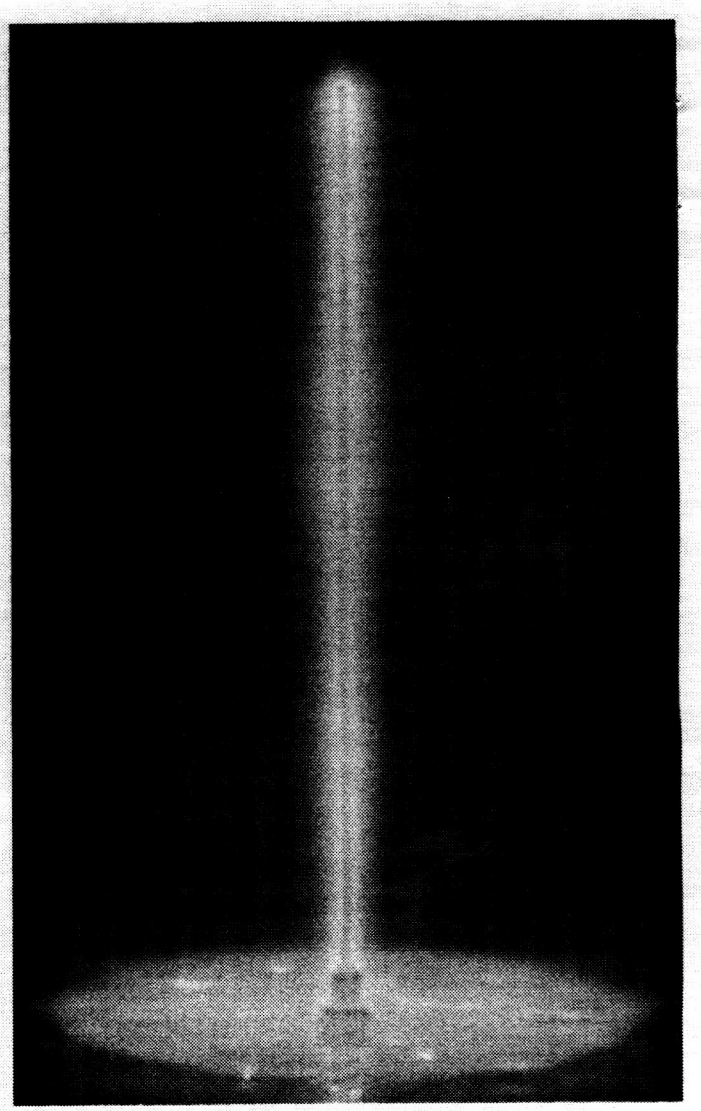

Fig. 6. Breakdown at 0.37 torr (180,000 ft) with 150-W input

altitude of 220,000 ft with 200 W of power applied is shown in Fig. 4.

Figures 5 through 9, respectively, show corona at 0.17 torr (200,000 ft) with 170 W input; 0.37 torr (180,000 ft) with 150 W input; 0.763 torr (160,000 ft) with 100 W input; 1.6 torr (140,000 ft) with 70 W input; and 3.5 torr (120,000 ft) with 70 W input.

The maximum available power input to the antenna under matched conditions was 200 W. The VSWR fluctuated extensively as the pressure approached the critical region and the reflected power randomly varied between 0 and 50 W during the time when corona was being experienced. These variations indicated that the antenna impedance was varying and that the mismatched condition was not permitting the transmitter to deliver the full 200 W.

Standing waves of ionized gas moved up and down the antenna as gas was bled into the chamber. A voltage null appeared near the top of the antenna, Fig. 5, at 200,000 ft; a short time later, a voltage peak appeared at nearly the same point. Fig. 6 (180,000 ft). At a pressure slightly above 3.5 torr, the gas deionized and the power input to the antenna went back up to 200 W.

Photographs of a helical-antenna-over-a-cup for use at S-band frequencies which was tested in all the gas mixtures with an input to the antenna of 62 W with no evidence of corona are presented in Figs. 10 and 11.

The feed system and rotary joint for an S-band parabolic antenna system are shown in Figs. 12 and 13. This antenna feed system was subjected to 62 W in the simulated atmospheres with no indication of breakdown.

It is evident that radio communications can be adversely affected by this corona which wraps the antenna in a lossy plasma, reduces the output of the transmitter, and then tries to make the transmitter dissipate some of the power that it is trying to radiate.

The breakdown characteristics of the atmospheres of Mars and Venus will presumably fit within the composite curve of Fig. 3; however, because the critical pressures on Mars and Venus do not occur at the same elevation as on earth, the problems of corona will occur at a different point in a Mars or Venus mission than on earth. Corona will be an ever present problem on the surface of Mars where the pressure is thought to be in the neighborhood of 5 to 20 torr. This would put the pressure at the surface of Mars at about the same pressure as earth's atmosphere near 100,000 ft. The critical region will extend to an altitude of about 250,000 ft.

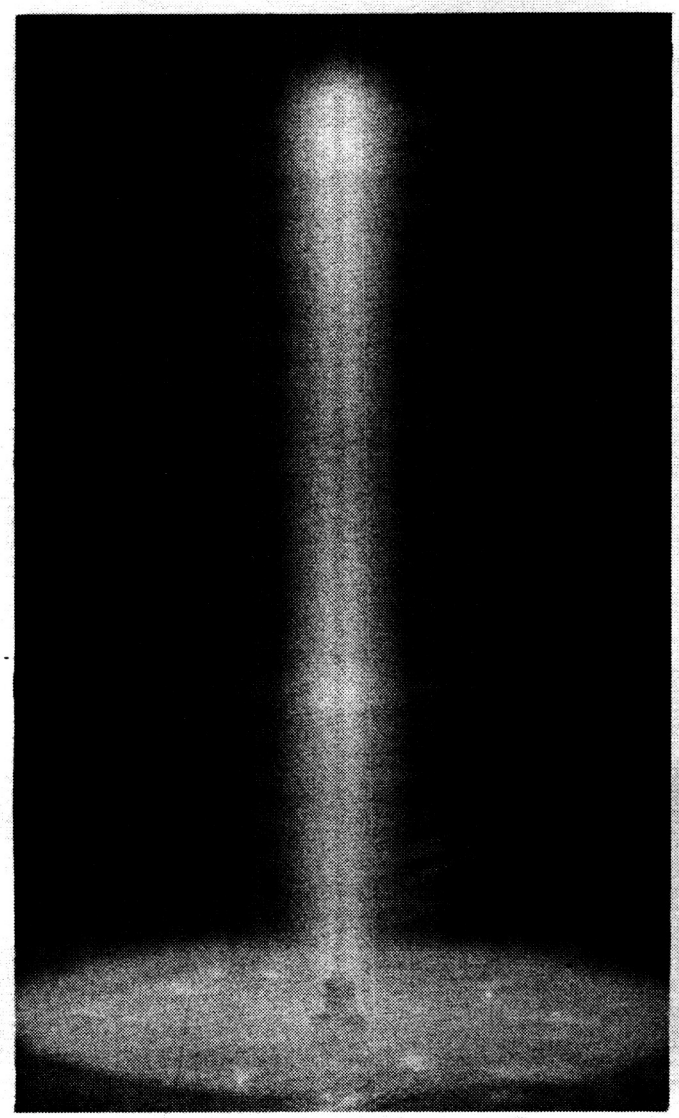

Fig. 7. Breakdown at 0.76 torr (160,000 ft) with 100-W input

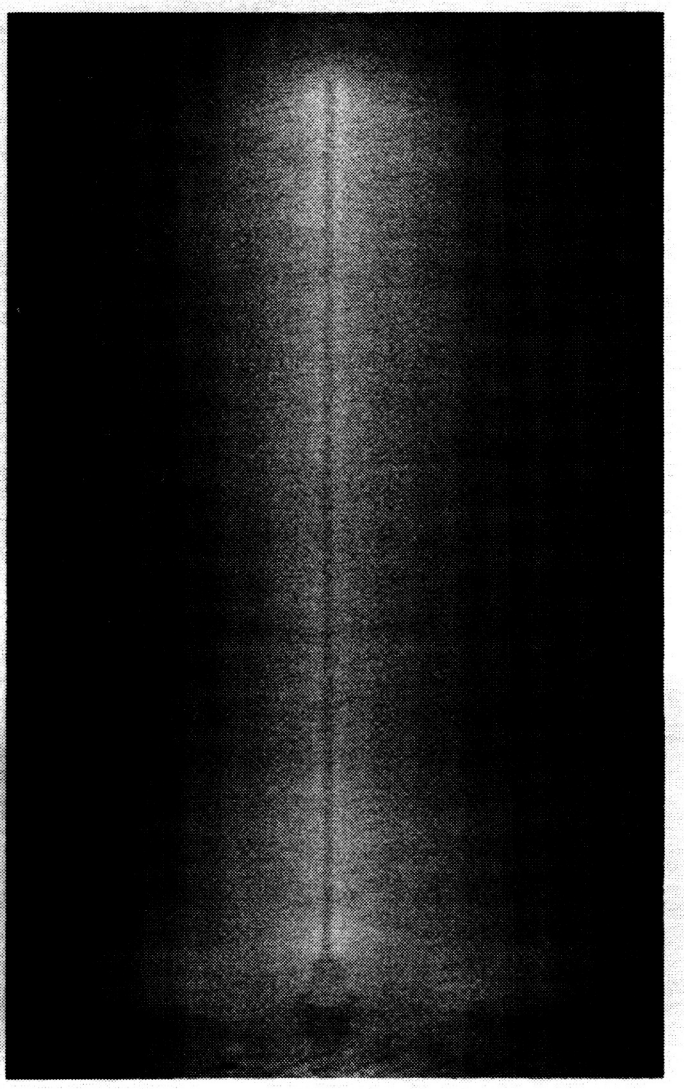

Fig. 8. Breakdown at 1.6 torr (140,000 ft) with 70-W input

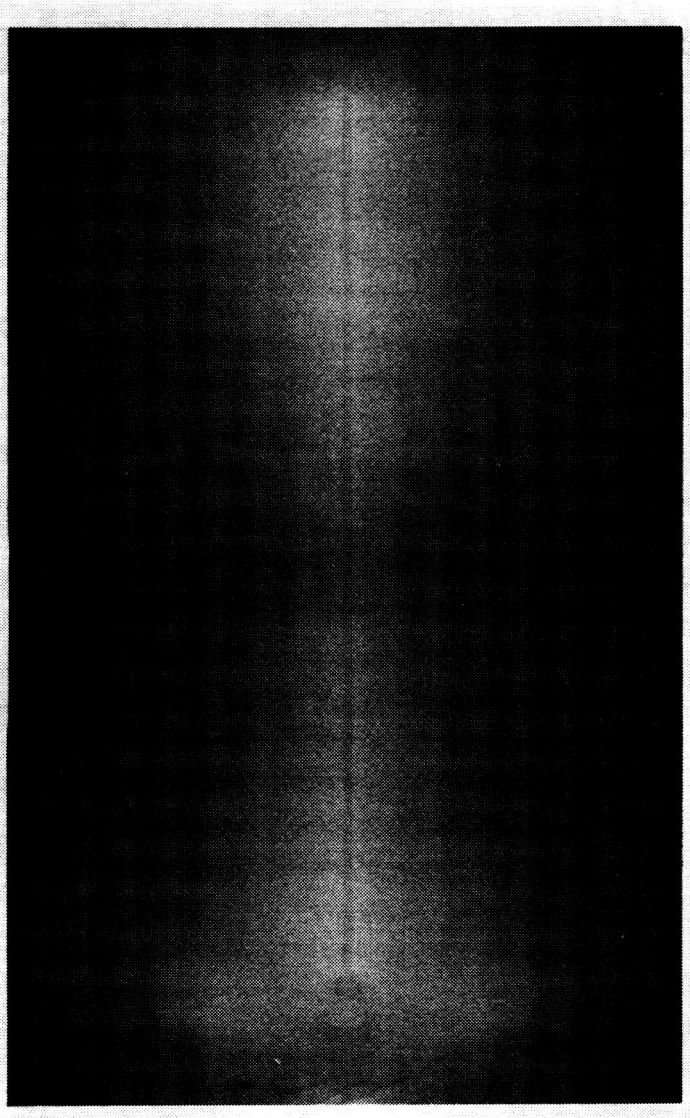

Fig. 9. Breakdown at 3.5 torr (120,000 ft) with 70-W input

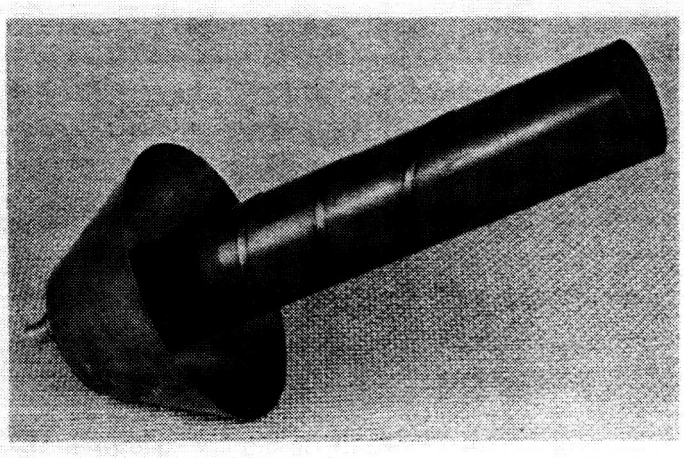

Fig. 10. A 2300-MHz helix-over-a-cup antenna

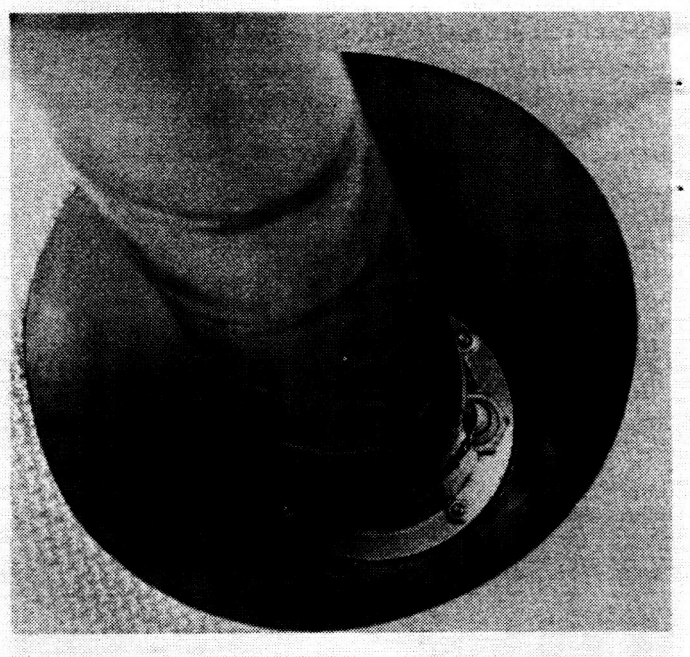

Fig. 11. A 2300-MHz helix-over-a-cup antenna showing connector helix interface

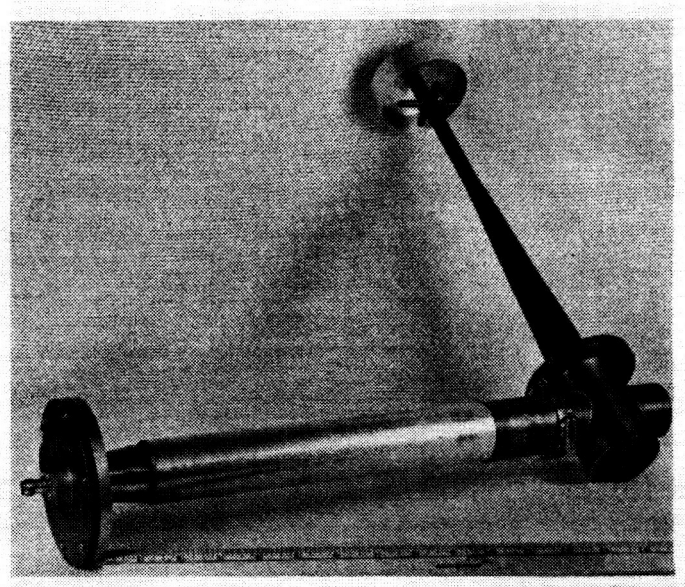

Fig. 12. A 2300-MHz crossed-dipoles-over-a-cup parabolic antenna feed

Present information indicates that the atmospheric pressure on the surface of Venus is about 100 times the pressure on earth. This would eliminate the possibility of antenna breakdown due to the ionization of gases at the surface; but, greater attenuation of RF signals from that surface would be expected. Problems of ohmic losses, and leakage and contamination might be anticipated. Assuming the gases of the Venesian atmosphere

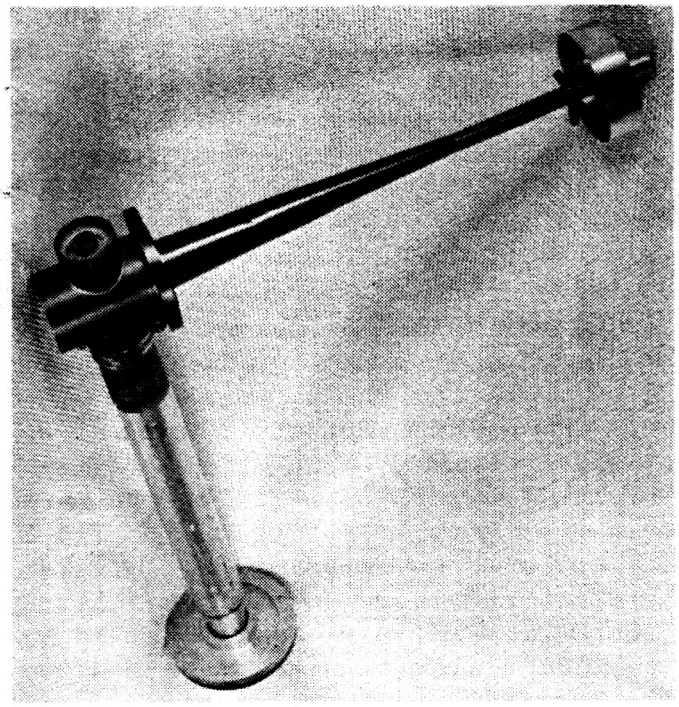

Fig. 13. A 2300-MHz crossed-dipoles-over-a-cup showing ball bearing rotary joint

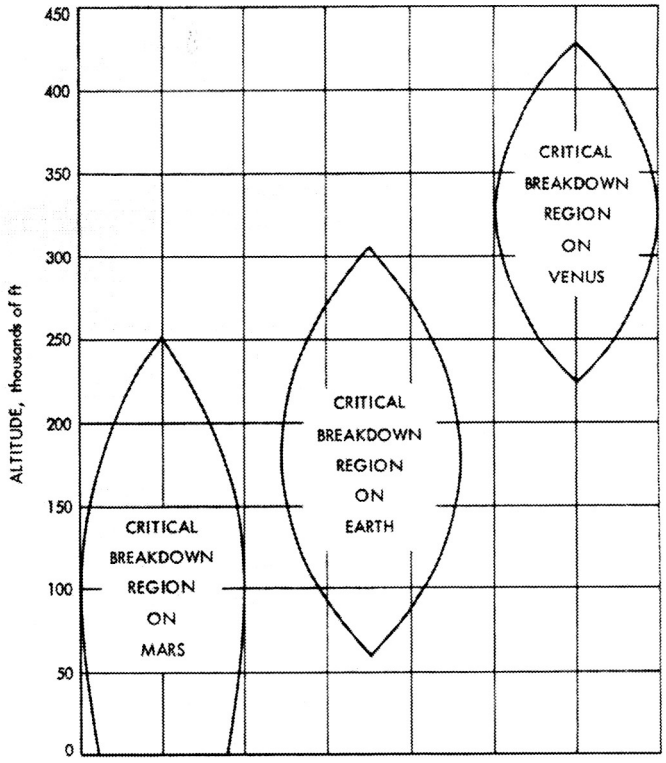

Fig. 14. Regions of critical breakdown

would have the same breakdown characteristics as previously described, corona problems would be expected in the region from about 230,000 to 430,000 ft above the planet's surface.

A comparative picture of the critical breakdown regions on earth, Mars, and Venus is presented in Fig. 14.

The choice of frequency for use on Mars and Venus probes is also important because the critical pressure at which breakdown occurs is frequency sensitive. It has been determined that in earth's atmosphere the minimum breakdown point occurs in the region where the product of the pressure in torr and the wavelength in centimeters falls between 10 and 40. The smaller number applies to physically-small, electrically-large antennas for the higher frequencies and the larger number applies to physically large, electrically small low-frequency antennas.

The frequency at which breakdown will occur most easily plotted against the pressure and altitude in earth's atmosphere is shown in Fig. 15. If the atmospheric pressure on the surface of Mars is 5 to 20 torr, low-power breakdown can be anticipated at S- and X-band frequencies.

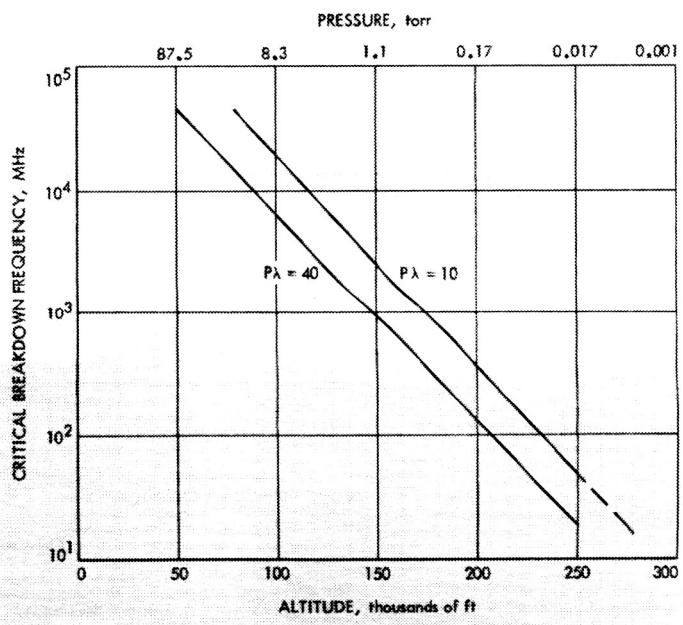

Fig. 15. Critical breakdown frequency vs pressure and altitude

In addition to the problem of voltage breakdown in a free-flowing atmosphere, there is another area where the same problem can occur as a sort of delayed action.

In order to make antennas as small as possible and still appear the proper size electrically, dielectric materials are used as antenna fillers. These fillers, whether solid dielectrics or foams, tend to outgas in reduced pressure environments. This outgassing is not limited only to materials used in antennas and at radio frequencies but can occur in all types of electronic materials and at dc voltages as well as RF.

Instances of corona-type failures in spacecraft systems after more than two weeks of operation in a vacuum have been experienced on *Mariner* (Ref. 11), *NIMBUS*, *OSO*, and *OGO* (Ref. 12).

In a test performed on a foam-filled caity-backed slot telemetry antenna, the antenna operated satisfactorily with 200 W of power applied throughout the range of pressures from earth surface to 0.046 torr at an equivalent altitude of 230,000 ft. The antenna was left in the vacuum chamber for three days and tested again; it broke down at 80 W. The outgassing of foams and other materials is a recognized problem and efforts are being made to determine how to overcome this problem.

The high-temperature sterilization requirements for Mars and Venus probes are certain to magnify the problem of outgassing of materials not only in antennas but throughout the spacecraft.

Several antenna schemes are being pursued today in which more than one transmitter is to be connected to a single antenna. Combining RF signals into a single antenna causes the antenna to see an input power equal to the instantaneous peak powers of the transmitters. A beat of power peaks at the frequency equal to the difference between the transmitter frequencies will occur. This means that if simultaneous transmission from more than one transmitter is to feed a single antenna, the power from each individual transmitter must be reduced to keep the total power below the corona onset level.

A test was performed using two transmitters: one operating at 245 MHz and the other at 250 MHz. Their outputs were fed into a multiplexer and the output of the multiplexer was fed through a wattmeter to a 1-½-in. diam quarterwave monopole antenna. When either of the transmitters was turned on, the antenna experienced breakdown at about 80 W. When both transmitters were turned on and power to the multiplexer increased in 1 W steps from each transmitter, corona breakdown was experienced when each transmitter was delivering approximately 30 W. A cavity-backed slot antenna replaced the monopole and broke down at 60 W from either transmitter and with approximately 17 W each when both transmitters were on.

Another test was made with some multiplexers at 419.5 and 425.5 MHz. Using an 8-in. diam monopole, the antenna would break down from 5 to 8 W from either transmitter. With both transmitters on, only 2½ W were required for breakdown.

Furthermore, once the gases surrounding an antenna have become ionized and the corona formed, it may be necessary to completely remove the RF excitation before the corona will extinguish.

Discussion

August: Fonti and Mullin in the *IEEE Transactions on Antennas and Propagation* I think about two years ago had a paper on multifrequency breakdown of antennas, and their basic conclusion was that you essentially got no increase in power-handling capability; in other words, your sum powers, that all your frequencies was at most equal to single-frequency breakdown power, or somewhat less. I have been interested in the subject because of problems of noise radiation. To my knowledge there is only one experimental paper in which this problem of multifrequency breakdown has been studied, and that was with two and three frequencies. So, I would appreciate your publication, and one additional comment: this problem of multifrequency breakdown on a single antenna I think is in reasonably good shape.

I have been worrying about noise radiation and multifrequency radiation from other types of structures, such as log periodic or spirals in which the radiation is essentially from different portions

Discussion (contd)

of the structure, and it appears on those that you can get somewhat increased power-handling capability.

Heuser: What was your criterion for a breakdown of the antenna? Was it just a visual observation of corona?

Brockmeyer: That is primarily what it was. We could watch the voltage standing wave ratio on the reflectometer and we generally could detect that we were approaching breakdown before we were actually able to see it. The voltage standing wave ratio began to fluctuate quite wildly.

We were trying to see if there was any correlation between VSWR and breakdown, and everything was so wild we couldn't find it.

Heuser: We have used some photomultiplier tubes to detect breakdown, and we could see evidence of a breakdown before it was visible to the naked eye.

Another question I would like to ask is: had you ever put the antenna in a slightly charged-particle environment, that is, put a UV tube in there to slightly ionize some of these gases beforehand?

Brockmeyer: We tried it without and we also used a couple of polonium 210 sources inside the chamber. We found that unless we did this, since it was dark and we had no external light, that the repeatability of our breakdown measurement was almost impossible unless we did use some sort of an ionization source in the chamber.

References

1. Herlin, M. A., and Brown, S. C., "Breakdown of a Gas at Microwave Frequencies," *Phys. Rev.*, Vol. 74, pp. 291–296, August 1948.
2. Herlin, M. A., and Brown, S. C., "Electrical Breakdown of a Gas Between Coaxial Cylinders," *Phys. Rev.*, Vol. 74, pp. 910–913, October 1948.
3. Herlin, M. A., and Brown, S. C., "Microwave Breakdown of a Gas in a Cylindrical Cavity of Arbitrary Length," *Phys. Rev.*, Vol. 74, p. 1650, December 1948.
4. MacDonald, A. D., and Brown, S. C., "High Frequency Gas Discharge Breakdown in Helium," *Phys. Rev.*, Vol. 75, pp. 411–418, February 1949.
5. MacDonald, A. D., "High Frequency Breakdown in Neon," *Phys. Rev.*, Vol. 88, p. 420, October 1952.
6. MacDonald, A. D., "High Frequency Breakdown in Air at High Altitudes," *Proc. IRE*, Vol. 47, p. 436, March 1959.
7. Kelly, D., and Margenau, H., "High Frequency Breakdown of Air," *J. Appl. Phys.*, Vol. 31, pp. 1617–1620, September 1960.
8. Chown, J. B., Scharfman, W. E., and Morita, J., "Voltage Breakdown Characteristics of Microwave Antennas," *Proc. IRE*, Vol. 47, pp. 1331–1337, August 1959.
9. Scharfman, W. E., and Morita, T., "Voltage Breakdown of Antennas at High Altitude," *Proc. IRE*, Vol. 48, pp. 1881–1887, November 1960.

References (contd)

10. Linder, W. J., "Critical Altitudes for Radio Frequency Breakdown" in *Proceedings of the Workshop on Voltage Breakdown in Electronic Equipment at Low-Air Pressures,* Technical Memorandum 33-280. Jet Propulsion Laboratory, Pasadena, Calif., Dec. 1966.

11. Bunker, E. R., Jr., "Voltage Breakdown Problems at Low Air Pressures Encountered in the *Mariner IV* Spacecraft," in *Proceedings of the Workshop on Voltage Breakdown in Electronic Equipment at Low-Air Pressures,* Technical Memorandum 33-280. Jet Propulsion Laboratory, Pasadena, Calif., Dec. 1966.

12. Street, H. W., "High Voltage Breakdown Problems in Goddard Scientific Satellites," in *Proceedings of the Workshop on Voltage Breakdown in Electronic Equipment at Low-Air Pressures,* Technical Memorandum 33-280. Jet Propulsion Laboratory, Pasadena, Calif., Dec. 1966.

N70-32289

VHF Breakdown on a *Nike-Cajun* Rocket

J. B. Chown, J. E. Nanevicz, and E. F. Vance
Stanford Research Institute
Stanford University
Stanford, California

This paper was presented by G. August of the Stanford Research Institute.

The Stanford Research Institute (SRI) has been involved in voltage breakdown studies over a period of several years. This paper demonstrates that even with such extensive experience, complete solutions to the problem have not yet been found.

This paper addresses itself to the laboratory testing of a VHF quadraloop antenna (Fig. 1) identical to one used in a *Nike-Cajun* flight; laboratory testing was performed on several antennas, however, we have confined this report to the former.

Prior to the particular *Nike-Cajun* flight in question, a VHF antenna was tested at the SRI laboratory. It was thought that a reasonably conclusive investigation had been performed. After the flight, however, it was concluded that flight test data did not agree with laboratory findings. Subsequent analysis indicated that flight conditions had not been properly simulated.

A sketch of the VHF quadraloop antenna is shown in Fig. 2. It is a standard quadraloop antenna designed to operate at 260 MHz. The antenna's cavity is filled with dielectric to maintain rigidity. During the flight, unfortunately, there were two instances in which the VSWR shifted abruptly; it is suspected that either there was a loose screw or an anomolous mechanical pressure resulting in the VSWR change.

The high-field region is situated in the back (or open) end of the antenna; i.e., an essentially shorted quarter loop. The electric field is zero at the closed end; on the *Nike-Cajun* this is the apex end or the front end of the vehicle.

The quadraloop was designed to be power modulated in operation at about once-per-second with a trapezoidal wave form. The purpose of the modulation was to make it possible to observe both breakdown initiation and breakdown extinguish.

In laboratory tests, the same approximate modulation was induced; however, a trapezoidal shape was not achieved. The shape was sinusoidal and reasonably similar. The incident peak power was 25 W; the power initially delivered to the antenna was about 17 W immediately following the first VSWR change. Later, the

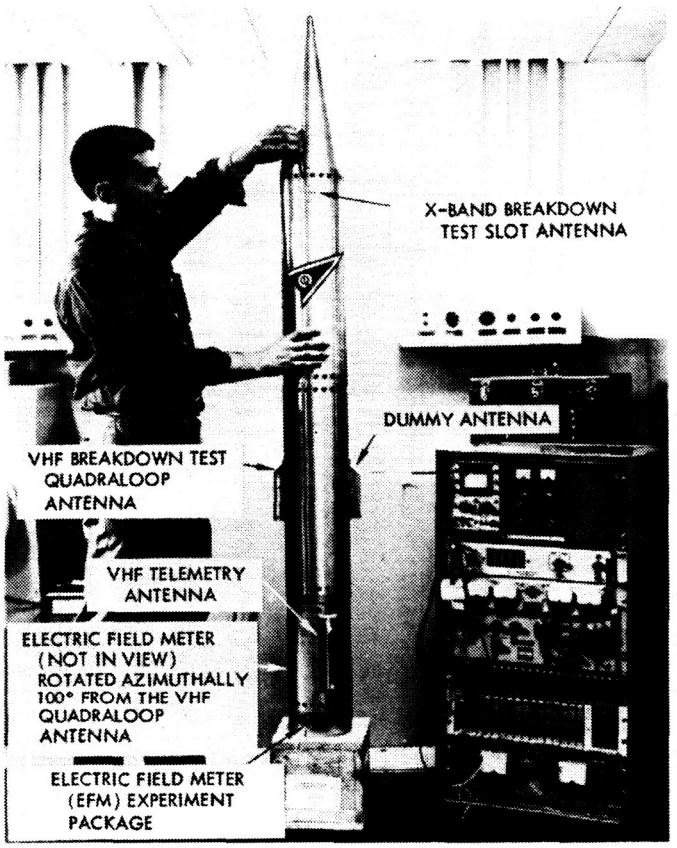

Fig. 1. *Nike-Cajun* payload

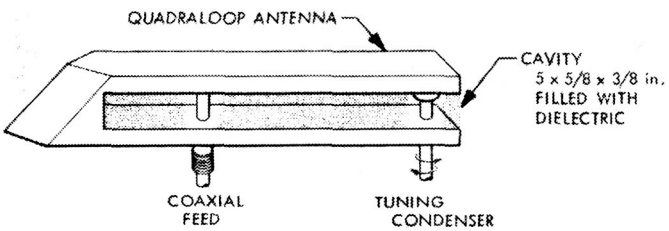

Fig. 2. VHF voltage breakdown experiment antenna

power increased to about 23 W after the second VSWR change, which lowers the VSWR.

In addition, the once-per-second modulation was slow enough during the flight test to enable taking breakdown and extinguish points at a reasonably stationary altitude. This was a supersonic flight and the altitude change was relatively insignificant. A large telemetry bandwidth was not necessary for recording the data.

A typical telemetry record is shown in Fig. 3. The antenna incident power, shown at the bottom of Fig. 3, was monitored. Antenna-reflected power and the ground-received signal are shown by the middle line; as can be seen, the wave form is trapezoidal. At this point the reflected power is reasonably high; i.e., about a 3.6 VSWR. These data were received prior to the VSWR changes. On breakdown initiation, a notch in the incident power appeared; a small notch in reflected power also became manifest. At the beginning of the notch, the received signal on the ground dropped abruptly. On extinguish, the reverse process occurred.

For predicting breakdown levels of various antenna types, both empirical data and theory are relied upon. A reasonably well established theory for predicting antenna breakdown in terms of field strength exists. Since the exact field strength distribution on many antennas is not known, some laboratory testing is required.

We proceeded with our laboratory tests and thought we had the problem relatively well established. We know what the breakdown curve should look like at relatively low altitudes. It is attachment-dominated, and you get the familiar U-shaped curve where you are on the one end of the U; as you get higher in altitude the breakdown power decreases until you go through a minimum. At sufficiently high altitudes you are in a diffusive dominated regime, which determines the breakdown power.

Unless you are operating on a pulse basis or at frequencies where the electron densities get so high that recombination effects are important, you ignore these things. You can do a reasonably good job with CW theory. Since we were supersonic with the *Nike-Cajun*, we thought convective effects might be important in modifying the simple CW theory. We know from a lab test, for example, on slot antennas in shock tubes that if the shock is moving at sufficiently high speed, convective effects change power breakdown because they essentially sweep out electrons that are created by the RF field. We didn't think this would be important for this particular antenna.

A mockup of our VHF quadraloop antenna is shown in Fig. 4. It is mounted on a cylinder, because we found that at the frequency of 260 MHz there was an axial mode excited on the *Nike-Cajun* which was significant in the radiated power, so we had to somewhat duplicate that by constructing a cylinder to simulate the body.

Our test procedure is relatively simple. We pump it down to the desired pressure. Polonium sources provide electrons for reliable starting of the discharges. Break-

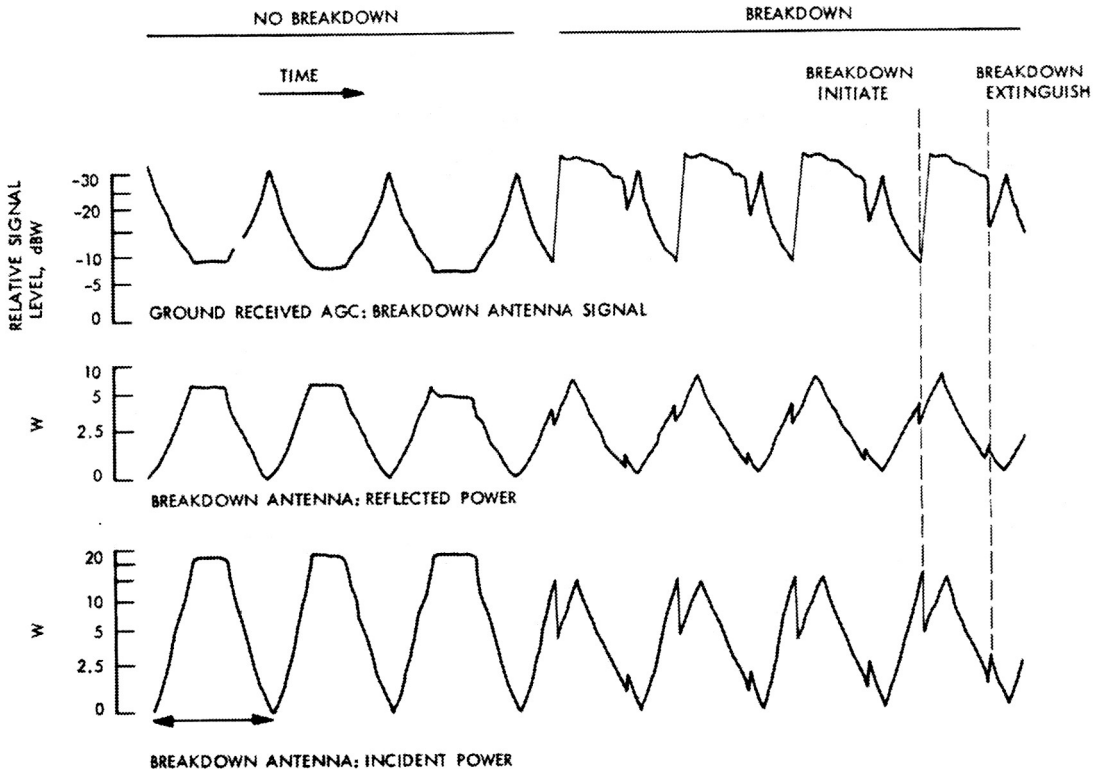

Fig. 3. Telemetry record of VHF antenna voltage breakdown

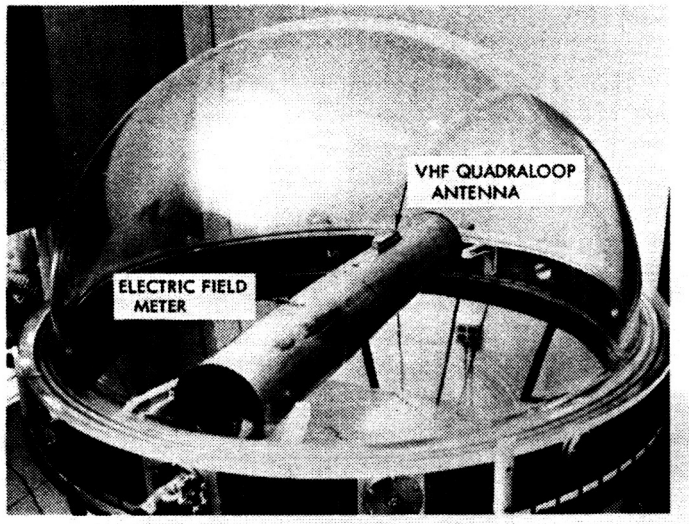

Fig. 4. Mockup of VHF antenna and EFM experiments

down points of net antenna power are recorded (not incident power since we have taken out reflected power). As can be seen in Fig. 5, we have the standard U-shaped breakdown curve with regions of attachment control and diffusion control as a function of pressure. Also, in this illustration, we have an extinguish curve which is lower by something on the order of 8 dB below the initiate curve. This is what might be expected because when you have ambipolar diffusion in the presence of many electrons, the threshold for breakdown drops by 6–10 dB. The conditions governing extinguish should be reasonably close to those of ambipolar diffusion initiate.

When sufficiently low pressure was achieved, we found we were getting multipacting; this is indicated by the constancy of breakdown power vs pressure over about three orders of magnitude of pressure.

This experiment was also performed with plasma in our vacuum chamber. For this experiment, we used an auxiliary multipactor source driven at 50 MHz to provide an ambient plasma which we monitored to be about 10^4 to 10^5 electrons/cm^3, comparable to that in the ionosphere.

Measurements of plasma density are a little difficult to take in this range, but that was the best we could do. It may be off by a plus or minus factor of 2 or 3. As you can see, for the frequencies we were using and the relatively low electron densities, we didn't get much shift in breakdown threshold with plasma or without, as

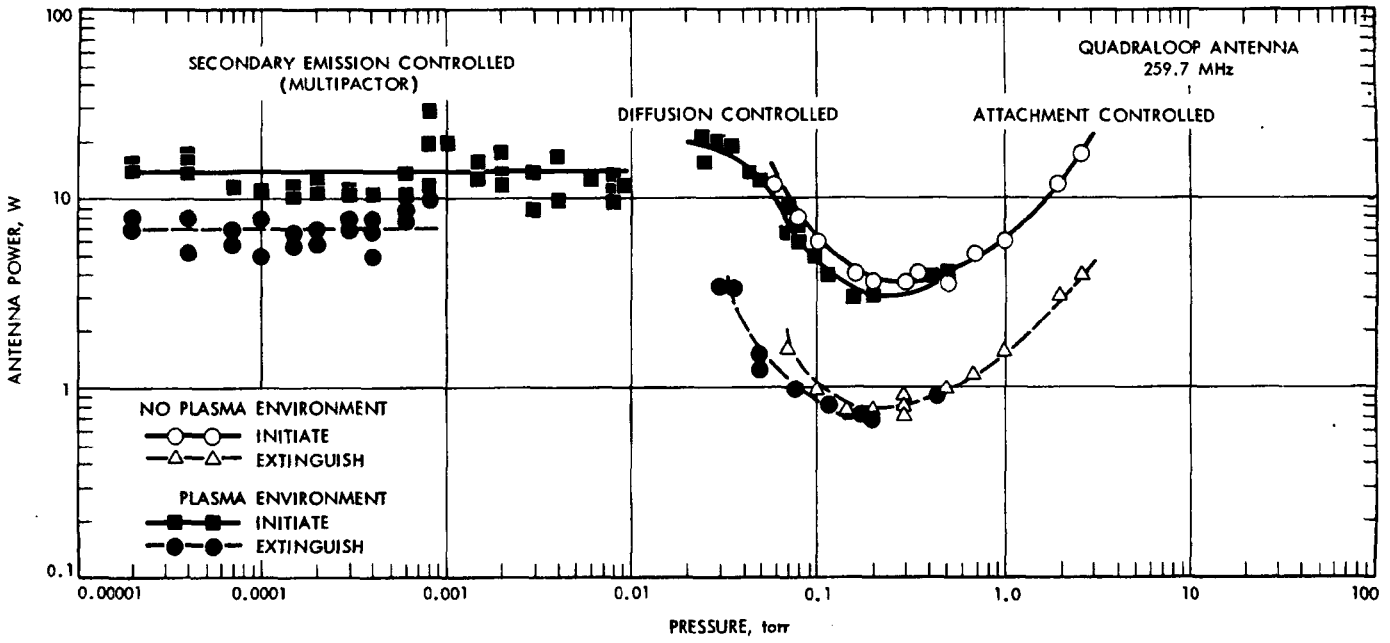

Fig. 5. VHF antenna breakdown: laboratory test

compared to without. The same is true of the extinction levels. This result is expected in the case of extinction because, after all, a breakdown plasma is created which is furnishing most of the plasma about the antenna.

A similar result held for the multipacting points. I don't want to go into the theory of multipactor here, but there isn't any particular reason that a plasma environment should lower the breakdown threshold appreciably; you might expect a dB, or so, because the plasma prevents some of the electron losses that normally occur in multipactor discharge.

We don't have an altitude scale in Fig. 5, but, at the minimum, at about 100 microns, the pressure is equivalent to 214 kft, and there is a roughly 50-kft change per decade.

In the very low altitude regime, beginning at 10^{-2} microns, our multipacting was very erratic. It was flickering; it would go on for a few seconds, go off and then it would restart. Sometimes it would run for as much as a minute and then stop and start again rather unexpectedly. This is typical of relatively low-voltage multipactor environments. These points were taken not on a CW basis but on a pulse basis, most of them, so the discharge was coming on and going off, and we weren't continuing to clean up the multipacting surfaces by constant running of the discharge.

We have found in most of our experiments, as I am sure many of you have, who have worked with multipacting, that if you allow a discharge to go on for a long time you can clean it and it stabilizes, and you don't have problems in maintaining it; however, the starting voltage usually goes up after you have cleaned it.

Also, below 10^{-3} torr which is about 300 kft, we could not see the multipacting by a change in incident or reflected power in our static laboratory tests since the magnitude was too small in comparison with the errors in the system. We were able to see it visually, however; Fig. 6 shows what it looked like. This was a long-time exposure; you can just barely see our quadraloop. This is at 4×10^{-4} torr, which should be around 320 kft.

There is a very diffuse blue-white multipacting illumination around the antenna. It spreads quite a bit because the pressure is so low that the electron mean free path is high. There is nothing to interfere with the electrons, and they just spread out. We hadn't really expected multipacting in this geometry because of the arrangement of the electrode surfaces on the quadraloop antenna. Although there is an upper electrode and a lower one there aren't really a pair of parallel surfaces where multipacting normally occurs. Nevertheless, we were getting multipacting in this arrangement.

A comparison of flight test records and laboratory records is shown in Fig. 7 for the ascent portion of the

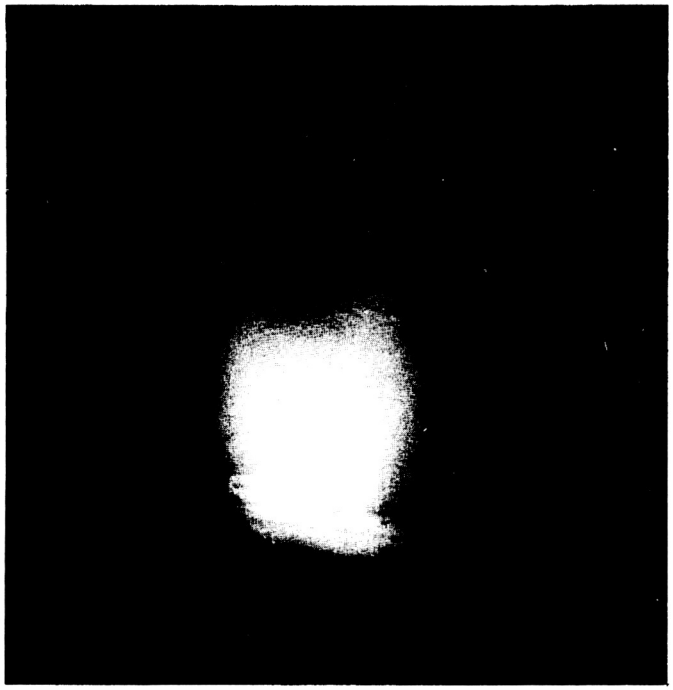

Fig. 6. Breakdown glow of VHF quadraloop antenna at 4 × 10^{-4} torr

flight is shown. We don't have a velocity scale here, but we see some strange things happening.

First of all, our laboratory data, which is indicated by the solid and dashed curves, in Figs. 7 and 8, are appreciably displaced from our flight test records. There is something like 50 to 100 kft between where breakdown during flight actually occurred and where breakdown occurred in the laboratory; the familiar U-shaped curve is very, very broadened. It is not as one might expect it to be on theoretical grounds, and shows up both in the initiate levels and in the extinguish levels.

The multipacting data begins, as one might expect; it goes at about 10 microns. We are seeing essentially a steady breakdown curve, i.e., a steady value in watts at about where we expected it in the laboratory so that the multipacting level is not appreciably disturbed in the flight test record.

The only thing that seems to be wrong is that the extinguish levels at very high altitudes are a lot lower

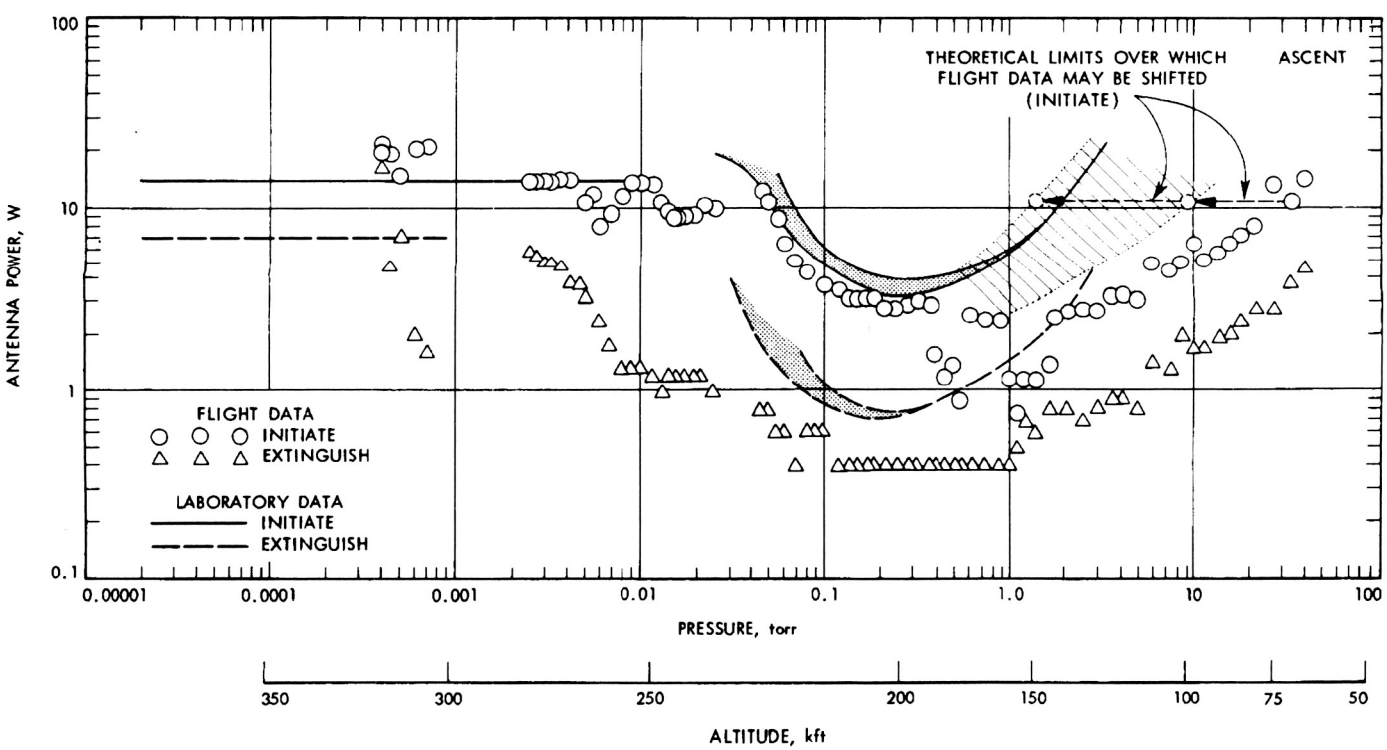

Fig. 7. VHF antenna breakdown during ascent: flight test

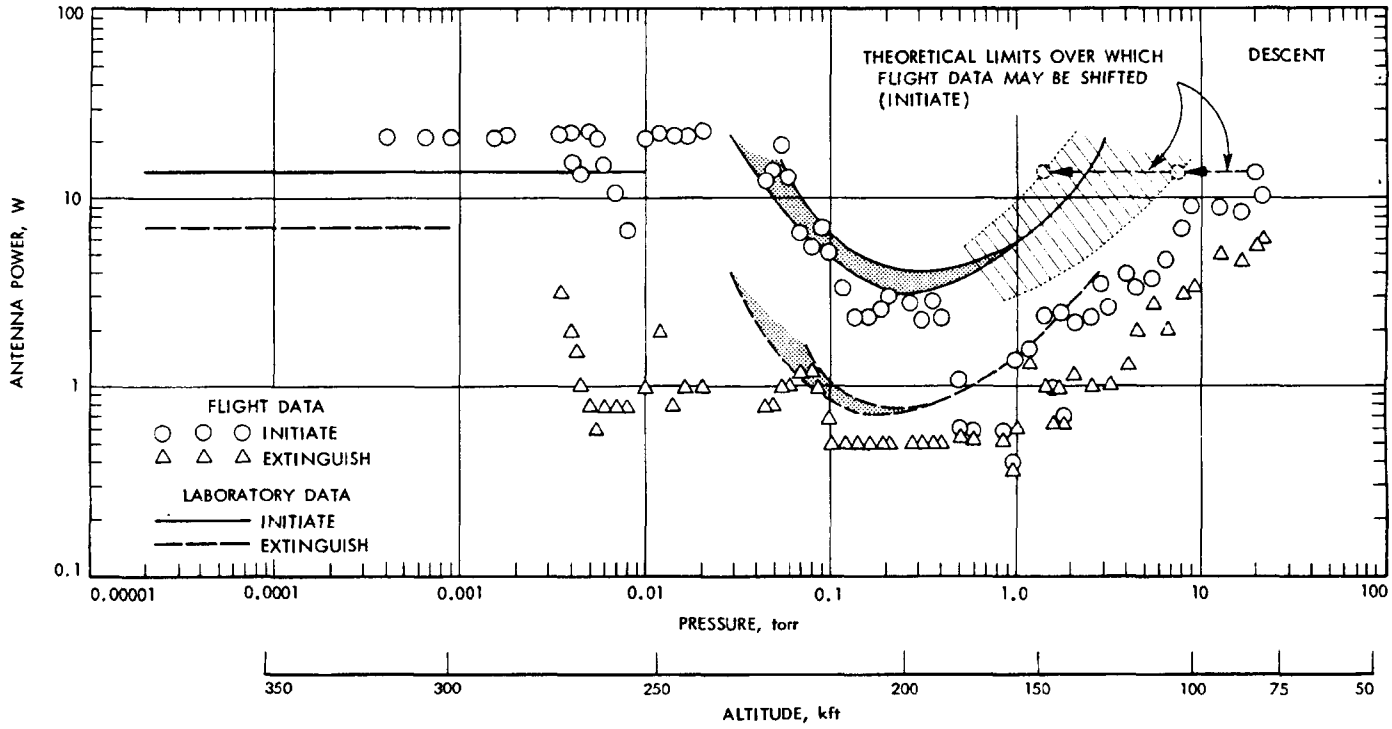

Fig. 8. VHF antenna breakdown during descent: flight test

than one might expect. Normally, one expects a multipacting to only produce a very slight modification in incident power and reflected power, so the multipacting should begin at this level and remain.

The points below are discrepancies in that the extinguish levels are much further down. On the descent portion of the flight we got a somewhat similar sort of result. I won't bother to go through it in too much detail; that is, the difference between the flights.

Let's talk about why this happened: we analyzed the data from the flight test and, considering the theory, concluded that one of the things that we had neglected in the static laboratory tests was the aerodynamic effects taking place. Since we are flying a quadraloop antenna, protruding from the surface of a *Nike-Cajun* and since it is flying at supersonic speeds, at least at lower altitudes, and since there are boundary layers, shocks set up around various portions, particularly around the front edge of the quadraloop. If you examine the theory of what the boundary layers should be, you can find that the quadraloop is actually protruding from what should be the boundary layer on the *Nike-Cajun* body itself. Furthermore, because there is a sharp discontinuity at the back of the quadraloop, where it steps down to the vehicle surface, there should be a flow separation passing over the top of the quadraloop; as with most flow separations, you get a partial vacuum behind them. We think that what happened during the flight test was that the local pressure in the high-field area, which is the breakdown area right at the back of the quadraloop, was not the ambient pressure, so there is no particular reason to expect the two to agree.

We looked through the theory as best we could, and it has to be approximate, because the shock theory and the aerodynamic theory are not well defined for arbitrary shapes and as for something like a quadraloop, and we estimated the basis on which the altitude levels over which the flight test data could be shifted to correspond to ambient values.

We think these were a different local pressure and we shifted them to what we thought was the actual local pressure right in the high-field area. As a result, a little better agreement is secured when we shift all of these points to this range. We don't know precisely how much we are supposed to shift it; we just have a range. However, the lowest breakdown points fall into this range where we actually observed our laboratory data; thus, we are reasonably convinced that this is what happened at low altitude on both ascent and descent.

We simply got aerodynamic effects, a lowering of the pressure behind the quadraloop, and that shifted the breakdown data from the ambient data that we had measured in the laboratory.

There were some instances of anomalous breakdown at high altitudes where we were supposed to get multipacting; we weren't supposed to see extinguish values down here, and we looked into this too. I will discuss this a little later, but right now I will go to some of the other data.

Now, this is a comparison of most of the things that we did, including some things I don't want to discuss. The important things here are the measured quadraloop breakdown power on ascent and descent, and our ground-received telemetry data and AGC signal, which show when we got breakdown by significant loss in received signal level.

As can be seen from Fig. 9, when breakdown occurred at sufficiently high altitudes during ascent, a decrease in ground-received signal level took place. This might be expected because we experienced our breakdown on the aft end of our quadraloop antenna. At high pressures or low altitudes it is confined to only a small portion, whereas the major portion of the radiation is probably coming from the rest of the loop. Thus, we should not expect to see too much ground-received attenuation. Furthermore, the breakdown power is so high and the initial increase in reflected power is so low that we aren't attenuating it severely.

Altitude is increased, and the plasma spreads because the mean free path becomes longer, it gradually envelopes the antenna, resulting in a greater reduction in received power.

We have two sets of data plotted in Fig. 9: one is total VHF experimental loss, including the impedance effect. That is, we plotted for a given incident power, what the net power to the antenna was, which is what we might expect to see radiated to the ground. We also plotted the signal loss during the antenna breakdown, excluding the impedance effects; this curve represents basically the plasma attenuation and any pattern changes caused by the plasma around the antenna. You can see that that gradually increases as altitude is increased and the breakdown plasma spreads. Results were approximately comparable.

One significant thing happened in that our telemetry signal, which was about 225 MHz as compared to our VHF experiment at 260 MHz, we noted some attenuation in the telemetry antenna. As you will recall from Fig. 1, this was mounted aft of our breakdown quadraloop antenna.

What we think happened here is that we probably got some diffusion at these altitudes of our breakdown plasma around our telemetry antenna. The breakdown value we would expect for the telemetry antenna with the plasma, that is, the extinction level was about 0.4 W, whereas the thing was actually radiating about 2 W per telemetry antenna. Therefore, if we got sufficiently high plasma, it would see an ambipolar plasma around it and break down; this might cause the reduction in telemetry signal.

On the other hand, the spreading plasma from our breakdown experiment might produce sufficiently high attenuation to give us that value up there, so we did see some breakdown results at a different location on our telemetry antenna.

Now, I would like to talk about the high-altitude breakdown which was due to multipacting. We considered what the discrepancies were in the high-altitude breakdown, which we believed was multipacting. The major discrepancy was that it appeared to act as a gas discharge; in other words, the reflected power was higher than one would anticipate for a multipactor discharge on the basis of our laboratory experiments. We wondered why this was happening; were we really seeing gas discharge or was there something else?

We decided that the probable cause was the fact that the vehicle was outgassing rather slowly during flight because the total flight time was only about 5 min. When we test something in a laboratory we pump down for an hour and sit at a low vacuum for quite a while. Thus, everything has a chance to become reasonably outgassed.

It was thought that maybe what was happening was the multipactor was starting off and there was sufficient local pressure, as distinct from ambient pressure, due to outgassing around the quadraloop antenna that was simply going into a gas discharge. We decided we would try and simulate this in the laboratory and find out. Fig. 10 shows the altitude–time profile of the rocket flight.

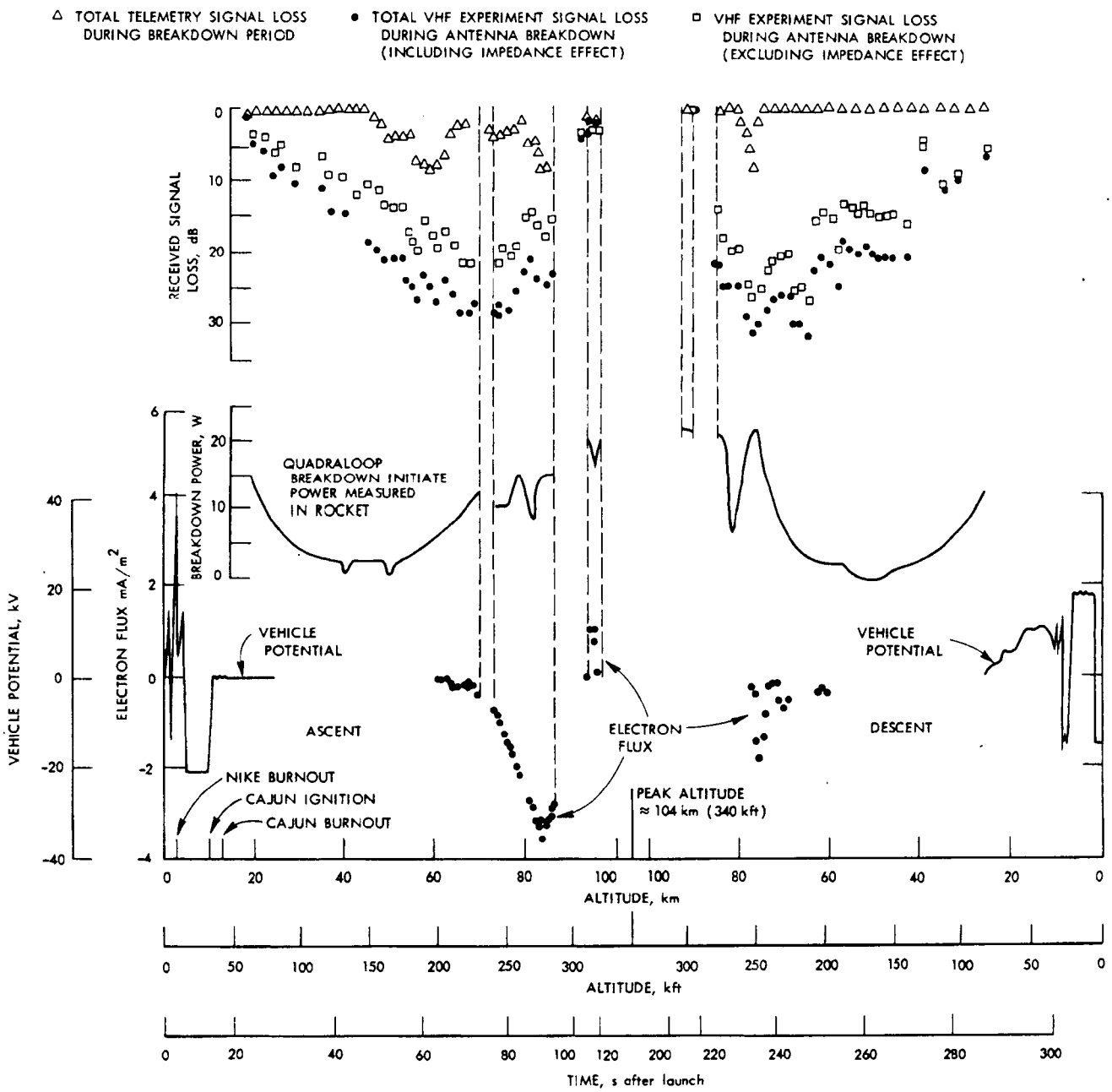

Fig. 9. Correlation between data from various experiments

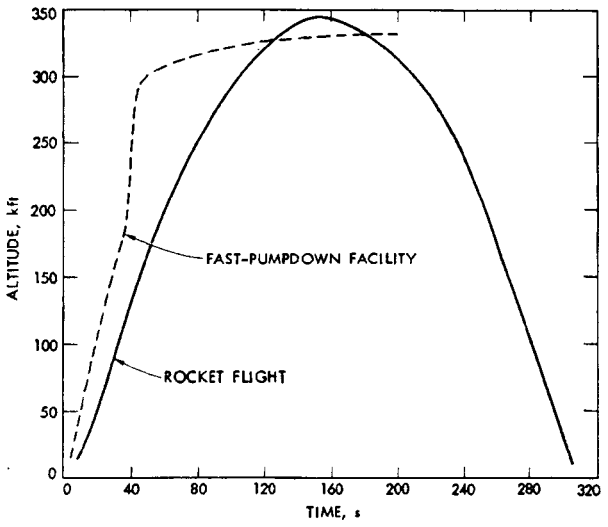

Fig. 10. Altitude-time profile obtained in fast-pumpdown facility compared to rocket-flight profile

A small bell jar was secured and the quadraloop antenna was placed in it, on a cylinder again, and a separate chamber was pumped down, which we opened up and dragged the vacuum down in a hurry. Then we turned on the already-hot diffusion pump in the bell jar and sucked it down the rest of the way.

The top of the curve is very flat because our bell jar is outgassing to the wall so fast that we can't pull down our vacuum, but we are able to simulate at least the rapidity of the rocket flight.

We turned on our quadraloop antenna, again pulsing at once per second with an approximately sinusoidal wave and we decided to see what was happening. We were shocked because results were obtained that completely disagreed with our original multipactor tests run under static conditions.

Rather than go into complete detail, I will explain what is happening. In Fig. 11 the number of cycles represents the time from when our power was turned down. This particular figure was taken when we had pumped the thing down to 1 micron pressure, equivalent of 300 kft; we let it sit for 60 s. This is not exactly a fast pumpdown but we got the same or worse results on the fast pumpdown test.

When we first turned on the power, we found we were getting what we call quasi-gas breakdown. Figure 11 represents the incident power, the reflected power, and a photomultiplier trace. When breakdown occurred, we had adjusted the photomultiplier so that it saturated during gas discharge but was unsaturated and down at a very low level for multipacting.

We turned on our power at the equivalent of an ambient altitude of 300 kft, and we got what looked like a very high reflected power. The scales are not the same. This is about 2.3 W of reflected power for about 22 W incident power, whereas our normal reflected power was down quite low. We had a VSWR of only about 1½. The multipactor was driving gas off the surfaces of the antenna and the nearby cylinder, and we went into a gas discharge.

We saw this thing happen for a variable number of cycles on a typical run. We tried clean surfaces and we tried dirty surfaces. Dirty surfaces which we had deliberately contaminated, for example, with finger oils or salt spray, because we were trying to duplicate conditions that might be prevalent at Wallops Island where the flight occurred, gave us quasi-gas breakdown cycles as long as 77 in number for over a minute. Now, a minute represents a significant portion of our high-altitude profile, since the entire flight takes place in only about five min, so if you have contaminated surfaces, they can cause a lot of damage.

Eventually, however, we began to clean enough gas off the surface so that it didn't continuously give the saturation and the sort of things I call "transition cycles."

Cycle 8 in Fig. 11 is a transition cycle in which we began to see reflected power; breakdown suddenly

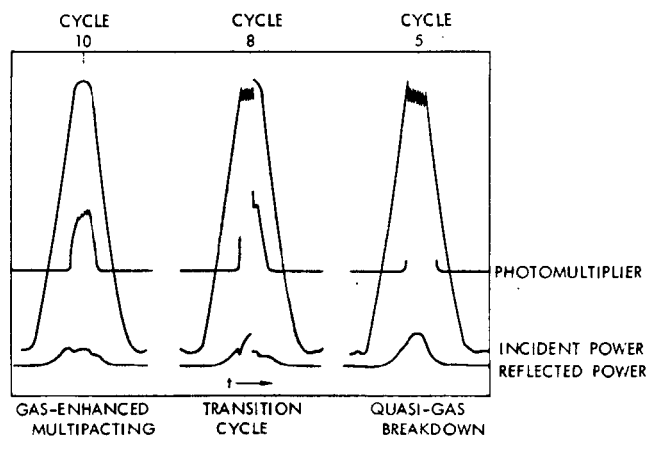

Fig. 11. Modulation cycles during gas-augmented multipactor design

occurred in a gas discharge as shown by saturation of the photomultiplier trace.

We stayed up near the peak of the power cycle, and suddenly it seemed that all the gas was cleaned off and the power dropped abruptly. The photomultiplier trace came back to a relatively low level, reflected power dropped, and the incident power shot up; i.e., we weren't absorbing as much. At this point we got out of the quasi-gas breakdown and went into what we think is straight multipacting. We examined this visually, and recorded the events on motion picture film; you can see these happening during the cycle.

After a variable number of these cycles, again depending on the surface condition, a partially gas-enhanced multipacting takes place. Some photomultiplier output can be seen, but not as low as it eventually will become if you continue to run this thing until a pure multipactor develops where the level of the photomultiplier signal is down low, monitoring light output. Some effects can be seen on the reflected power which tend to be a saturation; i.e., you suddenly move off the plateau here when multipacting stops and you drop down on the smooth, normal reflected power condition.

We carefully examined the flight test records, and were able to establish that all sorts of behavior were obtained during the flight test records. Sometimes, in the laboratory tests, we would start off multipacting on one of these transition cycles and then suddenly go into a gas discharge, so that reversal took place. We saw those things on the flight test record as well. This and some other internal evidence told us we were pretty sure we were getting gas effects in the multipacting at high altitudes.

I will summarize by saying that here was an instance in which two unexpected results were obtained from the flight tests: one, an aerodynamic result which wasn't duplicated in our original laboratory test, and the other was an outgassing result which wasn't duplicated in our original laboratory tests for multipacting. Both results, had we more carefully considered them, might have resulted in our anticipating them and taken them into consideration in our laboratory records.

As it was, the first laboratory test provided results which didn't turn up in flight. The second laboratory test showed us that at least the multipacting could have been anticipated from outgassing going on in the initial multipacting cycles. An analysis of shock theory showed us we could expect some reduction in local gas density and a change in breakdown thresholds.

I think one needs both laboratory tests and flight test records to check each other and to make sure one isn't missing anything.

Discussion

Question: How did you measure the low electron density in your simulated plasma?

August: Langmuir probes.

Question: Did you state that you had 10^4 to 10^6 electrons cm^{-3}?

August: As best we could determine, we had 10^4 to about 10^5.

Question: Do you believe your probe measurements?

August: Yes, I believe our probe measurements. We have some probe experts at SRI too, and we checked this in a variety of ways and with a number of different-sized probes of varying axial parameters; i.e., length-to-diameter ratio. Furthermore, I recently have also been using a flat Langmuir probe guard ring. These things are very hard to measure at these low electron densities, as any of you who have tried know.

Incidentally, our electron temperatures were about 4 or 5 eV. They aren't typical of the ionosphere, but if you are just worried about multipactor, if you are just worried about breakdown due to ambipolar diffusion, they suffice for giving you the appropriate number of electrons. They don't take care of the sheaths.

N70-32290

Development of Packaging Techniques for an Amplitron and Power Supply

P. Felsenthal
Arthur D. Little, Inc.
Cambridge, Mass.

D. Grieco and J. Fridman
Raytheon Space and Information Systems Div.
Sudbury, Mass.

I would like to outline the topics that we will cover, and then get into the details. I will explain the equipment function, give some of the details of the old construction and the failures that occurred with it; then get into some of the nitty-gritty of the new construction, including detailing heat sink parts, potting techniques, and module testing. That leads into some of the details on ignition experiments on which Jonathan Fridman will report. Finally we will provide a brief rundown on testing of tubes and wires and one of the microwave components, and then try and step back and give some sort of philosophical summary of what we think the generalities are that come out of the work performed.

The equipment is shown in Fig. 1. It is a dc to dc converter and redundant amplitron system. Along the mounting flange the system is symmetrical, so that on the bottom of the system there is another amplitron and another high-voltage power supply.

The 10-kHz low-voltage power supply that drives the high-voltage power supply is outside of the case.

We will be concerned with examining the potting techniques of this high-voltage module, and in examining, briefly, the testing of the amplitron tube and some of the RF problems in the microwave circulator.

The power supply, incidentally, gives anything from 1700 to 2500 V at 30 mA. The amplitron delivers around 24 W at 2.2 GHz. The amplitron takes three-quarters of a W drive to start it; it has no modulation provisions; the modulation occurs on the input signal. The old potting is shown in Fig. 1. It was a rigid potting, and the original specifications were that the unit would operate from room pressure to very low pressures, on the order of 10^{-6} torr; testing occurred at room and at low pressures. However, as people began to detail some of the actual flight configurations of the vehicle, they found

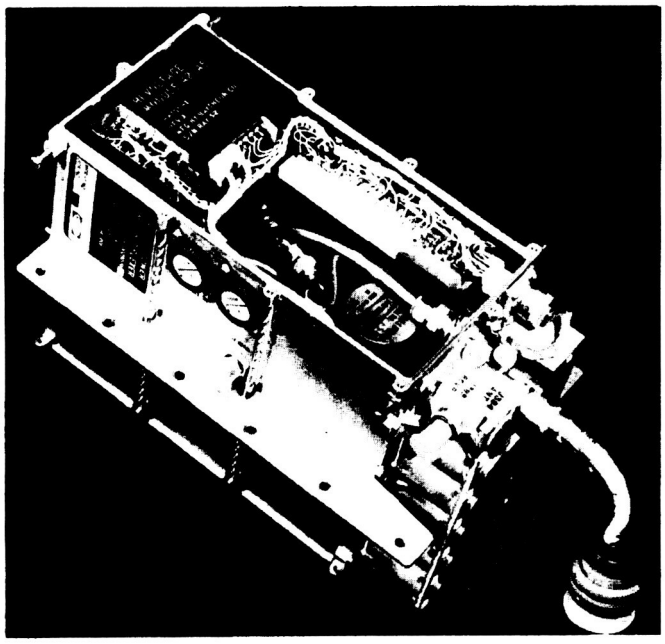

Fig. 1. S-band power amplitron and diplexer

that you may very well operate in the critical pressure region. Tests were run with the unit in the critical pressure region, therefore, and a number of failures occurred.

It looked as though the failures occurred because of poor adhesion of the components to the potting compound and because of problems with differential temperature coefficients of expansion. Operating temperature range or ranges are quite reasonable, 25 to 165 ° F, but storage temperature ranges are much more extreme. A quick fix was tried, putting on a thin layer of epoxy material over the module; this also failed. Therefore, about 1-½ yr ago a program was initiated to redesign the high-voltage module; at the same time, the program was initiated to design a pressurized case, taking the same envelope and seal configuration and making a sealed unit. We were involved in the redesign of the high-voltage module as well as some of the other parts.

The physical configuration of the high-voltage supply is shown in Fig. 2. As can be seen, it is of cordwood construction with a fairly high density of parts. The white is the heat sink. It is a magnesium heat sink, and the original heat sink had a Dow 17 coating on it that was in the order of 0.0002–0.0004 in. thick and provided no particular insulation quality.

We made certain that the heat sink was properly tumbled, that all sharp edges were removed, and that another insulating coating was sprayed over top the Dow 17 coating. This was a urethane coating which was 6 to 8 mils thick. The urethane coating was examined with a test probe on the outside surfaces. The probe was run at about 3 kV and about 1.5 kV on the outside surfaces (just to prove the integrity of the coating).

We originally started out with a clear coating, but found it was a little easier to check whether there were problems in the coating if we colored it; so you see in Fig. 2, a white urethane covered heat sink. In placing components into the heat sink, we tried to do it in such a way that, for instance, the ends of the resistors were not flush with the heat sink walls, thus providing straight field lines between the axial resistor lead and the grounded heat sink.

We also tried to be careful in the staking of the components in the heat sink before potting. The staking compound was put in the middle of the hole so there would be a minimum of entrapped gases. During the potting process, the compound had a chance to permeate the holes as much as possible.

A different view with a different-colored urethane coating is shown in Fig. 3. It does show the point-to-point

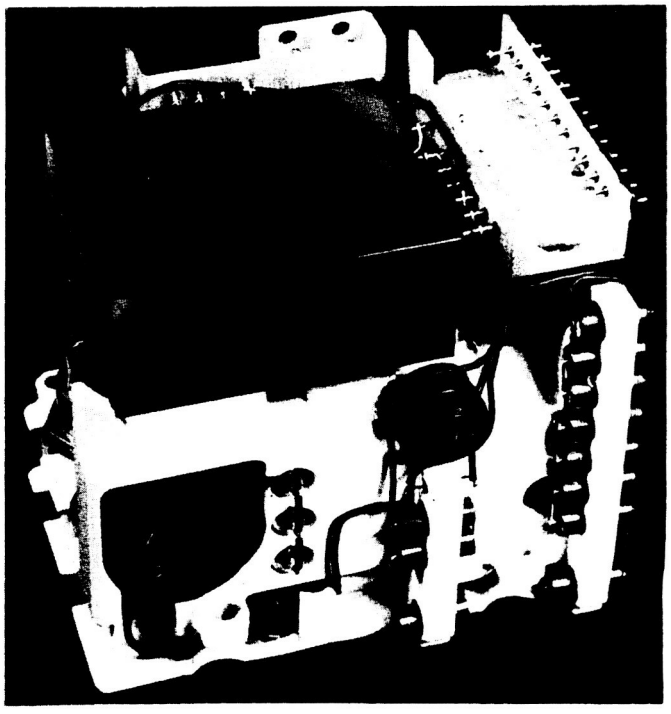

Fig. 2. High-voltage supply

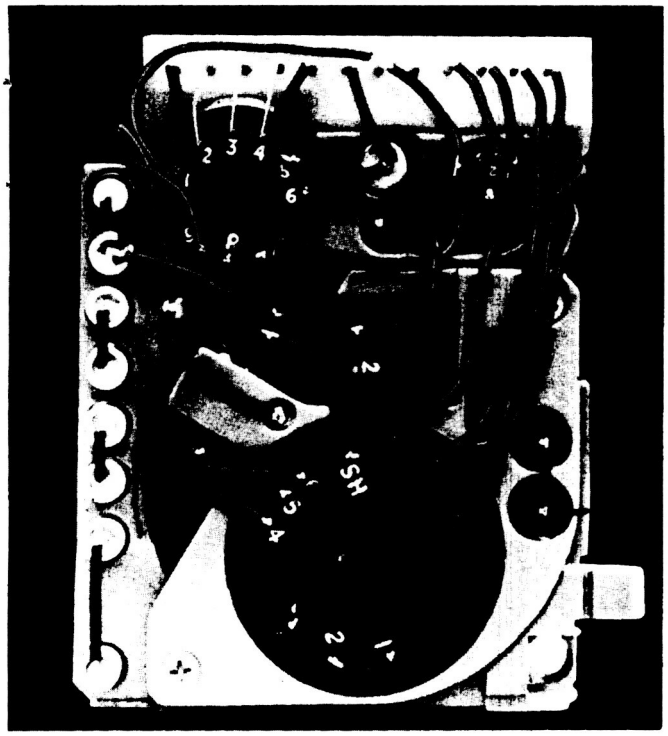

Fig. 3. Point-to-point wiring in high-voltage supply

wiring involved. We used welded wiring with shrink tubing on it.

Components originally used for this unit were not corona-tested; however, after experiencing a resistor failure, which we found was due to a potted void in the resistor, and experiencing one magnetic component failure, we went to corona testing of all the components that make up the power supply.

Our criterion for rejection of components, except for one component, the solid-state rectifier bridge, was that any corona was suspicious. It was established that any corona at operating voltage was criteria for rejection, so we ended up with having at least 60-Hz corona-free components in the unit. We found that we could not believe manufacturers' specifications as to whether components were corona-free; even though the magnetics were bought with a corona specification. We found a fair percentage that did fail.

Corona testing, on the small components and larger ones, was simply accomplished by wrapping a ground plane around the component, either in the form of a sheet or a wire, and immersing the component in a Freon bath. The solid state rectifier ended up at operating voltage having corona on the order of 20 to 30 pC.

We examined this with the manufacturer and reviewed his manufacturing techniques. He claimed it was due to avalanche noise in the rectifiers. We were never completely convinced that this was the case, however. It was a pressure-molded case that was well immersed in the potting compound in the final configuration, and we let it go.

The potting compound for the high voltage supply, as shown in Fig. 4, was very carefully chosen to avoid what we surmised were the problems in the previous units, viz., the fact that the potting compound was inflexible and there was differential shrinkage between the components. Hairline cracks occurred and breakdown could occur in the critical region. We chose a polyurethane compound that had many of the characteristics we wanted but many disadvantages.

The compound was flexible; it adhered to all the surfaces involved in our particular unit, had a relatively high tensile strength, and provided all the mechanical and shock endurance we wanted. However, it did have

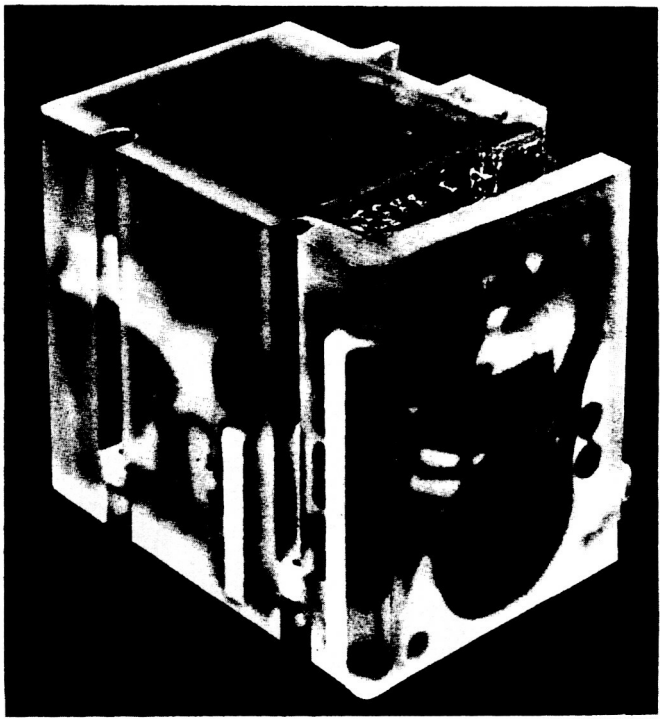

Fig. 4. Potting compound for high-voltage supply

a high dielectric constant. It was very difficult to pot, and was subject to moisture absorption.

Volume resistivities went down two or three orders of magnitude with moisture absorption. Actually, we didn't feel this was such a disadvantage because it could supply at least a little more uniform voltage gradient in the compound. The fact that the compound is transparent worked both for us and against us. It allowed us to see where we were having problems in potting and where there were large void areas; on the other hand, it allowed all the quality control inspectors to spot any void and take appropriate action.

The potting procedures and cleaning up the units for potting turned out to be very elaborate, and I can't really emphasize how important it turned out in our units to get successful potting, to go into the manufacturing operation and come down very hard on all the items of cleanliness. For instance, we couldn't store parts in polyethylene bags after a certain portion of the cleaning cycle because the bags contained an agent which, although approved by the FDA, didn't help the polyurethane to adhere to the components. Likewise, we found that, although vapor degreasing was being used, the units were being taken out of the liquid side of the vapor degreaser rather than out of the vapor side. Thus, any advantages of vapor degreasing were minimized.

We also found that we had to enforce a schedule for changing the solution in the vapor degreaser. The potting chamber is a two-stage type, and you can control the pressure in the mixing bath and the pouring bath separately. We put the unit in and baked it at its highest temperature for 6 h ahead of time at 10^{-6} torr. We then brought the pressure back up to the level at which we had to pour (which was about 3 torr). Great care was exercised in the mixing cycle.

If we were more than three min off in timing the pour from the beginning of the mixing, we ended up with poor castings. The unit was poured at about 3 torr, then pressurized with filtered clean nitrogen and allowed to cure for six h in the chamber at atmospheric pressure.

With all these cautions, we eventually were able to produce consistently good units. Module testing was accomplished in two stages. We would make operational tests on the module in the prepot condition, and we also arranged our circuits so we could make corona tests on the module in the prepot condition, too.

Then we would pot the module, make a corona check, and operational test, before a 100-h thermal vacuum test. Thermal vacuum testing consisted of many different cycles, but, in essence, you go from room pressure to 10^{-3}, going slowly through the critical range.

We also had two modules which showed high corona, e.g., on the order of 1500 pC, which we ran for 1000 h through this sort of a cycling in and out; no failures occurred.

It was found that although we put in to the potting unit a module with corona-free components, after potting we would have corona on the module. Our assumption was that the corona came from the wire and shrink tubing, and we ran separate tests on the wire and showed this, indeed, was the case.

The corona, due to the wire, seemed to decrease as a function of time, either during operation or while sitting on the shelf. In looking at this corona source, we examined a great many different shrink tubings and methods of coating the wire in order to get rid of the corona problems. We ended up where we started, i.e., with the polyolefin-shrink tubing being the one which provided minimum corona.

The bare wire, of course, provided even lower corona, but, because we had to run an operational test before potting, we were not able to use the bare wire because of lead dressing.

During module testing, we noticed exterior glows in a number of areas. In some of these areas we were able to put on corona shields, that is to say, ground planes within the potting, that prevented the glow.

In other cases we were not able to do this, and we ended up with glows in the critical region on the outside of the module.

It was observed that certain sections of the high-voltage power supply, even though improved by replacement of the potting material, insulation of the heat sink, etc. still indicated a consistent glow at critical pressures around certain sections.

We wanted to make very sure that none of this corona, or glow—we didn't know which it was at that time—could in any way create a hazard to the materials that were being used in the construction of the high-voltage

power supply. We wanted to establish limits to determine the conditions at which any of these materials may ignite.

There is little, if any, technical literature available or work that has been performed on the effects that low-pressure gaseous discharges have on the ignition levels of various materials and combustible gas mixtures.

Data on the degeneration of materials, such as dielectrics, epoxy resins, various plastics, and electronic circuit components (for conditions when these particular substances are exposed to corona and glow discharges or more intense arcs) aren't available.

The only data available are data on the ignition points of dust clouds and explosives; these, in turn, are usually subject to microsecond or nanosecond interval ignition spark discharges. There are no data available on the ignition points of different materials at low pressures. In order to tackle this problem, we decided to simulate, as best we could, the corona levels observed on the equipment. Measurements were made and a corona level of about 60 μJ was observed in critical spots on the high-voltage power supply. With this in mind, we simulated the physical situation with a very simple experiment.

Figures 5 and 6 illustrate the experiment that was devised.

In Fig. 5 we have a gas discharge bottle 8-in. long and 3-in. in diam with two copper electrodes, 3 mm in diam, sharpened to a point. We evacuated this bottle down to 1 torr to make corona glow discharge, abnormal glow discharge, and arc discharge measurements between these two points. A point discharge was used because the electric field being nonuniform, we are able to obtain breakdown points at lower potential and thus one can contain a glow discharge or an arc discharge with better stability.

After establishing the current voltage relationships at which these different types of discharges take place—and I will come to that later, we suspended materials between the electrodes to observe, in time, the physical history of these materials.

As shown in Fig. 6, the discharge was subject to a frequency of 10 kHz because this was the operating frequency of the high-voltage power supply, and transformed up to 3,000 V. Measurements of the current and

Fig. 5. Gas-discharge bottle

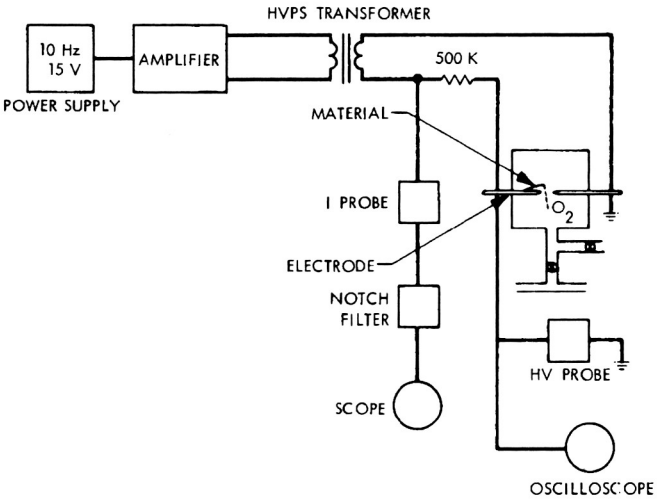

Fig. 6. Schematic for ac oxygen gas-discharge measurements

voltage at the electrodes were made. In addition to that, we also made some corona measurements by means of this circuit. We eliminated the 10 kHz excitation frequency with a notch filter to observe the high-frequency corona components that may be in the gas discharge.

By making measurements of the current and the voltage across the discharge and plotting these, we then correlated what we observed visually with the effects that these had on the materials.

A theoretical curve of the discharge characteristic common to all discharges is shown in Fig. 7. Here we are plotting current versus voltage in a dc discharge.

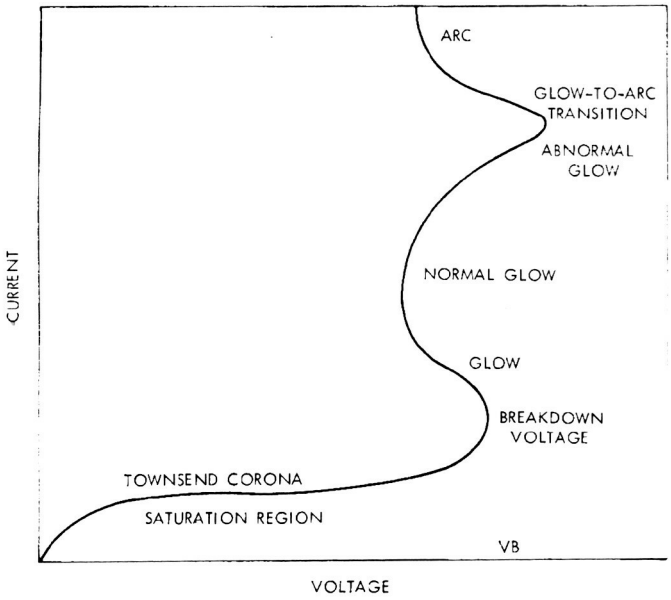

Fig. 7. Discharge characteristics

What happens is that at first, between any two points as you increase the voltage, there are going to be a certain amount of electrons generated in the electric field. The electron current is going to increase, and finally it will saturate when the regular production of electrons is equal to the losses suffered. Hence, the rate at which the discharge is increased is a function of the mobility of the electrons and the recombination or attachment processes prevalent.

At a certain point, and this is when a glow usually is first observed one usually obtains a corona with a non-uniform electric field. At a certain point, any increase of voltage will suddenly create a breakdown, and one begins to observe the glow around the electrodes. As one goes beyond this point, the voltage drops back and the current increases. As a result, depending on the pressure regions examined, a very vivid glow is obtained. As one increases the current, at a constant voltage, a normal glow prevails and the entire structure then begins to glow.

Beyond that, once again a reversal takes place wherein an additional increase of voltage will trigger a much higher increase in the current. A transition from a glow to an arc discharge then prevails. The characteristic of the arc is that its breakdown voltage is less than the breakdown voltage for the normal glow.

This phenomenon, in terms of the measurements, is shown in Figs. 8 and 9.

In Fig. 8 you can see the two electrodes within the discharge bottle. Three pictures just correlating the dis-

(a) FAINT GLOW DISCHARGE AT 1 torr O_2 PRESSURE

(b) GLOW DISCHARGE AT 1 torr O_2 PRESSURE

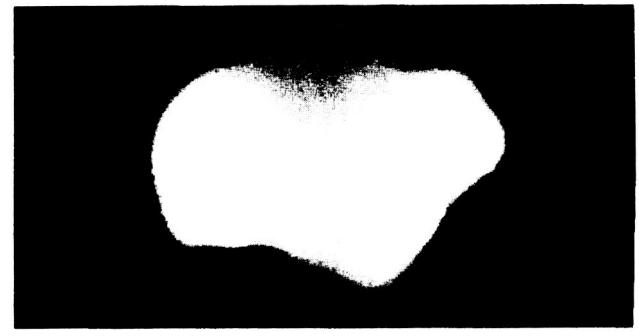

(c) ARC DISCHARGE AT 100 torr O_2 PRESSURE

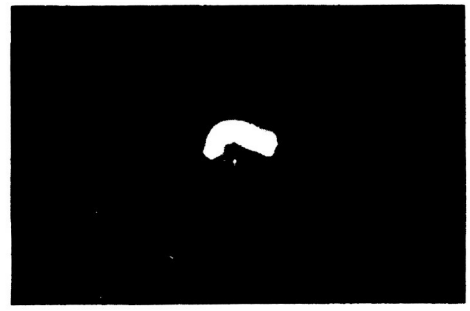

Fig. 8. Arc-discharge characteristics

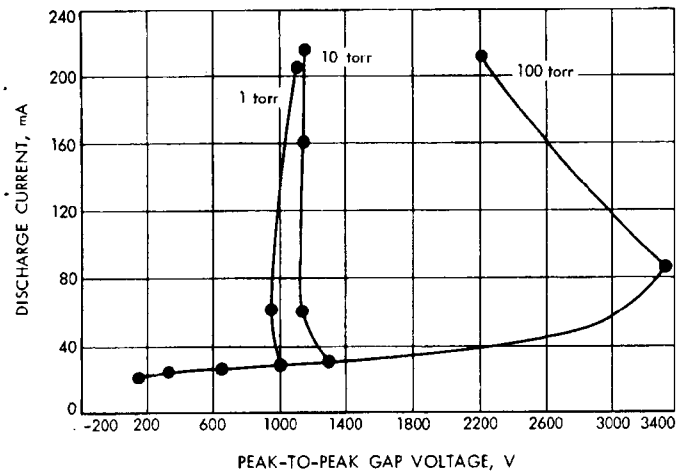

Fig. 9. Oxygen-discharge characteristics for 6-mm gap

charge characteristics to the actual measurements of the current and voltage plotted in Fig. 9 follow. Figure 8(a) was taken at 1 torr line, and we observed a glow at this very point.

In Fig. 8(b) was also made at 1 torr. In each of these cases, the discharge is in pure oxygen in order to ignite these materials with high reliability. This picture corresponds to a condition somewhere along the 1 torr plot in Fig. 9. Limitations in our circuitry did not permit measurement of the current and voltage corresponding to an arc discharge; however, Fig. 8(c), which is a very clear arc jumping across the two electrodes, corresponds to a current-voltage point on the 100 torr line.

The above operating conditions were established and different samples of materials were suspended in between the electrodes to observe them on a time and material basis; however, one great limitation in all of this was the lack of data on the ignition points of these materials. In order to acquire the ignition-point data of test materials, such as for polyurethane, lens paper, chunks of wood, and steel wool, we performed other experiments. Figure 10 shows the setup. A sample of the material was placed in an oven evacuated down to a pressure of 1 torr in pure oxygen, and heated to observe the ignition point electronically by means of a thermocouple instrumentation and visually.

These tests generated Table 1 which is a tabulation of ignition levels of material samples in oxygen for lens paper, gauze paper, wood, the polyurethane used in the construction, and steel wool in oxygen at different pressures.

In every case, as the pressure went down, as was to be expected, the ignition point of lens paper and wood went up. Now, for the critical case of the polyurethane, we never observed burning. What we observed was that at 760 torr the material did ignite (very, very dramatically), but at any other pressure it would first transform itself into a liquid state from a solid state and then carbonize, never really igniting.

The ignitability of these materials in actual measurements can be seen in Figs. 11 and 12.

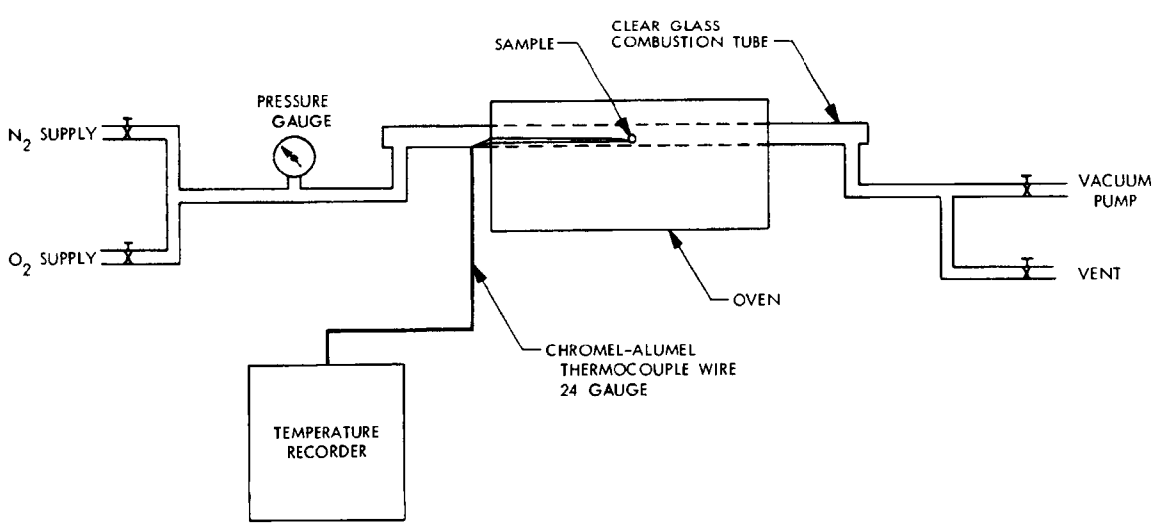

Fig. 10. Combustion test for ignition temperature measurements

Table 1. Ignition levels of material samples in oxygen

Atmosphere	Pressure, torr	Lens paper, °F	Gauze paper, °F	Wood, °F	Polyurethane PRC-1538, °F	Steel wool
O_2	760	548-635	593-622	573-593	678-793	[a]
O_2	500	592-635	630-643	660	[b]	[a]
O_2	100	678-699	746	729-797	[b]	[a]
O_2	50	708-831	770	868-872	[b]	[a]
O_2	10	846	[b]	[b]	[b]	[a]
O_2	2.5	[b]	[b]	[b]	[b]	[a]
Air	760	703-707	662-668	777-801	885-889	[a]

[a]Samples oxidize completely before ignition temperature is reached.
[b]Samples do not ignite, but oxidize and carbonize.

(a) PAPER SAMPLE IN LOW INTENSITY 1 torr O_2 GLOW DISCHARGE

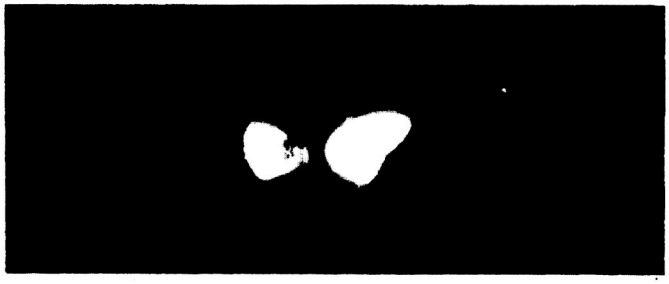

(b) PAPER SAMPLE BURNING IN O_2 AFTER BEING HIT BY ARC AT 100 torr

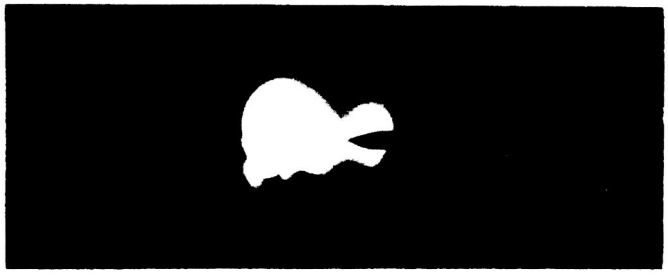

Fig. 11. Ignition of a paper sample

(a) POLYURETHANE PRC-1538 SAMPLE IN GLOW FIELD AT 1 torr O_2 PRESSURE

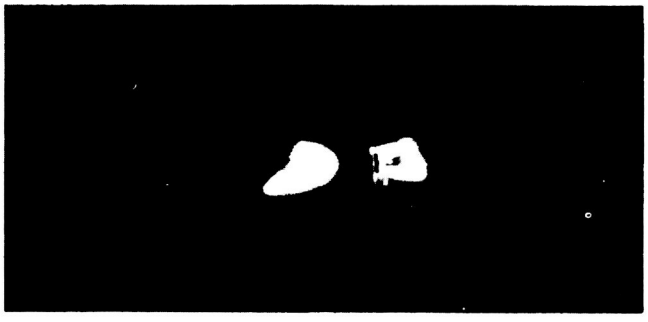

(b) POLYURETHANE PRC-1538 SAMPLE IN BRIGHT GLOW AT 2.5 torr O_2 PRESSURE

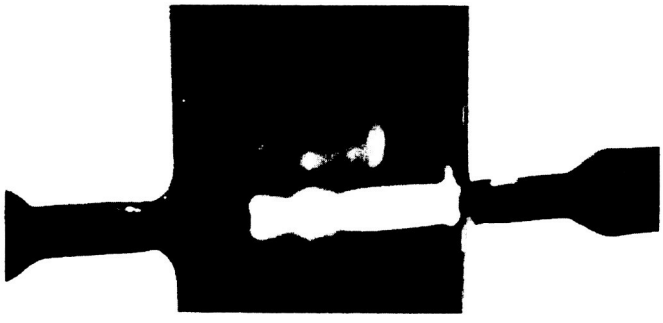

(c) POLYURETHANE PRC-1538 SAMPLE IN ABNORMAL GLOW DISCHARGE AT 50 torr O_2 PRESSURE

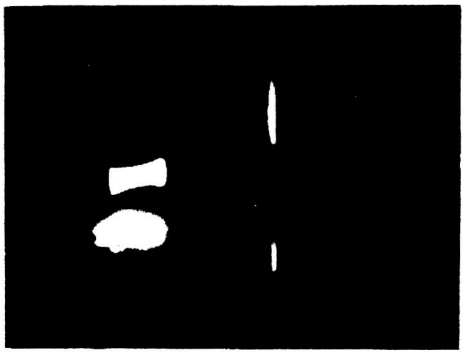

Fig. 12. Glow discharge of polyurethane

Figure 11 shows a paper sample in a 1 torr oxygen glow discharge left in that state for 8 or 9 h; it never burned. This is evidence that the glow discharge does not have sufficient energy to burn the paper. The paper ignited dramatically when struck with an arc at 100 torr. We couldn't get arcs below that point.

In the case of the polyurethane, shown in Fig. 12, the same events at 1 torr oxygen pressure occurred; i.e., no destructive effects were noticed. When the polyurethane was subjected to a 2-½-torr discharge environment, and this is the critical pressure within the high-voltage power supply module, nothing happened to it, either. No evidence of any degradation of the material or loss of its properties was observed when left in such a state for many hours.

When it was placed in an abnormal glow discharge, pretty close to an arc—the polyurethane began to transform itself, and, as you can see in Fig. 12, a bead had formed; i.e., the substance has transformed itself into a liquid state. In a way, this assured us that in no way could the glow discharge levels of 60 μJ, observed in the high-voltage power supply, expose the material to any dangerous situation.

We determined from several measurements and from the specific heats that it takes about 2J of energy to ignite the paper. These measurements correlate very well with some work that has been done at A. D. Little Inc. in measuring the ignition levels of wool and cloth subject to spark discharges. Thus, our value is 5J; their value is 2J; we're in the same ball park. It takes 1J to ignite the polyurethane. Since the levels of corona observed in the high-voltage power supply were 60 μJ, essentially we have a factor of safety of 16,000. This reassured us that there was no physical danger in any way to the components and to the materials used in the high-voltage power supply that may create any undesirable hazard.

I would like to discuss, briefly, the tube and wire testing, and one of the microwave components.

These two components illustrate the situation that you can get into if you manufacture components without full specifications firmly in mind and aren't aware of what it is you are going to face in terms of testing and operation of the equipment.

Figure 13 is an illustration of the amplitron tube. Silicone-covered wires come out and go to a potted-in connection on the high-voltage power supply, discussed earlier. In the tube, the wire goes through a foamed area into a potted pin, which then leads directly into the vacuum envelope.

Fig. 13. Amplitron tube

During testing of complete amplifier units, we experienced two failures in the tubes. We attributed these failures as follows: (1) to a mechanical problem between a wire and some of the mounting screws, and (2) to a void in the potting. In looking over the tube-manufacturing procedures, it was realized that the tubes were not evacuated during potting and pouring, and that there was a possibility of voids occurring in the potting of the tube where the high-voltage stud goes through the vacuum seal.

In order to get some idea of the probabilities of this void giving us problems in the critical region, we tested 16 tubes and wires for a period of 300 h at critical pressure, cycling in and out of critical pressure, or running the tubes for about 100 h. We experienced no failures, but we certainly did measure corona under these circumstances, and I mean dc corona.

There were separate measurements with the wire running about 1,000 h, that indicated no degradation of the wire under these conditions, but it is still a little suspicious.

The second problem we experienced was within one of the module tests. We had problems with a 2.2 GHz microwave circulator. After going to the supplier and subsequent inspection, we found that his circulators were fine as far as microwave specifications are concerned. They had not considered breakdown at all, however. This was because they had never had problems with high voltage and had never worked in the critical region. We took some of the units apart and looked at the manufacturing procedures. We think we have this problem straightened out now, but, again, it is another illustration of the fact that you have to look very carefully at the specifications of the unit and design accordingly.

Finally, I would like to step back a minute and see if we can draw any generalities from the work that we have done.

The first thing that occurs is that in commercial applications such problems would not have occurred. If breakdown takes place on commercial equipment you simply make it larger and put in a lot of oil or grease; you determine some inexpensive solution, and you don't have to go to the expense that we have to go to with a piece of flight hardware to make it work because we have firm constraints in terms of envelope, space, and weight.

The second point is that we redesigned the potting and the high-voltage power supply from a mechanical point of view to prevent breakdown. We cannot operate this power supply over a certain rated voltage because of some of the component characteristics; therefore, we don't know how far we have gone to overdesign the high-voltage protection system.

Normally, you like to trade off overdesign versus cost. In this case, however, we don't know where the trade-off lies. We may have designed an insulation system for 7,000 V; we may have designed it for 2,600 V; but, this, again, is one of the penalties you pay in flight hardware.

The third point: The first speaker spoke about a very rational engineering procedure in the designing of equipment. This is fine, if you are aware of the problems ahead of time you can do this. You can go through the prototype testing and construction, but often you can't do this. You find you have a delivery schedule for a piece of hardware that is supposed to fly in July and you must have the parts in March. Suddenly you have found a problem, so you are often working under schedule constraints that force fixes and engineering solutions that are not optimum and are certainly not the least costly.

A questioner of the first speaker asked if he had defined *E* over *P*, *PD* products, and I assume the appropriate parameters for microwave breakdown in terms of what things produced breakdown. Well, in my opinion, in our situation and some of the others I have seen, although we may be able to put an order of magnitude on these things and relate them to experiments in axisymmetric cases or uniform field cases, theory only puts us in the ball park. When you are talking about arbitrary shapes, manufacturing tolerances, and all the rest, it is really applied technology, and science helps but does not provide the final answer.

Finally, one fairly obvious point in breakdown situations: If you have a unit that doesn't work; what breaks down is the weakest link. If you adjust that, then the next weakest link goes. Therefore, you must be very careful when you look at the design problem so that you are not just trying to fix the weakest link. You have got to look at the whole system.

Discussion

Scannapieco: Can you tell me what the other insulations you looked at were; and were any of them Teflon?

Felsenthal: For the wire, yes, we did look at Teflon and we looked at polyimide insulations. The ones that we could get were wire-wrapped, not extruded installations, ended up with gas spaces next to the wire; these gas voids are then trapped in the potting compound and they light up under our corona test. We found that the shrink tubing, if you were very careful about it, gave us the minimum voids. You put the heat gun in at the center of the wire and then work out.

We took one module which had been carelessly constructed, and it showed one corona level, like 300pC, and we went back at it and went at the wiring with a heat gun and reduced the corona level to 60pC.

Scannapieco: Were any other shrink tubings looked at?

Felsenthal: Yes, they were. I have a detailed paper which I would be glad to show you afterwards.

Yorksie: My first question relates to your actual insulation system capability. I am wondering: couldn't you have tested parts of the system individually, if not in a complete operating assembly, to find out exactly what the capability of your insulating system was?

Felsenthal: They were tested at room pressure. Once you load them in the heat sink, you have a different physical configuration, and, of course, once you put the potting compound on, you have another physical configuration. I don't see how, in our particular geometry (maybe I don't understand your question).

Discussion (contd)

Yorksie: Well, two components in particular, the transformer and the rectifiers, couldn't they have been tested individually?

Felsenthal: Yes, they were tested individually. They met specification at room pressure. I am not sure that we tested them at reduced pressure. We did look at their corona values. We did not have failures with the magnetics or with the solid state components. Our failures mainly involved terminations on the smaller components, on the capacitors, or on the resistors and their relationship to the ground planes of the heat sink.

Yorksie: You talked about the ignition point of your potting system; I was wondering, what consideration did you give to the fact that you may have corona in your system that would cause a gradual deterioration of your potting system in the vicinity of this corona; i.e., not a catastrophic failure initially, or not presenting a fire hazard, but present a long-term degradation problem.

Felsenthal: My assumption has been that if you have corona, you have a long-term degradation problem. Then you want to put a number on how long it takes to degrade to the point that the system is not operational. To do this rigorously requires statistics.

Well, as we all know in space flight hardware, assemblies statistics are difficult to obtain because of expense. We did take two units which had among the highest corona ratings we had. We ran these units for 1,000 h each in critical pressure, measuring the corona values in between, and we found that the corona decreased for the first 500 h and then gradually increased. In no case did it come back up to near the initial level; so, although we know we have degradation due to corona, at least in the power supply itself, we don't feel this limits the life of the over-all system.

Yorksie: Did you do any tests to find out on individual components what the actual corona inception voltage was?

Felsenthal: Yes, it was measured on every component and it was tabulated. Once it was initiated, the voltage was then run down to see whether, if it was once initiated, whether with high-voltage spikes it would still maintain at operating voltage.

York: You said something about considering a pressurized design. Apparently you threw that out?

Felsenthal: No. The fact is that a pressurized design was initiated at the same time that a redesign of the high-voltage module was begun, which was probably the same time you began rework on yours. In March of last year, the pressurized design proved feasible from a mechanical point of view. In January of this year, the pressurized case was again instituted and just this week completed qualification. I assume that in the *LEM* following the one now circling us, if all goes well, it will contain a pressurized case with the components which I have described inside.

York: Does this unit contain an RF filter and is it sealed?

Felsenthal: I believe it did. The dc power has RF filters on it.

York: I meant an S-band filter.

Felsenthal: Well, there are two. It is not a filter. There are two microwave components. One is a circulator and one is a diplexer. One comes to us pressure-sealed with a small percentage of helium so we can check its leak rate. The other is an open strip line configuration, except where the ferrite and the high-dielectric constant material are, and that is not pressure-sealed. It has been presenting problems, but tests presently indicate we have solved those problems in a fairly straightforward manner.

York: Your diplexer, then, you say is sealed?

Felsenthal: Yes.

Stern: What do you call the critical region in which you examine your power supply and components?

Felsenthal: One might pick as criteria the Paschen curves or the microwave breakdown curves, of course, the microwave breakdown curves vary as far as the critical region goes, depending on the frequency, and what have you. We took a very operational approach to it. The area which gave us breakdown and/or corona is at 0.10 to 10 torr. In the case of corona, it seemed to peak very nicely at 0.8 torr. In the case of a microwave breakdown, it seems to depend on what the equivalent PD product is, as to where it is, but it is in the same general region for our dimensions and frequency.

Stern: You mentioned corona testing in Freon. I would like a little further information on that.

Felsenthal: Well, if you take a magnetic component or a resistor and you wrap a wire around it, you have got a lot of air between the component and the current carrying leads. If you run this 60-cycle corona test, you can light up the air around the ground plane that you put on there. If you place it in Freon, you assume that Freon takes up these air spaces and that if anything lights up, it is an entrapped void.

Stern: Was this Freon a liquid Freon or a gas Freon?

Felsenthal: Yes, a liquid Freon; that is, duPont Freon, TF, the ordinary clean room cleaning agent which is, I believe, Freon 113.

Dunbar: I would like to make a comment on the red wire and the white wire, for people interested in this. On that particular test, which we also ran, after 300 h, if you looked at the wire, the white wire had virtually no pin holes; it was clean. The red wire, unfortunately, did have many small holes in it. This was a separate test from the one Mr. Felsenthal is talking about; there were many small holes in it, very small. They were definitely a decomposition of the silicone into silicon and gas with the carbon track into it. At 300 h, it started to lower its corona onset voltage.

Heuser: One comment I would like to make is that even though a corona does not bother your particular piece of equipment, it could very well bother what you are connecting to or the telemetry system of the spacecraft.

Felsenthal: Yes, it could. In our case, since we are generating 24 W of 2.2 GC, our equipment is in an RF sealed box; it meets all sorts of RF sealing requirements. There are RF filters on the dc lines coming in, so we felt any corona in our unit would be isolated from the rest of the system.

PRECEDING PAGE BLANK NOT FILMED.

N70-32291

Development of Electronographic Image Converters for Far-Ultraviolet Space Astronomy Applications

G. R. Carruthers
Naval Research Laboratory
Washington, D.C.

At the Naval Research Laboratory (NRL), we have been developing a series of electronographic image converters for far-ultraviolet stellar spectroscopy and for direct star field imaging in selected far-ultraviolet wavelength ranges.

The principle of operation of the electronographic image converters which we have been developing is illustrated in Fig. 1.

Incoming light from the star field, or whatever is being observed, is brought to a focus by the concave mirror and forms an optical image on a front surface, photocathode, which is an evaporated film of an alkali-halide, salt on a metallic conducting substrate. This photocathode emits electrons under the influence of ultraviolet radiation, which are then accelerated toward the grounded collecting mirror by maintaining the photocathode at a negative high voltage on the order of 20 kV.

The electrons simultaneously are focused by an axial magnetic field produced by the surrounding solenoid or permanent magnet assembly and form an electron image at this plane which is a duplicate of the optical image that was produced on the photocathode. The electron image is then recorded on a nuclear track emulsion.

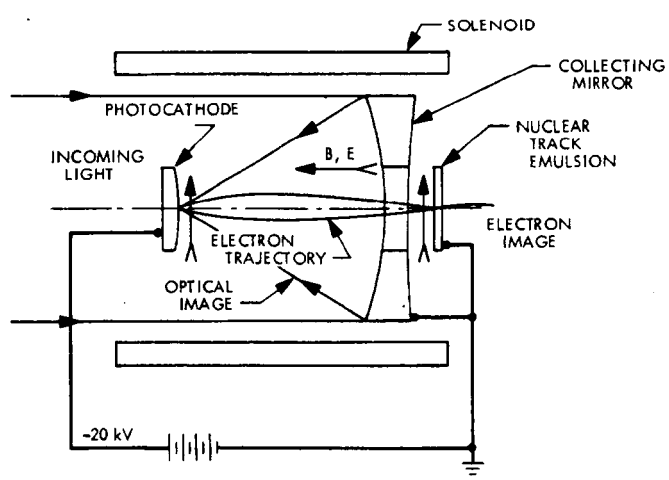

Fig. 1. Operating principle of the electronographic image converter

Due to the fact that these electrons have 20 to 30 kilovolts energy, they are recorded in the nuclear track emulsion with almost 100% efficiency. Each high-energy electron leaves an individual track of developable grains in the emulsion. The quantum efficiency of the photocathodes in the far ultraviolet can be very high, in excess of 50% in wavelengths below 1216 Å. Therefore, the overall efficiency of the system is the product of the photocathode efficiency times the collecting efficiency of the optics.

On the other hand, if one uses even the very fastest photographic films, such as SC 5, these have only about 1—3% efficiency for recording ultraviolet protons directly as developable grains.

Therefore, the speed gain of this system over conventional photography is on the order of 10 to 30, which is quite considerable, especially for sounding rocket flights where you have only a very limited observing time available. When working in the far ultraviolet, one often has to use a windowless type of system because the available window materials have either a very low or zero transmission of ultraviolet radiation in the wavelength ranges of interest; even where window materials can be used, it is impractical to use a sealed-off evacuated-type configuration; e.g., as in the commercially-available image tubes which have a phosphor screen-type output.

Therefore, the devices we have been developing are of open construction and depend on the ambient space environment to provide the high vacuum required for operation. Since accelerating potentials on the order of 20 kV are used, problems of high-voltage breakdown and corona are of prime importance, particularly in the case of sounding rocket flights where only a very limited time is available for pump-down before the instrument is turned on.

Hence, I would like to recount to you some of the problems which we have encountered in the development of these devices and the solutions adopted to overcome them. I would also like to discuss the results of three sounding rocket flights which confirm the feasibility of open construction, electronographic image converters, and which also proved helpful in indicating improvement and modifications that were necessary but which could not be readily indicated by the ordinary laboratory tests.

One of the first things we discovered, the hard way, was the importance of using the proper types of connectors and cable terminations. As many of you have also discovered, a loose wire end with a high voltage on it will produce a corona in a vacuum system, even if the pressure is as low as 10^{-6} mm because of the fact that there is trapped gas between the wire and the insulation which escapes right along the wire and provides a source of gas for corona at the place where the wire is cut off.

Two types of connectors which we have developed and used with very good results in our image converters are shown in Fig. 2. The first one is a cable termination for attaching to our photocathode assemblies. We use Belden cathode ray tube lead in our cables, which is readily available commercially and consists of a center conductor, a plastic insulation, and an outer red plastic jacket.

This wire is rated at 25 kV. We have not had any particular problems with it other than the fact it doesn't take very much heat. We strip the wire, solder it, and then strip the jacket further up and pot the whole thing in epoxy so as to provide a rigid end which will not let any gas escape from either between the wire and the insulation or between the insulation and the jacket. We also take care to smooth off the ends of the lugs and not leave any sharp edges or sharp wire ends which can produce corona problems. We have had very good success with this. For cable connections we came up with the type of assembly, shown in Fig. 2(b), where we use O-rings to seal the wire and prevent any gas from escaping.

Generally, we don't have too much of a problem here because there is either very little gas trapped or else it

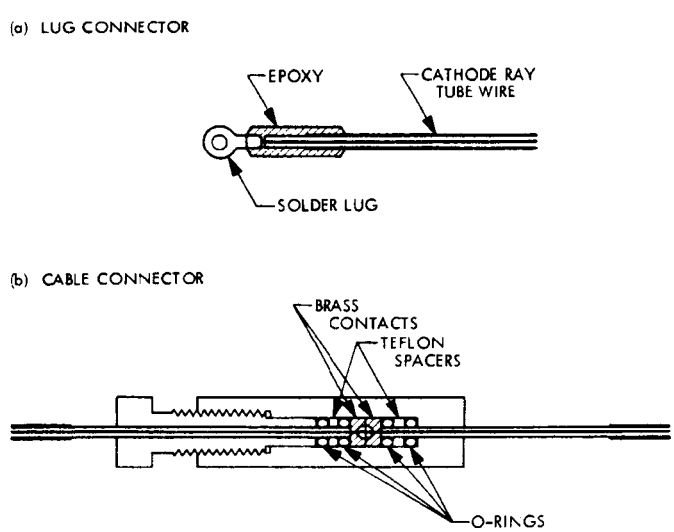

Fig. 2. Image converter connectors

pumps out very quickly. The main thing is to be sure that this part is well sealed.

Another factor of great importance is that the high-voltage electrodes must be kept clean and free of all sharp edges; bits of steel wool, for example, are particularly bad on high-voltage parts.

Here again, the internal parts of the image converter obviously cannot be potted because they have to be exposed to the ultraviolet radiation. Therefore, we have to have a completely open and bare type of electrode structure. Hence, all parts must be scrupulously clean and free of all sharp edges. The nuclear track film is a very sensitive indicator of the presence of corona and will come out black in a few seconds exposure at a corona level which is completely invisible to the dark-adapted eye.

Generally, if all sources of corona are eliminated and there are no sources of positive ions in the vacuum system, there is no stray background on the film, even at gas pressures as high as 2×10^{-4} mm. Above this point, however, things start to become unstable and high-voltage breakdown or glow discharge is produced.

The nuclear track film that we use has Kodak NTB 3, emulsion on a 35-millimeter wide, 4-mil thick ester base. This base has definite advantages over the regular cellulose acetate base films in that the cellulose acetate tends to charge when used in these image converters. When the film does discharge, it leaves black lightning-like streaks all over the images. It also has the secondary disadvantage that it tends to crack on long storage in a vacuum.

In early developmental tests of some of our devices, a very serious problem was encountered in that discharges occurred resulting in total blackening of the film whenever the film was advanced, by our transport mechanism, even when the film had been outgassed in vacuum for many hours. This discharge was, in fact, visible to the dark-adapted eye looking into the front end of the device when the film transport was pulsed. It was felt this was due to a sudden release of water vapor from the emulsion as a result of mechanical flexure of the film. It was found that the discharge could be completely eliminated by placing a grounded grid made of tungsten stocking mesh about one inch ahead of the film plane between the film and the photocathode.

Apparently this creates a field-free region in which the gas released from the film has a chance to expand before it emerges into the region of high axial field strength between the photocathode and the grid. In sounding rocket flights, the time available for evacuation of the instrument is very limited, and, therefore, it is essential to assure elimination of all sources of outgassing and to reduce the amount of evacuation required in flight before one reaches a safe operating pressure. We have made a practice of evacuating our rocket payloads before launch, therefore. The evacuated section is equipped with an O-ring sealed door which is ejected in flight to allow the instruments to view the star fields of interest.

Typically, this occurs about 72 s after launch for an *Aerobee 150* rocket, at which time the ambient pressure is less than about 5 microns. The payload is typically evacuated in the tower to about 10^{-6} mm, and then is closed off and the pump apparatus removed about two h before launch.

During this time, the payload leaks up to typically 20 microns of pressure; however, in laboratory tests in which the diffusion pump was closed off but not removed for this length of time, it was found that the system would pump down to below 10^{-4} mm almost instantly when the gate valve to the diffusion pump was open. Consequently, we felt it was safe to assume that after the door was ejected in flight the pressure within the instrument is essentially equal to the ambient pressure after door ejection.

A problem which is encountered in space applications, which is not generally present in laboratory vacuum systems, is the presence of ionospheric ions and electrons. Positive ions in the ambient ionosphere are attracted by the high negative potential on the photocathode. The positive ion bombardment of the photocathode would result in secondary emission of electrons. This can result in film fogging or even high-voltage breakdown at pressures as low as 10^{-7} mm.

We have discovered this in the laboratory using an ion gauge, for example, as an ion source. Since the positive ion densities in the ionosphere are considerably greater than can be easily produced in the laboratory vacuum system, at least at the present time, it was obviously of great importance to ensure that we had properly designed grids and vents to exclude positive ions from the interior of the instrument.

Due to the complex geometries and field distributions involved, the design of ion repeller grids and baffles is largely by trial and error; however, an order of magnitude estimate of the requirements can be made by treating the device as a triode electron tube in which the grid is used to prevent positive ions from being attracted by the high negative potential photocathode. In other words, this is the cutoff condition in electron tube terminology, and for testing the grid systems in the laboratory we found that the most satisfactory ion source is a plasma jet-type device, shown in Fig. 3.

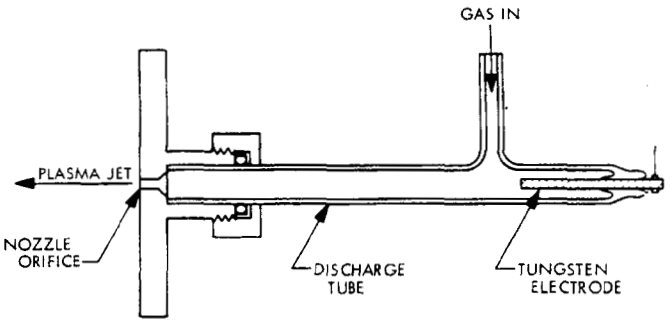

Fig. 3. Plasma jet-type device

In this device, air or another gas of interest leaks into the vacuum system through a glow discharge, one electrode of which is the nozzle by which the ionized gas enters the vacuum system.

We find this device to be more suitable for our purpose than ion gauge-type sources because we have essentially a thermal plasma in our vacuum system, and there is not the abundance of high-energy electrons that one gets from an ion gauge which we have found to give spurious results.

In the case of a triode consisting of infinite plane electrodes, the amplification factor μ and the ratio of plate voltage to the negative of grid voltage, for the cutoff condition, and this is given by the following approximate expression

$$\mu = \frac{-2\pi\, d_{gp}}{a\, ln\, [2 \sin (\pi\, S/2)]}$$

In this equation d_{gp} is the grid-to-plate spacing, a is the spacing between grid wires, and S is the screening factor.

In the grids that we have used, which consist of a commercially available tungsten stocking mesh, the screening factor is 0.05. It is 95% transmitting gauze and the spacing between grid wires is about 0.040 in. Therefore, the amplification factor is about 85 d_{gp}.

We find that the optimum voltage for the ion repeller grid is about 12 V positive relative to the vehicle. If we have a higher voltage than this, electrons can be drawn into the instrument with sufficient energy to ionize the residual gas within the image converter. These ions are, therefore, attracted by the photocathode and can result in a background which increases with increasing positive voltage on the repeller grid. Consequently, if we have 20 kV on our photocathode, and if we approximate it by an infinite plate. Then the grid-to-plate spacing would have to be about 19-½ in. for +12 V on the grid. However, in the actual image converter this plane-parallel approximation is a very poor approximation, as the photocathode does not resemble an infinite plane seen from the grid. We can get by with much less grid-to-plate spacing, and it generally is less than half of this. We find that this arrangement still works quite well using the 95% transmitting tungsten mesh; however, for safety and redundancy we generally use two grids which are spaced by about ¼ in. and use separate sources of voltage. Thus, if one is shorted out accidentally we still have protection by the other.

Figure 4 shows three basic types of instruments based on the electronographic principle shown in Fig. 1. On the left is an instrument using an all-reflecting or Schwartzschild-type optical system which has two mirrors. The photocathode is between the two mirrors with the electrons going up through the secondary mirror to the film transport. The other two types are Schmidt-type systems which are essentially as shown in Fig. 1 but with a corrector plate at the center of curvature of the primary mirror. In the all-reflecting instrument we use a grid to keep out positive ions. In the Schmidt-type systems we use vent baffles, since these have the corrector plate to exclude direct entry of positive ions into the instruments. In the case of baffles, even the grid terminology doesn't apply, and we use trial and error techniques, almost entirely, for designing those.

Our first rocket flight was of an all-reflecting-type system, but it was an earlier version which used a solenoid coil instead of the permanent magnet array, Fig. 4.

The instrument worked very well and a spectrum of a very hot star, Gamma Velorum, in the far ultraviolet is shown in Fig. 5; however, in the center of the field we find an ion spot which was very intense early in the flight

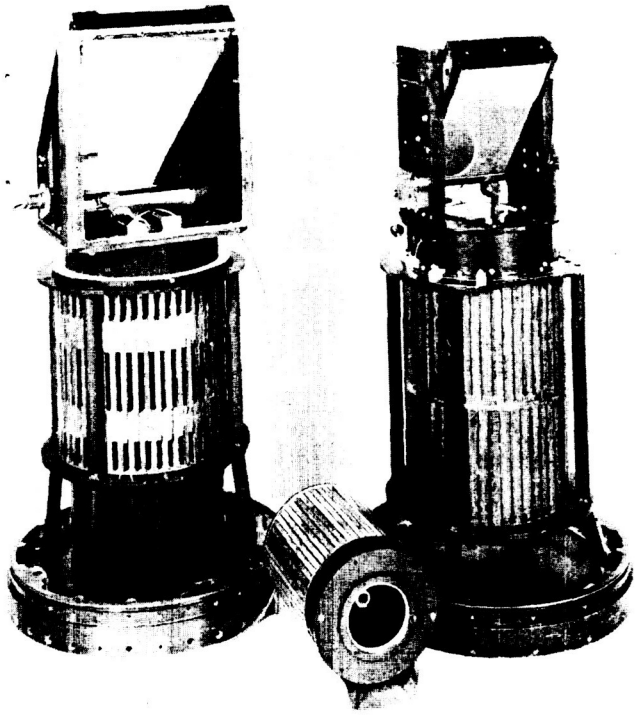

Fig. 4. Basic electronographic instruments

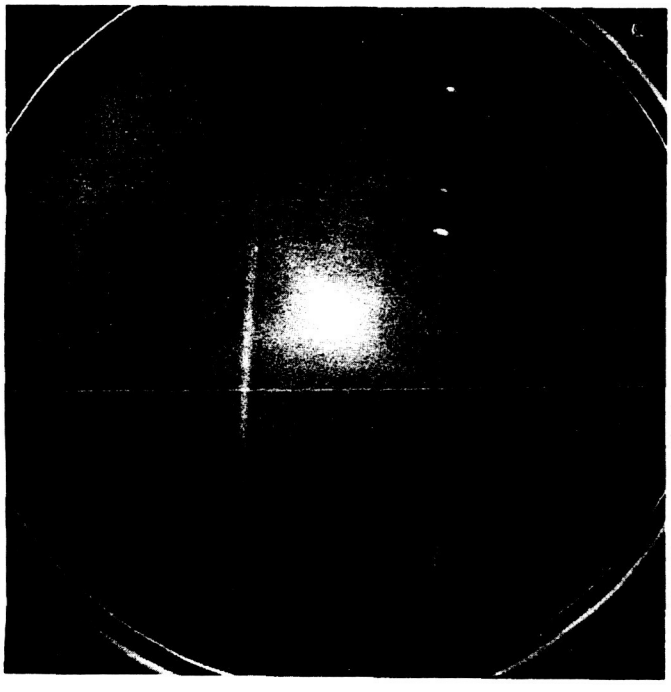

Fig. 5. UV photograph of Gamma Velorum

but gradually decreased and was almost gone at the end of the flight, which was approximately 4 min later.

Since we had evacuated the payload before launch and this ion spot was not present in the laboratory tests we ran just before launch, we assumed this was caused by outgassing of parts of the payload outside of our experiment cylinder. The prime suspect was the nose cone of the rocket which was vented and which contained all of our electronic equipment and wiring.

Another possibility which may have contributed to the ion spot, though it would not cause it by itself, was that this was before we had discovered that if you go above 12 V on the ion grid you actually get an increase in background. We used 28 V on the grid in this particular flight.

Our second flight was of a Schmidt-type system, such as the one on the right of Fig. 4, and used a vent baffle.

I might add that in the first flight we did not have the suppressor grid between the film plane and the photocathode because we did not run into that problem until we were testing the instrument that was used in the second flight, which was the Schmidt-type system.

Unfortunately, due to a programming error in the rocket control system, we did not point at the stars we were wanting to observe, and we did not get any useful spectra; however, there was no trace of the ion spot in this flight. As this instrument was not sensitive to the night air glow radiation at 1216 Å, which produces a uniform background in exposures with the all-reflecting instrument independent of the ion spot, the films had no background whatsoever, and there were just a few faint star images to show that the instrument was actually operating.

The most recent flight was on the Jan. 30, 1969. A typical result of this flight is shown in Fig. 6.

Here, again, we used the sealed nose cone, and the ion spot is completely eliminated. There is only uniform background of the Lyman alpha the night air glow; however, we discovered, for the first time something that we had never noticed in a lab test, handy, that the suppressor grid between the film and the photocathode does cast a very undesirable shadow pattern which is quite evident in this exposure, because of the night Lyman alpha air glow background.

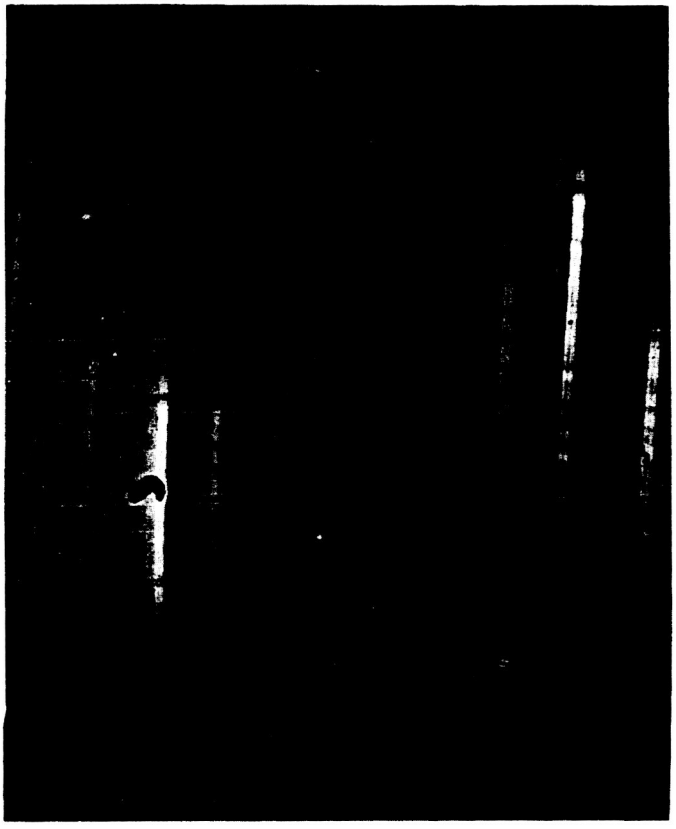

Fig. 6. Night air glow recorded on Jan. 30, 1969

In the laboratory test we just used paint (or slit) light sources not a diffuse source, and hence we did not notice the shadow pattern. We hope to get around this problem by using a focal plane shutter instead of a suppressor grid. The shutter will close just before film advance and open just after film advance. Thus, we can make our exposures without having the grid shadow pattern superimposed.

We are presently continuing our development work on these image converters, both in the laboratory and in sounding rocket flights, and hope eventually to use them in manned orbital missions in which the film data is recovered by astronaut extra-vehicular activity.

We are also developing other types of image converters based on this same general principle, for use in the far ultraviolet and also in the X-ray range, middle ultraviolet from 2,000 to 3,000 Å, and possibly the visible and near-infrared. Certainly in the visible and near-infrared, we expect to run into many new problems in high-voltage breakdown because of the fact that this requires the use of highly active cesium compounds, whereas the alkali–halides we use in the far ultraviolet are relatively inert.

An electronographic Schmidt camera was flown successfully in September 1969, obtaining starfield images in the Orion region of the sky. This camera used the focal-plane shutter system described in the text, and no background due to film outgassing was encountered.

It has been found that, in the all-reflecting instrument, neither a suppressor grid nor focal plane shutter are necessary to prevent discharge during film advance. Apparently, the large open area of this instrument allows any gas released by the film to escape more readily than in the Schmidt-type instruments. The instrument which was flown in January, 1969 was flown again (without suppressor grid or focal plane shutter) in March, 1970. Spectra of stars in Perseus were obtained, and the exposures were free of shadow patterns or ion spots.

Discussion

Lagadinos: I wonder whether you considered the possibility of using the EG&G XR film for this application. This is a multilayer, multi-exposure type of film which allows you to penetrate, based on the variable intensity of light, so that you can't really overexpose the film, and it is a fairly high-speed film.

Carruthers: No, actually I hadn't really considered that, but, in any case, we are talking here about exposure to electrons rather than to visible light, and I presume that this film that you are talking about is for visible light.

Lagadinos: Well, not quite. I think the ASA number of the film is in the neighborhood of about 30,000, and EG&G has been using that film for photographing spectrums of nuclear detonations.

Carruthers: Well, generally we find that the characteristics of films under exposure to electrons are quite different from what they are in the visible; for example, our nuclear track film is very low sensitivity to light, but it has very high sensitivity to electrons.

Lagadinos: The other question is in regard to the lead termination. In the past, we had the problem of having a sharp edge around the lug termination which you really secured at the next point of connection; and what we have done to cure that problem is to take a sphere which has been drilled and tapped and placed over the termination. This expands the field distribution to the level which is far beyond the corona level based on the voltage levels that you are concerned with.

Question: Did you happen to try any microwave discharges of plasma source? You said you used the triode and the plasma gun.

Carruthers: No, we hadn't really tried to use a microwave discharge other than external to the vacuum system in the same way as we

would the two electrode discharge, in which case this would be the type of microwave diathermy light source that is often used in vacuum UV light sources.

Question: Right. That is just what I was going to suggest, that it is often used, and you can operate it at a higher pressure and use a flow system to get a low energy plasma.

Carruthers: Yes, we have used that.

Yorksie: You made a reference to your electronics package being vented. Does that mean that all your electronics package, including your high-voltage system, was not of the potted type or encapsulated type?

Carruthers: Our high-voltage power supply was a potted high-voltage supply which we got from Pulse Engineering, and it was in the vacuum system with the electronographic image converter. Therefore, it was all in hard vacuum at all times.

PRECEDING PAGE BLANK NOT FILMED.

N70-32292

Low-Voltage Breakdown in Electronic Equipment When Exposed to a Partial-Pressure Nitrogen Environment Containing Water Vapor

R. F. Sharp, E. L. Meyer, and D. E. Collins
RCA Corporation
Astro-Electronics Division
Princeton, New Jersey

I. Introduction

A recent investigation has been completed at the RCA Corporation (RCA) Space Center relative to a practical evaluation of operating special electronic equipment in a critical pressure environment containing a mixture of nitrogen and varying amounts of water vapor. The results indicate that the addition of water vapor raises rather than lowers the voltage breakdown threshold, and that in typical electronic equipment extreme care must be taken when applying the Paschen curve to predict critical pressure.

While the objectives of this investigation were directed toward solving an equipment problem unique to RCA, many of the results may be of interest to those concerned with designing equipment for similar environments. An example of this may be the Martian atmosphere where surface conditions exert a pressure in the order of 11 torr with a gas composition of nitrogen, carbon dioxide, and water vapor.

II. Approach

A cursory review of the specific application established a need for additional information that would be oriented toward a given problem. As a result, the following objectives were established for this investigation:

(1) An evaluation of the voltage breakdown susceptibility of the electronic equipment, including margins of safety at anticipated operating levels.

(2) A determination of the effects of low pressure on voltage breakdown.

(3) A determination of the effects of humidity on voltage breakdown in a low-pressure environment.

To achieve these objectives the investigation was conducted in three parts, as outlined below:

(1) Background literature search. Some insight was provided for understanding the mechanisms involved in voltage breakdown phenomena.

(2) Test of a simulated unit. Critical circuits were simulated in a mechanical mockup.

(3) Electrode testing. A controlled gap for a quantitative evaluation of humidity effects was provided.

III. Background

As an aid in understanding the test problem, it is first necessary to review the basic theory concerning the mechanisms of ionization and voltage breakdown* (Fig. 1).

For the purpose of the review, it is assumed that initial ionization is caused by an electric field. However, this initial ionization can also be the result of a radiation field, photoelectric emission, or thermal excitation.

The main prerequisite for field intensified ionization is a few free electrons within the electric field. The increased energy imparted to the electrons by the electric field must be sufficient so that, upon collision with neutral molecules, additional electrons are released from the neutral atom. Each collision then creates an additional free electron and a positive ion. The free electrons then repeat the process supplying more free electrons and, thereby, create a current path. Since the massive positive ions are not accelerated to velocities for ionization by collision, they become ineffective ionizers.

The positive ion bombardment of the cathode, however, causes secondary electrons to be released (secondary emission) which further intensify the ionization current.

Voltage breakdown occurs if there is a net accumulation of electrons and positive ions. For the discharge to be self-sustaining, each initial electron must produce enough ionization to cause emission of one electron from the cathode.

While the ionization process is under way, the deionization process simultaneously neutralizes the ionization. A simplified diagram of the deionization process is shown in Fig. 2.

The deionization process results from volume recombination and/or diffusion. Volume recombination, shown in Fig. 2, takes place when a free electron, after a number of collisions, becomes attached to a neutral atom to form a negative ion. This negative ion, in turn, combines with a positive ion producing two neutral atoms.

Diffusion, as diagrammed in Fig. 2, occurs when a positive ion and an electron collide at a surface, such as

*Cobine, J. D., *Gaseous Conductors*, McGraw-Hill Publishing Co., New York.

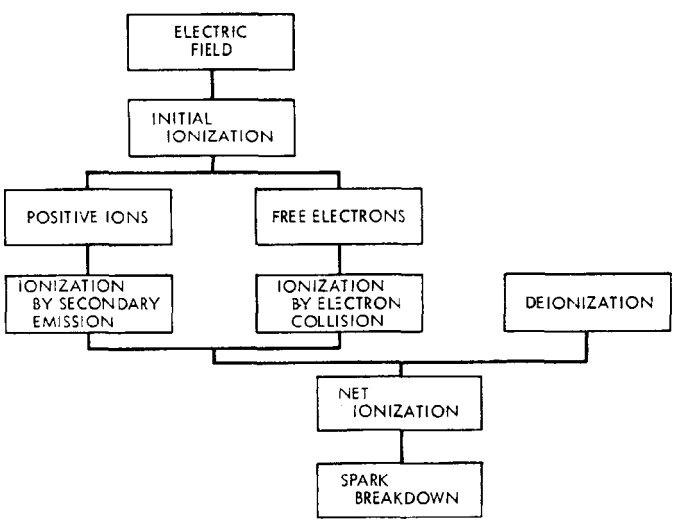

Fig. 1. Voltage breakdown

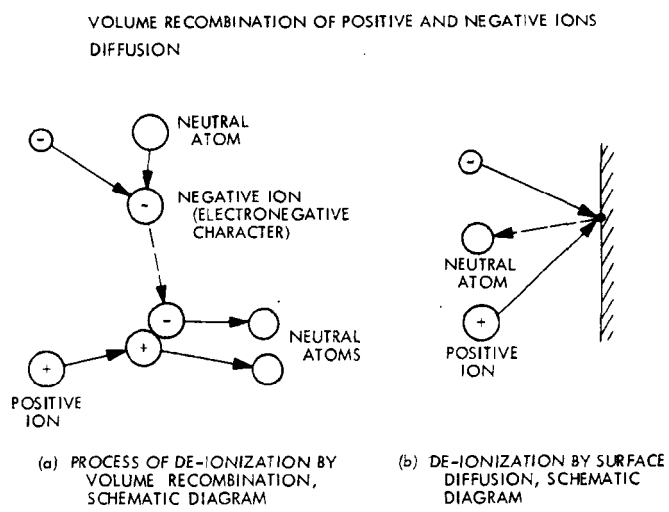

Fig. 2. Deionization process

the chamber wall, and combine to form a neutral atom. As is often the case, the chamber dimensions are much larger than the mean-free-path (MFP); therefore, deionization by diffusion is a minor effect. Volume recombination then is established as the chief mechanism of deionization.

In dealing with deionization by recombination it is found that environments composed of certain gases tend to promote the attachment process to a significantly greater degree than do other gases. This is because the molecules of these gases have an affinity for free electrons; this property of some neutral gases is termed electronegative character. The greater the electronegative character, the greater the tendency of neutral atoms in the environment to combine with free electrons. Because the attachment of free electrons is the necessary first step in the recombination process, it is seen that a highly electronegative gas will provide a much more efficient medium for deionization.

The coefficient of attachment of some common gases is provided in Table 1. The coefficient, in turn, is a measure of the relative electronegative character. Water vapor and oxygen exhibit a higher degree of electronegativity than nitrogen so that increasing the concentration of one of these gases in a nitrogen environment would tend to decrease breakdown susceptibility in the environment. This implies that water vapor, in general, should exhibit higher breakdown voltage characteristics than nitrogen.

Table 1. Deionization

Recombination	Diffusion
1. Major vehicle of deionization 2. Coefficient of electron attachment (δ) and electronegativity	3. Diffusion process considered negligible (MFP of electrons and ions very small with respect to chamber dimensions).

GAS	δ[a]	t[b]
N_2	$\rightarrow \infty$	$\rightarrow \infty$
AIR	2.5×10^5	0.63 μs
O_2	0.4×10^5	0.194 μs
H_2O	0.4×10^5	0.141 μs

[a]δ Average No. of collisions before attachment (lower δ indicates higher electronegativity).

[b]t mean time before attachment.

IV. Simulated Test

The initiation of a breakdown investigation at RCA was prompted by the proximity of circuit elements, particularly diodes and transistors, in an item of equipment which may operate in a partial pressure environment. As has already been mentioned, this environment could contain water vapor.

The essence of our approach was to build a test specimen which accurately duplicated those portions of the equipment at which the maximum voltages appear; maximum voltage differences were on the order of 120 V. This specimen would be subjected to a range of partial pressure/breakdown tests to determine problem areas and a margin of safety. This approach had three distinct advantages: (1) it would not require interpretation and application of "classical approach" data, (2) it would not require that actual fabricated equipment be subjected to a potentially hostile environment, and (3) the safety margin could be explored by use of voltages considerably in excess of normal operating levels.

Two basic types of simulated circuit were to be studied: the first involved actual circuit components with layout and wire routing duplicating that of the equipment design. Five similar circuits were constructed on the test specimen (Fig. 3), each one accentuating some condition thought to increase the likelihood of breakdown. The second simulated circuit, shown in Fig. 4, sought to recreate the effect of a ground plane above a row of bifurcated terminals.

A. Environment

The environment simulated in the test chamber consisted of the 100% dry nitrogen (N_2) and dry nitrogen with various amounts of water vapor to approximately 90% relative humidity (RH). The RH is defined as the ratio of the partial pressure of water vapor at a temperature to the partial pressure of saturated water vapor at the same temperature.

Control of the vapor pressure in the chamber consisted of pumping the chamber down to approximately 0.05 torr; at this pressure, the rough pump is blanked off, and water is injected by bleeding through a needle valve to the desired vapor pressure while applying heat to prevent freezing (Fig. 5). To achieve the desired mixture of N_2 and water vapor, N_2 is backfilled into the chamber until the desired total pressure is attained.

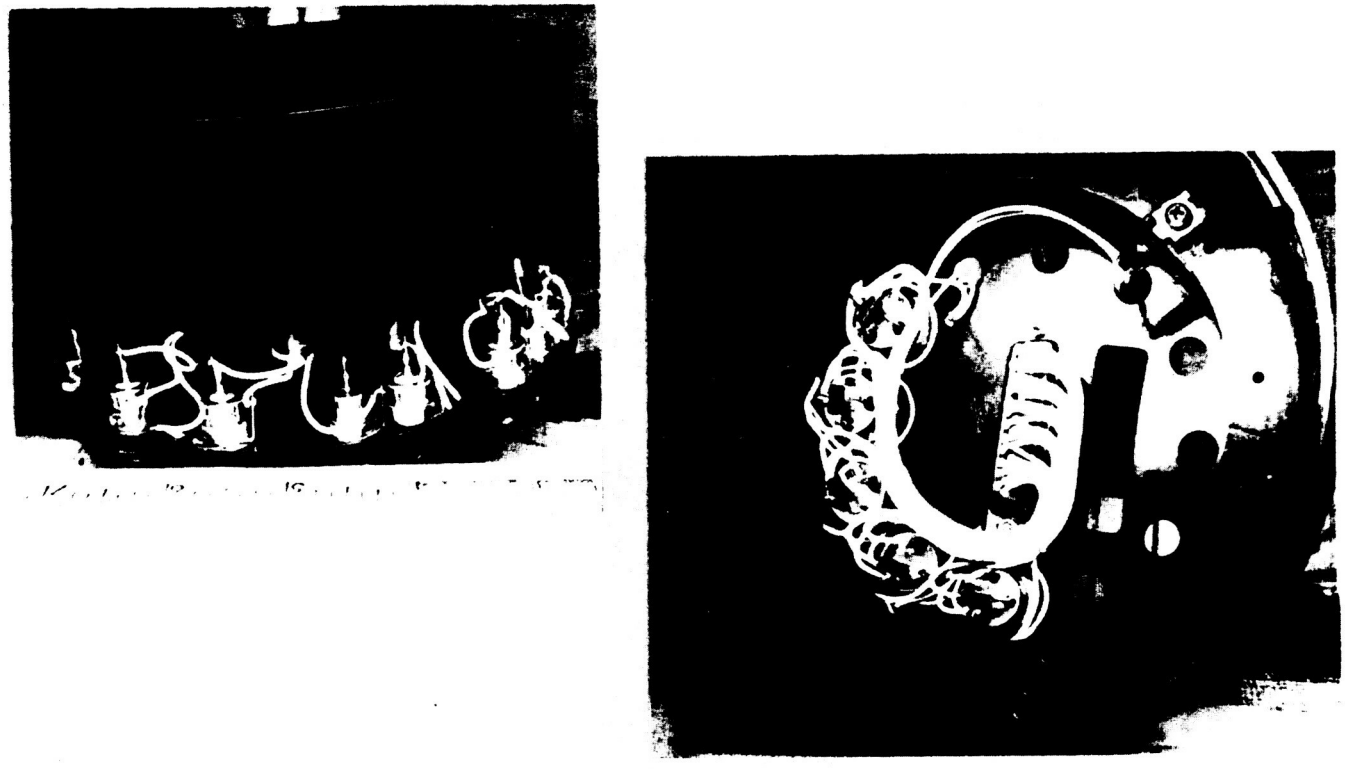

Fig. 3. Test specimen

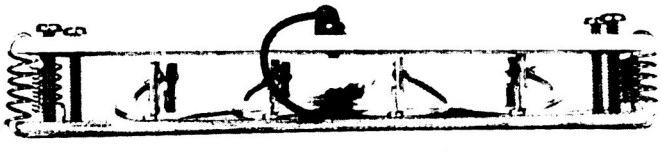

Fig. 4. Simulated terminals

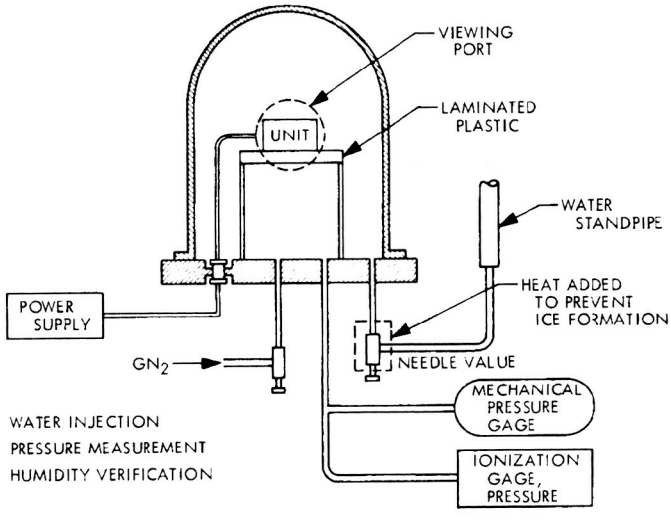

Fig. 5. Mechanical setup for testing of the simulated unit

Measurement of total pressure was accomplished by the combination of an ionization pressure gage and a mechanical gage. Use of the mechanical gage was necessary since it responds to total pressure; however, it is inaccurate at low pressures. The ionization gage, in contrast, measures the pressure by ionization of the gas and is accurate over a wide range of pressures; some error in exhibited, however, when used with a gas different from the calibration gas.

Verification of the humidity measurement was accomplished by installing a temperature-compensated humidity sensor in the chamber which translates vapor pressure into resistance. This is converted on the indicator to a percentage of RH.

B. Test Procedure

Three types of test voltages were employed in the test series as shown in Fig. 6: dc, chopped dc, and ac superimposed on dc. They were chosen to permit evaluation of each characteristic of the voltage waveform.

Electrical discharge detection was accomplished by two methods. The first method was by visual (unaided eye) observation of the corona, which was not always reliable. The second method employed an oscilloscope for monitoring the discharge current through a 100-kΩ series resistor. Voltage stress was applied for a period of approximately 7 s at one level. The voltage was increased and the stress again applied for 7 s. The process was repeated until spark breakdown occurred. Breakdown threshold was recorded by noting the first significant current, either dc or a series of pulses. The dc current type of discharge was predominant.

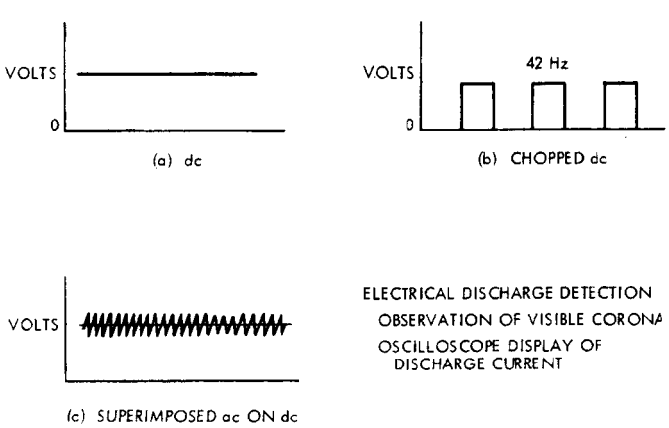

Fig. 6. Test procedure

C. Results

Voltage breakdown levels and pressure readings for the simulated unit testing are plotted in Figs. 7 through 10. Terminal gaps set at 0.06 and 0.15 in. are shown in Fig. 7. The curves exhibit a minimum breakdown voltage characteristic as expected from Paschen's law. Departure of the two curves can be expected because of the lack of symmetry between the setups.

Both gaps with different types of voltage wave shapes are plotted in Figs. 8 and 9. Tests were conducted in dry nitrogen. The lowest breakdown to be exhibited by the dc with a 3-kHz superimposed sine wave is shown in Fig. 8. The difference is small, and no explanation of this is offered; however, it is felt that it does not represent high-frequency effects. Except for the gap size, test conditions for the data of Fig. 8 were identical to those for Fig. 9. The results summarized in Figs. 8 and 9 indicate that the effects attributable to the different types of test voltage were negligible for the purpose of the study. All further testing was with a dc test voltage. Several runs with various humidities for the simulated unit are represented in Fig. 10. The trend of the curves indicates

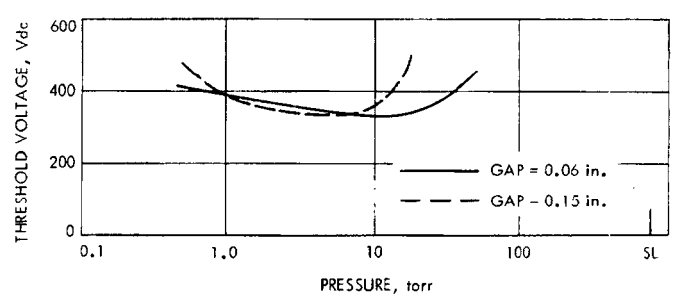

Fig. 7. Effect of gap distance on corona in terminal-type gaps, low RH, dc test voltage

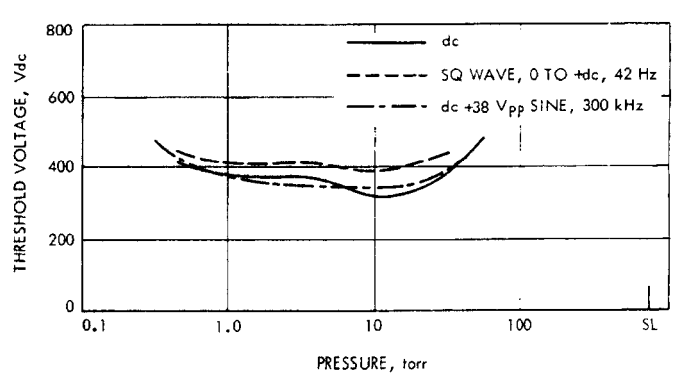

Fig. 8. Effect of various types of voltage on corona in an 0.06-in. terminal gap with low RH

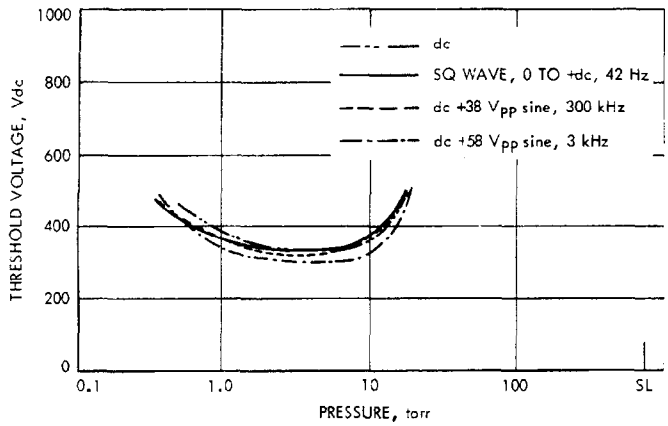

Fig. 9. Effect of various types of voltage on corona in an 0.15-in. gap with low RH

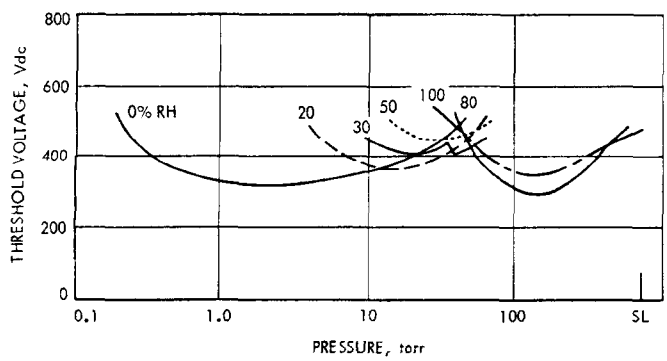

Fig. 10. Effect of humidity on corona in heat sink circuit No. 1, dc test voltage

an increased breakdown voltage with increase in humidity, to a point. At higher humidities, however, this trend appears to reverse. The latter effect was unexplainable, but could have been the result of a different breakdown path within the equipment; perhaps a surface path resulting from condensation at the higher humidity levels was the cause. However, no traces of condensation were found upon breaking vacuum.

The questions raised by these unexpected results prompted the study to be extended to a new phase to determine more accurately the effects of water vapor on breakdown.

V. Electrode Test

The electrode test was designed to eliminate all variables except the composition and pressure of gas which comprises the test environment. Only in this way could the effects of humidity be isolated.

The test specimen consisted of a pair of aluminum electrodes, 0.25-in. in diam, 6-in. long, and machined to a 45° point. Selection of the diameter and angle of the electrodes was intended to provide a point gap while still maintaining an electric field which, although nonuniform, was somewhat less sensitive to gap alignment than would be required by needles.

A. Environment

The environment for this test consisted of the following constituents:

(1) One hundred % dry nitrogen.

(2) One hundred % water vapor at partial pressures ranging from 0.3 to 24 torr.

(3) Dry nitrogen with various amounts of water vapor to approximately 80%.

Control of the vapor pressure in the chamber was the same as in the previous testing. The setup, however, was changed to eliminate all possible corona points other than the electrodes. If this is not done, "stray breakdown" can occur and, as such, will cause erroneous test data. The mechanical setup for this test is shown in Fig. 11.

B. Test Procedure

A gap width of 0.010 in. was chosen empirically to provide data in a pressure region compatible with that encountered with water vapor.

In an attempt to eliminate any anomalies which might result because of subtle differences in setup conditions,

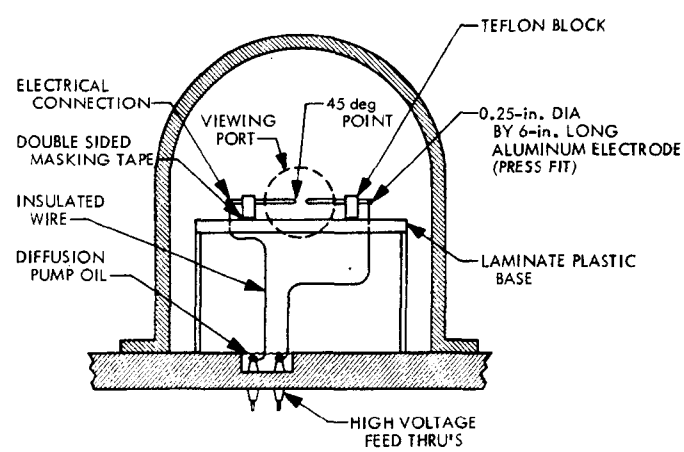

Fig. 11. Aluminum electrode voltage breakdown test setup

2

the following sequence of steps was used in all the test runs:

(1) Polish electrodes; clean with alcohol.

(2) Install in Teflon blocks and set gap.

(3) Pump-down to 0.2 torr or less, back-fill with dry nitrogen to 750 torr.

(4) Pump-down to 0.2 torr, back-fill to first pressure step (approximately to 0.5 torr).

(5) Apply voltage across electrodes for approximately 7 s. Increase voltage and repeat until breakdown threshold is reached.

(6) Backfill with dry nitrogen for next pressure increment.

(7) Apply voltage between electrodes for approximately 7 s. Increase voltage and repeat until breakdown threshold is reached.

(8) Complete pressure range as desired for 100% nitrogen.

(9) Pump down to 0.05 torr.

(10) Inject water in chamber to desired vapor pressure.

(11) Apply voltage between electrodes for approximately 7 s. Increase voltage and repeat until breakdown threshold is reached.

(12) Back-fill with dry nitrogen for next pressure increment.

(13) Apply voltage between electrodes for approximately 7 s. Increase voltage and repeat until breakdown threshold is reached.

(14) Complete pressure range as desired.

Each humidity run was preceded by a dry nitrogen run to provide for a more meaningful correlation of relative humidity and threshold voltage.

C. Results

Voltage breakdown levels and pressure readings for the electrode test series are plotted in Figs. 12 and 13.

Figure 12(a) shows the threshold breakdown voltage for water vapor and for dry nitrogen, individually. The increased breakdown voltage of the water vapor is predictable on the basis of the vapor's electronegative character. The pressure range of the water vapor curve is limited because the saturation vapor pressure is 28 torr at 77°F.

The breakdown voltage for approximately 22% RH is shown in Fig. 13(a). The apparent decrease of breakdown voltage in the nitrogen/water vapor mixture is considered to be brought about by the dilution of the water vapor as more nitrogen is introduced. Humidities of 30, 40, and 80% are shown in Figs. 12(b) and 13. In each of these plots, the 0% RH condition was run to obtain a meaningful correlation; i.e., where all other test conditions were identical.

All of the previous curves for a trend indication are plotted in Fig. 12(b). The dry nitrogen curve is actually an average of nine tests under the same conditions.

These results indicate that water vapor, when mixed with nitrogen, which does not exhibit an electronegative

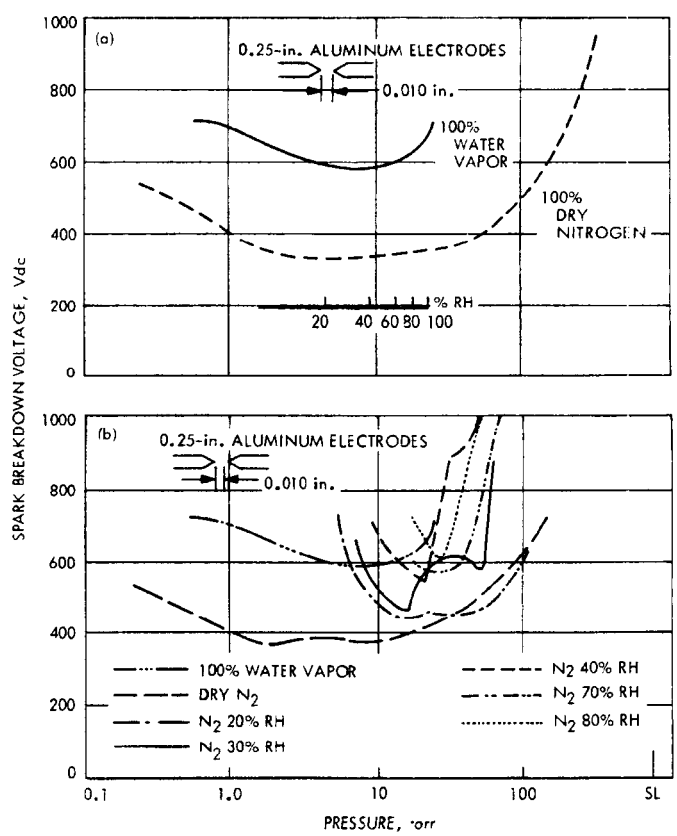

Fig. 12. Spark breakdown threshold as a function of the pressure and gas environment

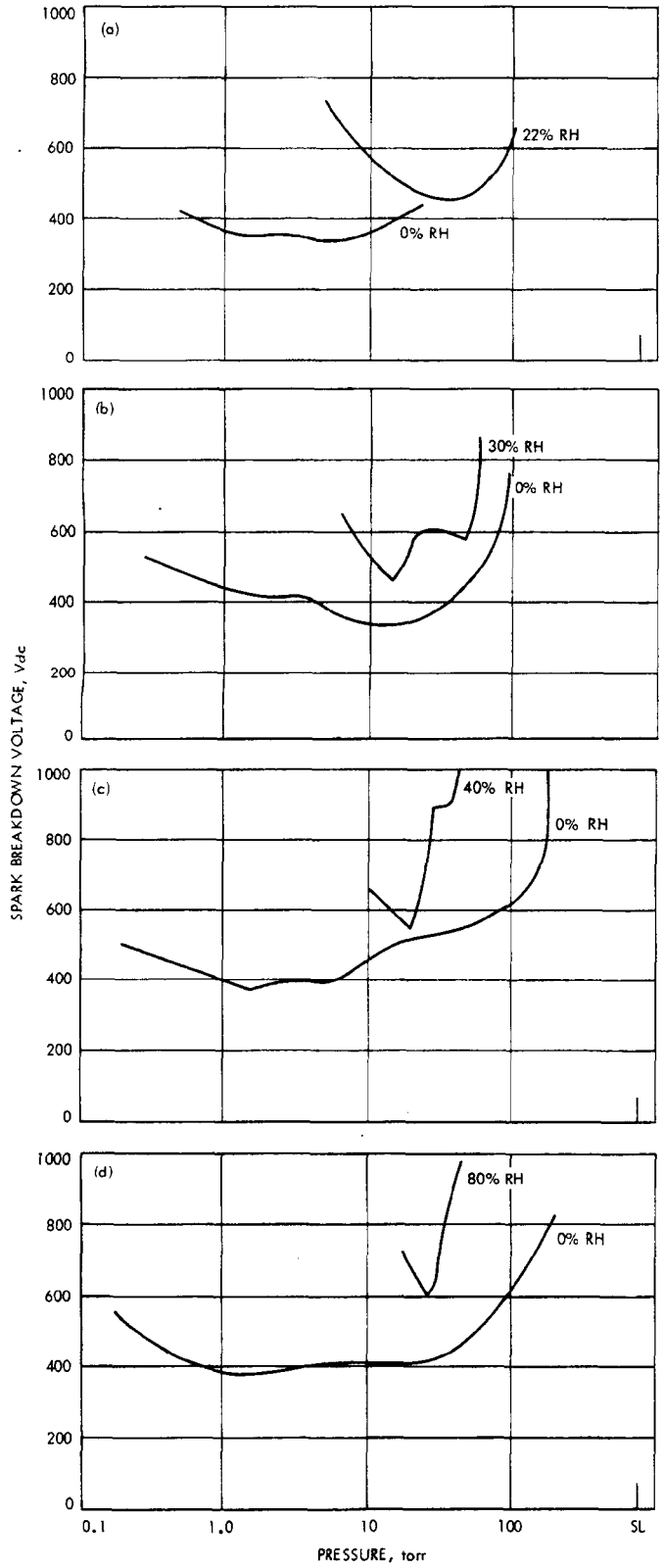

Fig. 13. Spark breakdown in nitrogen with and without water vapor, 0.010-in. gap

character, will increase the breakdown voltage. The larger the percentage of water vapor to the total pressure, the greater the increase of breakdown voltages. However, it is not known what effect humidity will have when higher voltages are used; e.g., in kV. For this testing, voltage levels were limited to 1200 V.

VI. Conclusions

The following conclusions were drawn from the results of this study:

(1) Voltage breakdown curves in 100% water vapor exhibit the same general shape as the familiar Paschen curve.

(2) Voltage breakdown levels in 100% water vapor are significantly higher than those in 100% dry nitrogen.

(3) Typical electronic equipment exhibit a multitude of possible breakdown paths so that it becomes impossible to apply the classical Paschen curve to predict critical pressure. It should be re-emphasized that the Paschen law relationship cannot be applied indiscriminately to physical circuits.

(4) Addition of water vapor to a nitrogen gas environment will increase the breakdown threshold; in addition, the breakdown voltage increases with increasing humidity.

Discussion

Piemersma: In your measurements on the sparkover voltage of these various gases and at points you plotted, how many tests does each point represent? What I am trying to say is the variability of sparkover, particularly with that type of geometry almost necessitates that you statistically analyze your data in order to get a valid comparison. I am wondering how many data points you took to plot your curves.

Meyer: Well, in most cases we took very few. However, the last curve averaged the dry nitrogen run, and with a fair amount of repeatability in those points. We did go back a few times and repeat voltages of breakdown levels, but essentially there was no statistical values for those.

Piemersma: I think it would be worthwhile for your application, because with my experience with sparkover, the variation can be as much as 100% from test to test.

Discussion (contd)

Meyer: That is right. This is why we ran the dry nitrogen run preceding the water vapor run. The slightest change in the configuration or alignment, could throw the value off by a considerable amount.

August: I am a little confused about that because some of our experience has been contrary. First off, it looks as though you have a poor Paschen curve there. The minimum is spread over more than an order of magnitude in pressure, and, second, we expect, at very low pressures where diffusion is important (and it seems that you have gone down to those pressures) that the attachment contributed by water vapor should be negligible, and it should be diffusion-dominated. Therefore, you should expect your curve to coincide for dry air and for various amounts of water vapor. Any explanation?

Meyer: Well, we had, first of all, diffusion. The chamber dimensions were very large and the mean free path of the electrons and the ions is very small, so that there are many collisions before the diffusion would come in.

August: Well, diffusion to walls is not necessarily important; it is really diffusion in the area where your electric field strength is high, and that can be over a short distance. Thus, your diffusion length can easily be several times the gradient in the electric field strength. What about the spread in the Paschen curve at the minimum? Why is it so broad?

Meyer: Well, as I said before, this is sort of a practical solution to a particular problem we had. We realized, using electrodes, that we were looking for trouble, and we wouldn't get a very good Paschen curve, but we weren't really interested in plotting a very accurate Paschen curve. If we were, we probably would have taken uniform fields and used special equipment to do that. We were not really interested in plotting Paschen curves in nitrogen or anything like that.

Stern: I think Ed has found a problem that all investigators in observing voltage breakdown have found, namely, that if you don't have a really good, uniform system, something in which you can be certain of your electric field, you are going to have some apparent strange behavior. We, too, have gone through this problem at Goddard.

Dunbar: I am a little bit confused over your drawings. It showed your minimum for nitrogen in the vicinity of above 300 V, dry nitrogen, and my experience with uniform and nonuniform fields (I include down to points and wires) to be well below 300 V. However, in our dry nitrogen bottles that had water in them or were previously filled with oxygen by a certain company we bought from, we did run into the problem you did have, and I am questioning your dry nitrogen data.

Meyer: Well, let me say we took no special care in using the dry nitrogen. I assume it was dry nitrogen. In other words, we didn't filter the nitrogen, coming in with any kind of filter to remove any water that might be in it.

Dunbar: Did you check it against a theoretical curve?

Meyer: Well, we have the Paschen curve in nitrogen for uniform fields, and that ran at about 270 V, but we were not concerned too much with the difference of 270 and 300 V; again, this was kind of a—

Dunbar: Well, that is the point I am making. Dry nitrogen will repeat at about 270 V with nonuniform as well as uniform fields, especially when you get down near the minimum of the Paschen curve, down at that minimum, if you had real dry nitrogen. If you have impurities in it, though, almost anything will bounce it up 30 to 40 V, and it is very difficult to handle.

Meyer: That is right, and if you go one step further, by introducing water vapor you can raise that level to 100 V, so that is right.

PRECEDING PAGE BLANK NOT FILMED.

N70-[illegible]

The Bendix OAO Star Tracker High-Voltage System and Its Design Considerations

W. Mitchell
The Bendix Corporation
Navigation and Control Division
Teterboro, New Jersey

I. Introduction

As with some other vehicles using high voltage systems, the first *Orbiting Astronomical Observatory* (*OAO*) star tracker showed indications of discharges in orbit, but not during vacuum chamber testing. The star trackers on *OAO I*, though not made by the Bendix Corporation, had a similar high voltage system in that they both must be operated outside a critical pressure region. After the failure, a re-evaluation of the vehicle-star tracker configuration concluded that there was a high probability of a non-vacuum environment existing in the vicinity of the star tracker for a considerable period of time (Ref. 1). In view of the inability to specify the time-pressure characteristics of the star tracker ambient and the disruptive nature of arcing, the National Aeronautics and Space Administration (NASA) subsequently required the Bendix Star Tracker, which was designed for the same vehicle, to operate at all pressures between sea level and space.

II. Design Constraints

Both the initial and modified high-voltage systems had several design requirements; these were:

(1) A shelf life greater than 2 yr.

(2) An operating life in excess of 1 yr.

(3) Operation and survival between temperatures of -55 and $+55°C$.

(4) Operation without discharge between the following pressures:

(a) For the original system: at room pressure and pressures of $< 1 \times 10^{-3}$ torr.

(b) For the modified system: at any pressure.

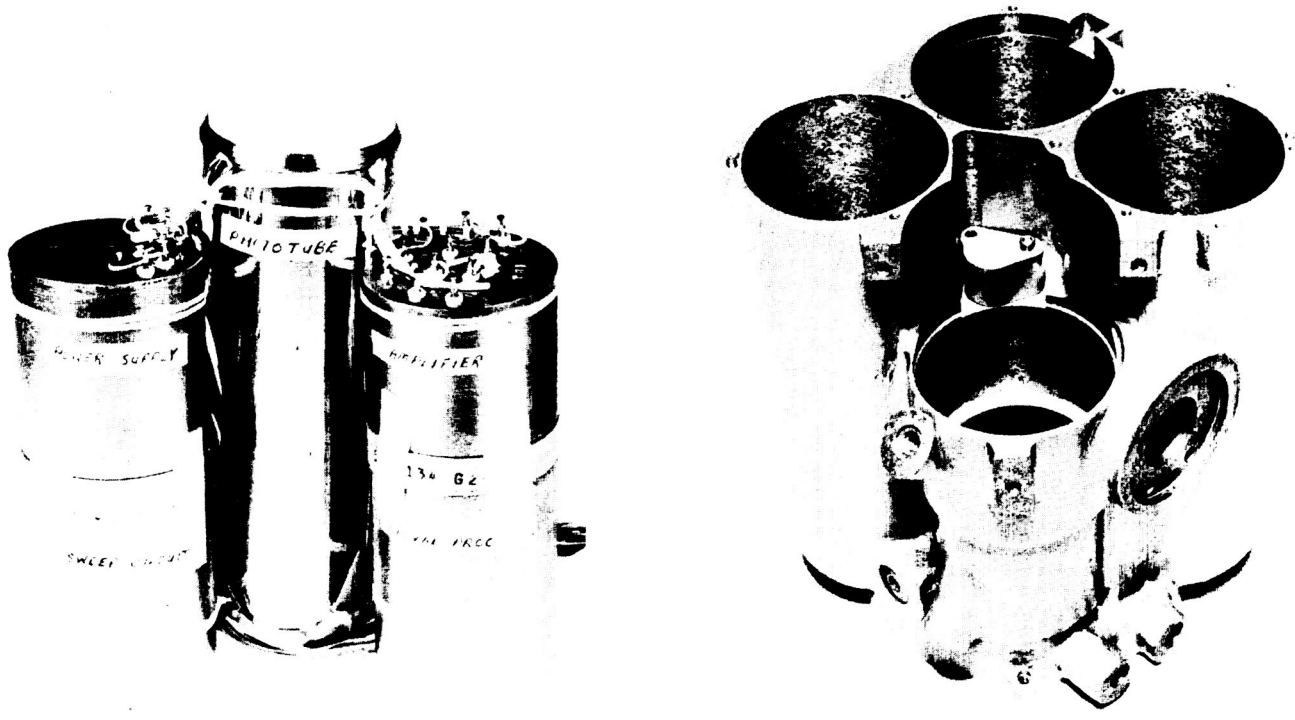

(a) ELECTRONICS

(b) TELESCOPE HOUSING

Fig. 1. Bendix OAO star tracker telescope: (a) electronics, (b) housing

III. Original High-Voltage System

The high-voltage system consisted of the following three main elements:

(1) A 2-kV-dc power supply.

(2) The high-voltage terminations and transmission.

(3) An FW 143 phototube and its resistive divider network.

The telescope's electronics are shown in their respective positions along the housing in which they are contained in Fig. 1. The high-voltage system is shown alone and more detail in Fig. 2. The phototube was potted in its magnetic shield with the RTV-11 without the use of a primer. Its divider network is affixed directly to the base pins. The high voltage is transmitted with a piece of teflon insulated wire from an exposed terminal on the high-voltage supply. The high voltage supply consisted of a dc to ac converter, a voltage quadrupler, and a low pass filter.

The original high-voltage container was vented to the housing which, in turn, was vented to the local star tracker ambient. The supply was conformally coated with Hysol 12007 A/B to "current limit" discharges to nondestructive levels in the event the ambient would go through the critical pressure region. In testing, this exposure was inadvertently given without occurance of

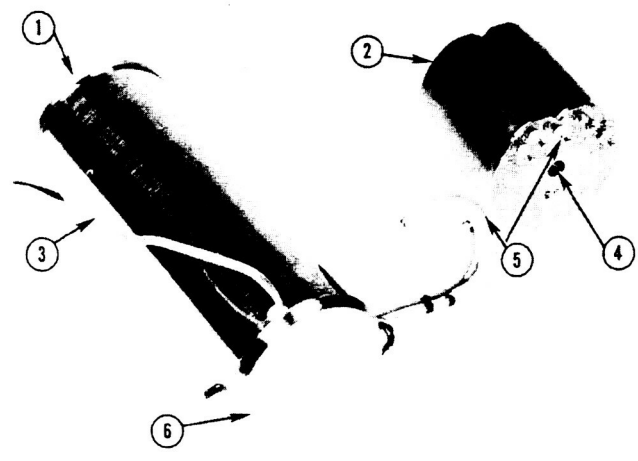

1. PHOTOTUBE-SHIELD ASSEMBLY
2. HIGH VOLTAGE POWER SUPPLY
3. ANODE OUTPUT
4. VENT
5. HIGH-VOLTAGE WIRE AND TERMINAL
6. RTV-11 POTTED DIVIDER NETWORK

Fig. 2. Original high-voltage system

failure. At best, however, this procedure would be disruptive to normal spacecraft operation due to radiated and conducted transients.

As a result of using air as a dielectric, the original high-voltage system could not be operated at all reduced pressures. The nature of the dielectric strength of gases is such that for a particular electrode spacing, geometry, and potential, there will be a critical pressure range above and below which the gas will not break down. Due to the complex geometry of the many areas where air was the dielectric, the range was experimentally determined to be between 0.06 and 90 torr. It should be noted that this type of design will not function properly, if not fail, if the ambient is ionized.

IV. Modified System

The original design was pressure sensitive as it used an air dielectric in several regions. Modifications to allow operation at all pressures required elimination of the ambient as a dielectric. The actual modifications consisted of providing stable dielectrics and the means of terminating the potential field within them.

Theory describing the type of discharge occuring in this application is well developed and has appeared in the published literature for decades. The application of materials to realize a desired design, however, was often found to yield the most troublesome problems.

In order to allow the star tracker to operate at any pressure, changes were required in four areas: (1) the high-voltage wire and its terminations, (2) the high-voltage power supply, (3) the phototube base and resistive divider network, and (4) the phototube window. This last item was not fully appreciated until the first system was beginning qualification. Prior to the construction of a qualification unit, a substantial amount of materials evaluation and testing of prototypes was performed.

Discharges at the tube base were prevented by applying a potting which adheres to all surfaces in the region. A cross-section of the phototube shield assembly is shown in Fig. 3. The RTV-11 was completely removed from the base and divider network components. To allow adhesion, unetched teflon materials were replaced with etched types and eliminated where possible. Teflon etching does not provide true adhesion and the material was only used in noncritical areas. In general, use of Teflon is

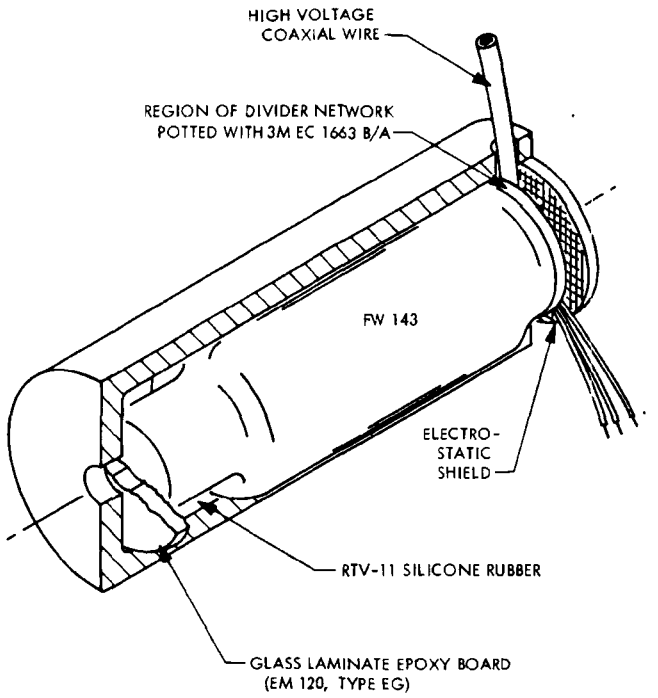

Fig. 3. Simulation of phototube and shield

not recommended for high-voltage systems. The region was carefully cleaned, primed, and then filled with 3M EC 1663 B/A potting material. A mesh screen was impressed in the outer surface of the potting. This screen serves as a ground plane constraining potential gradients to remain within the potting.

The modified design uses a high-voltage coaxial wire, already space proven, to transmit the high potential. In the wire, the potential is constrained to remain in a silicone rubber dielectric. The terminations are also potted in 3M EC 1663 B/A material, which is electrostatically shielded.

The high-voltage power supply has many electrodes at potentials above the minimum sparking potential of air, $\approx$330V. The electronics and new hermetic package are shown in Fig. 4. In an attempt to avoid damaging seals, materials were chosen which required working in widely different heat ranges; e.g., seams of the can and the electrostatic shield were welded, the filler tube and ground lugs were braised, and different temperature solders were used in applying the feedthrough terminals and the main seal. The supply was filled with a 90:10 mixture of nitrogen and helium at 17 lb/in.^{2}. This mixture is both a good dielectric and provides for leak detection using standard equipment. Based on the OAO

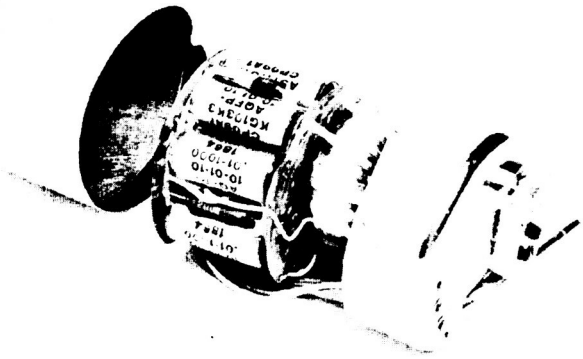

Fig. 4. Assembly showing the hermetically-sealed can and electronics module

mission objectives, the maximum initial leakage rate was 12×10^{-2} μm-ft^3/h. Background readings of two orders of magnitude lower were attained.

Eight power supplies and six tubes, with the modifications just described, were constructed and their parameters measured before and after a thermal-vacuum exposure. Two phototubes mounted in an open thermal vacuum chamber are shown in Fig. 5. An observer tube mounted externally for viewing window discharges is shown in Fig. 6.

Figure 7 shows 500 ft of high-voltage wire mounted in a small vacuum chamber. It was operated at 3000 Vdc and the leakage current and input power was monitored at several pressures for 25 days. Additional testing was also performed on several potting materials to determine their mechanical properties.

Materials tested were RTV-11, Sylgard 182, and 3M1663 B/A. All were found to exhibit generally similar characteristics; the 3M material was chosen primarily for its adhesion properties. Of particular significance was the low temperature characteristics which were very similar for the three materials. The rate of contraction and hardness increased drastically below −55°C. At this point the "brittle point" is being approached and the material can cause considerable damage to the component below.

At this point, a qualification unit was constructed with modifications to all areas except the phototube window. Figure 8 shows this system at an intermediate stage of

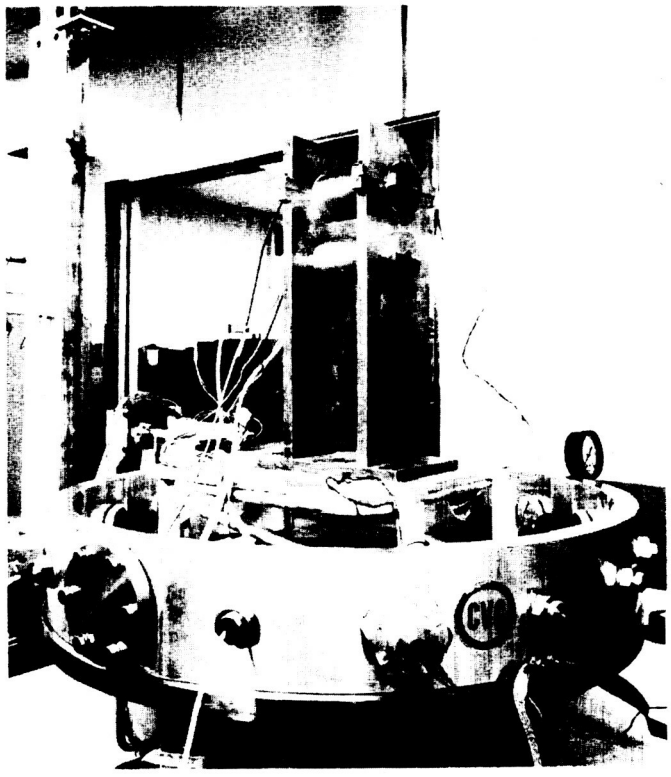

Fig. 5. Thermal-vacuum testing of simulated phototubes

development. It was successfully exposed to reduced pressure tests at −55, +25, and +55°C. These tests required approximately 5 days of exposure during which continuous strip recordings of input voltage and current, output voltage, and anode current were made. The anode output was further observed on a pulse height basis by: (1) a pulse counting technique, and (2) visual observation on a wide bandwidth oscilloscope.

After the five-day exposure, the phototube and high voltage supply were then assembled with the rest of the electronics in a set of gimbals. A substantial amount of high vacuum exposure had been covered at −55 and +25°C without difficulty. This time, however, problems developed at high temperature. After documenting the details of behavior, the power supply and tube were removed from the star tracker and placed in a small thermal-vacuum chamber. The problem was restricted to the tube by separately varying the temperature of the tube and power supply. A discharge at the window was confirmed through the use of an observer tube in the chamber directed at that region. An impulse of anode current occurred coincidently with a similar detection by the observer tube. The characteristics of the discharges are shown in Fig. 9.

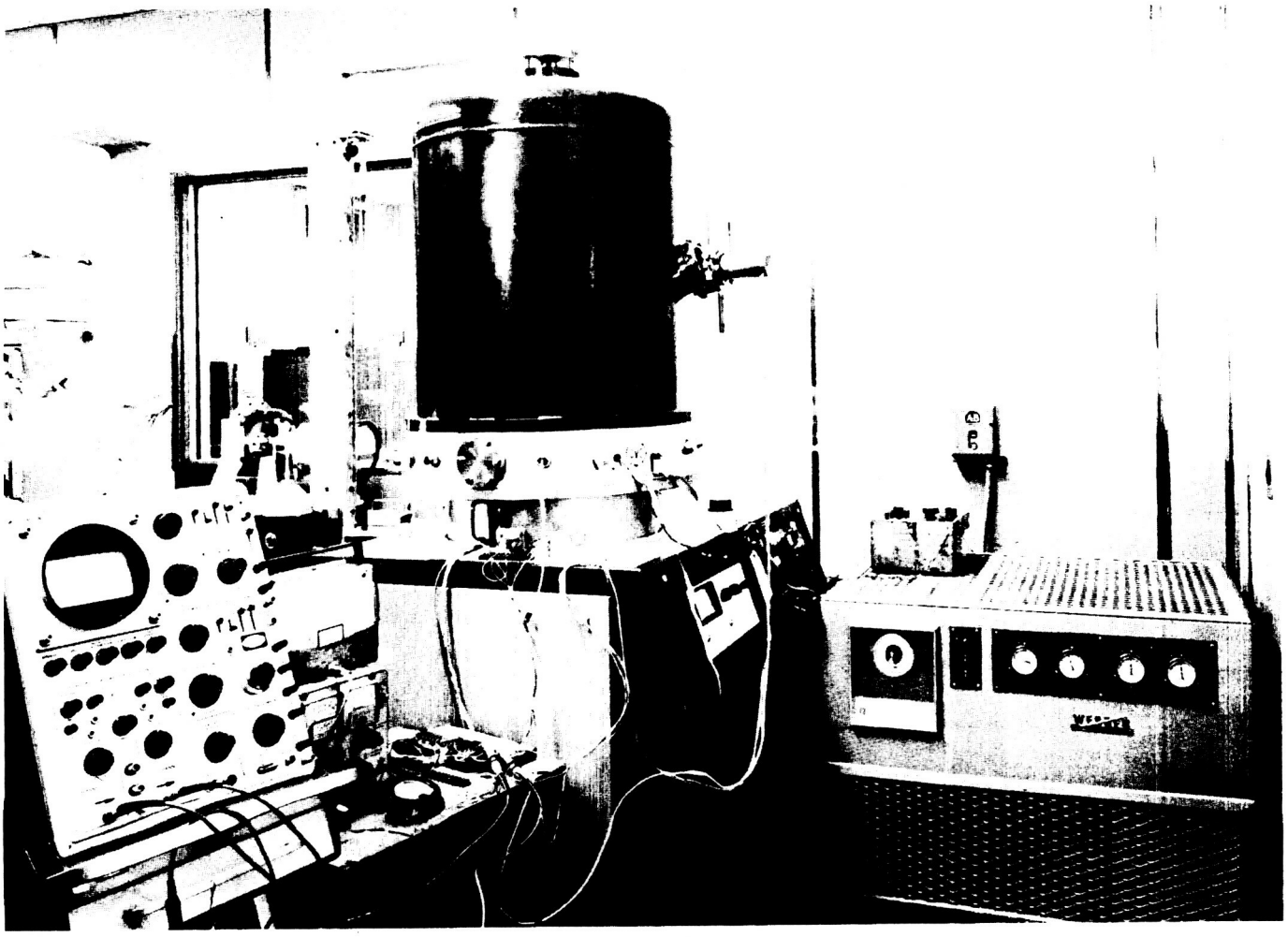

Fig. 6. Thermal-vacuum facility showing observer tube

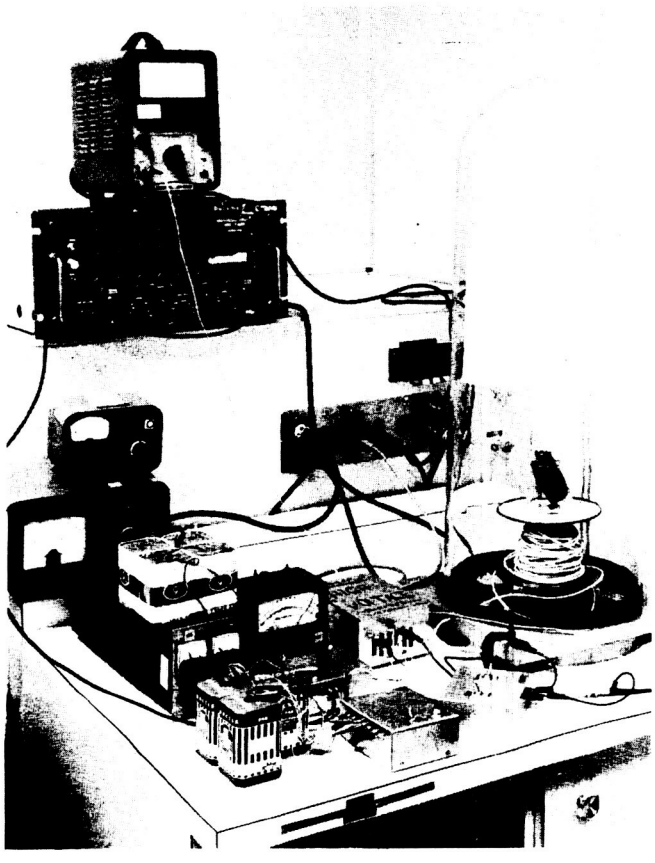

Fig. 7. Vacuum testing of coaxial wire

Fig. 8. Intermediate testing of the modified high-voltage system

CHARACTERISTICS OF WINDOW DISCHARGE

ANODE TRANSIENT: AMPLITUDE IS EQUIVALENT TO SATURATED TUBE OUTPUT; 300μA FOR < 1μs. REPETITION RATE IN CRITICAL REGION IS FUNCTION OF TEMPERATURE

CRITICAL PRESSURE-TEMPERATURE REGION

NONRECURRING TRANSIENTS OUTSIDE CRITICAL REGION OCCUR: DURING FAST PUMP DOWN, AND DURING FAST BACK FILL

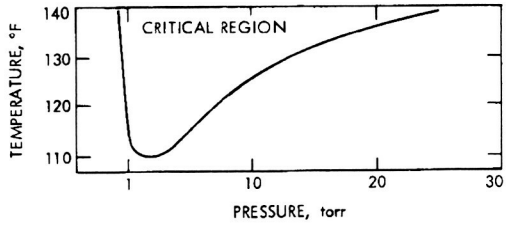

Fig. 9. Characteristics of window discharge

V. Definition of the Problem

At this point it was apparent that a discharge was occurring at the phototube window under several different sets of conditions resulting in an impulse of saturated anode output. Foremost, it was apparent that the window was not below the sparking potential. The correlation of the critical region and Paschen's curve is apparent; the analogy is not perfect as all of Paschen's conditions were not met, but seems to substantiate the same type of phenomena. It now remained to develop a model to evaluate this problem and its solutions.

A. Electrical Characteristics of Glass

Before getting into the details of this mode, a few electrical properties of glasses will be discussed. Glass has historically been considered a near-perfect dielectric, but the fact that it does have some conduction is now causing problems. A plot of volume resistivity as a function of temperature is shown in Fig. 10. It is interesting to note the strong temperature dependence. The window material's resistivity used in the tube under consideration drops two orders of magnitude in going from 25 to 55°C.

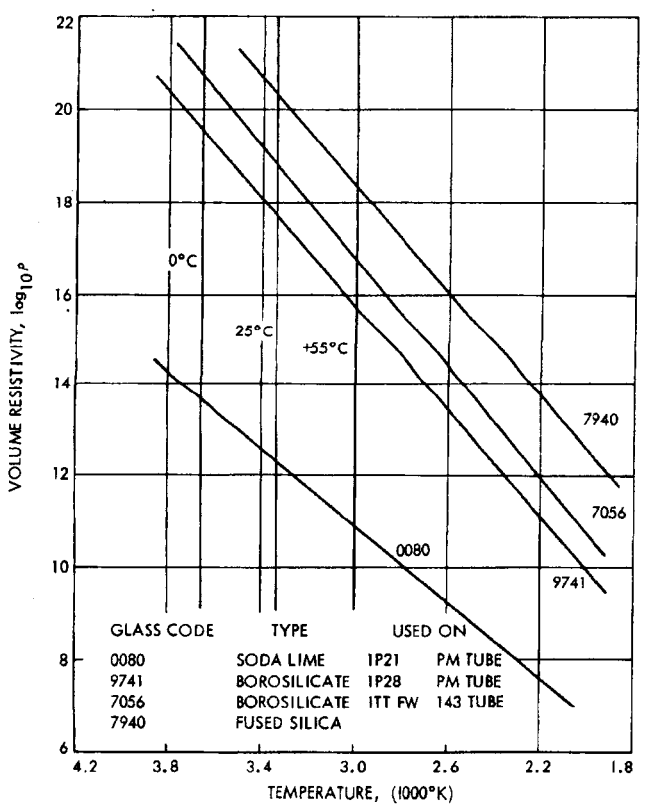

Fig. 10. Volume resistivity of gases as a function of temperature

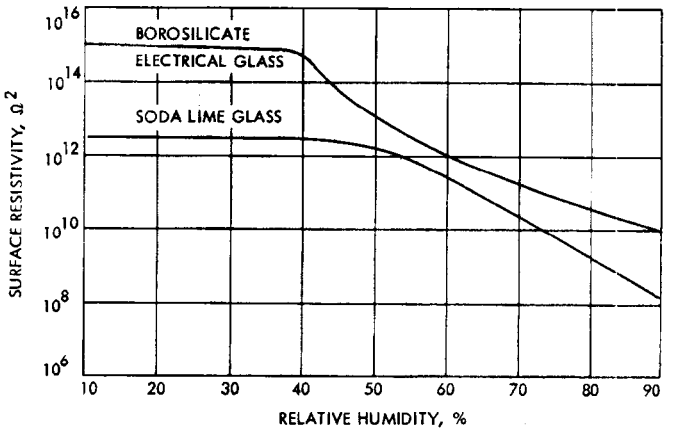

Fig. 11. Surface resistivity of glasses vs relative humidity

Another interesting characteristic of glass is surface conduction as a function of relative humidity (Fig. 11). It will be noted that water vapor alone can change this parameter by several orders of magnitude. Thus, due to the very high values of surface resistivity, it is easy to see how other contaminants can change the resistivity.

The third point of concern is in the application. As elimination of the present problem requires removing the gradient out of the region in front of the window, a likely place for it is in the window itself. It should be noted that not all glasses are of electrical grade in which case this can not be considered. Glasses with high alkali content, in particular, are subject to alkali migration; this results in a decrease in volume resistivity and may result in a permanent failure after prolonged exposure.

B. Model of the Phototube Window

Several situations developed in the course of the program where two dimensional potential distributions were sought for complex boundaries. Since extreme accuracy was not needed and exact solutions were too costly to develop in terms of time and effort, an approximating technique was used (Ref. 2).

It is similar to the relaxation methods in that it employs first order approximations, but differs in two areas: (1) it does not require an inerative procedure for convergence of the solution, and (2) the node density can easily be changed to account for boundary details. The technique changes the distributed fields problem to a lumped parameter networks problem. When the technique was developed, computers were not yet of age

and the physical construction of a resistive network was an improvement over the iterative technique obtained by hand. Today, however, generalized computer circuit analysis programs (Ref. 3) are available which can give the results quickly and with negligible effort.

MacNeal's method, as used in the window problem, is an approximate solution to Laplace's equation. The objective is to reduce the distributed parameters of the material to lumped parameters. In the case at hand we can assume a uniform conducting sheet, which is to be approximated by discrete resistances connected between nodes at which the potentials are desired. By referring to Fig. 12, the voltage between two typical nodes A and B is the line integral of the dot product of the divergence of ϕ and dl. The first order approximation of this is the product of the length of the line segment between AB and the magnitude of the divergence of the ϕ multiplied by the cosine of the subtended angle. The current flowing between A and B is the negative of the line integral of σ times the dot product of the divergence of ϕ and a unit vector normal to the AB taken between points 1 and 2. The first order approximation of this is the negative of σ times the product of the length of the line between points 1 and 2 and the magnitude of the divergence of ϕ times the cosine of the included angle. The resistance, R_{AB}, when taken as the quotient of the above two approximations becomes the ratio of the line length between AB and $1-2$ times the resistivity.

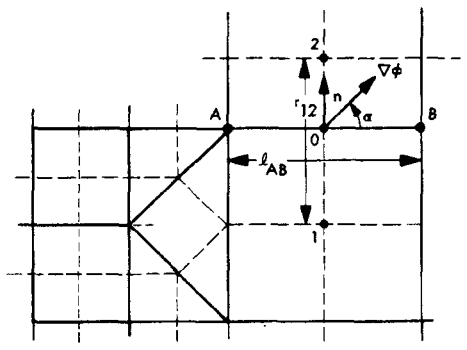

$$\nabla \cdot (\sigma \nabla \phi) = 0 \qquad \text{LAPLACE'S EQUATION}$$

$$V_B - V_A = \int_A^B \nabla \phi \cdot d\bar{l} \qquad \text{VOLTAGE ACROSS } R_{AB}$$

$$I_{AB} = -\int_1^2 \sigma (\nabla \phi \cdot \bar{n})\, dr \qquad \text{CURRENT THROUGH } R_{AB}$$

$$\left.\begin{aligned} V_B - V_A &\cong \ell_{AB} |\nabla \phi|_o \cos \alpha \\ I_{AB} &\cong -\sigma_o r_{12} |\nabla \phi|_o \cos \alpha \end{aligned}\right\} \text{FIRST ORDER APPROXIMATIONS TO VOLTAGE ACROSS AND CURRENT THROUGH } R_{AB}$$

$$R_{AB} = \frac{V_A - V_B}{I_{AB}} = \frac{\ell_{AB}}{\sigma r_{12}} \qquad \text{LUMPED PARAMETER RESISTANCE}$$

Fig. 12. An asymmetrical finite difference network

Using a similar approach and accounting for the dielectric constant, distributed capacitances can also be modeled. A simplification of these results can be made if the material being modeled is homogeneous. Since the solution will require solving a set of linear simultaneous equations, σ will be a common factor and may be taken as 1, if only the potential distribution is desired.

A cross-section of the phototube window-shield region, where discharges were found to be occurring is shown in Fig. 13. The maximum potential occurring on the surface of the window was desired. The photocathode was taken as a conductor on the inside of the window at -2 kV. The glass-laminate epoxy has a volume resistivity six orders of magnitude below the window material and is taken to be at zero potential, as it touches the shield, which is grounded. The potential in the window has rotational symmetry and is symmetrical about its center line. As the worst case was desired, the surface conductivity, which is difficult to evaluate practically, was neglected.

Owing to the symmetry, only half of the window was modeled. A section of this model with the branch-node designations and node potentials determined with the computer program ECAP is shown in Fig. 14. The figure shows the usefulness of the asymmetric technique in that it allows placing the highest node density where the field is most distorted. The input data format for ECAP is shown in Fig. 15. The program is user-oriented in that a simple format is used which topologically describes the network.

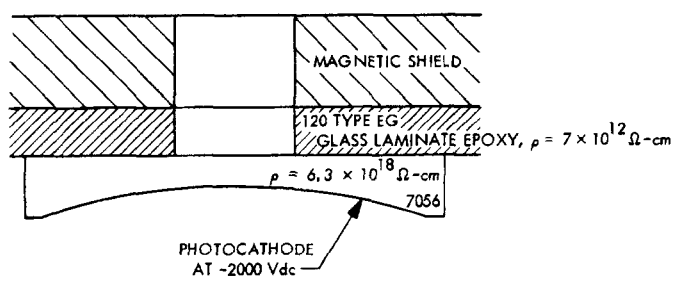

Fig. 13. Cross-section of phototube window-shield assembly

NODE VOLTAGES

NODES	VOLTAGES			
1- 4	-0.10004552D 04	-0.10019150D 04	-0.50290395D 03	-0.10097008D 04
5- 8	-0.51953057D 03	-0.15156857D 04	-0.54135124D 03	-0.10541406D 04
9- 12	-0.28939480D 03	-0.31388897D 03	-0.60467798D 03	-0.11170552D 04
13- 16	-0.36148311D 03	-0.66706336D 03	-0.92771788D 03	-0.46498012D 03
17- 20	-0.77437448D 03	-0.12372267D 04	-0.72406290D 03	-0.93659448D 03
21- 24	-0.11300020D 04	-0.98126544D 03	-0.10040443D 04	-0.11179385D 04
25- 28	-0.14000303D 04	-0.16998783D 04	-0.11929103D 04	-0.13696593D 04
29- 32	-0.13212632D 04	-0.13967316D 04	-0.15639367D 04	-0.14496162D 04
33- 36	-0.14949256D 04	-0.15855444D 04	-0.18449952D 04	-0.17836177D 04
37- 40	-0.17561930D 04	-0.18171427D 04	-0.18384671D 04	-0.18859917D 04
41- 44	-0.19113035D 04	-0.19557292D 04	-0.19769436D 04	-0.19906557D 04
45- 48	-0.19942604D 04	-0.19976586D 04	-0.19976586D 04	-0.19806948D 04
49- 50	-0.19994506D 04	-0.15654100D 04		

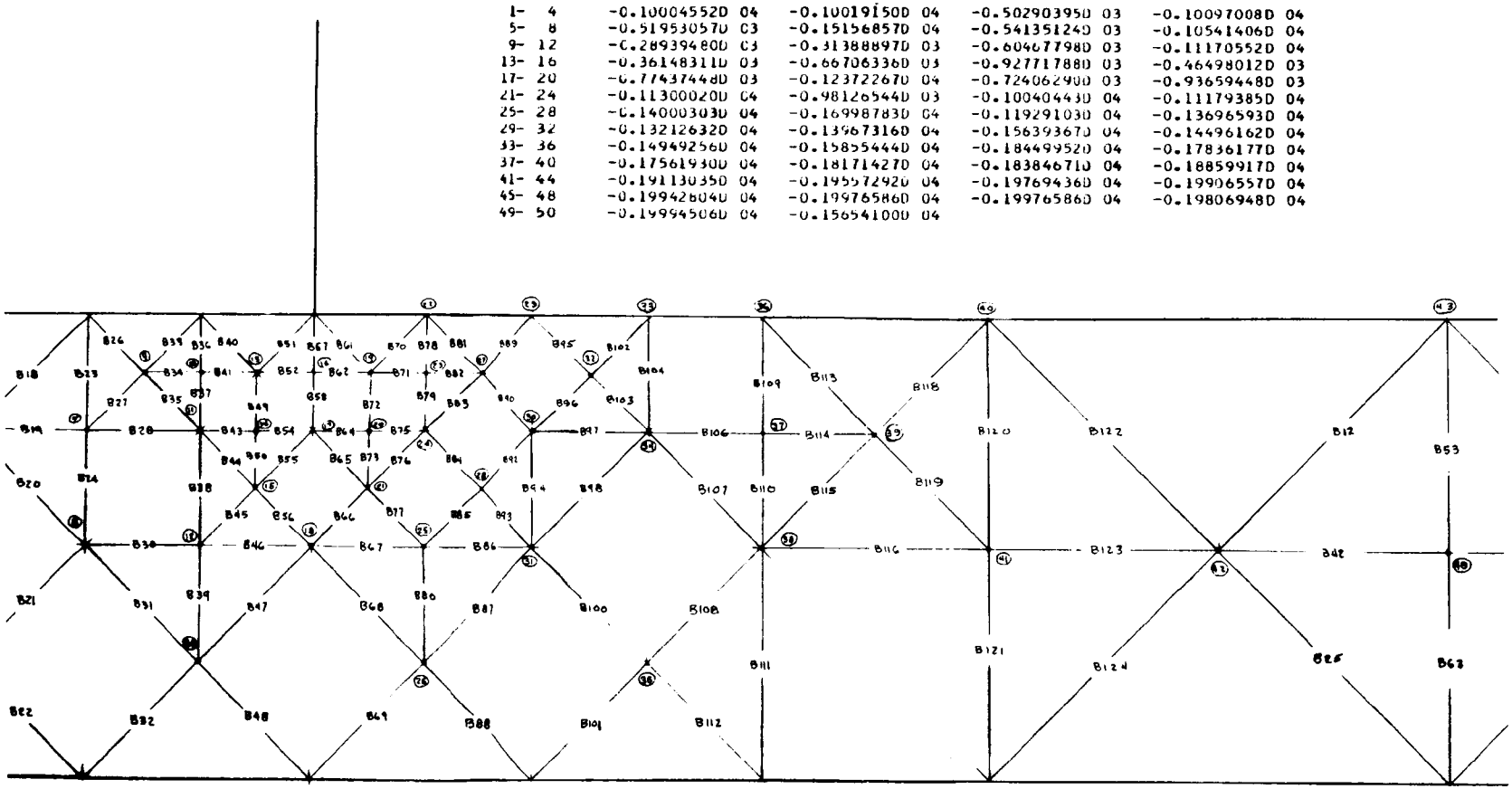

Fig. 14. Phototube window branch-node configuration

```
C     POTENTIAL GRADIENT IN PHOTOTUBE WINDOW
C     IBM 360  19 SEPT 1967   WM J MITCHELL
C
      DC ANALYSIS
C
 81   N(49,0), R=0.0001,E=2000
 82   N(0,1), R=1
 83   N(1,49),R=1
 84   N(2,1), R=1          856   N(15,18),R=1          8106  N(37,34),R=1
 85   N(0,2),R=2           857   N(0,16),R=1           8107  N(34,36),R=2
 86   N(2,49),R=1          858   N(16,17),R=1          8108  N(38,35),R=1
 87   N(0,3),R=1           859   N(44,46),R=1          8109  N(36,37),R=1
 88   N(3,2),  R=1         860   N(44,49),R=2          8110  N(37,38),R=1
 89   N(4,2),R=2           861   N(0,19),R=2            8111  N(38,49),R=2
 810  N(0,3),R=1           862   N(19,18),R=1          8112  N(35,49),R=1
 811  N(3,4),R=1           863   N(46,49),R=1          8113  N(36,39),R=2
 812  N(43,42),R=2         864   N(20,17),R=1          8114  N(39,37),R=1
 813  N(4,49),R=2          865   N(17,21),R=2          8115  N(39,38),R=2
 814  N(0,5),R=1           866   N(21,18),R=1          8116  N(41,38),R=2
 815  N(5,4),R=1           867   N(25,18),R=2          8117  N(47,46),R=1.053
 816  N(4,6),R=1           868   N(18,26),R=2          8118  N(40,39),R=1
 817  N(6,49),R=1          869   N(26,49),R=1          8119  N(39,41),R=1
 818  N(0,5),R=2           870   N(22,19),R=2          8120  N(40,41),R=2
 819  N(7,5),R=1           871   N(23,19),R=1          8121  N(41,49),R=1
 820  N(5,8),R=2           872   N(19,20),R=1
 821  N(8,6),R=1           873   N(20,21),R=1
 822  N(6,49),R=1          874   N(45,44),R=1
 823  N(0,7),R=2           875   N(24,20),R=1
 824  N(7,8),R=1           876   N(24,21),R=2
 825  N(42,49),R=2         877   N(21,25),R=1
 826  N(0,9),R=1           878   N(22,23),R=1
 827  N(9,7),R=1           879   N(23,24),R=1
 828  N(11,7),R=2          880   N(25,26),R=1
 829  N(43,44),R=2         881   N(22,27),R=2
 830  N(12,8),R=1          882   N(27,23),R=1
 831  N(8,50),R=2          883   N(27,24),R=2
 832  N(50,49),R=1         884   N(24,28),R=1
 833  N(0,9),R=2           885   N(28,25),R=1
 834  N(10,9),R=1          886   N(31,25),R=2
 835  N(9,11),R=2          887   N(31,26),R=2
 836  N(0,10),R=1          888   N(26,49),R=1
 837  N(10,11),R=1         889   N(29,27),R=1
 838  N(11,12),R=2         890   N(27,30),R=1
 839  N(12,50),R=1         891   N(44,49),R=1
 840  N(0,13),R=2          892   N(30,28),R=1
 841  N(13,10),R=1         893   N(28,31),R=1
 842  N(48,42),R=1         894   N(30,31),R=2
 843  N(14,11),R=1         895   N(29,32),R=1
 844  N(11,15),R=2         896   N(32,30),R=1
 845  N(15,12),R=1         897   N(34,30),R=2
 846  N(18,12),R=2         898   N(34,31),R=2
 847  N(18,50),R=2         899   N(45,46),R=0.932
 848  N(50,49),R=1         8100  N(31,35),R=1
 849  N(13,14),R=1         8101  N(35,49),R=1
 850  N(14,15),R=1         8102  N(33,32),R=1
 851  N(0,13),R=2          8103  N(32,34),R=1
 852  N(16,13),R=1         8104  N(33,34),R=2
 853  N(43,48),R=1         8105  N(46,49),R=0.932
 854  N(17,14),R=1
 855  N(17,15),R=2
```

Fig. 15. Input data for ECAP

The results of this simulation are plotted in Fig. 16. From this, it can be seen that most of the window is above the minimum sparking potential for air. If the photocathode surface resistivity was reduced through contamination, this result would change drastically as the steady-state currents establishing the field are extremely small. If a conductor at ground potential was placed on the clear sector of the window at 25°C, a current of only 2.8×10^{-14} A would flow; thus, it is easy to appreciate that surface contamination may not be insignificant.

At this point, several hypotheses can be developed to account for some of the observed phenomena. First the delayed occurrence of repetitive discharges were probably due to contamination. This first appeared after a thermal vacuum exposure at low pressures and temperatures from −55 to +55°C. This exposure probably served to vaporize a major portion of the volatile residues, thus changing the potential distribution and the pressure-temperature range of discharge. Second, outside the critical region, the surface can sustain a higher potential without discharge. As the pressure is dropped or raised quickly from outside the critical region, the charge does not have time to "leak off" through the gas and/or across the surface and discharges. If the pressure is changed slowly, nonrecurring discharges do not occur lending credence to the concept that leakage does occur.

C. Solutions

The solution, as in the rest of the high voltage system, requires that potentials above the minimum sparking value be removed from the gas. The particular application may impose additional constraints on a realizable approach. First, the solution should not attenuate or restrict the spectral transmission of the window. Second, as already noted, the gradient can not be constrained within all glasses, as dielectric failure may occur.

Several solutions are available. A conductive thin film could be applied to the tube directly or to a fused-silica disc which would be applied to the window. The former, would constrain the gradient in the window, the latter, in the disc. Similarly, as shown in Fig. 17, the potential can be controlled using discs of different volume resistivity glasses. A disc of 0080 glass placed on a window of 7056 glass would place most of the potential in the window; if an additional section of 7940 fused silica were used between the above, the potential would be in the silica. A somewhat novel approach would be to constrain the potential in a stable gaseous element; this is illustrated in the bottom of Fig. 17. Two specimens for shielding with glass are shown in Fig. 18; Fig. 19 shows one using a gas.

As an example, Fig. 20 shows the potential distribution for a 0.025-in. disc of 0080 glass placed directly on the window. The highest potential on the window surface is in the order of 100 V. An engineering tube, which was confirmed to exhibit window discharges under the same set of conditions as the qualification unit, was outfitted with an 0.050-in. disc of 0080 (Fig. 21). This tube was potted in a shield using the other modifications already described and was exposed to reduced pressures at temperatures up to +70°C; a thermal exposure beyond this point would cause permanent damage to the photocathode and would be well beyond our immediate requirements. The above solution was found not to result in any unusual tube response in terms of sensitivity or dark current.

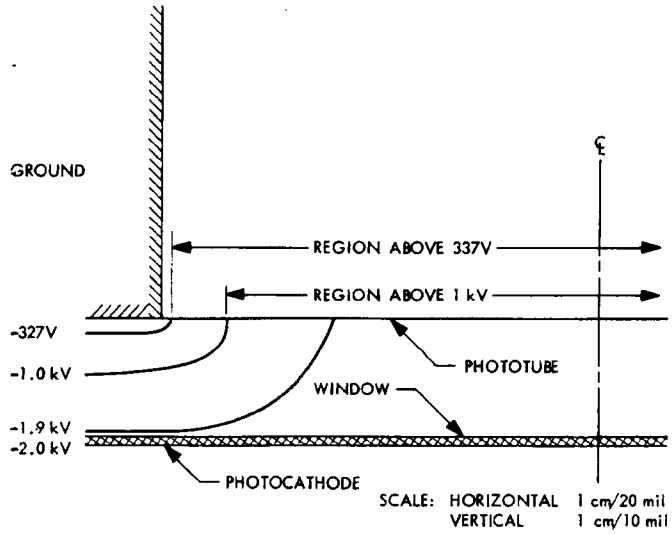

Fig. 16. Phototube window potential distribution

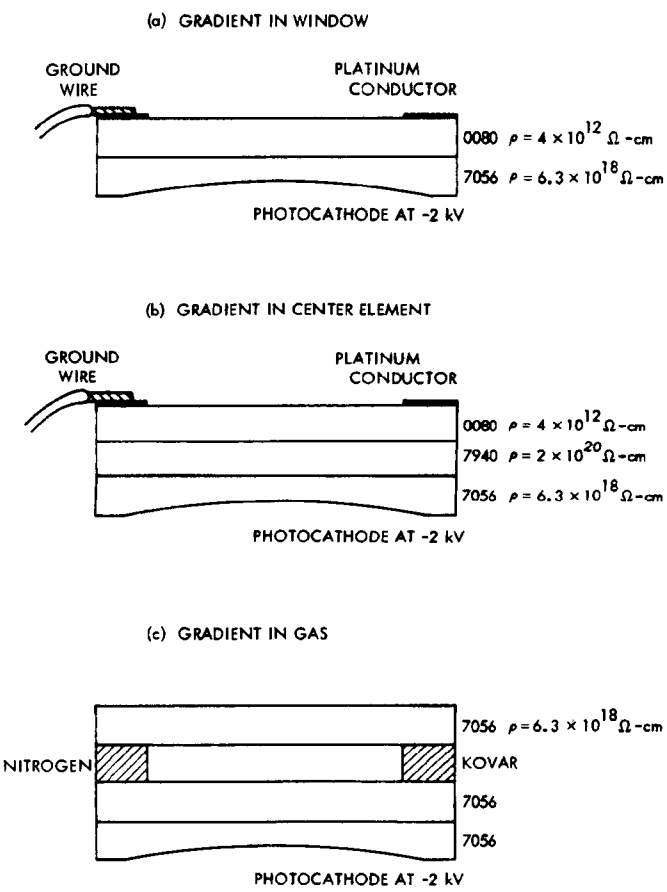

Fig. 17. Cross-sections of window shields

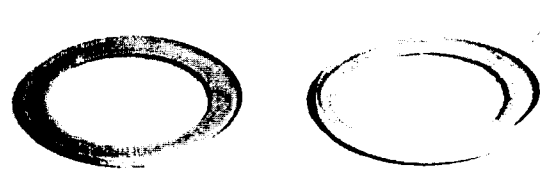

Fig. 18. Shielding with glass

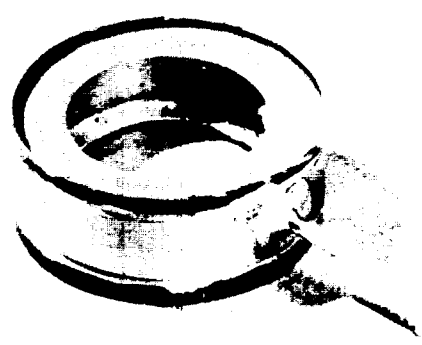

Fig. 19. Shielding with glass

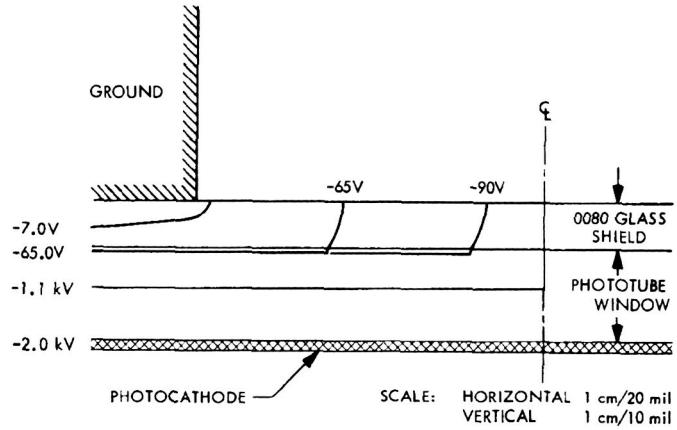

Fig. 20. Phototube window potential distribution with glass shield

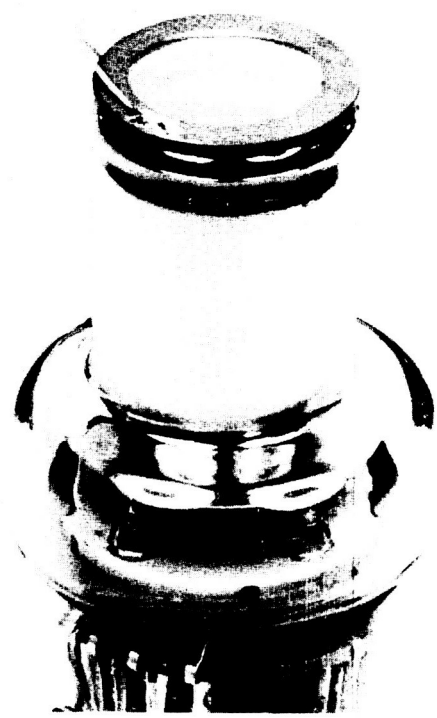

Fig. 21. Disc of No. 0080 glass shield applied to phototube

Appendix

Modeling Distributed Capacitance

If the potential on the boundary of a material is time-varying, the potential distribution becomes a function of both conductivity and permittivity. For this case, and others already considered, it is assumed that the conductivity of the electrodes on the boundaries is very high compared to that of the enclosed material.

If a system has two dimensional plane symmetry, lumped capacitive and resistive elements can be used to model the distributed system. This is a very restrictive requirement in a practical situation, but the speed with which results can be obtained makes it useful in understanding relative effects and bounding the actual results.

A typical volume element is shown in Fig. A-1. The discrete resistance between nodes A and B is as before

$$R = \frac{-\int \bar{E} \cdot dl}{\sigma \oint_S \bar{E} \cdot ds} = \frac{V}{I}$$

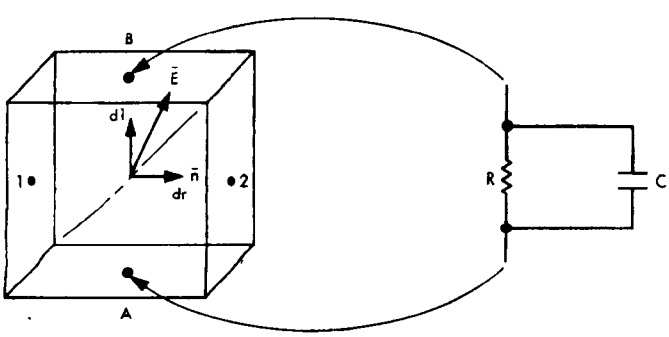

$$R = \frac{-\int \bar{E} \cdot dl}{\sigma \oint_S \bar{E} \cdot dS} = \frac{V}{I} \cong \frac{1}{\sigma K}\left[\frac{\int_A^B \bar{E} \cdot dl}{\int_1^2 \bar{E} \cdot \bar{n}\, dl}\right]$$

$$C = \frac{\epsilon \oint_S \bar{E} \cdot dS}{\int E \cdot dl} = \frac{Q}{V} \cong \epsilon K \left[\frac{\int_1^2 \bar{E} \cdot \bar{n}\, dl}{\int_A^B \bar{E} \cdot dl}\right]$$

Fig. A-1. Time varying model

which is

$$R = \frac{1}{\sigma K} \frac{\int_1^B \bar{E} \cdot dl}{\int_1^2 \bar{E} \cdot \bar{r}\, dl}$$

where the ratio of the two integrals approaches the ratio of the line length A-B to the length 1-2. The two constants σ and K represent the bulk conductivity and material thickness, respectively.

Similarly, the distributed dielectric properties can be accounted for with discrete capacitors in shunt with the resistors. The technique is such that the branch-node model, Fig. 14, used in determining the resistors can be employed to evaluate the capacitors. The discrete capacitors are equal to

$$C = \frac{\epsilon \oint_S \bar{E} \cdot ds}{\int \bar{E} \cdot dl} = \frac{Q}{V}$$

which, taking the same consideration as for the resistors, is

$$C = \epsilon K \frac{\int_1^2 \bar{E} \cdot \bar{r}\, dl}{\int_A^B \bar{E} \cdot dl}$$

Thus, it is seen that the ratio of integrals is the inverse of that arrived at for the resistor case. As such, the information to determine the discrete capacitors is known if the permittivity ϵ is known.

This network of shunt resistor-capacitor combinations is easily handled with the same user-oriented computer programs already noted. These programs have the capability of generating time functions on the boundaries. Thus, the steady-state ac, dc or the transient potential distributions can be determined.

Discussion

Bunker: You mentioned you had space-proofed high-voltage wire. I wonder first of all, was it shielded? In other words, a coaxial configuration; and, two, what were the insulation materials?

Mitchell: I can't give you the number for the insulating material. It is manufactured by Haveg Industries, of Winooski, Vermont, and it was used on the Nimbus program, for one. Some people from RCA might be able to provide further information as to exactly what the wire was. I believe they used it also. And, yes, it was coaxial. The dielectric was a silicone rubber and it had an outer Teflon shield over an outer braid.

Stern: Why didn't you perhaps try avoiding the problem of a breakdown at the window by having the photocathode at ground potential and using your anode at high positive potential?

Mitchell: Well, as I said originally, we had purchased several pieces of hardware and we had to use the existing design.

References

1. Bosch, T., *Spaceborne Corona and Sparking in Spaceborne Photomultipliers,* GAEC Report No. AV-252R-329.0, August 2, 1967.
2. MacNeal, R. H., *Quarterly of Applied Mathematics,* Vol. XI, Brown University, Providence, R. I., pp. 295–310, 1953.
3. Anon., "Electric Circuit Analysis Program," in *User's Manual,* ECAP-1620-EE-02X. Internal Business Machines Corporation.
   Molmber, A. F., and Cornwell, F. L., *Network Analysis Program,* NET-1, Los Alamos Scientfic Laboratory, Los Alamos, N. M.
   Anderson, J. G., *Septer,* Air Force Weapons Laboratory, Kirtland AFB, N. M.

N70-32294

A Vented High-Voltage System for Satellite Applications

D. Laffert
Sylvania Electric Products, Inc.
Needham Heights, Mass.

By a vented high-voltage system for satellite applications, I mean that the system sees the ambient, whatever it is, atmospheric pressure, a partial pressure, or a high vacuum. Before going any further, I would like to state that in my opinion, in most cases, the best approach for high-voltage packaging in satellite applications is to use a solid potted technique. In some special situations, this approach just isn't desirable or maybe it is impractical. Hence, the question may be asked, what can be done?

We have designed, built, and partially tested a high-voltage vented system which I intend to discuss. The work was performed on the *Orbiting Astronomical Observatory (OAO)* program for an experiment designated *PEP*. It is the last in the *OAO* series and is basically an orbiting telescope for measuring ultraviolet light from stars. The high voltage is required to power the photomultiplier tubes which are the data gathering devices.

This particular system is especially well suited for a vented technique for the following reasons:

(1) It is required to operate one full year in orbit.

(2) It is only required to operate properly in the hard vacuum.

(3) The initial turn-on time after injection of the satellite into orbit can be quite long; i.e., over a week.

It is understood that in spite of these ground rules it is possible and, indeed, is extremely likely in fact that arcing may still occur. This can happen for many reasons:

(1) The power supply could be improperly energized in the partial pressure region.

(2) During tests, man-produced faults can occur.

(3) Even at hard vacuum, momentary pressure changes could occur resulting in arcing/breakdown.

Bearing these facts in mind, we have defined one simple design ground rule as follows: the high-voltage supplies must be capable of operating at all pressure and all conditions without failure to themselves or to adjacent components and circuits.

We have taken the basic vented approach using good common high-voltage techniques and added a few modifications of our own. Very briefly, the modifications are (1) current limiting in the power supply, (2) arc detection in the power supply, (3) protection of adjacent circuits through shielding, (4) protection of adjacent circuits

through special electrical design, (5) component selection, and (6) ruggardized vented mounting techniques.

Current limiting is accomplished electronically. We simply sense and limit the input current. Basically, this feature is intended to protect the power-supply regulator when the output is shorted or overloaded; however, it has a second, more attractive, feature. Once the overcurrent circuit has been energized and the power supply shuts itself off, it stays off until the input voltage has been commanded off and then on again. This feature is intended primarily to protect the supply against shorts on the output or corona that cannot be detected as an arc. Because the load current is relatively constant, changes to the output load can be sensed in the input. Therefore, if the input current increases above a specified level the supply is automatically shut down and no further damage can occur.

An electronic arc-detector circuit has also been included in the design. The circuit monitors the current return from the high voltage. If an arc, fairly large current, occurs the circuit senses a voltage transient on the ground and stops the power oscillator. The effect is identical to that of the current limiter; i.e., it shuts the power supply down until the supply is commanded off then on again from the ground. The advantage of this feature is that arcs cannot continually occur until some component fails.

The adjacent circuits have been critically examined to determine their susceptibility to arcs and transients on the line. One type of circuit of particular interest is the preamplifier circuit associated directly with the photomultiplier outputs. During testing of the PMT's, we found that if the PMT's arced, the arcing produced large transients on the preamplifier inputs causing semiconductor failures. Therefore, we added some simple input circuitry, two diodes and a resistor; now the preamplifiers can withstand 5000-V transients on their input without damage to any of the components.

All adjacent circuitry has been protected by containing all high voltage in shielded vented containers. This required using shielded high-voltage cable to run high voltage from one container to another. Screening has been added on all vent holes. In addition, we have taken great pains to isolate the low-voltage portions of the high-voltage power supply from the high-voltage portions. An interesting case is the high-voltage transformer. We found that we could reliably impregnate the windings of the transformer but that arcing could occur at the high-voltage terminals inside the case. Therefore, we designed a sort of hybrid potted/vented transformer where the core and windings are impregnated and the high-voltage terminals are exposed to the ambient.

Component selection has also been critically considered. Much system improvement can be accomplished in the areas of components. For example, one component manufacturer was quite indignant that we were using his part to suppress voltage transients. He threatened to write us a letter stating that if we used his component in this way he would divorce himself of all responsibility for its proper operation. We did, and found that the part performed very well. Later, we ran extensive tests on the device in our special application. The manufacturer looked at the data and decided that, in fact, his device would perform in this situation. Therefore, in special cases, such as high voltage in space, the manufacturer doesn't know very much about his product. Some trouble was experienced with high-voltage diodes failing short for unexplained reasons. The diodes extremely high-reliability types and were being operated well within specified ratings. Investigation showed that when the power supplies were purposely arced, for testing, the output capacitors discharged directly through the diodes to ground and the surge currents, which were quite high and of very short duration, caused diode failure. Once the problem was defined, the solution was quite simple. We selected diodes capable of conducting large current surges and added small current limiting resistors in series with the diodes. Therefore, selection of high-reliability components must be complimented with detailed circuit considerations.

Assembly and mounting techniques for an improved vented system were also considered. We were looking for a good rugged modular assembly which could also be easily vented. Due to the severe vibration and acceleration requirements of the *PEP*, we felt that a ruggedized but lightweight assembly was absolutely necessary. In addition, we wanted to assemble the system such that all components were firmly held by the potting compound but that all high-voltage connections were vented (Fig. 1). The following procedure worked well: all components were mounted on a printed circuit board whose etch runs had been carefully examined to reduce voltage gradients (maximum voltage stress in the order of 5 V/mil). All solder connections were carefully rounded and general, good high-voltage practices were observed. Next, the assembly was conformally coated with two thin layers of epoxy. Finally, the printed-circuit cards,

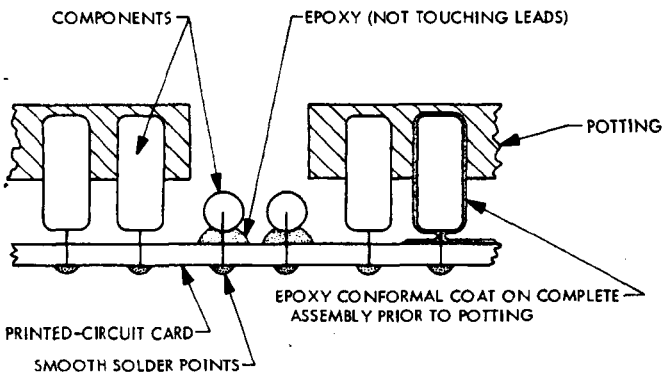

Fig. 1. Ruggedized mounting technique

with the components, were inserted upside down in a special mold to achieve the rugged assembly shown in Fig. 1. The end result was a layered type of structure which was approximately 50% open with easy venting routes from all open portions to the external vent holes.

All preliminary testing, so far, has been confined strictly to vacuum and thermal vacuum tests. To date, we have had no failures. As expected, testing at hard vacuum produced no arcs or detectable corona. All vacuum tests were conducted at hot temperature to encourage outgassing and to simulate the effects of radiation and at cold temperature for worst-case mechanical stress. Under these conditions, no arcing/corona was detected. Tests were also conducted where the protective circuitry, the arc detector, was purposely disabled and the chamber vacuum was maintained within the partial pressure range. Breakdown and corona were observed periodically throughout the duration of the test; the test continued for four days. At the conclusion of the test, the system operated properly either at ambient pressure or in a hard vacuum.

In the future, we plan to run the complete *PEP* system, not just the high voltage, through a detailed thermal vacuum test. At this time we hope to purposely cause the high-voltage power supplies to arc so as to check both the effect on the high-voltage portions of the system as well as on the adjacent low-level circuitry. Thermal plasma tests will also be conducted. Previous tests on the open-face photomultiplier tubes in the system caused the tubes to produce false counts. Considering this, it could be possible that the thermal plasma could also initiate corona in the high-voltage power supplies. If so, we are prepared to add ion traps to all vent holes in the power-supply package. Finally, we have prepared a proposal to perform additional tests to study the effects on the high voltage due to thermal plasma, trapped radiation, ultraviolet light, gamma radiation, and cosmic radiation.

This proposed high-voltage system works well for our special application because of the following additions and improvements to the basic vented approach:

(1) Current limiting.

(2) Arc detection with automatic shut off.

(3) Protection of adjacent circuits through shielding.

(4) Protection of adjacent circuits by special design.

(5) Proper component selection.

(6) Ruggardized venting and mounting techniques.

Discussion

Piemersma: I can see where your system works very well, but could you specify the advantages of your system over the fully encapsulated system?

Laffert: We have high-voltage photomultiplier tubes with no faces on them, open to the environment, and they must operate without arcing, or if they are arcing it doesn't matter if the power supply is arcing at the same time.

Heuser: You mentioned you had a corona detection system in the high voltage or a return for your power supply. Could you give me an idea what this detection system was?

Laffert: It basically looks like two transistor type of SCR, and all we do is monitor the ground return. If we see a large transient on this thing, it triggers the SCR and this shuts the power supply off.

We did some work along those lines to verify that the transients on the line couldn't cause the thing to trigger and we also have a large safety factor in there.

Diamond: First of all, I recall you said at the beginning you favored complete encapsulation of supplies; why?

Laffert: Well, that wasn't just to get the wolves off my tail, I really do. This is a special situation that we have. We have these open-faced PMT's, the supplies are remote from the PMT's, unfortunately.

Diamond: Let me interrupt. It is not special to us. We have exactly the same situation.

Stern: Stan, I don't want to make any comments at this time, but you also have a lot of problems with your system too.

Diamond: Well, I am reporting no problems at this time. What sort of impregnant do you use in your transformer system?

Discussion (contd)

Laffert: We use the 3M 235/253 system. If I recall, the 235 is very thin. It can run inside the laminations and the 253 is a little heavier and we put that on as a secondary operation.

Diamond: So the 253 is not so much an impregnant as an encapsulant?

Laffert: That is correct, and they are very compatible with each other.

Michaels: What is the urethane that you use for this coating and what is the upper temperature at which you have actually tested it?

Laffert: I haven't got the exact name of the urethane. I can find out for you. We test in thermal vacuum up to 85°C, but we don't envision any high temperature at all in space. Our nominal operating temperature is going to be somewhere between 0°C and −30°C and that was part of the stated problem. Maybe I didn't state it at first and maybe I should have.

We expect to go to −55°C. We even anticipate, if the system isn't turned on, going down to −80°C.

Michaels: Have you used any special preparation methods? Most of the urethanes I am aware of have fairly high vapor pressures at that temperature and I would expect problems with that construction.

Laffert: Unfortunately, I don't have the name of it. Maybe I can get quickly. If I recall, this particular urethane is very, very good for outgassing consideration.

N70-22295

Open Construction Magnetic Components for the *SERT II* Power Conditioner

D. S. Yorksie
Westinghouse Electric Corporation
Aerospace Electrical Division
Lima, Ohio

J. Lagadinos
Raytheon Company
Microwave and Power Tube Division
Waltham, Mass.

I. Introduction

The purpose of the *Space Electric Rocket Test II* (*SERT II*) mission is to demonstrate the feasibility of a mercury-bombardment ion-thrustor propulsion system for long-duration space missions. The *SERT II* power conditioner operating at a power level of approximately 1 KW supplies the necessary ac and dc voltages required by the thrustor. The power source is a solar photovoltaic array. The main thrustor requirements are:

(1) Positive 3000 Vdc at a nominal power of 750 W.

(2) Negative 1800 Vdc at a nominal power of 3 W.

(3) Various low-voltage ac and dc supplies operating at the positive 3000-V potential of the screen supply.

(4) Other low-voltage ac and dc supplies.

High-voltage isolation at 2:1 derating is provided by magnetic components in the *SERT II* power conditioner which is vented to the space vacuum.

The *SERT II* mission requires continuous operation for 6 mo in the space vacuum. In addition, the magnetic components are required to operate at room ambient conditions but not at low pressures between the two operating points. Maximum vacuum operating pressure is defined as 1×10^{-6} torr.

The philosophy of open-construction magnetic components was applied to all of the magnetic components used on the program and included:

(1) Power transformers with high-voltage windings.

(2) Power transformers with low-voltage secondary windings operating at high voltage.

(3) Low-voltage power transformers, saturating transformers, current transformers, magnetic amplifiers, and filter inductors.

(4) Low-voltage inductors operating at high voltage.

The primary design objective in developing open-type construction magnetic components was to take advantage of the inherent dielectric strength of the space vacuum. Such construction provides for minimum weight and avoids problems resulting from outgassing of encapsulating compounds. The space vacuum provides a predictable and stable operating environment independent of the mission duration.

The approach used on the program to accomplish these objectives was to eliminate potential problem areas through selection of the most suitable materials, simplified construction, and experimentally-proven design practices. Tradeoffs were made according to the established program priorities, as follows

(1) *Reliability.*

(2) Efficiency.

(3) Schedule.

(4) Weight.

Approximately 6 mo were available to implement the primary design objectives of open-construction magnetic components and to supply the first complete sets of breadboard magnetic components meeting the electrical and mechanical requirements of the power conditioner design.

This paper describes the development program which led to and the essential characteristics of the open-construction magnetic components developed on this program. Emphasis is placed on the high-voltage power transformers.

II. Configuration Evaluation and Design Criteria

Configuration evaluation, the formulation of design criteria, and the selection of suitable insulating materials was an iterative process. Certain decisions regarding configuration and materials had to be made early in the program. This permitted work to start immediately in the evaluation of magnetic materials, insulating materials, and coil bobbin construction to obtain the necessary data to optimize the selected design. During this process, changes were made in the original concepts where necessary and additional materials were evaluated as they become known. At the start of the program, DU laminations were selected for the high-voltage power transformers because of the following advantages:

(1) DU laminations are adaptable for use with layer wound coils, allowing the manufacture of coils that are properly protected against voltage breakdown. Conventional windings and winding techniques can be used. This allows for more reliable insulation and better control in manufacturing resulting in finished coils of more consistent and reproducible quality.

(2) The DU laminations allow two coil construction to be used on units; this type of construction is best from a volume utilization viewpoint.

(3) Mechanical characteristics for vibration and shock are improved and superior mounting to the heat sink is obtained.

The high-voltage magnetic components can be categorized as follows:

(1) Output power transformers with low-voltage output windings operating at the positive 3000 V potential of the screen supply.

(2) Output power transformers with high-voltage secondary windings; i.e., the screen supply power transformers with individual transformer outputs of 1000 V in series on the dc side to obtain the +3000 V screen potential, and the accelerator supply power transformer with 2 secondary windings of 900 V in series on the dc side to obtain the 1800 V accelerator potential.

Test coils were designed, fabricated, and tested to develop the design criteria to be used in designing corona-free coils. The test coils were designed with sufficient insulation to prevent the occurrence of corona due to interwinding stresses. The main objective of these tests was to determine the required voltage creep paths and voltage strike distances in vacuum. This information was essential in determining coil-end margins required for corona-free operation in a vacuum. Margin width is one of the criteria determining final unit size. Although solid bobbins were contemplated for use on final units, thus adding extra barrier and creep path to the end-coil margins, some determination of creepage characteristics over various materials in a vacuum had to be made before design work could start. The results of the initial tests are provided in Table 1. The results showed that secondary lead breakout and spacing between these

Table 1. *SERT II* summary, corona tests on specimen coils

Core	Cell tube	Primary wire	Primary margins and layer insulation	Insulation over primary	Insulation over shield	Secondary wire	Secondary margins and layer insulation	Corona starting voltage between secondary and primary and core grounded	Corona level at instant of starting	Ambient and vacuum at which test was run	Stress on interwinding insulation at corona level	Where flashover occurred	Flashover voltage	Impregnant
I. 0.5 × 3 in. 29 GA M6X 0.5 in. stack	0.060 in. epoxy glass & 3 × 0.005 3M-MX-2300 Fibrous Isomica	No. 24 ML 71 turns	1/8 in. single layer	5 layers 0.005 in. thick Mylar & one layer 0.005 in. 3M-MX-2300 Fibrous Isomica	No shield	No. 24 ML 71 turns	1/8 in. single layer	5500 V RMS	Measuring equipment not available at time of test	32°C 2×10^{-6} torr	188 V/mil RMS	From secondary lead breakout to core	7500 V RMS	3M No. Em-250
II. 0.004 in. thick DU-50 Super MU 40 0.5 in. stack	0.040 in. epoxy glass & 3 × 0.0055 epoxy mica (Macallen No. 98604)	2 × No. 20 ML 22 turns	15/32 in. 0.0055 epoxy-mica (Macallen No. 98604)	2 × 0.0055 in. epoxy mica over & under	10 × 0.0055 in. epoxy mica under primary shield 9 × 0.0055 in. epoxy mica over secondary shield	Sec. No. 1 = No. 27 ML Sec. No. 2 = No. 32 ML	15/32 in. 0.0055 in. epoxy mica	Sec. No. 1 to primary and ground 4000 V RMS Sec. No. 2 to primary and ground 3500 V RMS	300 pC 250 pC	32°C 2×10^{-6} torr	73 V/mil RMS	Was not brought to breakdown point	—	None
III. 0.006 in. thick DU-37 HY-MU 80 0.5 in. stack	0.040 in. epoxy glass	2 × 21 HML 29 turns per leg	0.25 in. 0.005 in. Kapton	2 × 0.005 in. Kapton	6 × 0.005 in. Kapton	No. 28 HML 245 turns per leg	3/4 in. 0.005 in. Kapton	1000 V RMS	Unable to measure because of flashover	32°C 4×10^{-6} torr	34 V/mil	From Secondary lead breakout to shield tab	1000 V RMS	None
IV. 0.006 in. thick DU-37 HY-MU 80 0.5 in. stack	0.040 in. Teflon	2 × 21 HML 29 turns per leg	0.25 in. 0.005 in. Silicone Isomica 3M No. 2855	2 × 0.005 in. Silicone Isomica 3M No. 2855	6 × 0.005 in. Silicone Isomica 3M No. 2855	No. 28 HML 245 turns per leg	3/4 in. 0.005 in. Silicone Isomica 3M No. 2855	3000-3500 V RMS occasional spikes at lower voltages	400-500 pC	Core & coil at 32°C 2×10^{-6} torr	117 V/mil	Secondary lead breakout point & core	3500 V RMS	None

PRECEDING PAGE BLANK NOT FILMED

leads and the ground plane were the major problems with the test specimens and provided the minimum margin requirements. Corona measurements were made using a Biddle Catalog No. 665878 corona test set with calibrator.

A. Electrical Stress Limits

The electrical stress limits used in the design of the *SERT II* open-construction magnetic components are detailed below. In addition to the limits used, the normal limits in each case are stated for comparative purposes.

1. Layer insulation. The maximum working stress on layer insulation is 150 V/mil. This applies to both toroidal and bobbin units and assumes a uniform field distribution. Normally, the materials used for layer insulation in the program would be rated at 250 V/mil.

2. Voltage creep and strike. The maximum working stress relating to voltage creep and strike is 12 V/mil. This level assumes a uniform field distribution and applies to bobbin and toroidal units. The normal stress limit would be 15 V/mil.

3. Coil margins. The maximum working stress on coil margins for layer wound units is 8 V/mil. The normal stress limit would be 15 V/mil.

4. Magnet wire. The maximum wire insulation stress limit is 80 V/mil and applies to toroidal and bobbin units. The normal stress limit would be 170 V/mil.

5. Current density. The maximum current density is 290 circular mils/amp. The interrelationship of operating mode, unit size, efficiency, heating, weight, and reliability combine to set the limit for each design.

B. Mechanical Stress Limits

Working stresses have been calculated for the hardware used in the magnetic components; this information is presented in Table 2.

C. Mechanical Configuration

The selected mechanical configurations result from the type of core considered most appropriate for each application.

Table 2. Mechanical stress limits

Material	Allowable stress, lb/in.^{2}	Maximum working stress, lb/in.^{2}	Safety factor
Aluminum, 5052-H32	17,500, endurance limit	5100	3.4:1
Silicone glass, laminate G7	18,000, ultimate strength	3460	5.1:1
Stainless steel, type 302	34,000, endurance limit	8000	4.2:1

1. Toroidal units. Toroidal cores were selected for all low voltage magnetic components. Low voltage was considered present when the wire enamel was sufficient to sustain the voltage between the windings. In those cases where more than 100 V exists between windings, Kapton insulation is used for additional protection. In order to limit crossovers, one should obtain a tight winding without overstressing the wire, and avoid twisting the wire; wire sizes 22 AWG to 29 AWG are wound by hand. Smaller diameter wires (30 AWG to 34 AWG) are wound by machine.

The terminal panels of fiberglass laminate for toroidal units are secured to the units by means of a bolt which passes through the center hole remaining in the toroid after winding (Fig. 1).

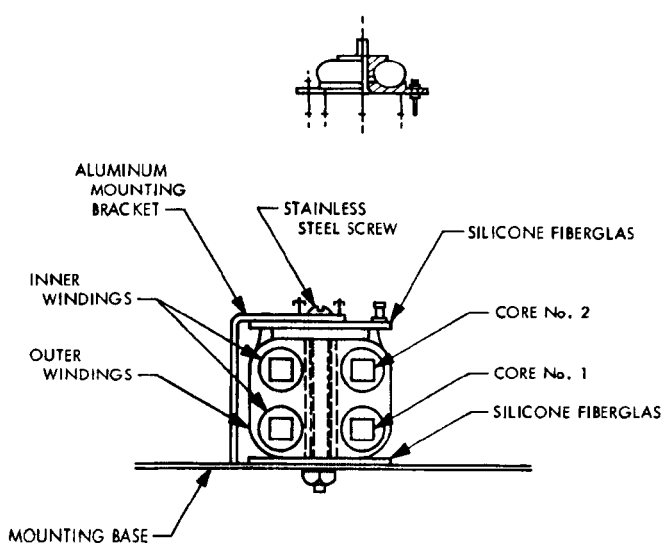

Fig. 1. Typical mounting configurations for toroidal units

2. *Bobbin wound cores.* All of the main high-voltage transformers have the same general configuration differing slightly in size. As previously discussed, DU-type laminations were selected as the core configuration for these units.

The high voltage transformers are designed for 2-coil construction. The criteria used in selecting this type of construction were (1) maximum volume utilization, (2) reduction of voltage gradient, (3) provision for termination separation, (4) improved heat transfer from windings to core, and (5) improved coupling between primary winding halves.

Bobbin-type construction was selected for layer-wound coils. This selection was based on voltage and mechanical considerations. The use of bobbins provides a solid barrier at the ends of the coils for added voltage protection.

Since this barrier or end plate is an integral part of the coil tube, it will retain its position under mechanical stresses. The end plates also provide locations for high-voltage terminations.

Certain types of coils require extremely tight coupling. The following procedure is used on this category of magnetic components:

(1) One half of the low-voltage winding is wound on the coil tube including its coil insulation.

(2) An electrostatic shield is wound over this and covered by insulation.

(3) The high-voltage winding is placed in position and its coil insulation is emplaced.

(4) A second electrostatic shield is then wound on this and covered with insulation.

(5) The other half of the low-voltage winding is wound over the shield wrap.

(6) All required interconnections are made external to the coils.

When winding interleaving is not required, the sequence is as follows:

(1) The low-voltage winding, its coil insulation, and the electrostatic shield are wound on an inner coil tube which fits over the laminations.

(2) The high-voltage winding is wound on a separate coil tube whose inside dimensions coincide with the outside dimensions of the low voltage assembly.

(3) The two subassemblies are then assembled coaxially and the bobbin end panels are placed in position to form the completed coil assembly.

(4) Lead breakouts and the shield tabs are brought out directly through holes in the end panels.

The copper electrostatic shields serve two purposes: (1) they shunt high-frequency signals to ground and,

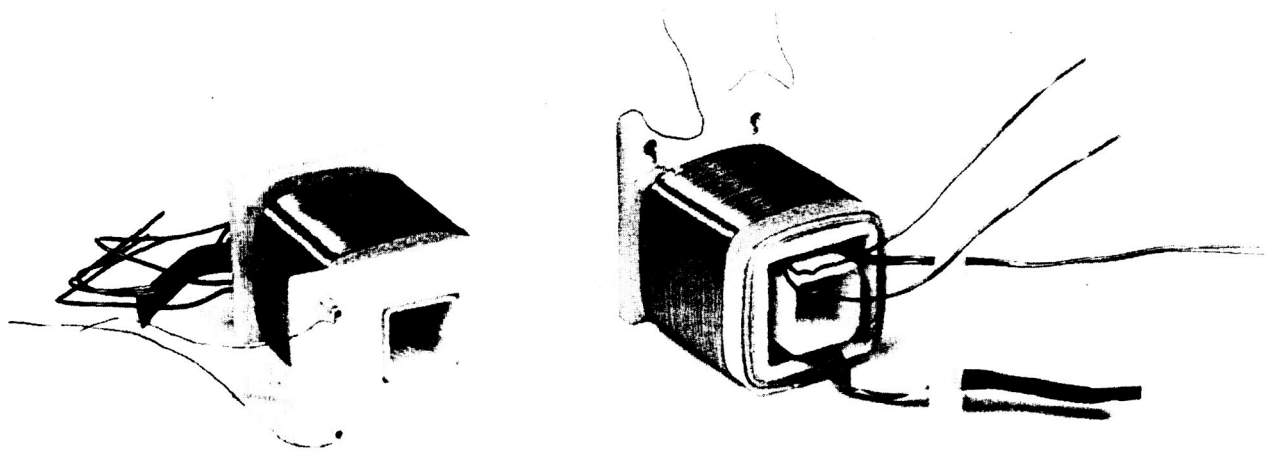

Fig. 2. High-voltage power transformer bobbin

thereby, protect the low-voltage primary circuits from harmful transients, and (2) the shields are connected to the core by copper tabs which serve to conduct heat from the center portions of the coils.

Details of a high-voltage power transformer bobbin are shown in Fig. 2.

III. Design Considerations and Selection of Materials

The vacuum encountered in space will have three important effects on the *SERT II* magnetic components. They include (1) evaporation of materials of construction or of a volatile constituent of the material, (2) loss of the layer of adsorbed gas present on the surface of the parts and also loss of absorbed gases, and (3) elimination of convection heat transfer.

The specified radiation flux of 10^{11} electrons/cm^2 of 1 MeV electrons is not considered a strong field. The magnetic components as installed in the power conditioner will be shielded from direct exposure to this particulate flux as well as ultraviolet radiation. The materials selected have good resistance to ultraviolet radiation deterioration due to small doses of exposure over a long period of time.

To operate reliably in the space vacuum, materials having high-volatization points at the operating temperature are required. It is extremely important that all materials lend themselves to rapid and thorough outgassing by baking and vacuum pumping. Metals which would tend to allow surface evaporation in vacuum and subsequent redeposition of materials on cooler insulating surfaces must be avoided. Electrical insulating materials should, therefore, have the following three desirable characteristics: (1) low initial volatile content, (2) rapid release of initial volatile matter under high vacuum, and (3) extremely low long-term outgassing rates.

A. Insulating Materials

A number of materials with potential for use as layer insulation, magnet wire insulation, or bobbin material were selected for preliminary screening by vacuum outgassing tests. Selection was made on the basis of known chemical and physical composition of the materials. These included polyimides (Kapton H, AI-220 wire insulation), aromatic polyimides (Nomex), and silicone-treated mica and mica-glass composites (the Isomicas).

Test samples were mounted in a fixture in a 3-in. diameter by 3-in. high metal cylinder with loosely fitting top and bottom covers. The cylinder served as an isothermal heating surface surrounding the samples and was indirectly heated by a concentric heating coil. Temperature was maintained at 130°C ±2°C throughout the test and monitored with thermocouples. The vacuum chamber consisted of a glass bell jar 18 in. in diameter by 30 in. high and included a liquid nitrogen trap in the vacuum line close to the bell jar mounting platform. Vacuum inside the bell jar near the samples was monitored by an ionization gauge and over the test period ranged from 2×10^{-6} to 6×10^{-6} torr.

Materials were selected on the basis of thermal stability, outgassing characteristics, mechanical properties, and electrical properties. The materials selected were those exhibiting the lowest outgassing rates of the materials available in their respective categories, provided the other selection criteria were fulfilled.

The question of whether or not mechanical and electrical criteria were fulfilled by the investigated materials was decided largely on the basis of the designer's experience in working with the materials over a period of years. In cases where a number of the candidate materials met the criteria of thermal stability and low outgassing, final selection was made on the basis of superior mechanical properties and fabricability.

Descriptions of the insulating materials finally selected are provided below:

(1) Magnet Wire. The selected wire is coated with an aromatic polyimide, commonly referred to as ML insulation. The material is characterized by high thermal stability and is rated for long term use at 200°C. After release of the initial moisture content of approximately 1%, the outgassing rate is less than 0.01%/100 h. All magnet wire used to fabricate the high reliability magnetic components was inspected 100% prior to coil winding.

(2) Coil Bobbins. The material selected for this application is a laminate of woven electrical-grade, fiberglass-cloth bonded with silicone resin (MIL-P-997, Grade GSG). Strength-to-weight ratio is high and temperature rating is 180°C. Initial volatile content is approximately 0.02% and after 24 h at 130°C the outgassing rate is less than 0.01%/100 h. This type of material was also used in the annular seal of metal toroidal cases.

(3) Layer Insulation. Layer insulation is Isomica 4350 (3-M Company), a 5-mil laminate of mica paper, silicone treated and bonded to woven fiberglass cloth. The fiberglass backing provides mechanical strength and cut-through resistance. This 180°C class material possesses excellent corona resistance properties. After post baking at 180°C to effect a complete cure of the silicone, the outgassing rate at 130°C is approximately 0.01%/100 h.

(4) Tying Cord. The windings of the open-construction magnetic components are secured with Nomex, high-temperature, polyimide tying cord, a material of outstanding thermal stability and tensile strength. The fibers are somewhat hygroscopic and absorb approximately 4% moisture at 50% relative humidity. Moisture is readily released and outgassing of dried material at 130°C is less than 0.01%/100 h.

(5) Insulating Sleeving. Varglass HC-2 (Varflex Corporation), a braided fiberglass silicone-treated material conforming to MIL-I-3190B, was selected. This 200°C class material has an outgassing rate of approximately 0.004% at 130°C after 24 h.

(6) Lamination Coating. Laminated core materials are coated with a magnesium oxide complex (Magnetics, Inc., No. 7) produced by spraying an alcohol solution of magnesium methylate on the lamination, then drying and heat treating in air. The outgassing rate of this material is negligible.

(7) Thin Film Insulation. Toroidal cores are insulated with a wrapping of 1-mil Kapton H film between core and winding. This material is also used as a gap spacer in inductor cores. Kapton H is a 220°C class material of extremely high-thermal stability and high-dielectric strength. After release of moisture (1.3% at 50% relative humidity) no outgassing was detected at 130°C.

(8) Elastomer. Elastomeric materials are used as fillers in interfaces where it is desired to improve heat conduction as, for example, between core and mounting bracket. The material chosen is Dow Corning 73-500 space grade encapsulant specially prepared for use in high-vacuum, high-temperature environments where outgassing and corresponding volatile condensates must be held to a minimum. Weight loss at 125°C after 24 h and 10^{-6} torr is 0.35%; volatile condensable materials at 25°C is 0.1%.

(9) Coating and Bonding Resin. Dow Corning 2104 has been selected as a bonding agent in the fabrication of silicone glass bobbins. It is a rigid resin rated at 200°C and after curing at 180°C exhibits an outgassing rate of 0.015%/100 h after 6 days at 130°C.

3M Company's No. 350 unfilled resin system was selected to hermetically seal all toroidal cores. Its low viscosity (1800 cP at 23°C) permits thorough impregnation with minimum accumulation. Manufacturer's data indicates a weight loss in air at 130°C of less than 0.01% over a 1000-h period. Moisture absorption is 0.3% at 96% relative humidity after 240 h.

Outgassing data on materials tested during the program and selected for use are summarized in Table 3.

Table 3. Outgassing of materials used in *SERT II* magnetic components

Material	Weight loss at 130°C and 2×10^{-6} to 6×10^{-6} torr			
	Loss, %	Test, days	Loss, %	Test, days
G-7 fiberglas laminate	0.013	1	0.026	14
Silicone fiberglas tubes	0.021	1	0.015	11
Isomica 4350, postcured	0.016	3	0.023	10
Nomex fiber	3.39	1	3.33	3
Silicone-fiberglas sleeving	0.043	1	0.054	11
MgO coated laminations	0.002	1	0.002	11
DC 2104 Silicone Resin	0.025	1	0.047	7
Mass spectrometer tests	**Loss rate, %/100 h after 1 day[a]**			
ML wire insulation	0.09 at 160°C and 10^{-6} torr			
Kapton H-film	0.018 at 200°C and 10^{-6} torr			

[a]Samples previously under vacuum of 10^{-6} torr, room temperature for 20 h.

B. Magnetic Materials

The operation of magnetic materials under the subject environment presents less difficulty than the construction of practical windings for various coil configurations.

However, the core materials and operating frequency are a very important consideration from the standpoint of efficiency, size, and weight. Core configuration also dictates the mechanical configuration.

A number of core materials were investigated for possible use with special attention focused on the family of nickel alloys and especially on the Supermalloy grade. Design studies over the range of 4–12 KHz eliminated ferrites from consideration and set the operating frequency at 8 KHz to minimize weight and maximize efficiency.

High-voltage power transformer laminations are of a 1-mil Supermalloy type material with a minimum permeability of 40,000 at 40 gauss; minimum permeability is 13,200 at 6,600 gauss with 60 Hz excitation. This material was specially annealed and transformed into a DU shape lamination through a photo-etching process followed by an insulating bath in magnesium metholate. Thicker 4-mil laminations are used as keeper laminations at the top and bottom of each stack.

The flux density level selected for operation of each specific design was the result of an evaluation of each design from the viewpoint of maximum efficiency while maintaining reliability. Copper and core losses were evaluated at many flux density levels; the level selected was that at which efficiency was maximum.

Square Permalloy 80, used in saturating transformers, is specified at 7500 gauss ± 150 gauss. Round Permalloy 80 is used in current transformers and magnetic amplifiers. Annular seals are fiberglass laminate, and the cores are hermetically sealed to prevent outgassing.

The Supermalloy grade material was selected for toroidal cores because of its high permeability and low losses at flux density levels from 3–6 kG. The actual flux densities selected are 5.5 kG for current transformers, 6.2 kG for magnetic amplifiers, and 6.8 kG (saturation value) for saturating transformers.

Molypermalloy powder cores used on the program were not coated since insulation was obtained by half-lapping with Kapton H-film directly over the core. Futhermore, Magnetics, Inc. is now using a new binder to sinter their powder Permalloy cores which optimizes the mechanical strength of the core and also minimizes the moisture absorption that previously caused a shift in the permeability of $\pm 3\%$ max.

IV. Typical Designs

The various types of magnetic components designed on the program are shown in Fig. 3. A high-voltage power transformer mounted in a protective carrying case is shown in Fig. 4. Table 4 lists the design specifications for this transformer. Actual weight was 0.45 lb. Table 5 contains the design specifications for the largest power transformer (similar to Fig. 4) designed and built on the program. Both the efficiency and weight specifications for this design were surpassed; actual efficiency was in the range of 98%, and actual weight was approximately 0.57 lb. Both designs just described successfully withstand a 6000-Vdc corona test (secondary to primary) and a 2000-V 60-Hz ac secondary winding corona test. Actual tests have indicated that these designs are capable of withstanding over 9000 Vdc between primary and secondary in a vacuum of 1×10^{-6} torr.

Table 4. High-voltage power transformer design specification; accelerator supply transformer

Transformer:	931A216
Circuit designator:	T601
General:	This is a high-voltage, high-frequency transformer. The voltage spike must be a minimum at no load to protect the primary circuit and to protect the filter capacitor. Transformer inductance must be sufficient to limit the surge current to 0.05 A when the output filter capacitor is initially charged.

Operating conditions:

Primary V peak	Primary A peak	Each Secondary V peak	Each Secondary A peak
54	1.74	810	0.05
60	1.74	900	0.05
75	1.74	1130	0.05
	(50% duty cycle)		(continuous)

Rated power: 100W (secondary)

Typical operating power 5W (secondary)

Operating frequency 8 KHz at 60 V, square wave operation

Design specifications:

Minimum efficiency: 96%

Maximum weight: 0.52 lb

Maximum hot spot temperature: 130°C

Maximum overshoot: 5.0%

Primary waveform rise time: 0.1×10^{-6} s

Derating: 2:1 on voltage
4:1 on power

Primary-to-secondary insulation for 6 KVdc operation

Leakage inductance between primaries: 2 UH

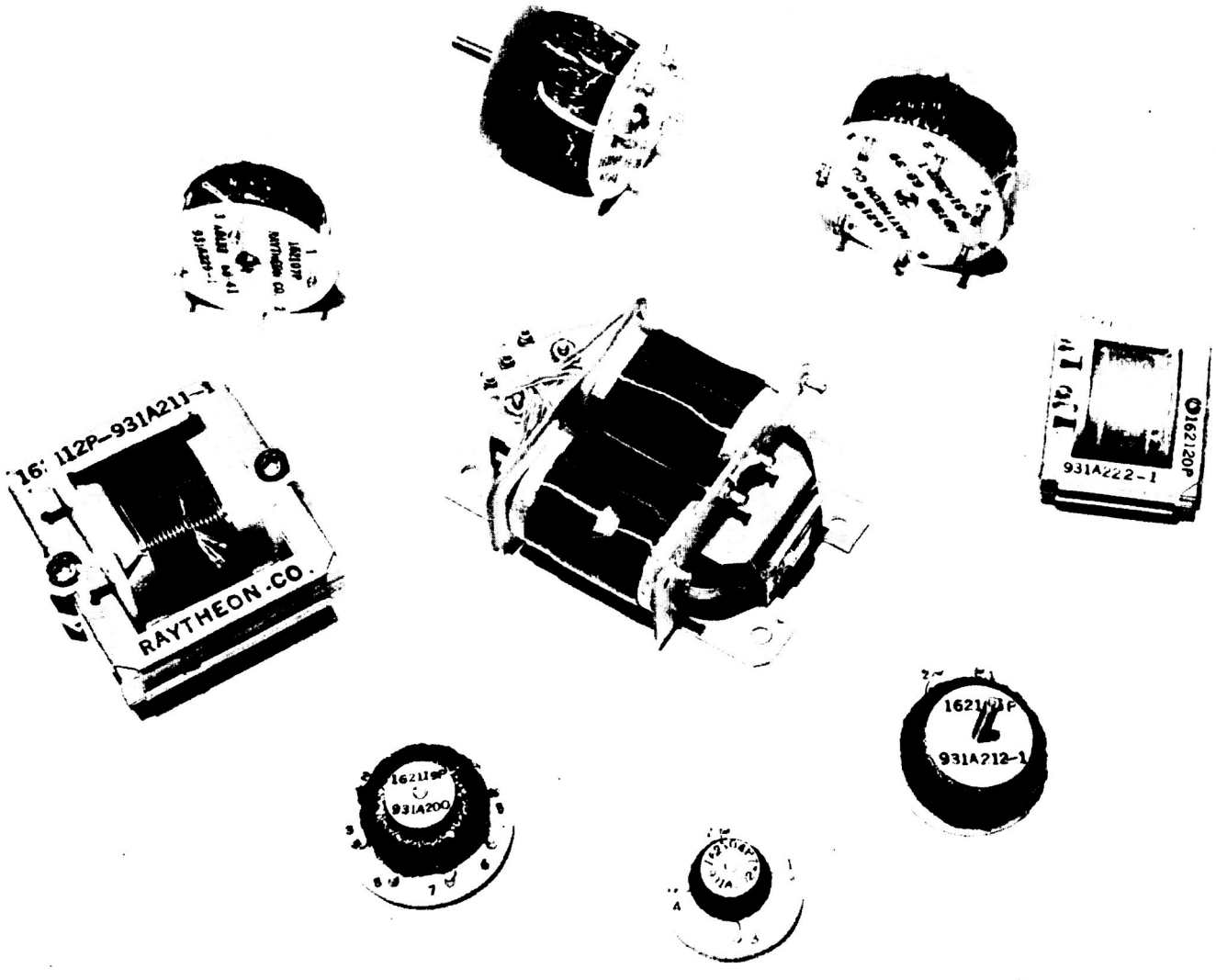

Fig. 3. Typical *SERT II* magnetic components

Table 5. High-voltage power transformer design specification; screen supply transformer

Transformer:	931A214
Circuit designator:	T501, T503, T505, T507
General:	This is a high-voltage, high-frequency transformer. The voltage spike must be a minimum at no load to protect the primary circuit and to protect the filter capacitor. Transformer inductance must be sufficient to limit the surge current to 0.26 A when the output filter capacitor is initially charged.

Operating conditions:

Primary V peak	Primary A peak	Secondary V peak	Secondary A peak
54	4.6	900	0.26
60	4.6	1000	0.26
75	4.6	1250	0.26
(50% duty cycle)		(continuous)	

Rated power: 260W (secondary)

Typical operating power: 250 (secondary)

Operating frequency: 8 KHz at 60 V, square wave operation

Design specifications:

Minimum efficiency: 96%

Maximum weight: 0.60 lb

Maximum hot spot temperature: 130°C

Maximum overshoot: 5.0%

Primary waveform rise time: 0.1×10^{-6} s

Derating: 2:1 on voltage
4:1 on power

Primary-to-secondary insulation for 6 KVdc operation

Leakage inductance: 2 UH

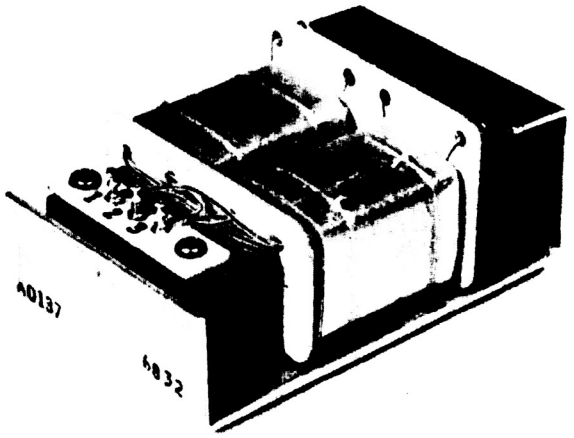

Fig. 4. Typical high-voltage power transformer

V. Conclusion

The open-construction magnetic components for all phases of the program including flight hardware have been built and tested. They meet all electrical and mechanical requirements. Selected designs are presently being qualified to the requirements of the *SERT II* program and the requirements of MIL-T-27B. Although the *SERT II* mission requirement is for 6 mo of continuous operation, the magnetic components designed and built on this program would be capable of many years of reliable operation in the space vacuum.

Discussion

Laffert: In order to clarify my earlier comments, I would like to state that in certain situations the vacuum environment can be used to good advantage. It is a very good controlled environment, and that is the primary reason why I think that the vented approach is best for our application; the fact that we have open-faced PMT's is secondary, but I don't want to push this. I think solid potting is probably best for most applications, but there are certain situations where this works very well.

Lagadinos: Well, what I would like to add to that is that based on the reliability figures we have on this approach the open-construction transformers can only get better, whereas the impregnated or encapsulated transformers could get worse.

I would like to point out a couple of the advantages of the approach we followed.

First of all, we had to meet a given temperature range, and, as you know, thermal shock problems exist. There is no way of knowing whether possible cracks within the impregnation could be potential problems for corona initiation and further degradation. I don't quite agree with the previous statement that if a company or an organization is not quite familiar in potting techniques it will go to an open approach. I think that Raytheon has demonstrated that capability in the LEM project and we were very successful. We were using a method of applying pressure and vacuum and temperature and even curing under temperature and vacuum. The results of this approach have been very successful.

The other advantages of the open approach is some savings in weight and volume. To my knowledge, there are also certain epoxy systems that probably could qualify at the temperature range that these components have to meet; apparently, however, the outgassing rate is far beyond the limit that can be tolerated.

When we began this investigation we couldn't come up with any epoxy, don't forget that we considered both approaches initially, and when we had a design review at NASA we presented potted hardware as well as the open approach. The advantages were quite obvious at that design review.

Yorksie: I might add that the power conditioner itself is a truly open-construction unit, so that outgassing of a potted transformer would certainly not be tolerated in the open-type design of the power conditioner.

Lagadinos: Of course, you have some problems there of not being able to hide any poor workmanship; it is obvious.

Harrison: When you have series secondaries, what potential do you prefer to keep the core at?

Lagadinos: The core is at ground potential and the coils are wound in such a fashion that the interlayers are approximately equipotential surfaces. One is wound in reverse direction to the other, so that when you look at the space in between the end layers, between the two coils, they are approximately at the same level. To answer your question then, the core is running at ground potential and the outer wiring is running at high voltage.

Harrison: One other comment: do you think there is a break point in voltage where you should decide to float the transformers; in other words, if the potential increases upwards of 100 kV perhaps, do you think it becomes advantageous to think about floating cores?

Lagadinos: I think you have more serious problems. One of the problems that we experienced was trying to conduct the heat away from the windings. Unless you improve an interface between the heat sink and the windings through the core, this is the only way that we can drive the heat away from a high-power transformer.

During one of the evaluations with the loads suspended within the chamber at 10^{-6} vacuum, we had a resistor evaporate. It is a pretty good indication that the temperature could be extremely high if you didn't provide a good heat flow path from the heat generator within the windings as well as the core.

I think that the temperature rise from between the coil and the core was approximately the same. We tried to keep the windings designed a little conservatively because we had to still go through the insulated barriers all the way from the outer space to the core, basically.

We tried to come up with an effective way of determining the maximum hot-spot temperature because I think the thermocouple method is not accurate unless you know where to place the thermocouple.

A thermocouple gives you an average reading only. So what we did was to replace the transformer itself, especially the windings, with the equivalent electrical circuit and the current generators. Each heat flow path was replaced by the equivalent thermal resistance. In this manner, we solved a complicated node-equation type circuit and came up with the maximum hot-spot temperature that was well within the maximum we could tolerate in the program.

This sort of analysis was also verified through the qualification program that is just about complete now.

August: This is sort of a side issue to what you are saying, but just a narrow comment on open versus potting. I think one of the problems you have to consider in any sort of an open structure is whether you are going to get any plasma in the operating environment as Mr. Carruthers found out this morning. If you do, you can have severe problems, and one of the things with the SERT is that it is used for an ion thrustor and we haven't really discussed any problems about rocket neutralization or whether you are getting any flow-back of ions. If you have surfaces which are potentially exposed to any non-neutralized plasma, you might have problems with open-type structures.

Lagadinos: I think you are introducing extraneous problems, because when we are looking at the design of the magnetic components we are faced with the design parameters. I can't really forecast certain problems that don't exist. Maybe Mr. Yorksie could answer something from a systems point of view.

I looked at these devices strictly on a magnetic component basis with the given requirements they have to meet.

Yorksie: I just want to add to your first remark that NASA has concluded, based on their SERT I mission, that they could effectively neutralize the plasma. Otherwise, there would never have been a SERT II.

August: You will always get some plasma neutralization because if you don't you have electric fields which would neutralize it. I am not trying to pick this apart, because your system is vented. In any event, the components aren't sticking directly out in the vacuum and they aren't directly where you have the high voltage. I am just saying that the problem of open versus potting should always be looked at if you have high electric fields or high-voltage components directly out on the surface where you can get plasma. Then I think you should worry about potting it. You aren't going to get the plasma inside. It is only going to be on the surface components.

Lagadinos: There is a cover over the power conditioner.

Carruthers: One thing I forgot to mention in my talk is that the presence of magnetic fields is also a very important consideration in the design of ion-repeller grids, as we found out in our magnetically-focussed devices. You can get a sort of funneling effect as in the case of the Van Allen Belt in which the ions and the electrons can come in along field lines. This can either hurt or help, depending on how you arrange your vents and grids.

Scannapieco: Can you tell me the technique you use for the weight work you did. Were they in situ measurements, or were they before-and-after measurements?

Lagadinos: We use two techniques. One was a qualitative as well as quantitative analysis through a mass spectrometer. Samples

were selected and placed in the spectrometer. We performed the test at temperatures: 70 C and 130 C. All of the results are tabulated. We have a copy of the general, more or less a synopsis of our final findings that could be made available.

Scannapieco: But the percent weight losses that you showed on the tables, they were before-and-after measurements, is that correct?

Lagadinos: Yes.

Scannapieco: The point I would like to bring up is this would not include a lot of the gases and moisture which would come off and go back into the sample before you would reweigh it again, and SERT is a ballistic shot, if I recall correctly, is it not?

Lagadinos: SERT II is designed for a polar orbit for six mo.

Scannapieco: I thought it was a short-term one like the first one. I was wondering about the initial weight losses that you have to consider in the first hour or two. This won't be a problem if you have six mo.

Lagadinos: It won't be turned on immediately once it is put into orbit. We have as much as 24 h of outgassing.

Stern: How long are your systems to be turned on when they are in orbit?

Yorksie: The figure that has been talked about between ourselves and NASA is somewhere on the order of 24 to 48 h. There is also the consideration, that this will be just a cold soak in the vacuum, and then the low-voltage circuits will be turned on for some time. That will, to a large extent, be determined by the type of telemetry data we get back from the unit as to when the high-voltage units will be turned on. There will be a fair amount of loss in the low-voltage circuits which will tend to heat the complete power conditioner and get rid of this initial high outgassing rate.

Stern: I just wanted to revive the problem of potting versus non-potting and the ambivalence in the group of people who design. You like that because of one reason and other people prefer to pot for other reasons, so the controversy goes on. Actually, it is not a controversy; it is just a matter of applying intelligent design techniques to the problem at hand.

PRECEDING PAGE BLANK NOT FILMED

N70-22296

Design Considerations for Corona-Free High-Voltage Transformers

Harold C. Byers
Transformer Electronics Co.
Boulder, Colorado

Many of our TEC toroidal transformers are used in power supplies for space applications. We have spent a great deal of time and money in finding ways to prevent corona. In cases where the power supplies were not required to operate until the low pressures of outer space had been reached, the corona problems were not so great. With space equipment becoming more and more complex, more of the electronic gear must operate through the critical air pressure region of low dielectric strength.

In this paper, I will explain some of the design considerations which we at TEC feel are important for the elimination of corona in high-voltage toroidal transformers to be used at low air pressures.

So that we all get a clear picture of the size and typical applications of the toroidal transformers which I will discuss, Fig. 1 is presented which shows a typical power supply designed for industrial applications at atmospheric pressures. A power supply such as this would require some modifications in materials, etc., to be acceptable for space applications.

The inner construction of the same type of power supply is shown in Fig. 2. I would like you to note the Teflon-insulating tape and the Teflon-insulated lead wires from the transformer to the PC board. These points will be discussed later.

In Fig. 3 a typical power supply package used in space applications is shown. This supply is rated at 4 kV output and is used to supply power to an ion pump. This power supply was only required to operate from launch to approximately 310,000 ft altitude and then it was turned off for the duration of the flight. We are now manufacturing a similar power supply in a hermetically-sealed package which is required to operate from atmospheric pressures to space vacuum and to continue to operate in space for at least 100 days without developing corona problems.

All of the high-voltage transformers which I will discuss have been wound on toroidal tape-wound cores. In Fig. 4 a typical tape-wound toroidal core is sectioned to expose the layers of tape in the center. The tape thickness varies from 0.5 to 14 mils.

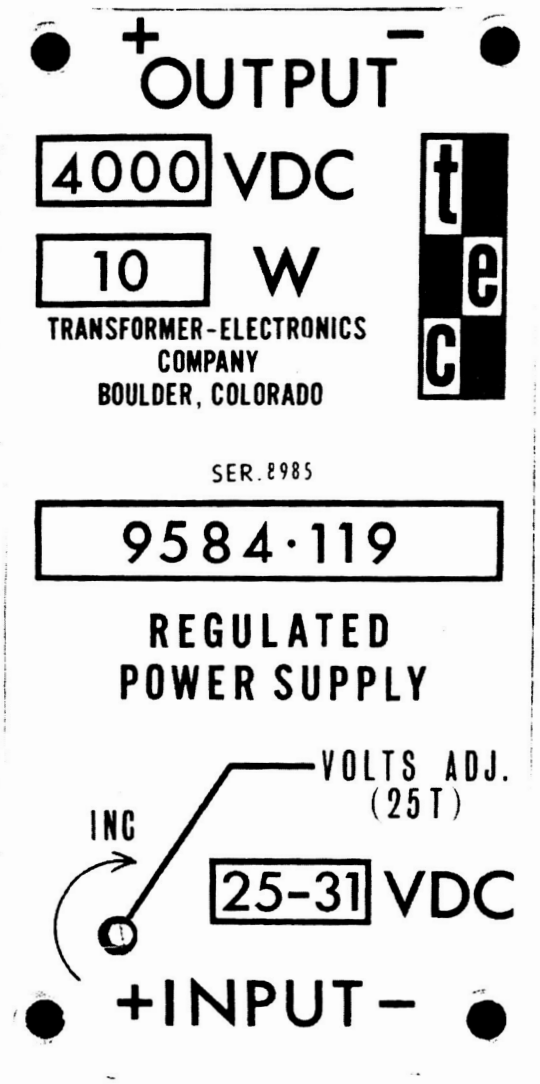

Fig. 1. DC-AC converter

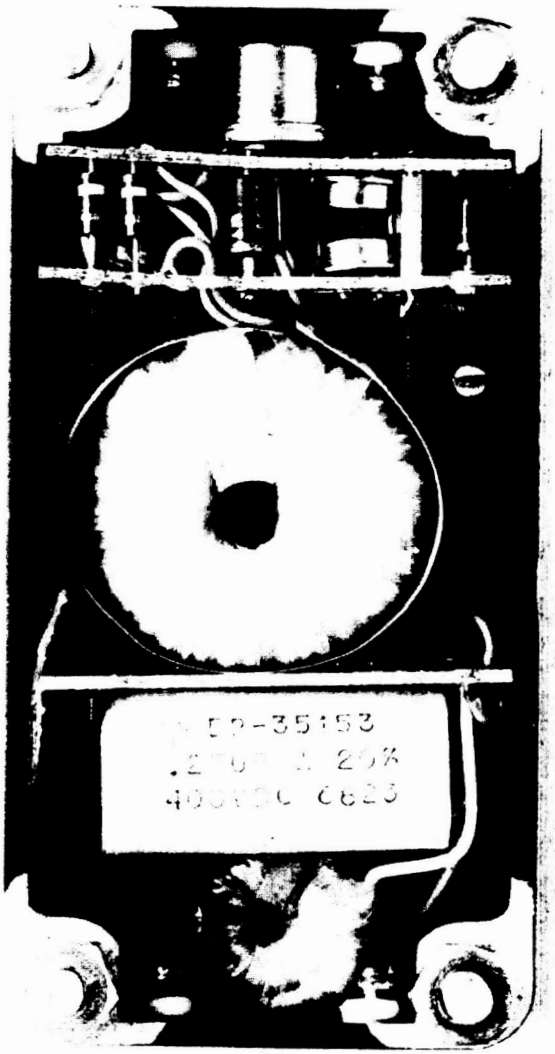

Fig. 2. Interior view, ac-dc converter

In the design of a high-voltage toroidal transformer, there is a definite reliability, size, and efficiency tradeoff. I would first like to discuss the considerations with regard to size.

The typical design requirements of a transformer are outlined in Fig. 5. We have an input of 20 V, an output of 500 V quadrupled to 2 kV, a power output of 300 mW, a frequency of 3.5 kHz, and an induction level of 6.5 kG. We have chosen two cores which will do the job very nicely. Notice that the secondary winding on the 52057-IF core is a No. 46 wire and the secondary winding on the 52374-IF core is a No. 42. This was done to save space, as the window in the 52057-IF core is smaller and there was not room to wind the No. 42 magnet wire on the secondary winding. The window in the smaller core is 0.625 in. in diameter and the window in the larger has a diameter of 0.875 in.

The area of the window in the larger core is actually more than twice that of the smaller core. To save space in the smaller core, one could raise the frequency and reduce the number of turns slightly. This would then

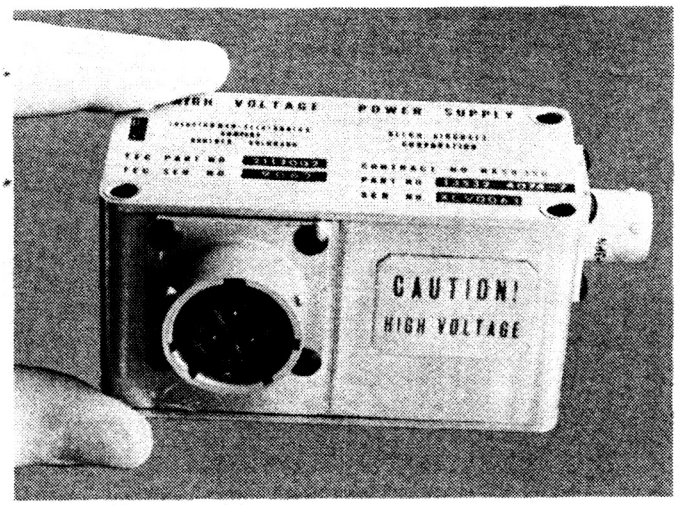

Fig. 3. Typical power supply unit

COMPARISON OF 2-kV TRANSFORMERS

DESIGN CRITERION

E_{in}	20 V
E_o	500 V QUADRUPLED TO 2 kV
P_o	300 mW
f	3.5 kHz
INDUCTION LEVEL:	6.5 kG
MANUFACTURER:	MAGNETICS, INC.

	52057 - IF		52374-IF
PRIMARY TURNS:	600	PRIMARY TURNS:	No. 600
SECONDARY TURNS:	12,000	SECONDARY TURNS:	12,000
PRIMARY WIRE SIZE:	No. 38,800 cm/A	PRIMARY WIRE SIZE:	No. 38,800 cm/A
SECONDARY WIRE SIZE:	No. 46		No. 42
FINISHED O.D.:	1.1 in.		1.4 in.
FINISHED HEIGHT:	0.5 in.		0.5 in.
MAGNETIC PATH:	5.48 cm		7.48 cm

Fig. 5. Transformer design requirements

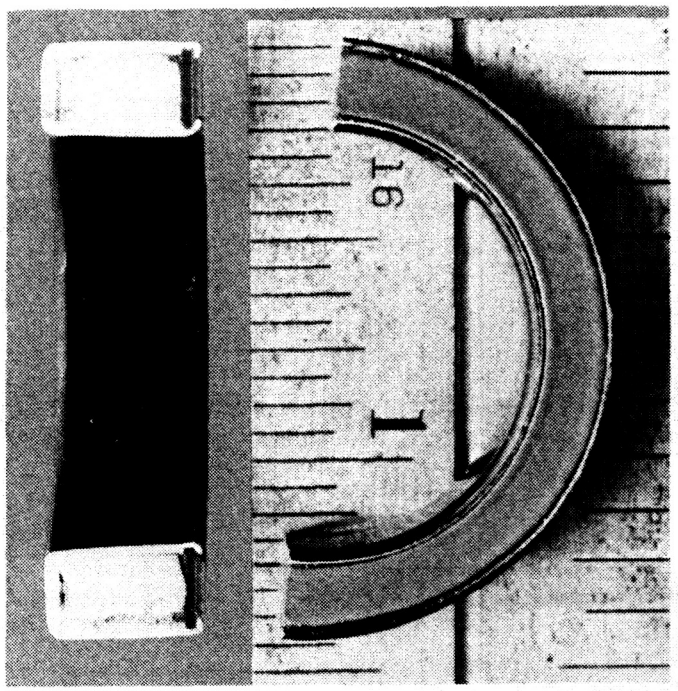

Fig. 4. Section tape-wound core

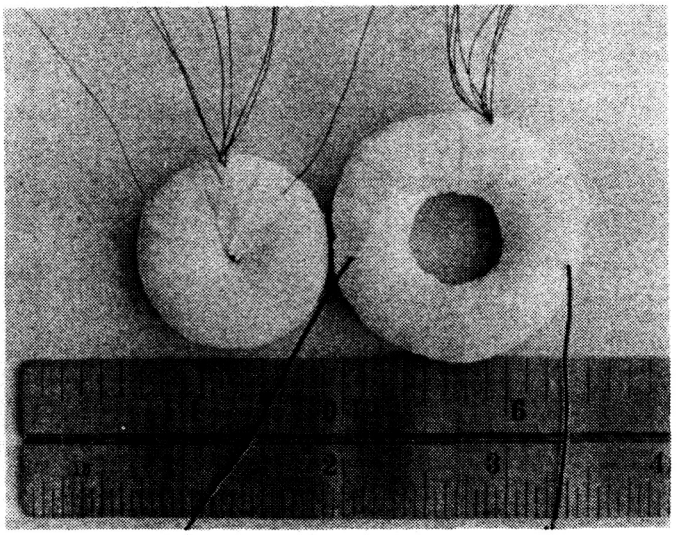

Fig. 6. Typical transformers

lower the efficiency of the core and the voltage gradients would be greater.

The transformers wound to the preceding specifications are shown in Fig. 6. Let us now consider the reliability of these two transformers; No. 42 magnet wire was used on the secondary winding of the larger transformer and No. 46 wire was used on the secondary winding of the smaller transformer. The insulation thickness of No. 42 double thick polyurethane-coated wire is 0.000250 in. The insulation material is rated at 1500 V/mil. This would give No. 42 wire insulation a breakdown voltage of 350 V. Number 46 (0.0016) wire has an insulation thickness of 0.000150. This would give it a breakdown voltage of approximately 225 V.

In the case of the smaller core, Fig. 7, the secondary wire insulation has a much lower breakdown voltage, yet greater stresses are applied to it than to the same winding on the larger core (as the start and finish of the high voltage windings are much closer to each other on the smaller core). It is well to remember that the smaller the magnet wire, the greater the chances are of damaging

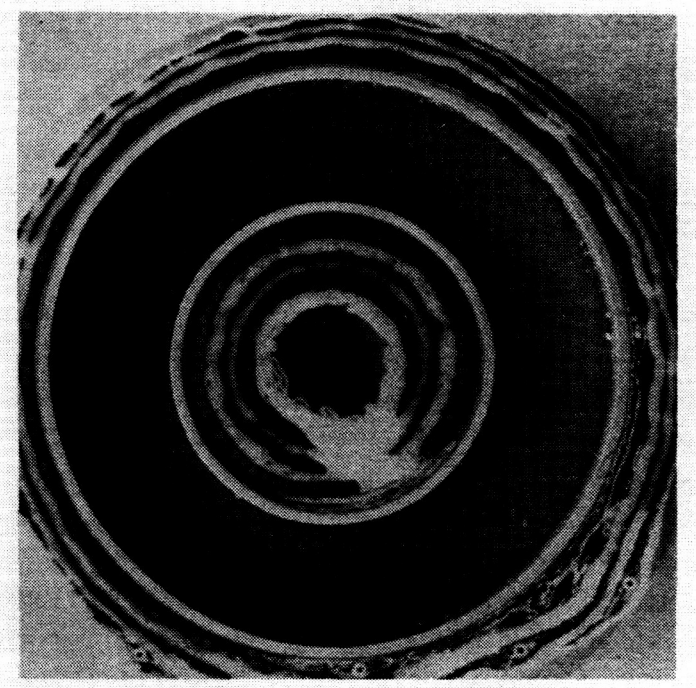

Fig. 7. Typical smaller transformer

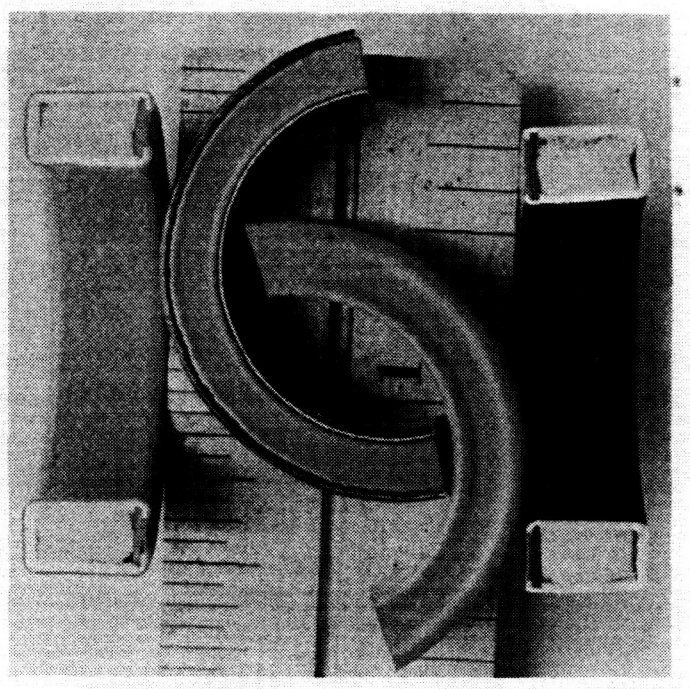

Fig. 8. Aluminum core cases

the insulation or stretching the fine copper wire during winding.

One can see the reliability dropping off quite rapidly as the interlayer insulation is decreased, the insulation on the magnet wire decreased, and at the same time the voltage gradients increased. From the foregoing information, it is obvious that the size of the transformer should be given considerable consideration when reliability and efficiency are important.

After the size of the core has been determined, one must select the core construction which will best satisfy his requirements. There are several types of cases used in the construction of tape-wound toroidal cores. The two cases shown in Fig. 8 are made of aluminum. There is also a phenolic case very similar to the aluminum ones shown. We chose the aluminum case because of its greater strength which gives better protection to the tape-wound core. Note the plastic ring inserted in the side of the case to break the electrical path around the core and to protect the tape laminations. The mechanical bond between the aluminum case and the plastic ring provides an air-tight seal. We selected a core with an epoxy coating, described by one manufacturer as a "GVB coating." The coating provides an extra seal to prevent the impregnating epoxy from entering the core and also gives an added 1000 V of insulation between the wire and the aluminum core case. This epoxy coating will not cold flow under the pressure of the winding. The epoxy coating on the core is compatible with the impregnating epoxy, thus avoiding incompatible interfaces between the core coating and the encapsulant. On the inside of this type of core, the air around the laminations is displaced with an inert silicone compound minimizing the chances of the air coming out during coil impregnation. This silicone material also acts as a cushion to dampen vibrations which might otherwise change or damage the core.

We will now discuss the subject of magnet wire insulation. It might be well to mention that most of these transformers are not required to operate above 125°C. In the selection of magnet wire, it is important that the encapsulating compound be bonded to the wire coating.

In Fig. 9 a Teflon-coated wire is shown surrounded by epoxy. You will see from the way the teflon insulation separated from the epoxy during sectioning of this sample that no bond whatever existed between the potting compound and the Teflon insulation of the wire. The teflon pulled away from the wire, resulting in a void here, too. This situation creates an interface which under the strain of the right voltage and air pressures would allow the development of corona between the wire insulation and the potting compound. In Fig. 2 a transformer with Teflon-coated lead wires was shown. This

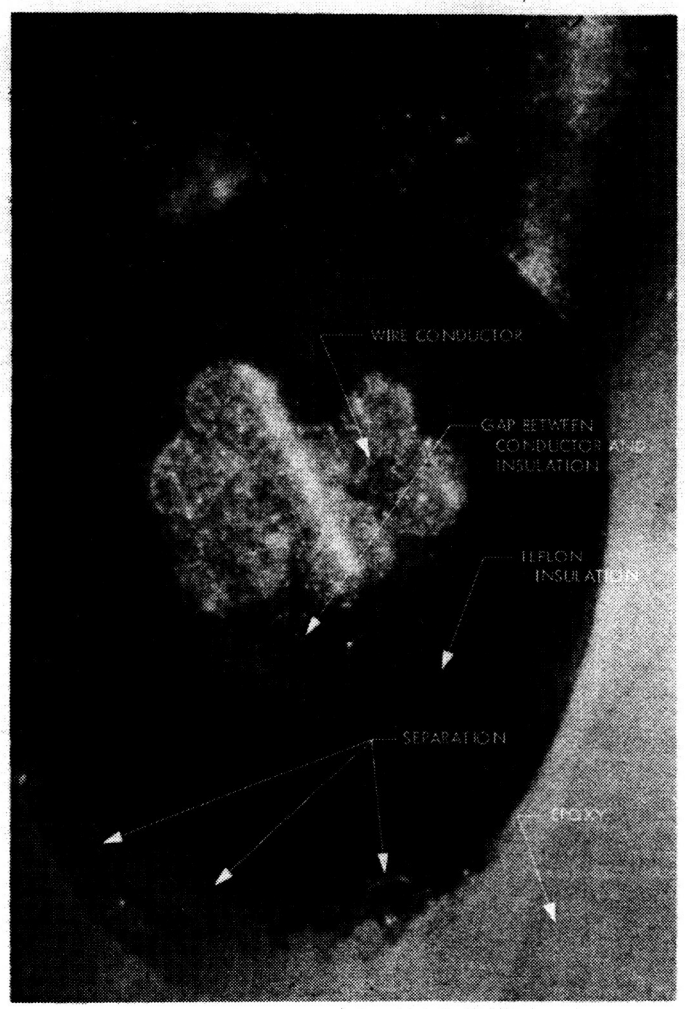

Fig. 9. Teflon-coated wire

type of design is used only when the transformer is to be used at atmospheric air pressures or in space applications where it is vented and turned on after it has reached the vacuum conditions of outer space.

Figure 10 is a microphotograph, (400 times size) of a polyurethane-coated wire embedded in epoxy resin. Under close examination it is seen that the epoxy bonded well to the wire insulation, avoiding incompatible interfaces for the later development of corona. After running various tests to determine wire insulation compatibility with various epoxies, we dicided to stay with either double-thick polyurethane or double-thick nylon-jacketed polyurethane. Another distinct advantage of the polyurethane-insulated wire is that the wire can be stripped in solder, thus eliminating chemicals which if not completely removed before encapsulation could cause failure of the joint at some later date.

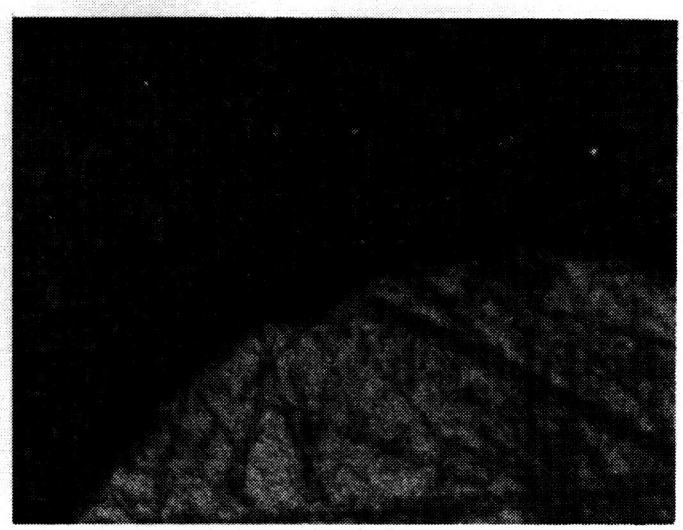

Fig. 10. Polyurethane-coated wire, microphotograph

One of the next major considerations in the design of high-voltage transformers is the interlayer insulation. By looking closely at Fig. 11, you will see what happens when Teflon tape is used. The complete lack of adhesion of the impregnating material to the interlayer teflon insulation can be seen. This kind of a situation creates numerous interfaces between the potting material and the insulating tape. The Teflon tape also tends to seal against itself (the epoxy was not able to get between the layers of insulation material) thus preventing a good impregnation of the transformer.

I might explain that when this particular transformer was cross-sectioned, the Teflon tape relaxed considerably and some of the magnet wire fell out making it look even worse than it actually was, but proving that there was no bonds to the wires, either.

A toroidal transformer which was potted using polyurethane coated wire and an open weave dacron tape used as an interlayer insulating material is shown in Fig. 12. Note the complete lack of visible interfaces. The dacron tape is completely impregnated with epoxy. There are no voids to create corona problems. Cleanliness of the dacron tape is very important. The operators must wear cotton finger cots or light cotton gloves. The wire insulation must be free from any skin oils or other contaminants. After the transformer has been impregnated, it should not be handled by bare hands. No oils, greases, or silicones should be allowed to contaminate the transformer before final potting, as these would probably create interfaces between the two epoxy systems.

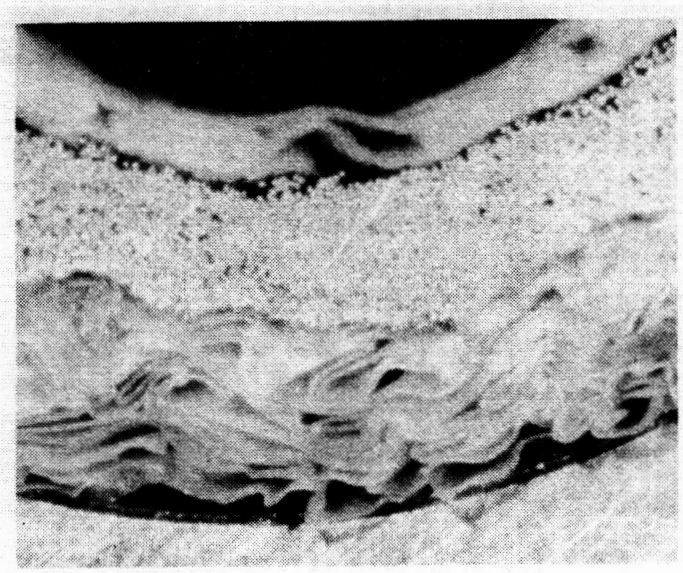

Fig. 11. Impregnated transformer

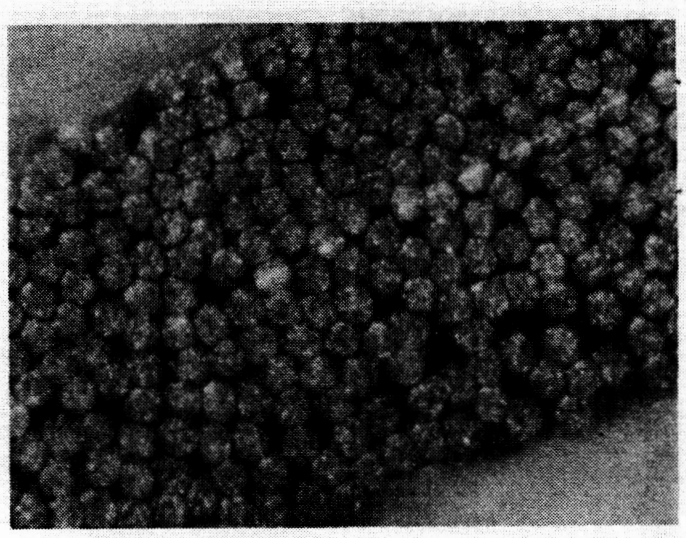

Fig. 13. Epoxy-impregnated transformer magnified 200 times

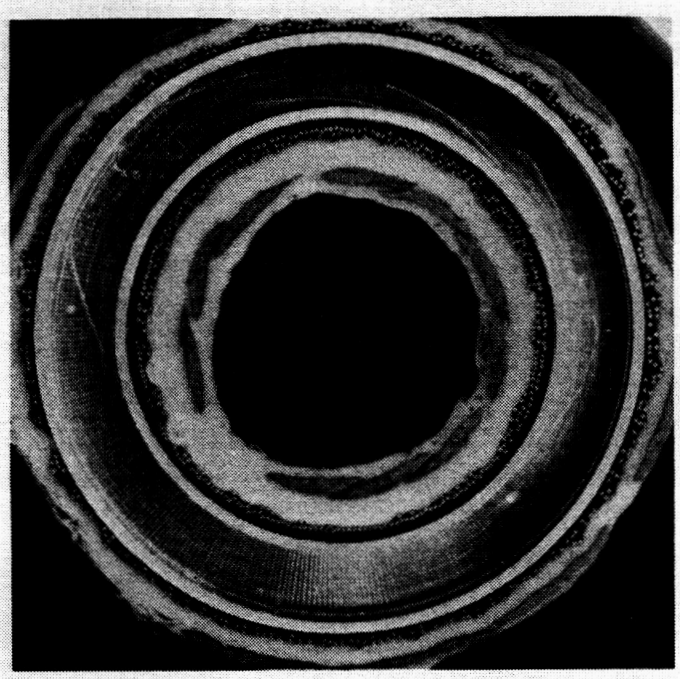

Fig. 12. Impregnated, dacron-wound transformer

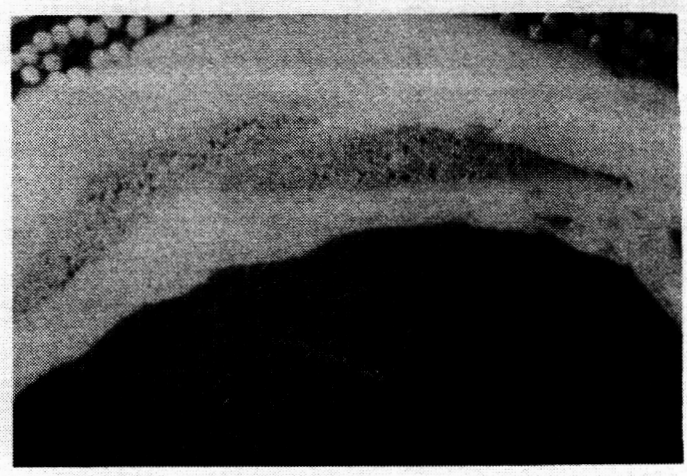

Fig. 14. Wire in epoxy

A micro-photograph of a section of the same transformer is shown in Fig. 13 enlarged 200 times. The wires are 2 mils in diameter. Notice how well the epoxy impregnated into even the smallest openings. Each wire is surrounded by epoxy. Incompatible interfaces between the epoxy and the wire insulation cannot be seen.

Figure 14 shows how well the dacron tape was impregnated. Although it may appear from the figure that there are voids, very careful inspection of the actual sample shows that none are present. The epoxy bonded firmly to the insulation of the wires, holding them firmly, thus protecting them from shock and vibration.

The wires in Fig. 15 are 10 mils in diameter magnified 200 times. Notice the complete lack of incompatible interfaces between the dacron tape, the wire insulation, and the core coating. There are no voids.

Referring back to Fig. 12, note the segment-shaped winding design. The transformer was wound in small segments, with a layer of dacron insulating tape between each segment, adding to the insulation of the transformer. By winding in this manner, voltage gradients in each

section are kept low. The highest voltage gradient in a 2-kV transformer probably would not be over 50 V in any one segment. Without additional insulation, the wire insulation would withstand 250 V. Therefore, a minimum of 500% safety factor is automatically built-in.

The success or failure of a high-voltage power supply often depends on the impregnating and potting compound used. We have settled on epoxies because of their compatibility with each other, and with wire insulations, etc. We have had best results impregnating the transformer with a low viscosity, low shrink, low exotherm, semi-rigid heat curing epoxy.

If the transformer is to be encapsulated in a case by itself, a rigid epoxy system would be used. If the transformer is to be encapsulated in a power supply along with fragile components, one would use a semi-flexible epoxy coating on all the fragile components and finish it off by encapsulating with a rigid, low shrink epoxy. There are many variations of rigid epoxies. Some become very brittle and crack at low temperatures. The epoxy selected must be tough to withstand low temperatures and still be a rigid system for low outgassing and weight loss.

A void which was created by a toroid having a poor seal is shown in Fig. 16. The air in the toroid escaped during the epoxy curing process. The epoxy used here was a high-shrink type which pulled the side of the core case apart. This points up the importance of a low-shrink epoxy.

A sample of two epoxies bonded together is shown in Fig. 17. One epoxy is a fully rigid system and the other a semi-flexible system. The coefficient of thermal expansion of the two epoxies is quite different. This sample was thermal cycled from −70 to +150°C every hour for 24 h. After thermalcycling the bond between the two

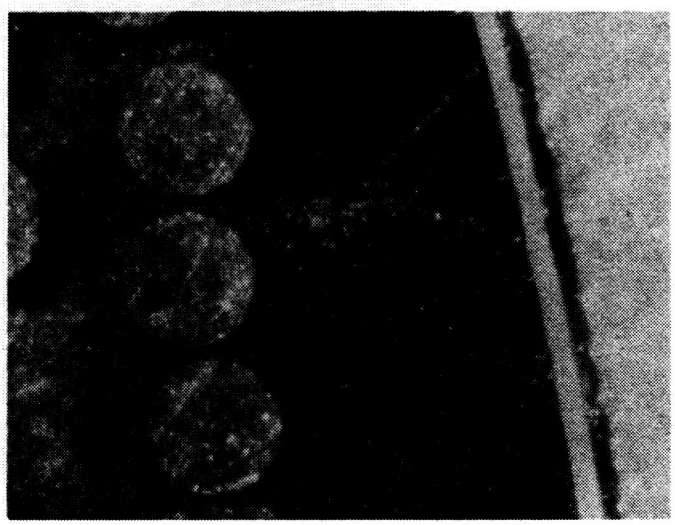

Fig. 16. Toroid with poor seal

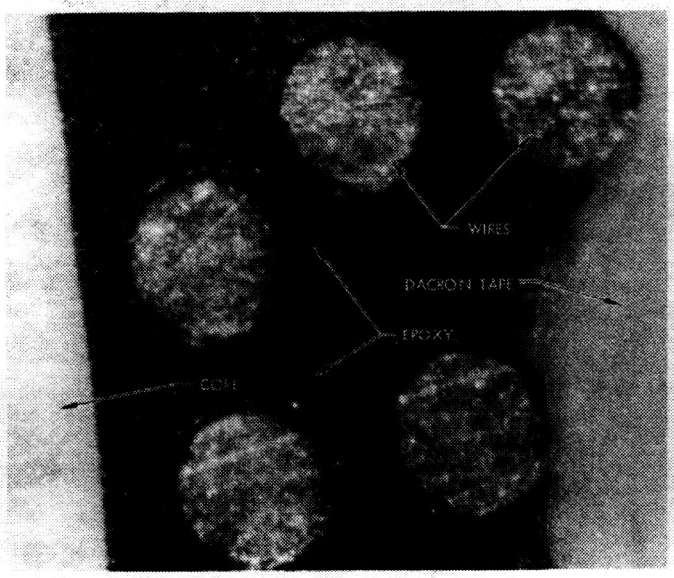

Fig. 15. Impregnated, dacron-wound transformer magnified 200 times

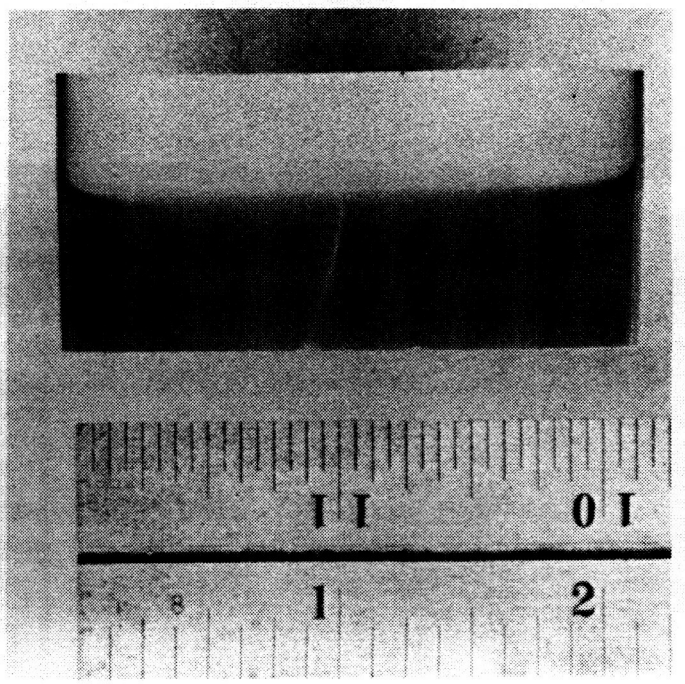

Fig. 17. Typical two-bonded epoxies

epoxies and the bond of the epoxy to the case was checked under a microscope. There was no fracturing of the bond. If more than one encapsulating material is used in a high-voltage application, they should be checked for compatibility to be sure incompatible interfaces are not introduced into the transformer or power supply by the separation of the two epoxies.

For those who are not familiar with epoxies, I might explain that the reason for using a rigid epoxy as a final encapsulating material is that usually rigid systems tend to outgass less than flexible systems. However, no decision to use a particular epoxy in space applications should be made until all the important parameters are known.

The following is a summary of items which, it is felt, are important in the design of corona-free high-voltage transformers: (1) choose a core of sufficient size and of the proper construction, (2) select wire of sufficient size for reliability, (3) select an interlayer insulating material compatible with the impregnating material to be used, and (4) choose impregnating and encapsulating materials which are compatible with each other and with core coating, wire insulation, and the interlayer insulating material.

Discussion

Reynolds: Can you describe the technique you used for making a joint between the wire and the lead out? I assume you did have a joint in there, you didn't lead out the magnet wire.

Byers: Well, in most cases we try to avoid the splicing of leads there. We try to run the magnetic wire, if it is of sufficient size, directly out from the transformer to the PC board. But, in cases where we can't, we try to stay with polyurethane-coated wires and then insulate under the connection and also over it.

Reynolds: You make some sort of splice by soldering?

Byers: In cases where we have to, we do have a splice, but we insulate with the dacron tape under and also over.

Bunker: Did I understand you to say you had a hermetically-sealed unit which would operate at any pressure and that it had a connector in it? I was wondering what kind of a connector you used.

Byers: In that particular case, we are completely hermetically sealing the package, coming out, even out of the package, with metal tubing. The conductor goes through the metal tubing and directly into an ion pump, which also is sealed at that end, thus, there are no connections of the high voltage.

Lagadinos: We used a similar process in the toroidal construction of our transformers, and we had a number of problems with the comparability of epoxies and Teflon. There seems always to be an interface.

The other problem that we had, when we impregnated a toroidal transformer was that we created some critical pressures within the core. If we tried to float the core, then we had corona levels at low voltages.

One way that we were able to get around this problem was to place the low-voltage winding on the core first, then impregnate the core over with a controlled thickness of impregnation. Then we placed the high-voltage winding over that impregnation. I wonder whether you had tried anything to that extent.

Byers: No, not with the epoxies. We have tended to put a number of layers of dacron tape between the windings and then completely impregnate. We have had very good results this way.

Lagadinos: The system that I just mentioned reflects on the LEM program which is operating right now.

Where is the magnetic material on the board that you are using? Is this a Permaloy or is it a Carpenter 49?

Byers: Could you tell me what the tape is on that thing?

Forsberg: It is a Permaloy.

Question: To what extent have you evaluated the materials which are within the sealed-core assembly and quantitatively evaluated the degree to which it is, in fact, sealed?

Byers: The only thing we have done with the cores to prove that they are sealed is to put them in boiling water and bring them up to heat to see if there was any quantity of air there; but, our approach is more to pot this thing in an epoxy. Whatever air happens to be in there, just lock it in, and leave it. It is supposed to be actually an airtight seal, and they are supposed to replace the air with silicone material, but I wouldn't want to guarantee that they do 100%.

Holbrook: Do I understand that you are still using Teflon?

Byers: No, definitely not.

Holbrook: And the reason was because of interfacial separations?

Byers: Yes. There is a lot of work being done to try to improve this bonding with Teflon, but I have tried several coatings that even Du Pont put out, and, of course, they were applied by a subcontractor. However, these coatings did not bond as well to the Teflon on the wire as they did to my epoxy. I was able to pull the wire right out of the coating.

Holbrook: Have you looked at the use of some of the proprietary Teflon etchings?

Byers: Yes. I have some right now on my desk that I have been working with. I tend to stay away from them, even with the etch, because in most cases you are not getting a bond; you are just increasing the length of the path down into the little separations, and so on.

N70-32297

High-Voltage Packaging Investigations in the Advanced Technology Group

E. Bunker, Jr.
Jet Propulsion Laboratory
California Institute of Technology
Pasadena, California

It was interesting to examine the list of attendees to this gathering. Very few of you were here three years ago for the previous workshop; however, approximately the same companies and centers are represented. I wonder whether this denotes a lack of interest or, rather, reflects changes brought about by promotion or personnel turnover.

Of necessity, some of this paper may overlap previous work.

The high-voltage packaging work performed in the Advanced Technology Group at the Jet Propulsion Laboratory (JPL) has three main objectives:

(1) The establishment of parameters and techniques for high-voltage packaging through the critical air pressure region and in the high-vacuum region.

(2) The improvement of instrumentation and establishment of test procedures to determine if corona exists in equipment and components.

(3) The preparation of specifications covering design and packaging of high-voltage circuitry.

To achieve these objectives, we conducted our own investigations and research, including design and tests. In addition, we visited other centers, vendors, and anybody else with whom we could speak, including holding and attending symposiums. The previous voltage breakdown workshop is a good example of such activity.

This is a progress report covering the objects we have pursued and their present status. The major objectives achieved during this period were the preparation of specifications for the *Mariner* '67 and *Mariner* '69 spacecraft projects. These began as packaging specifications, but guides for the designer were included; e.g., separation of conductors, maximal allowable stresses on insulation, and the statement that air was to be considered to have a zero dielectric strength. Some of these had to be taken into consideration to achieve a reliable high-voltage design.

These specifications applied to any equipment employing any voltage over 250 V, as 250 V was defined as high voltage.

Two classes of equipment were defined: Class I and Class II. The Class I equipment is that equipment designed to operate to specification in the critical air pressure region without corona or arcing. Of course, spark

gaps or devices that rely on arcing or corona for their proper functional requirement, were not excluded. Class II equipment was defined as equipment not subject to damage as a result of corona or arcing; however, operation to specification was not required.

This made it possible to design equipment which would not be free of corona but which would provide a means of protecting it and adjacent equipment.

We also included a description of tests, especially tests on transformers, to detect voids or defects in winding-to-winding insulation, and voids in the insulation between turns of the same winding. This was done to see if we could detect voids in the potting. From the tests performed on one transformer, it seemed we were successful.

One point of controversy, at the preceding workshop, was whether to use foam for high-voltage insulation. This problem resulted in considerable discussion.

I was interested in Mr. Brockmeyer's report on a foam-filled antenna that functioned well initially, at a power level of 200 W, and then, after three days in vacuum, would break down internally with only 80 W. This supports the contention that the air or the blowing gas in the foam exposed to a high vacuum will gradually leak out and the pressure will eventually go into the critical region, causing failure.

Since some of our advanced designs are for the Grand Tour spacecraft which is to be launched in 1977 for a 10-yr flight, plus testing, we are concerned with more than a few hours, a few days, or even a year. We have to be sure that our designs will last, as one person put it, virtually forever.

In an attempt to resolve the controversy over foams, we took various foam samples, put them in a vacuum, and tried to measure the pressure decrease in an internal cavity due to diffusion of the blowing gas. We were not too successful because any pressure gauge had a much larger volume than the volume we were trying to measure.

We decided to use the direct method of measuring the pressure in a cavity by determining the breakdown voltage of a fixed electrode configuration. Comparing this voltage with that of a calibration sample with an identical electrode geometry but with known pressures in the cavity would indicate the pressure in the unknown. Four samples, as shown in Fig. 1, were prepared. We

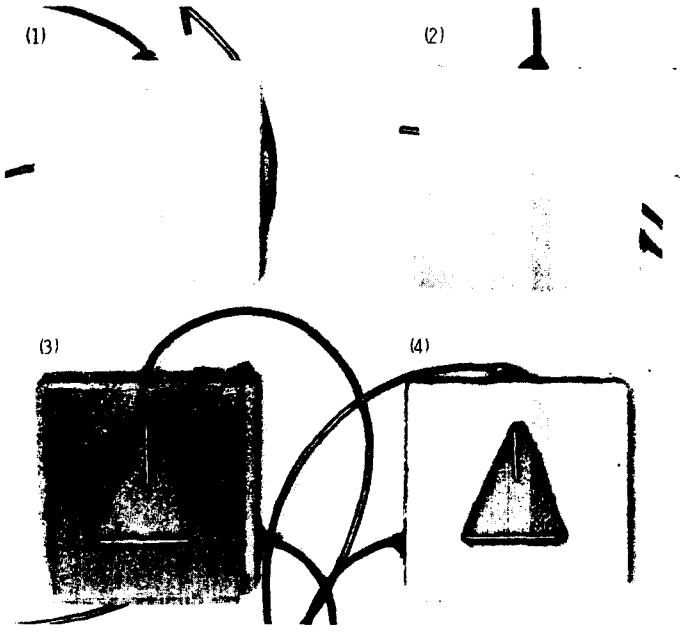

Fig. 1. CPR-8 isocyanate foam samples

cut four samples of CPR-8, isocyanate foam out of a block of material. The electrode configurations were the same in each which had a T configuration with a 1-in. separation. The points of the stainless steel rods were rounded to a 3/32-in. radius and polished.

The No. 4 sample was left open to the environment; the No. 3 sample had a plastic cover bonded over the triangular cavity so that the arcing or corona could be observed. The No. 2 sample was the same as No. 3, except that instead of a clear window we used another piece of foam. The sample we are really trying to test, No. 1, merely had holes drilled in it for the two rods. In other words, we were testing the foam between the point and the rod of the solid sample.

Sample No. 4 was our reference. It was run in the vacuum chamber at various pressures from 760 torr to 10^{-6} torr; we measured the breakdown voltage up to 10 kV ac and visually observed the type of breakdown across this gap. Using this as a calibration for breakdowns in the other three samples, we acquired a feeling for the average pressure between the electrodes.

All four samples were placed in the vacuum chamber, which was pumped down to a very high vacuum, and left for more than 300 days. From time to time each sample was checked for breakdown in order to determine what was happening inside.

Sample No. 1 never showed an arcing breakdown. Samples No. 2 and 3 went into the critical region. There was no discharge between the point of the rod in No. 4 since it was in a high vacuum; however, we thought there might be some leakage path around through the foam as it outgassed. This was not observed.

In No. 1, from time to time, various anomalies were observed on the scope that could be due to small corona bursts. Therefore, about halfway through the experiment the 10 kV voltage was applied continuously to see if the anomalies would break down; after a while they disappeared, and nothing further happened.

The color in sample No. 1 differed from the color of the other samples. They were all cut out of the same block of foam, but the bubbles in No. 1 were much smaller, which might have introduced an additional parameter in the experiment. Figure 2 shows the results for samples 2 and 3. The curves start out at room pressure, and then the points went up. We think this must have been due to the outgassing of the adhesive, which increased the pressure a small amount. As time went on, the pressure began to leak down because the corona initiation voltage became smaller and smaller until we got down into the arcing region from the corona region. Arcing occurred in both samples.

The scattering of the points is rather interesting; note that the curve drawn is not smooth, not an average, but zig-zag connecting each point.

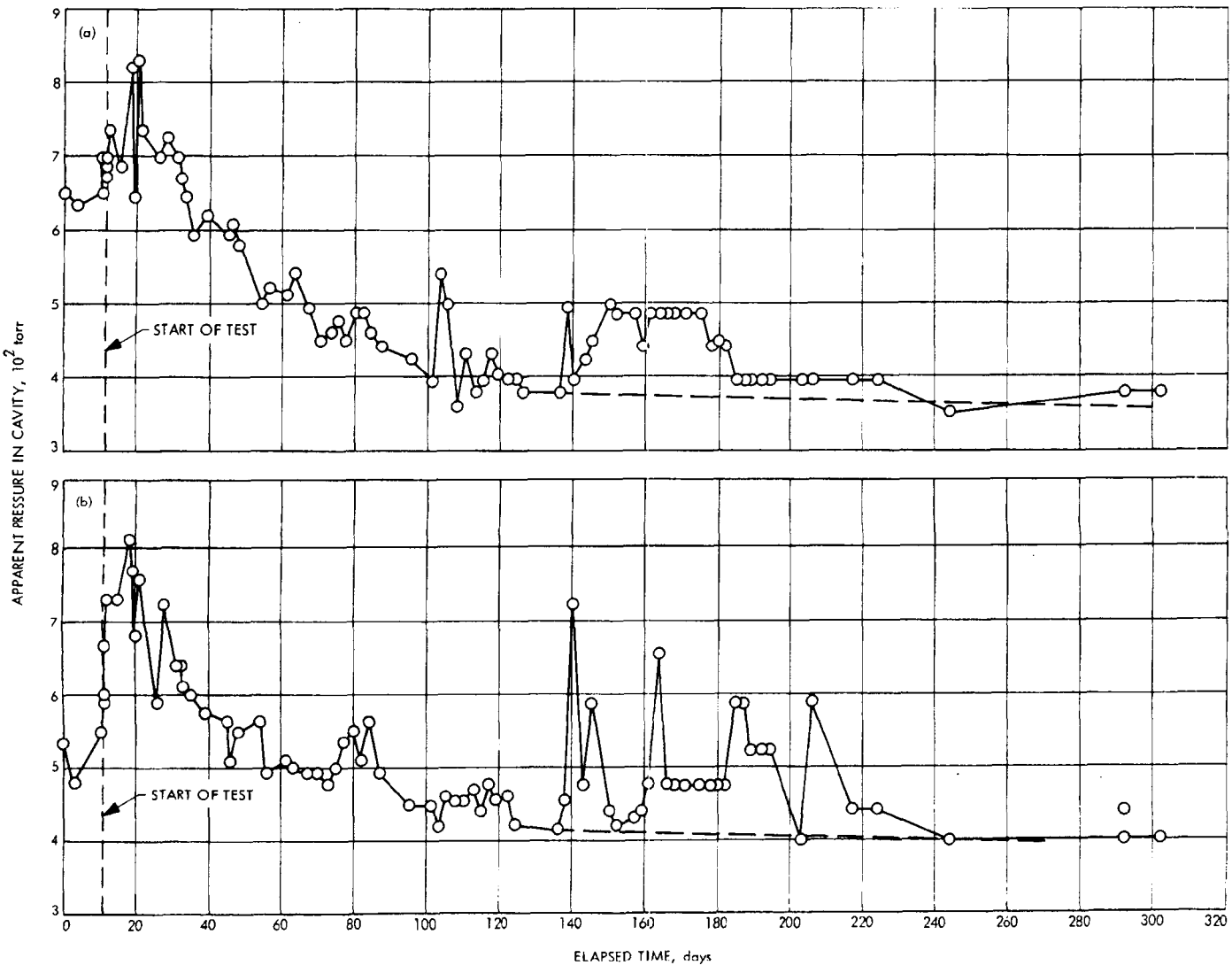

Fig. 2. Test results for samples No. 2 and 3

The point plotted for each day is a result of between five and ten readings, it is not just one voltage reading, so the pressure seemed to vary from day to day. Maybe the bubbles were ruptured in bunches releasing gas in surges; we don't know, but that is the reason this curve is drawn this way.

Both curves come down, and level off. Sample No. 2, which was all foam, came down faster to a lower level than the one with the window. So it showed that the extra foam on top provided an additional leakage path.

The experiment was terminated at 300 days because the data appeared to be asymptotic at around 400 torr. It wouldn't prove very much to continue the test. The data showed that at least where there is a cavity of larger dimensions than the bubbles, there is an outgassing and the pressure goes into the critical region. By extrapolation it seems reasonable to believe that the gas pressures in bubbles will do the same, though it may take longer.

Another part of our work is in Corona Detection Networks. We prefer the so-called series or Quinn type, instead of the MIL-T-27 type.

Figure 3 shows that the Corona Detection Network in MIL-T-27 is a corona-free, oil-filled capacitor tied into the high-voltage point, and then an inductance in series with the other end grounded and the node point connected to the input of the oscilloscope. Thus, any high-frequency noise generated by corona is coupled through the capacitor, with the inductor showing a large impedance to the noise voltage. This is the standard test set-up. and the IEEE has written specification on a sensitivity calibration of this.

The problem with using this in vacuum is, of course, that we can't make the high-voltage connection to the capacitor in vacuum. To make the connection we must bring the high-voltage level out through the vacuum chamber interface which may not be practical. Besides this, the capacitor is often larger than the equipment we are trying to test. For these reasons, therefore, we went to the Quinn, or the series type, shown in Fig. 4 which looks similar because it too uses an inductor and capacitor, but is not. The high voltage is applied only to the load, and the inductor is in the ground return. The radio noise generated by corona is capacitively coupled to the oscilloscope. This can be done outside the vacuum chamber; in fact, the voltage level is only a few mV, so that it is very handy and it can be included in spacecraft subsystem cabling. This method of being able to tie into a ground loop, actually monitor the complete subsystem for corona during the thermal vacuum test, has been accomplished.

This circuit, however, is an elementary one. During our investigation it was found that it was possible, under certain vacuum conditions, to get dc corona in which no radio noise was generated. A very dim corona could be seen on the point, but the oscilloscope gave no indication. Therefore, we went to the Type II, shown in Fig. 5, to which we added a neon bulb in series with the input, and another across the inductor. These would light up when corona current was present, but the neon bulbs were not sensitive enough as they took 20 μA to turn on. We then went to the Type III, shown in Fig. 6, which is a little more sophisticated and which we are presently using. The Type III is in series in the ground return of the high-voltage load.

Two zener diode bridges in series are used to rectify the ac corona and arcing voltages, which are indicated on the microammeter or milliammeter, respectively. The resistances in series with the meters are of such values that, with rated full-scale meter currents, the voltage

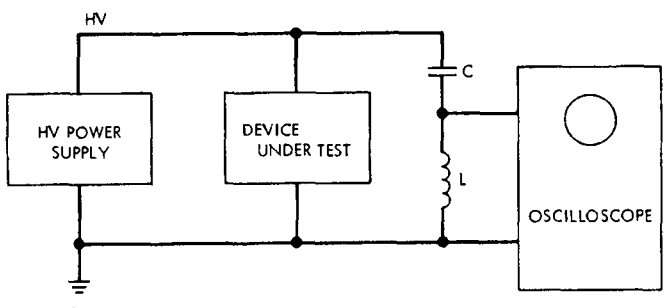

Fig. 3. MIL-T-27B corona detection network (shunt)

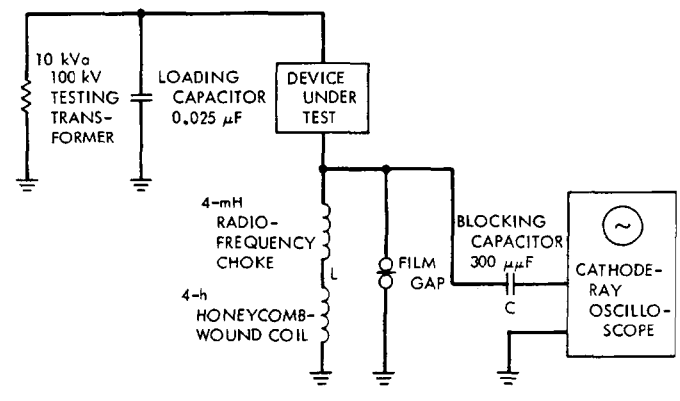

Fig. 4. Quinn corona detection network (series)

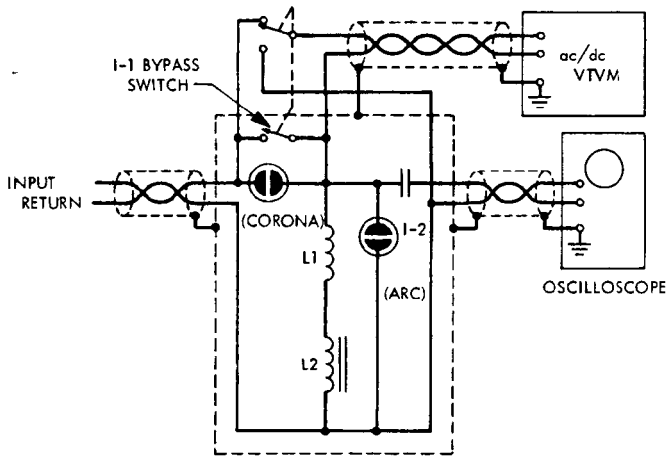

Fig. 5. Type II corona detection network

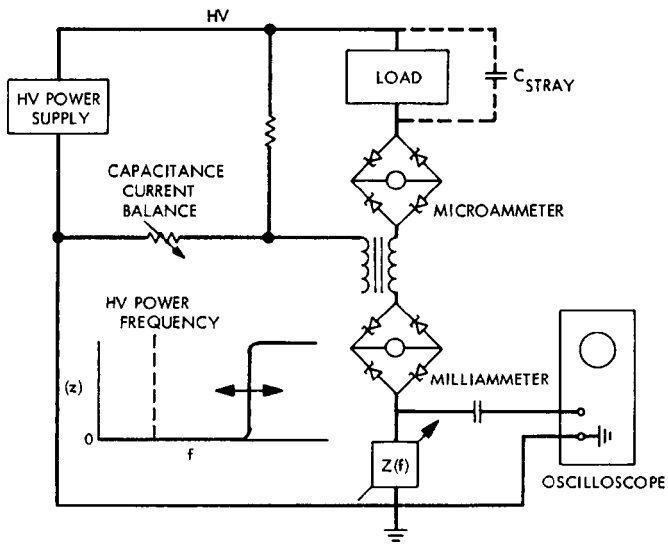

Fig. 6. Type III corona detection network

drop equals the zener breakdown voltage. In this manner, each meter is protected from current overloads or surges.

Reduction of the power frequency to a sufficiently low level so that the higher frequencies of very low amplitude corona may be detected as on an oscilloscope is accomplished by an inductance as in the Quinn circuit, or more ideally, by a more complex high-pass filter with a variable cutoff.

We also have proposed an added feature of adding a capacitive current balance for ac so that the current due to stray capacitance can be balanced out. Thus, the microammeter needle will not move until corona occurs.

As the high voltage is increased, the capacitive-coupled voltage is in proportion so we can null it out, essentially, and then go to a microammeter to indicate the corona current.

Another advantage is that the zener diode bridges work on ac or dc equally well. There is a dc path of either polarity through them as well as ac; however, the calibration of the meter is different.

We have built one such model and have used it in some of our work. We have some improvements to make in the capacitance current balance network. We also plan to calibrate its sensitivity so that it can be compared with the MIL-T-27 shunt type.

Since most spacecraft power sources supply 2500 Hz, or higher, we need to test the dielectric strength of the transformers and electronic equipment at this supply frequency.

Another of the objectives of the Advanced Technology Group was to obtain a power supply which would allow the use of higher frequencies, such as 2500 Hz. We sent our specification out for bid, on a 10-kHz, 10-kV power supply, with a 1-% distortion sine wave. The request was sent to 28 power supply companies; no bids, however, were received.

It was decided the effort should be performed in-house, using a little different approach; this approach is shown in Fig. 7. Using a linear power amplifier to drive a step-up transformer, we will have a high-voltage output of the same frequency as the input to the amplifier. Since there is no requirement to change frequency while operating, several transformers can be used to cover the range of the power amplifier.

Furthermore, there is another advantage; we can put other wave forms in and see how breakdown is affected

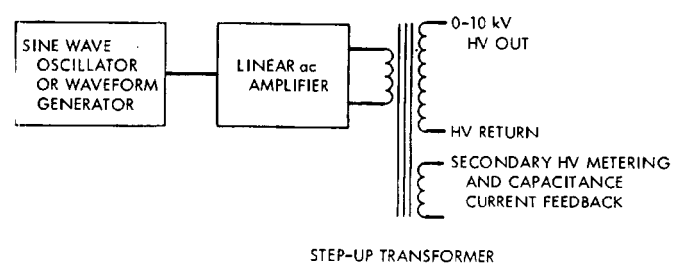

Fig. 7. High-voltage variable-frequency power supply

by waveform, e.g., a tone burst. Then we can see what kind of breakdown occurs in the critical pressure region.

Another project is an automatic equipotential plotter for the determination of equipotentials in a complex high-voltage geometrics. In the past, I have used the laborious and messy water tank method for drawing equipotentials. Starting out with the resistance paper method, the electrode configuration was drawn to scale with silver ink on resistance paper. As shown in Fig. 8, the paper was placed on the X-Y plotter and the ink column was used to pick up the voltage, compare it to a set point, and the difference then drives the Y axis motor. Using the X-scan, it follows along and draws the equipotential. By re-adjustment of the set point, starting over, and we could rapidly get a series of equipotential lines.

We had investigated other methods using digital computers, and found that any time you get other than a very simple geometrical configuration it becomes very cumbersome even for a computer.

We are not interested in the extreme accuracy obtainable with a digital computer; however, we would like to know where the regions of highest voltage stress would be for a given design, and what changes are necessary to alleviate the problem before actual fabrication.

Such equipment is still under development. The first model operated well, but the ink would not stick to the resistance paper. We changed ink, and got adhesion.

It is felt that this approach, which gives us a planar representation of a three-dimensional configuration, would at least provide an idea where the problem areas will be and what to do about them.

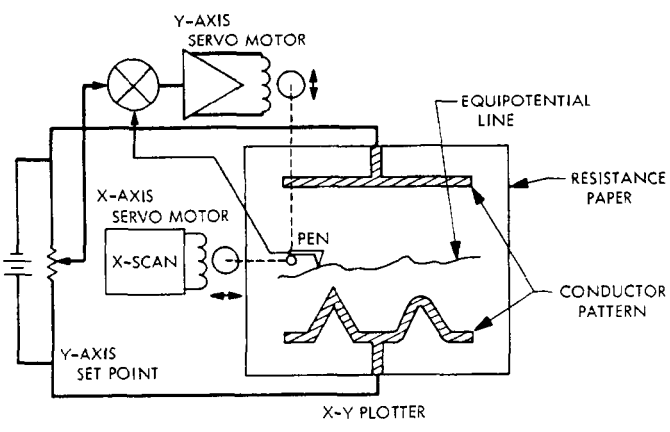

Fig. 8. Automatic equipotential plotter

We also did work on transformer encapsulation. I was very interested to learn if Mr. Byers was going to recommend Teflon for the insulation between windings, and yet be able to provide a void-free encapsulation. We are working with two types of transformers: a toroidal transformer with a 1-kV output and a pi-wound secondary transformer which has a rating of 12 kV. The specifications required the use of a porous tape material, not Mylar, between windings. There was quite a bit of discussion with the transformer vendors who insisted that Mylar was the better material to use; as with Teflon, however voids cannot be eliminated during encapsulation. Dummy toroidal transformers with micarta cores so they could be sectioned easily were fabricated.

There are several requirements for encapsulants which demand a void-free encapsulation for high-reliability space application. First of all, the encapsulants must have a very thin viscosity to be able to completely penetrate the windings. Secondly, they must bond completely to the high-voltage wire insulation.

Another frequently unappreciated characteristic of encapsulation materials, especially of the more rigid types, is the compressive forces applied to the electronic components at low temperatures. We have measured this in various kinds of materials, and are preparing a report. For example, Stycast 1090/11, which is frequently used, is very light in weight; but, when you get down to $-40°C$, it stresses the electronic components to something like 3000 lb/in.^{2} Some other popular encapsulents exert even greater stresses.

In addition, the encapsulent must not evidence heat damage because it will be used on equipment which will be dropped on planets, and, thus, should be heat-sterilized at 135°C for 600 h. Finally, it must have adequate dielectric strength, as well as ensure a complete bond with the lead wire insulation.

After trying various kinds of materials, Scotchcast 235/241 was chosen. For a while, Scotchcast 280/281 was considered the best choice because it was rated at a higher temperature; but, we found that Scotchcast 235/241 would withstand the sterilization temperatures.

A one-step encapsulation process using Scotchcast 280 was also tried. With it, we could simultaneously achieve impregnation as well as encapsulation. Its use was finally rejected because the 280 material, normally an impregnant, will crack in large masses.

Mariner '69 carries TV transformers that were designed to the specifications previously mentioned and tested for both interwinding and turn-to-turn voids. Several transformers that had rather interesting effects, which could be explained as corona occurring internally in the windings had been considered. These were rejected, however, in favor of those transformers for which anomalies were not indicated.

After the flight is completed, anomalous transformers will be available for testing and connected into circuits. At that point we will correlate, where possible, any failures to determine is the test results, which indicated a void between turns, actually a void or something else.

Tests performed on the transformers selected for *Mariner '69* were run at 2500 cycles at the rated voltage. The voltage and frequency was then doubled to get a twice turn-to-turn voltage stresses in all windings. At this point, some of the corona indication became apparent. Insulation between the high-voltage secondary winding was stressed by applying twice the operating power plus 1000 V rms at 60 Hz to one terminal of the winding, and grounding the primary through the Corona Detection Network.

Since there is doubt in some quarters that Teflon is ever really bondable, in spite of special surface preparation, one of the other things we did was to try and find high-voltage wire that is Teflon-free. None was available, and it is difficult to get vendors to make special wire in small quantities. We don't make very many spacecraft, so we really don't need too much of it.

A high-voltage wire is needed because in most cases the high-voltage power supply is in one place, encapsulated, while the load is in another; this requires a wire between them.

We have had failures of the encapsulation not bonding to the wire insulation; in fact, Fig. 9 shows a test set-up using Epoxylite 295-1, where the wire insulations are plain Teflon, polyolefin, nylon, and etched Teflon. An 0.25-in. section of insulation was removed and then the wire was encapsulated.

This sample was put in the vacuum chamber and high voltage applied to each wire in sequence. Due to lack of bonding between the plain Teflon and the Epoxylite, failure occurred after a few seconds, resulting in black streaks. There were no other failures, but this was not really too good a test because the wire was not shielded and it glowed. The corona quickly burned holes in the wire insulation.

We obtained some shielded high-voltage wire fabricated to a specification which would not allow Teflon.

Figure 10 illustrates the test configuration established to determine the bondability between various wire insulation materials and the encapsulant. Three sets of double

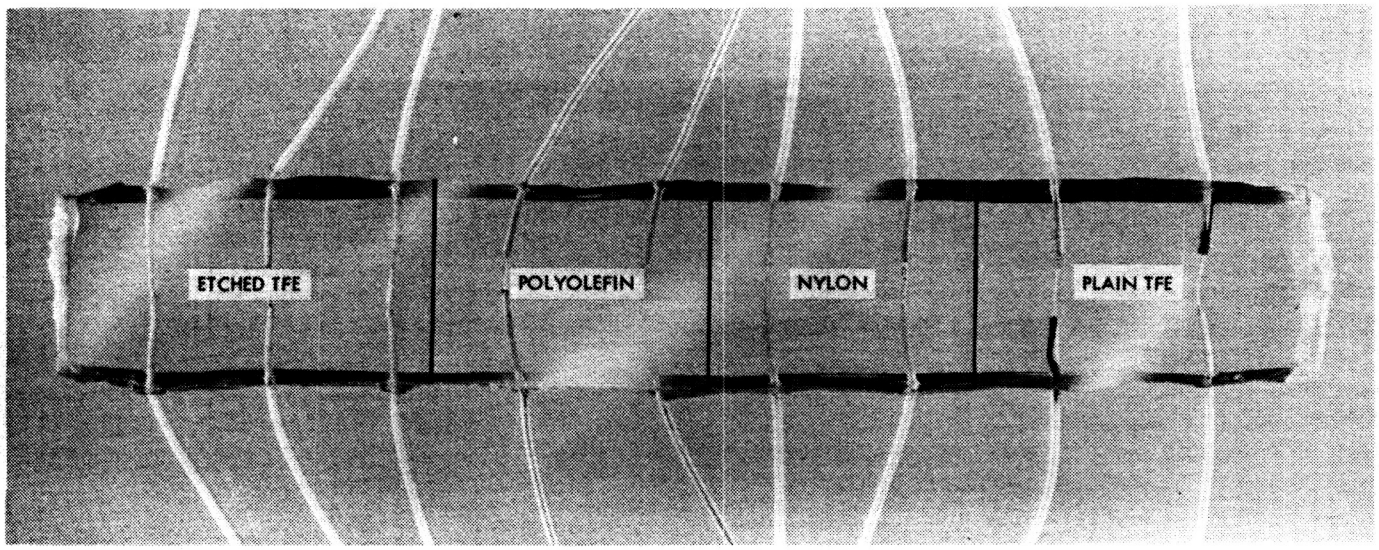

Fig. 9. Wire insulation samples for bonding test set-up

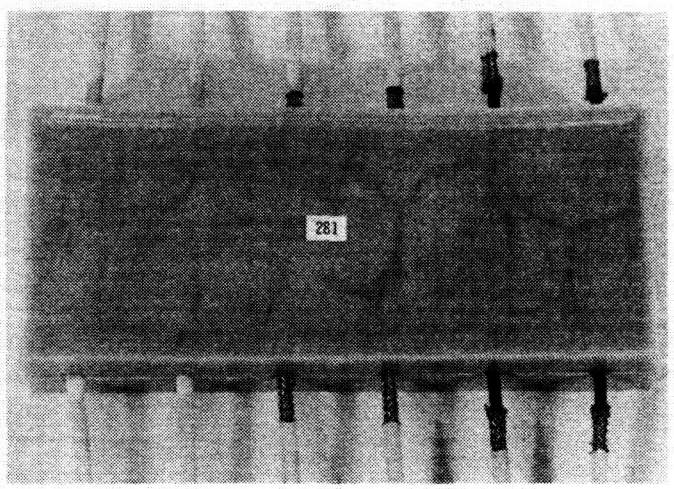

Fig. 10. Test configuration

wires were used. The first pair were jacket shielded and insulated, and each quarter-inch was exposed to bonding of the encapsulant, in this case, Scotchcast 281. The second pair had the jacket cut back so only the shield and insulation were embedded. The third pair had only the wire insulation with both the ends of the jacket and the shield exposed. We planned to put these samples in the vacuum chamber and apply voltage to them. The two wires that we were really testing were the ones with the sheaths embedded.

The other sample were simply designed to see what would happen if air got down the shield. We haven't tested any of these yet as the high-voltage wire wouldn't take more than 300 V because of the conductive powder smeared over the cut ends.

Figure 11 shows the configuration of the wire we obtained. It had an overall diameter of slightly more than a tenth of an inch and was rated at 7 kV operating. It was tested at 15-kV ac or 35-kV dc, with a conductor of 19 strands of 34 gauge. Next to the strands was a conductive plastic which smoothed out the stress from sharp points from the wire, thus protecting the dielectric. Next is the insulation dielectric and then the shield. What isn't noted is that the shield also had a layer of conductive powder to eliminate stresses from points, as well as assist in the fabrication. The presence of the conductive powder was not realized until after the test samples were made, when breakdowns were occurring at abnormally low voltages. A very thorough cleaning with 1,1,1, trichloroethane removed the powder, then the wire would withstand rated voltage, but, of course, could not be applied to the embedded ends.

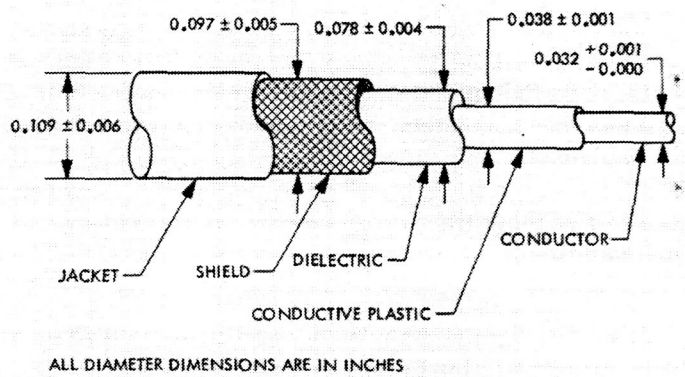

Fig. 11. High-voltage wire configuration

The insulation was all non-teflon, the dielectric was modified polyolefin, and the outer jacket was polyvinylidine fluoride. Presumably, a good bond could have been achieved with various encapsulating materials; we want to find something that would completely bond to a quarter-inch of encapsulating material.

Our long range plans are to go as high as 100 kV in our high-voltage designs.

Discussion

Holbrook: I would like to know, first of all, how do you define corona, either in terms of currents or energy levels, and, secondly, how does your Type III corona detector differentiate between ohmic conduction and the discharge currents caused by corona?

Bunker: Well, first of all, I define corona as a partial breakdown of a gaseous dielectric; an arc is a complete breakdown. In other words, corona is a high-impedance path; arcing is a low impedance path through the gas. I have assumed 1 μA was the lower limit of corona, but I have been able to detect corona currents at 0.3 μA, and I think there are some quite a bit lower, if we go to a photomultiplier-type detector, which we haven't as yet.

But, that is my definition. It isn't a good one, but that is the one I am using. I don't define it by energy levels. If someone else knows, I would appreciate the information. There is a definite point between the Townsend current, due to the free electrons floating around, and where the electrons are stripped off of the gas molecules and the gas is ionized. That is the start of corona.

Holbrook: It has been my experience this appears as an emission type, almost as a capacitive discharge when displayed, using an oscilloscope. I made my corona measurements by just measuring the voltage drop across the standard resistor and using well-shielded circuits. I have been able to detect these non-ohmic conduction levels down as low as 10 nA. It is interesting if you take samples and allow this condition to exist, to see these very low levels of non-ohmic conduction; eventually you see degradation of the dielectric.

Discussion (contd)

Bunker: Are you talking about dc?

Holbrook: Right.

Bunker: We are more interested in ac because it is harder to prevent corona due to the dielectric effect of the various insulating materials. That's the reason we can't use a resistor for ac, because the ac capacitance voltage would mask any corona occurring. You have to have a type of filter which is effectively what we have in the Type III corona network.

Holbrook: I have another question. How do the results of your X-Y equipotential plotter compare with field equation analysis for simple electrode geometries?

Bunker: We haven't got that far to try it out. We are still trying to iron the bugs out of the instrument.

Holbrook: Do you plan to do this?

Bunker: Yes. At the next workshop we may be able to tell you how we did it; or you come around and we will show you.

Young: Two questions: what do you recommend in place of urethane foams? Question two: what do you think about solithane as an encapsulant for high-voltage power supplies or packaging techniques?

Bunker: Well, my recommendation is that foam, and that is in our specification, not be used for high-voltage work. For solithane, we use a lot of it here. We use it for conformal coating, but don't use it so much for encapsulation, but it is quite effective for coating high-voltage circuits, as long as you don't have a sharp point which makes the solithane thin at that place making a breakdown possible. It is handy because it has a low-shear strength. You can tear it apart to repair something and seal it up again.

Zaiden: I notice most of the work is done on wires and so forth. How about connections? This is the main problem we have been having. We have found good wire as far as corona-free wire, but when we get down to the connection, this is where we are running into problems.

Bunker: By "connection," you mean termination or connectors?

Zaiden: Termination and connectors; such as the shield that you had in that picture there. How do you terminate your shield?

Bunker: In one design we have a power supply separate from the load, requiring a high-voltage cable in between. The high-voltage lead goes to a terminal that is in a recess in the power-supply encapsulant, but filled with solithane. To disconnect that wire, we dig away the solithane, unsolder the wire, and pull it off.

As for a connector, I don't know one yet that will work. We have an idea for one that we may try out for an actual high-voltage connector which you can put together and take apart.

Zaiden: Are you designing your own connectors?

Bunker: Designing is sort of a hard word. We make up a sketch of a prototype. Then we try to get somebody to build it for us. We wouldn't try to design it here, unless we could use standard hardware such as contacts, shells, etc.

Lagadinos: You mentioned a 12-kV transformer in your discussion. Do you care to elaborate slightly on the construction of that transformer?

Bunker: The transformer was originally designed for another group. It has 5 high-voltage pi's, each rated at 2-½ kV. It uses a C-type core, with the primary, a two-layer winding between the pi's and the core. The idea is to encapsulate the whole thing. We made some changes in it. The original design had the high-voltage leads between pi's come up and connect in order, start-to-finish, so you have quite a buildup of high-voltage interconnection wires, at high-voltage differences, and small size.

What we have done is taken the No. 2 pi and the No. 4 pi, reversed them, so that we can tie start-to-start, finish-to-finish, start-to-start, etc., and keep all interconnections right down inside the transformer between the pi's. We are in the process of encapsulating this now.

Lagadinos: Is the insulation tapered as you go along, since the voltage rating increases to the last pi?

Bunker: That would be nice, but it is so small that it wouldn't pay us. The whole transformer is about 4-in. long.

Lagadinos: Is this corona free at 12-kV ac?

Bunker: That is our objective. We haven't tried it yet. Other people have. I think we ought to be able to.

Cooper: Will you identify solithane, please.

Bunker: It is made by Thiokol and is a clear material, rubbery, doesn't adhere too well to things, which is its main disadvantage, but it is repairable.

Question: It is a polyurethane?

Bunker: Yes.

Goldlust: I think I am having the same trouble that the gentleman from Hughes had with your Type III detector. When you are using ac on that, are you doing your monitoring across the scope or using your ammeters?

Bunker: Both. The oscilloscope is used; it is the best detector when there is radio noise, because we have a very high gain in the oscilloscope x amplifier and we can adjust out the power supply frequency that's going into it. Under some conditions of dc, when there is no radio noise, we have to use the microammeters.

Goldlust: How do you separate the dc, the spurious pulses, corona pulses, from just the –

Bunker: Pulses on the scope.

Goldlust: Then why do you use the ammeters?

Bunker: The purpose of the ammeters – I didn't explain – they are set point meter types, so we can set it up and if we have a corona current more than half a μA, for instance, it will shut down the power supply and we won't burn anything up. So, we can leave it unattended. The main purpose of the ammeters is to serve as a technician-free monitoring system.

Goldlust: But you are depending on the oscilloscope for your measurement?

Bunker: Essentially, yes.

Stern: You had mentioned that your tests were made with the foams. Were these foams communicating cell types or closed cell types? If they were foam cell types, do you have any comment to make on the communicating cell types of foams as a dielectric for potting?

Bunker: This foam was supplied by a company and it was the closed cell type. You can look in a microscope and see the cells. You could see the cell walls bulge in and out as we would change the pressure. The communicating type, I have no feel for.

Question: What was the voltage in frequency, waveform applied in your foam tests?

Bunker: The voltage was 10-kV ac, 60 Hz more or less sine wave.

Question: In corona testing reactors, where you have a dc and an ac superimposed voltage, what is your feeling in regard to thoroughly testing those devices on a simulated basis?

Bunker: I have seen some data. I can't remember the exact figures or company involved, but I can give you the results reported. This company had a reactor they tested first with dc, and it would break down at 40 kV. They tested it at ac and it would break down at 16 kV. When you combine the two, it would seem reasonable that you should have a summation, but you still could put almost 40 kV dc and 16 V on top of that before it would break down.

Question: We had that problem. We consulted with James Biddle Company, and they felt that if the dc level is only 30% of the ac, then the ac is a sufficient test for the insulating properties of the device.

Bunker: I have this report, but haven't really studied it. It seemed interesting, but it didn't seem reasonable. I don't know if it was the configuration or not.

Holbrook: Why are you so adamant against the use of foam? Based on your test results, they would indicate that it is an acceptable material for short-term use in space, say, up to two and three years; however, you have taken the position, or apparently have taken the position that foam should not be used as dielectrics for high-voltage applications.

Bunker: Well, I am not as biased as I might appear. The reason I am personally against foam is we have had failures in our spacecraft equipment; in fact, there is one instrument that was to fly on Mariner '64, an ultraviolet spectrometer, but didn't because of a breakdown on a printed circuit board. This board had 2800 V, between conductors with inadequate separation. The conductor side was foamed with about a half inch of foam on it, afterwards a layer of solithane was brushed over it. After 75-100 h in thermal vacuum it broke down. I am in the position that if I recommend something contrary to our experience, like "use foam," and it breaks down, then this would be bad.

So I am taking the easy way out and saying no foam, because we have had failures with it, and there are other ways for accomplishing the same objective.

Holbrook: Was the circuit board entirely encapsulated, or was it just a foam coating? Could there have been an interfacial separation which caused the break down?

Bunker: It could have. It was a printed circuit board on one side with just a foamed-on block there. Now, the breakdown occurred between the foam and the board. If there was a bubble there, or something, we don't know, but how do you control it if you foam it in place? How do you know there isn't a bubble there?

Holbrook: Foam the entire thing.

Bunker: Another thing, of course, isn't it reasonable to assume that there will be a diffusion out of the blowing gas so the pressure in the bubbles will eventually go in the critical region? We asked the plastics people if we couldn't put some of this foam material in the vacuum chamber and foam it in the critical region with electrodes so that you end up with the pressure in the bubbles in the critical region, then apply voltage and see what happens. They threw up their hands and said no; so, I don't know.

N70-32298

Corona Evaluation of Spacecraft Wires and Connectors

W. G. Dunbar
Aerospace Group
The Boeing Company
Seattle, Washington

I. Introduction

Nonhermetically-sealed electronic assemblies installed in spacecraft will outgas as the spacecraft makes the transition from earth atmosphere to space vacuum. Some spacecraft will make a second transition from space to earth's atmosphere or to other planetary atmospheres. In addition, inadvertent pressurization can be caused by materials outgassing or engine firings. During these transitions electrical components and wires in pressurized electronic assemblies may see pressures between 20 and 10^{-2} torr, a range that includes where corona is most likely to form.

Corona between electrodes and insulated wires occurs whenever the voltage gradient in the air spaces between wires exceeds a critical value (Ref. 1). Corona manifests itself as a luminous glow or as a small current between energized electrodes. These phenomena result from localized critical gradients. Ultimately, a spark or arc carrying larger current forms if the critical gradient progresses across the whole spacing. Electrical discharges, including corona, in gases follow Paschen's Law, which states that breakdown voltage is a function of gas pressure times effective electrode spacing. Based on Paschen's Law, corona-onset voltage data has generally been presented for various insulated wires either as a function of gas pressure multiplied by effective conductor spacing or as a function of gas pressure for various insulated wires (Ref. 2).

The ionized gas created by corona degrades the electrical and physical properties of the insulation on wires (Ref. 3). This degradation is undesirable because, in time, it destroys the layer of solid insulation adjacent to the gas. Furthermore, corona within electronic wiring generates spurious high-frequency voltages that interfere with communication and may trigger sensitive circuits. Corona also wastes power and dissociates some materials, creating noxious gases and odors. Corona-free design is achieved by limiting electrical stresses in the gases between insulations and between insulation and conductor.

II. Background

The voltage applied to two insulated round wires will divide into three components: the voltage across each

of the two wire insulations, and the voltage across the space between the insulations. This voltage distribution is unlike that in series capacitors where the voltage across the air capacitor is proportional to the voltage across the solid-insulation capacitor for all applied voltages. With parallel wires, the thickness of the insulation is constant around the wire, but the thickness of the gap between wires varies from a minimum in the space between the wires to a maximum from the far side of one conductor to the far side of the other conductor. This results in a non-linear field between the conductors.

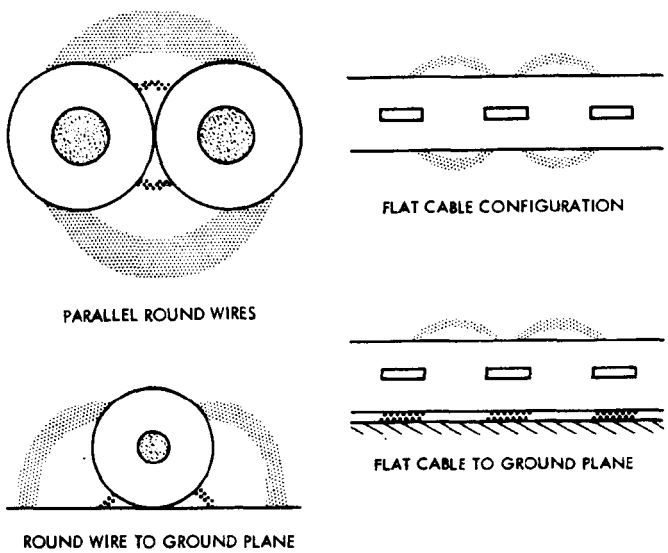

Fig. 1. Wire configurations

For pressures greater than 10 torr, and with conductors insulated and with at least 0.025-cm insulation, the corona will form in the narrowest air gap between the conductors (dotted area, Fig. 1). As the pressure is further reduced, the pressure-spacing relationship will be such that the corona will form at the wider spacing (cross-hatched area, Fig. 1). Thus the corona-onset voltage (COV) is reduced as the ratio of insulation thickness to air space is reduced (Fig. 2).

III. Round-Wire Tests

We measured the COV and corona-extinction voltage (CEV) of spacecraft electrical/electronic wiring, components, and systems. Detection of the presence rather than the magnitude of either corona or voltage breakdown, was required. The instrumentation was to be sufficiently sensitive to detect transmitted or conducted corona-generated interference of 1 mV in magnitude. These small signals are easily observed on the 5-mV scale of a Tektronix 541A Oscilloscope with a Type B plug-in amplifier (Ref. 4).

All of our tests have indicated that the minimum COV of a twisted pair is always greater than that of a spaced pair having the same wire size and insulation thickness.

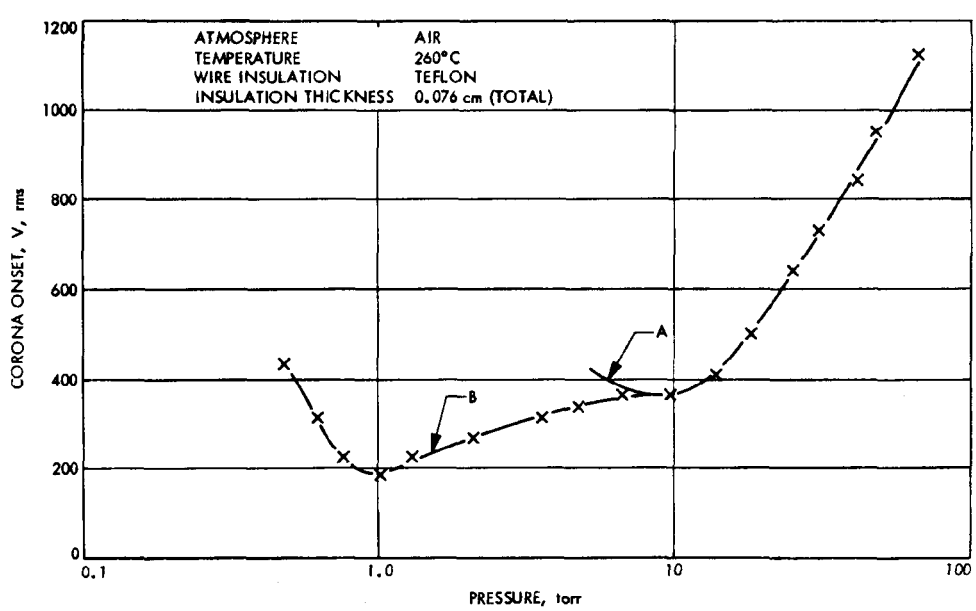

Fig. 2. Corona onset voltage of Teflon-insulated twisted wire pairs

The difference in minimum COV between a twisted pair and a spaced pair depends on the dielectric constant of the insulation, thickness of insulation, wire size, and voltage stress (Ref. 2).

In a series of round-wire tests, we determined the effect of insulation thickness by measuring the COV between a wire and ground plane and between twisted pairs. We used number 20 AWG nickel-clad copper-stranded conductors insulated with various thicknesses of Teflon. The effect of Teflon thickness on the COV of twisted wire pairs is interesting. Figure 3 shows both the calculated values and test values of COV for Teflon-insulated wires. Normalizing the test data shown from Fig. 3 on the basis of pressure times spacing produces an empirical relationship (Fig. 4). The COV at the minimum of the Paschen-law-type curve (Fig. 3) is shown as a function of insulation thickness in Fig. 5.

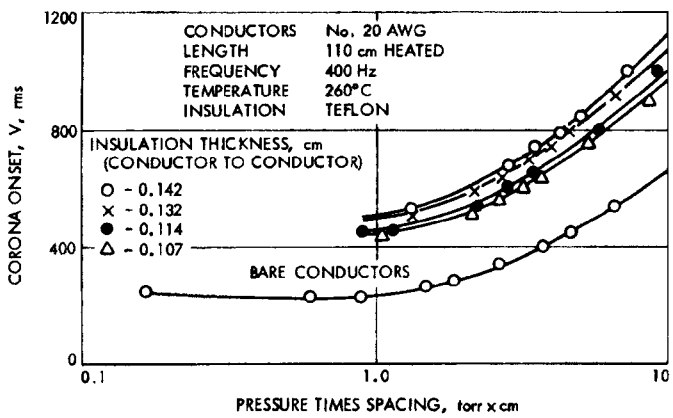

Fig. 3. The COV of Teflon-insulated twisted wire pairs

ATMOSPHERE	AIR
TEMPERATURE	23° C - 287°C
WIRE INSULATION	TEFLON, $\epsilon = 2$
PRESSURE RANGE	2 - 500 torr
INSULATION THICKNESS	0.02 - 0.2 cm, BETWEEN CONDUCTORS
PRESSURE x SPACING RANGE	0.85 torr-cm TO 10 torr-cm
WIRE SIZE	No. 20 AWG 19 STRANDS, RERATE FOR LONGER AND SMALLER SIZES

FORMULAS:

$$COV_2 = 230 + 3860 \frac{t_2}{\epsilon} + V\left(0.7 + 2.6 \frac{t_2}{\epsilon}\right)$$

$$COV_1 = 230 + 6100 \frac{t_1}{\epsilon} + V\left(0.9 + 2.6 \frac{t_1}{\epsilon}\right)$$

COV_2 = CORONA ONSET OF TWISTED PAIR

COV_1 = CORONA ONSET OF WIRE TO GROUND PLANE

t_2 = TWO THICKNESSES INSULATION

t_1 = ONE THICKNESS INSULATION

ϵ = INSULATION DIELECTRIC CONSTANT

V = TAKEN FROM CURVE AT SPECIFIED PRESSURE TIMES INSULATION THICKNESS, pd

Fig. 4. Round wire data

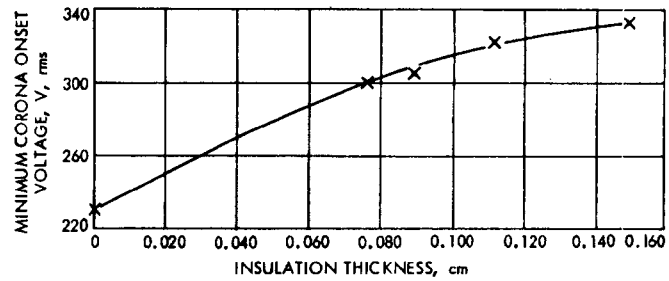

ATMOSPHERE	AIR
TEMPERATURE	-40° TO 260°C
WIRE INSULATION	TEFLON
PRESSURE RANGE	10^{-3} TO 10.0 torr
INSULATION THICKNESS	0 TO 0.2 cm, BETWEEN CONDUCTORS

Fig. 5. Minimum COV of twisted pair

IV. Flat-Wire Tests

Teflon-insulated flat-conductor cables (FCC) were also tested for COV. These cables were made of flat aluminum strips, side by side and embedded in and enclosed with layers of Teflon insulation.

The tests showed that the COV between conductors of both a cable supported in air and a cable bonded to a ground plane was higher than the COV of round conductors with the same insulation thickness (Fig. 6). Further, the corona-sensitive pressure was narrower for the flat conductors. These effects are attributed to the peculiar field between the two flat conductors. One disadvantage of FCC is that a cable placed close to a ground plane has a much lower COV at pressures above 20 torr than round conductors with the same insulation thickness.

V. Connectors

In measuring the COV of electrical connectors, it is important that the minimum COV of the connecting wire be greater than that of the component being tested. Inasmuch as the contacts within a connector must float in order to allow for manufacturing tolerances, there will be a small space surrounding each contact. Furthermore, small air gaps will form about the wire insulation unless

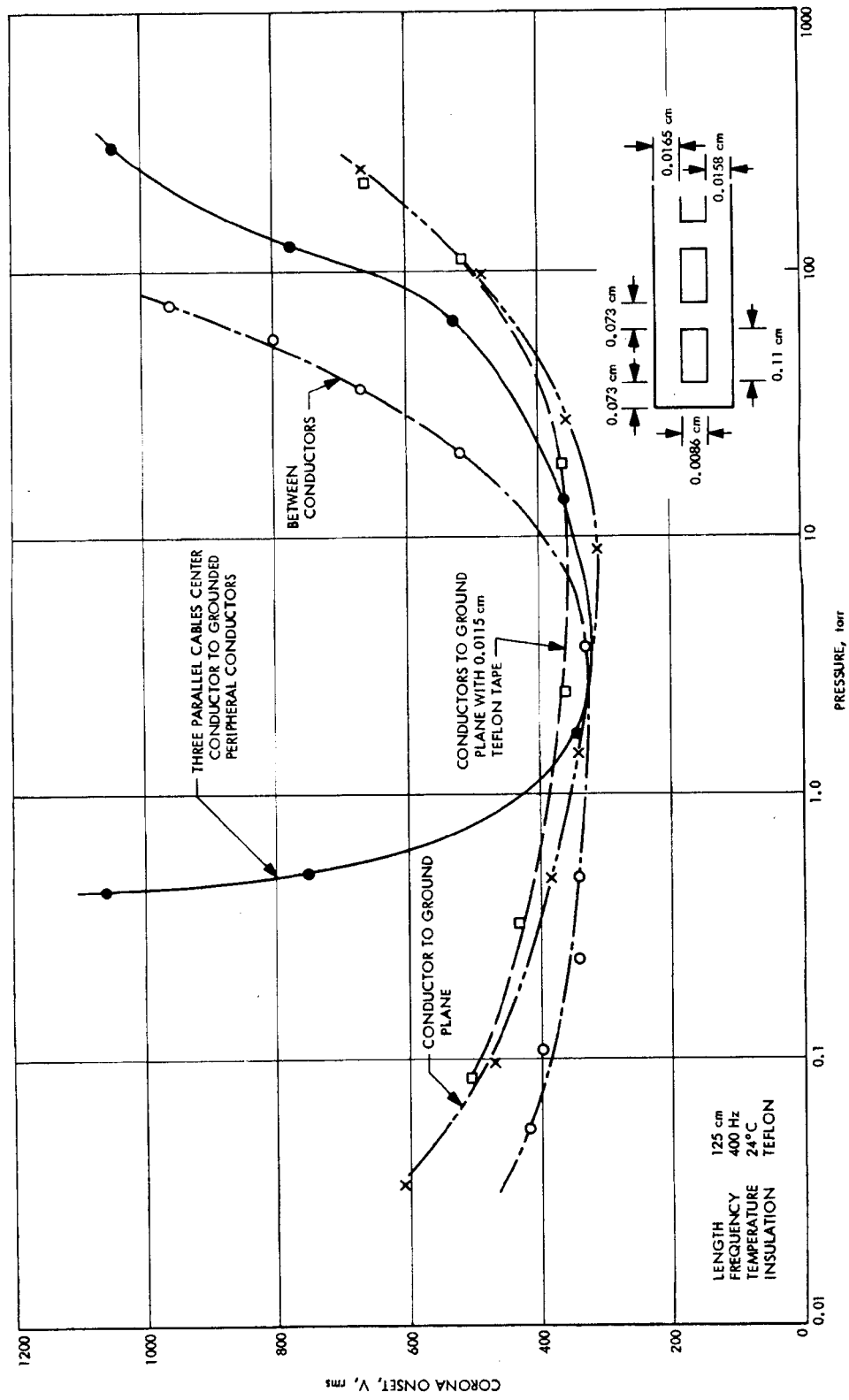

Fig. 6. The COV of Teflon-insulated flat conductor cable

it is pressed firmly against the contact. Many FCC connectors are made with spring-loaded contacts, which leave air gaps above each contact. These air gaps lower the COV (Fig. 7).

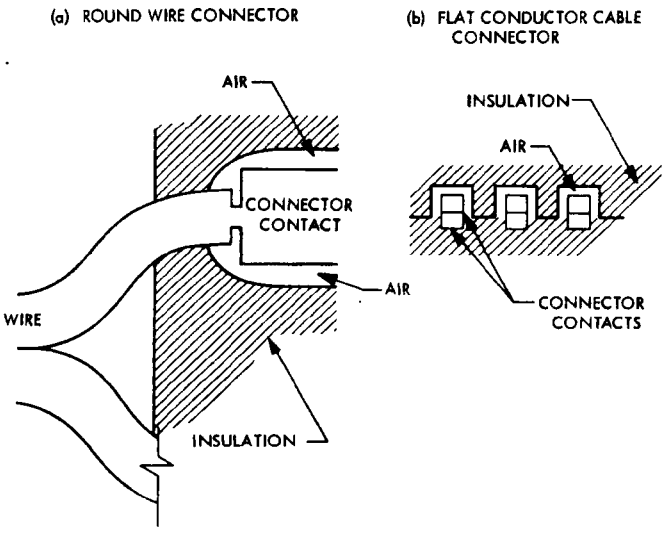

Fig. 7. Connector diagrams

Three COV tests were made with a 55-pin mated round connector. The connector shell was grounded and the connecting wires and unwired pins were encapsulated with at least 13 mm of silicone rubber.

In the first test, we connected a pair of No. 22 AWG round Teflon-insulated twisted wires to adjacent connector pins. The second test was the same as the first except that the connecting wires were connected to nonadjacent contacts. In the third test, one wire was disconnected from its contact and then reconnected to the corresponding contact on the mating half of the connector. In each test one wire was connected to a positive voltage source and the other to a negative source. The test chamber had corona-free feed-throughs.

The test results show that the true COV of the connector was obtained in the third test (Fig. 8). The curves from the first and second tests correspond to twisted wires

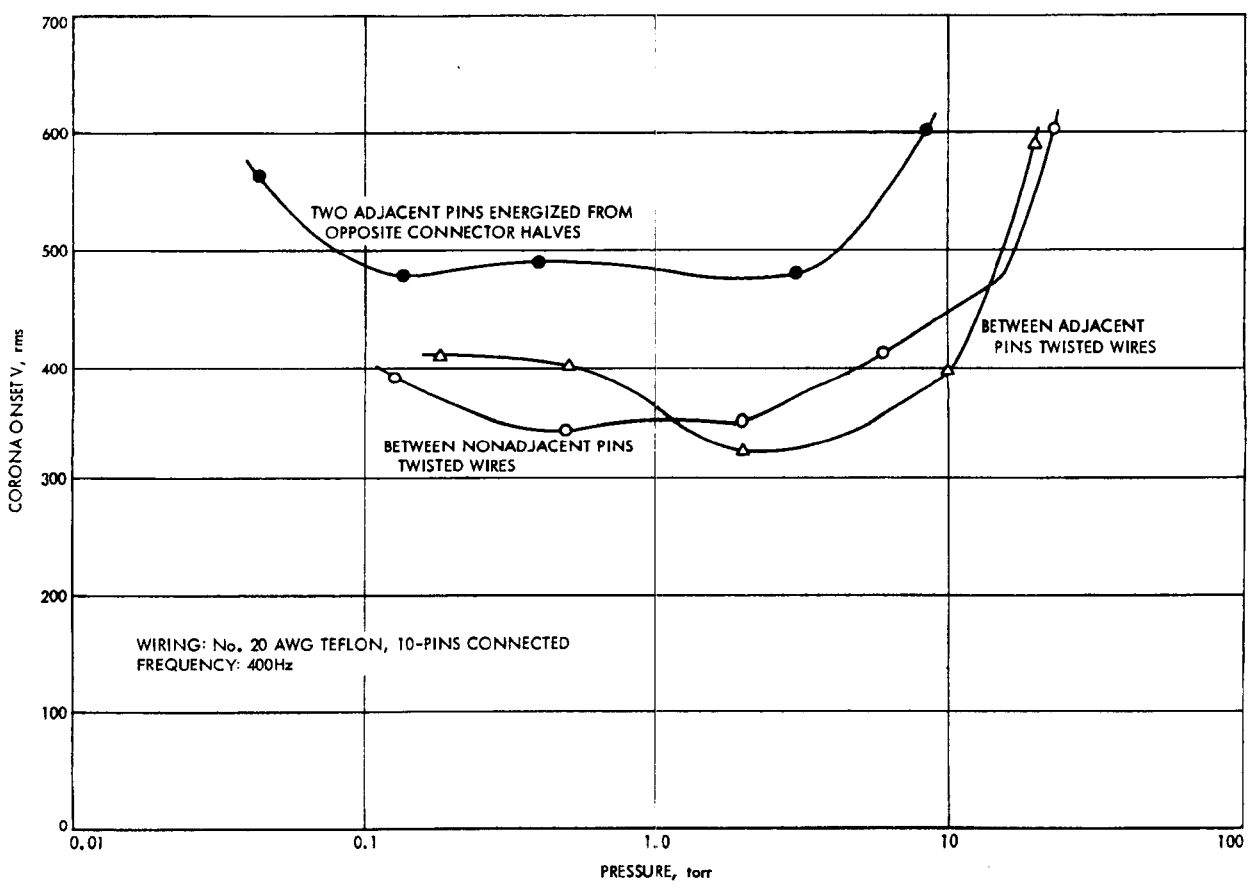

Fig. 8. Connector: 55 pins in air at 24°C, terminals not potted

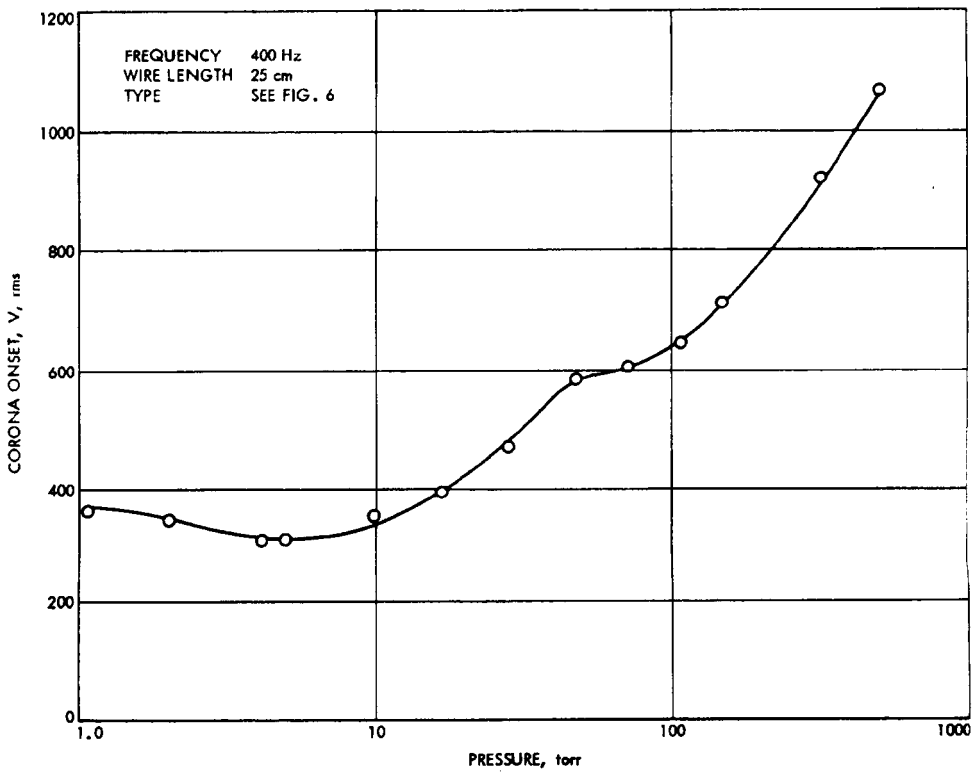

Fig. 9. Flat-wire connector system: 17 pins in air at 24°C, terminals potted

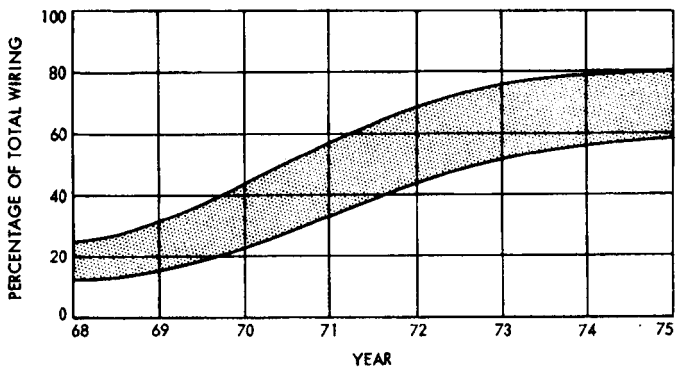

Fig. 10. Industry predictions of flat conductor cable usage for space, missiles, and aircraft

as shown in Fig. 5. If insulation voids had existed between adjacent connector pins, the COV would have been that of bare pins in the encapsulated gas.

An FCC connector was also tested. Its minimum COV was that of the cable (Fig. 9). The connector was so designed that it would have been difficult to apply voltage between contacts from opposite halves of the connector; therefore, only one test was conducted.

VI. Conclusions

These data show that FCC has a higher COV at minimum pressure-spacings than round-wire configurations. Many organizations have shown that FCC saves weight, and that FCC use will increase (Fig. 10). Connectors, breakouts, and terminations, however, continue to provide problems.

The application of electrical wire can result in interesting corona problems, as illustrated in Fig. 11, where the wire selection was based on dielectric strength of the insulation. The silicone-rubber insulated wire has a dielectric strength of 5000 V, which is 10 times its COV. This wire in low-pressure atmosphere will produce corona whenever its COV is exceeded. This corona will deteriorate the fine 5000-V insulation, decreasing the COV even further.

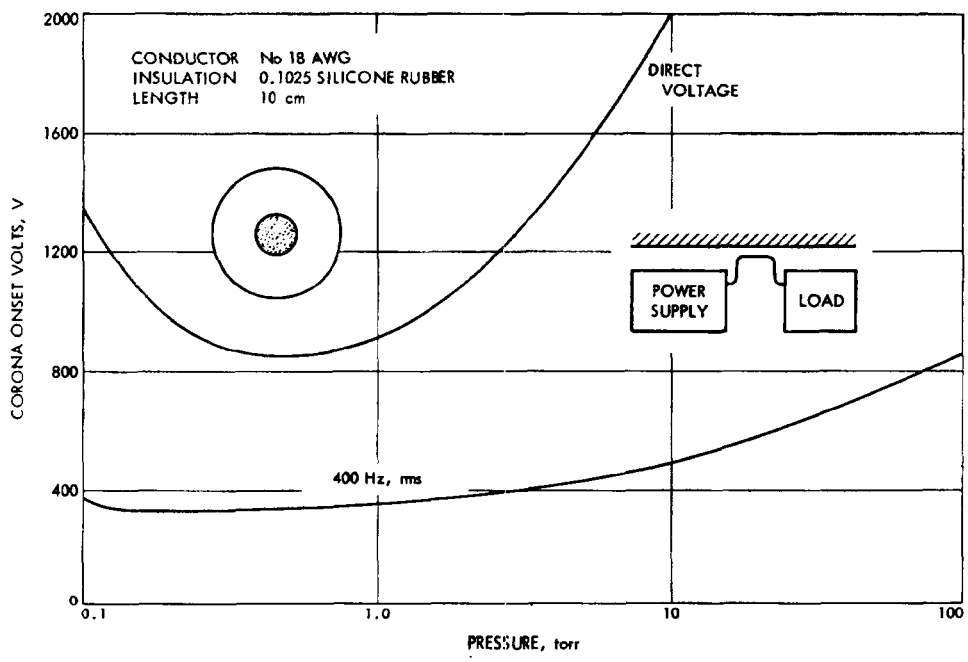

Fig. 11. The COV of silicone-rubber insulated wire to ground plane in air at 63°C

Discussion

Perkins: I don't have a question, because I have been battling with you on these problems ever since I have been here.

I would like to report that we have corroborated many of the things that you have reported. I don't mean that we disagree with the things that we haven't corroborated; we just haven't done the work in that area.

I will give you an example of some of the corroborative information obtained: we have run life tests on what I should call hookup

3

Discussion (contd)

wires. We would take a mandrel which is grounded and spirally wrap wire around it and run at a voltage that will provide a mild corona discharge between the outside surface of the insulation and the grounded mandrel.

Eventually, you get a failure; anyone would know that the stress is at maximum at the contact point between the insulation and the grounded mandrel. In the hundreds and perhaps thousands of tests that we have run in this fashion, we have never seen a single failure at that point. The failure is always around, away from the mandrel in the part of the insulation that is under tension as compared to that which is under compression. There you have the combination of this distance effect and the lower dielectric strength of material due to tension.

We obtained the same results on straight wires as Mr. Dunbar obtained.

We have also performed many calculations and measurements of corona levels, not with wires in twisted paths, but on wires against a ground plane. This provides different results from his simply because the voltage required is a factor of two lower in most instances than his.

Essentially, our calculations agree with his published data, and our measurements were made over the rather limited range of pressures, because we do not have the equipment available to him; however, we agree, in general, with what he has reported.

So, I would like to simply support your work.

Dunbar: Thank you. I might add a few remarks on long-life testing. We have tested wires with the following insulations: asbestos, asbestos glass, glass Teflon, Teflon, H-film which is called Kapton or polymide, and Teflon. We are finding that H-film, if left in an ionized field for a period of time, in our experiments breaks down in a considerably shorter time than does Teflon. After about 30,000 h, glass didn't breakdown, but one of the anomalies of glass is that it will absorb moisture and hence outgas for a long period.

Another insulation phenomenon found in reentry vehicles and high-altitude airplanes is breathing, which I did not mention in this paper or in any other paper I have written to date. If you allow insulation to breathe, noise will be generated; but, not from corona. It will be a thermal or material noise with a different wave shape, and different noise factor altogether.

We have taken Teflon up to 500°F for a test. We do not have 50,000 h on any insulation as yet.

References

1. Loeb, L. B., *Electrical Coronas*. University of California Press, Berkeley and Los Angeles, Calif., 1965, p. 5.
2. Dunbar, W. G., *Corona Onset Voltage of Insulated and Bare Electrodes in Rarefied Air and Other Gases*, Technical Report AFAPL-TR-65-122. Air Force Aero-Propulsion Laboratory, Research and Technology Division, Wright Patterson AFB, Ohio, p. 58.
3. McMahon, E. J., "The Chemistry of Corona Degradation of Organic Insulating Materials in High Voltage Fields and Under Mechanical Strain." IEEE Trans. Elec. Insulations, Vol. EI-3, No. 1, 1968, p. 3.
4. Dunbar, W. G., Corona and Breakdown Voltage in Helium-Oxygen Atmospheres, presented at Eighth Electrical Insulation Conference, Los Angeles, California, Dec., 1968.

N70-32299

Low-Level Corona Detectors

P. H. Reynolds and C. J. Saile
James G. Biddle Co.
Plymouth Meeting, Pennsylvania

I. Introduction

This paper discusses the problem of the detection of pulse signals in insulation systems resulting from the application of alternating voltage. Consideration is given to the effect of detection system bandwidth, response, and integration time. Particular emphasis is given to tests on insulation systems which may be considered to have distributed parameters or secondary resonances, rather than those which are lumped or simple 2-terminal specimens.

The techniques described which permit accurate measurements on distributed insulation systems are equally applicable to the case where lumped systems are to be tested.

II. Characteristics of the Corona Signal

The pulse to be measured is the result of a step voltage across a void in the insulation system. The step voltage liberates charge which produces a pulse voltage at the terminals of the insulation system. This pulse is typically of a few nanoseconds duration with fast rise and fall times. It is important to note that the area within the envelope of this pulse in volt-seconds is directly proportional to the apparent charge in coulombs. It is also important to note that the waveform of the pulse, as it appears at the input of the corona detector, may be significantly modified compared with its initial form.

The modification of the pulse is due to its propagation from the site of the corona to the input of the detector. Many insulation systems and their associated circuit elements look like a 4-terminal network with frequency-dependent attenuation characteristics. As has been shown in Ref. 1, although this transmission reduces the amplitude of the peak voltage of the wave, the apparent charge as indicated by the area of the wave does not usually attenuate. There will be some power attenuation of the signal, but in most practical systems this is not of major importance unless the insulation is of high-loss material.

III. Detection Systems

Detection systems may be classified in any combination of two characteristics:

(1) Broad or narrow bandwidth.

(2) Alpha or Beta response.

Consider Fig. 1, which illustrates a typical broadband system. The impedance Z may be a resistor, an inductor or a tuned circuit. The amplifier may be quite broadband, although it must suppress signals in the vicinity of the high-voltage supply frequencies and its low harmonics. Choice of a suitable inductor or tuned circuit will help in this respect compared with using a resistor.

Figure 2 illustrates a narrow-band system which represents typical present-day thought in detector design. This works on the principle of the ringing of a tuned circuit when excited by a pulse, to produce a response which is proportional to the energy in the pulse. In our case, this is the apparent charge of the corona in the specimen.

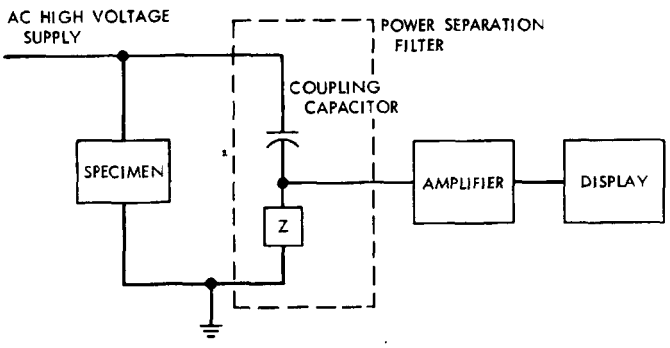

Fig. 1. Typical broadband system

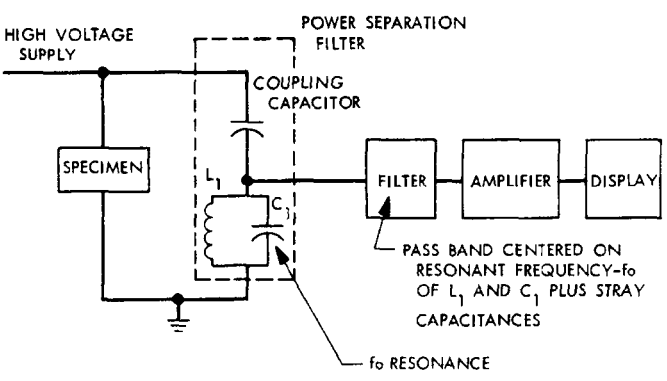

Fig. 2. Typical narrow-band system

The output waveform of the power separation filter is shown in Fig. 3. Note that the ratio

$$V_{p1} : V_{p2}$$

may be on the order of several hundred to one. However, the half cycle V_{p2} and its successive train will occur at the resonant frequency of L_1, C_1 in Fig. 2, as modified by various stray capacitances. This is the signal which is accepted by the filter, amplified, and displayed.

Note that the amplitude of V_{p1} is not directly proportional to change at this point, since there is no information on its duration. The amplitude of V_{p2} is directly proportional to charge since the wavelength is defined by F_o.

The sequence of events in making the measurement is, therefore, as follows:

(1) A corona discharge takes place which generates a pulse, whose volt-second area is directly proportional to apparent charge.

(2) This pulse appears across the resonant circuit, L_1C_1 in Fig. 2. The waveform may be considerably modified compared with that which occurs in (1) above, but the volt-second area is only modified by the power losses in the transmission path. In normal circumstances this is a minor source of error. The signal now appears as shown in Fig. 3, followed by a damped train of oscillation at the frequency of the tuned circuit. The area of

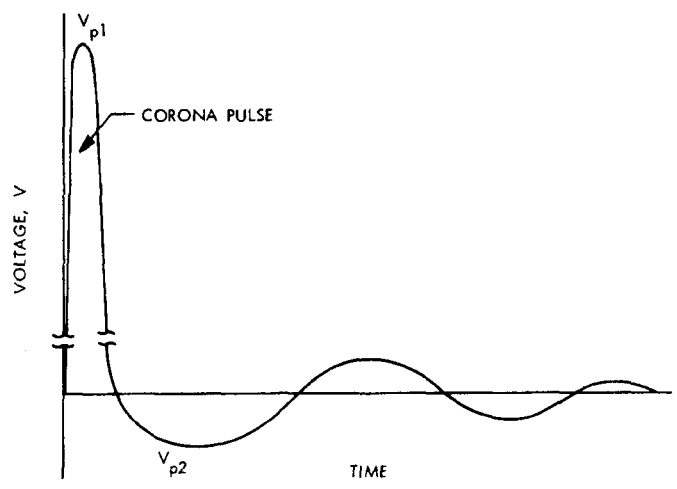

Fig. 3. Power separation filter output waveform

each of these half cycles is also directly proportional to apparent charge.

(3) This signal is applied to a filter which eliminates the initial pulse (V_{p1}) and passes the subsequent damped oscillatory train.

(4) The signal is now applied to an amplifier, which also integrates and half-wave rectifies the signal. This unidirectional signal has an amplitude proportional to the peak voltage of the resonant wave train and is known to be based upon the resonant frequency of the tuned circuit. Thus, the peak voltage is directly related to the volt-second area. This is the pulse which is displayed on the oscilloscope or other display.

(5) Calibration may be accomplished by injecting a signal of known magnitude having similar characteristics to those that appear at the terminals of the specimen. The calibration signal may be directly calibrated in apparent charge (picocoulombs).

IV. Alpha and Beta Response

The use of the terms Alpha and Beta response was originated by Dr. Kreuger (Ref. 1). It is used to describe the response of the corona detector to a pulse originating from corona.

Alpha response is defined as a waveform in which each successive half cycle is smaller than the preceding. Beta response occurs where these conditions do not apply. These are illustrated in Fig. 4.

The effect of these responses becomes significant where two or more corona signals occur within the same body of insulation where over-lapping of the pulses may take place, or where a reflection of a single signal can occur and arrive at the input to the detector at the same time as the desired signal. Both of these situations happen frequently in practical insulation systems.

Figures 5 and 6 show the effect of the summation of two signals with varying degrees of overlap, as shown by the time t, where the peak amplitude is assigned the value 1.0. As can be seen from the figures, the coincidence of the pulses can lead to errors. However, in the Alpha case they cannot exceed +100% and −0%. In the case of Beta response they can be +100% to almost −100%. Obviously minus errors are much more serious than positive errors.

Detectors with either Alpha or Beta response may be used to measure lumped-parameter insulation systems. With distributed parameter systems, the use of detectors with Alpha response is necessary to avoid serious errors. Since it is often difficult to decide if a complex insulation system can be considered lumped or distributed, the use of an Alpha-type detector is preferable under all circumstances.

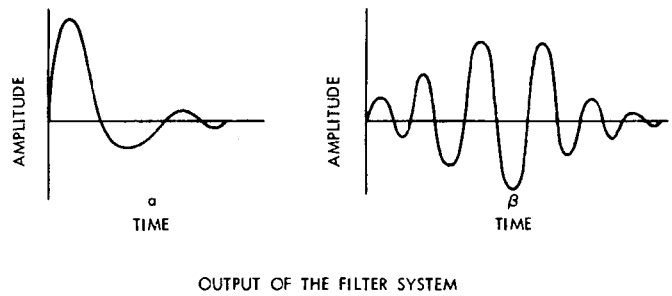

Fig. 4. Filter system output

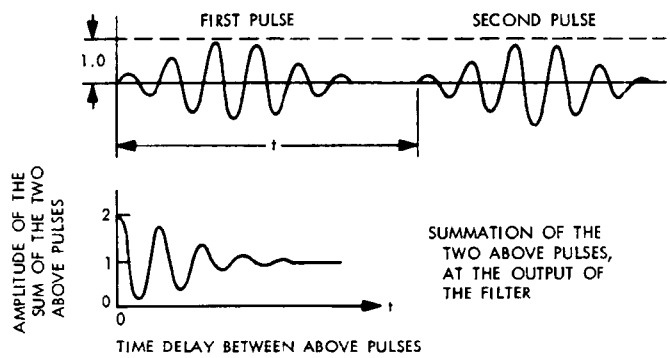

Fig. 5. Summation effects

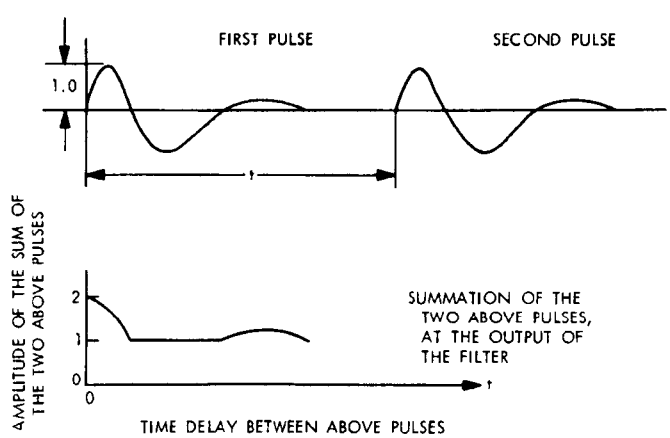

Fig. 6. Summation effects where *t* is longer

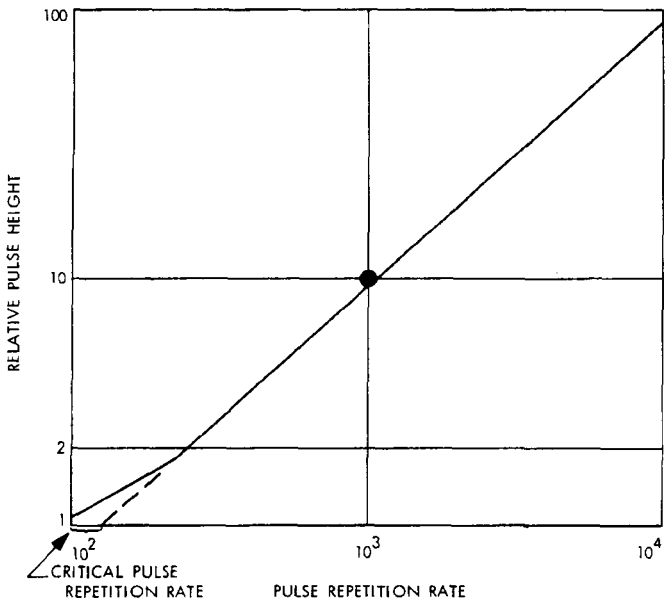

Fig. 7. Detector output vs repetition rate

V. Integration Time

Consideration of multiple discharges leads to the study of the integration time of the detector. The integration time of the detector may be established most conveniently by means of experiment. A pulse generator is required that is capable of producing unidirectional pulses of not more than 100 ns duration at a variable repetition rate and in bursts of known length. This is connected to the input of the detection system and the repetition rate increased while maintaining constant amplitude and duration of the pulses. A plot of the output of the detector against repetition rate will produce a curve as shown in Fig. 7. The reciprical of the critical pulse repetition rate is the integration time of the detector.

For a detector of Alpha characteristics, the integration time should be

$$T \text{ int} = 2\,T^{1/2}/\pi$$

where $T^{1/2}$ is the duration of the first half cycle of the oscillation (V_{p2}) that is generated by the pulse (V_{p1}).

VI. Noise Considerations

In practical situations, noise is frequently a problem in corona measurements. Under these circumstances there is an obvious advantage in the use of the narrow band technique. Man-made noise usually approximates to a constant power density at the lower end of the frequency spectrum. Consequently, the narrower the bandwidth the better the signal-to-noise ratio from this source. However, it is quite difficult to design a narrow-band system with a true Alpha response, correct integration time, and minimum overshoot. Compromises must be made to ensure reasonable fidelity of waveform with an acceptable signal-to-noise ratio.

One option that is available to the designer is the choice of the resonant frequency F_0, or more correctly the range of frequencies F_0 for a range of specimen capacitances. Experience has shown that 30 kHz is a good choice from the point of view of signal-to-noise ratio together with reasonable integration times. It should be remembered that choice of a relatively low frequency has no effect on the system's ability to detect very high-rise time pulses; consequently, the use of the term "narrow-band" is somewhat misleading. Other approaches to the noise problem include use of high-voltage filters, careful filtering of the detector power supply, and various shielding methods. A recent development has been the introduction of logic techniques to process the corona signal to:

(1) Extend the definition of corona inception. This we have defined as corona in excess of a specified amplitude on at least five successive half cycles of the test voltage.

(2) Extend the definition of corona extinction, which is the inverse of (1), above.

(3) Discrimination between point corona, on every cycle, and void corona, on every half cycle.

(4) Filtering on a time basis, to avoid responding to noise occurring when corona is not likely.

Use of these techniques permit very repeatable corona measurements to be made even in the presence of noise.

VII. Acknowledgments

The authors would like to acknowledge the assistance of Dr. Bahder of the General Cable Corporation for his helpful discussions of the subjects considered in this paper. We would also like to thank the authors of Ref. 4 for their permission to use some previously unpublished material concerning the summation of corona pulses.

Discussion

Question: How do you differentiate between void corona and point corona?

Reynolds: Point corona usually occurs on every cycle, and void corona occurs on every half cycle.

Dunbar: I have a tendency to disagree with your definition of corona. This is the occurrence of corona on five consecutive half cycles. Now, if we are going to operate a spacecraft or any other type of aero device, first of all, we are going to be down in the critical region most of this time. The degradation of the material as the function of time is dependent upon that stressing. In my laboratory, and maybe I disagree with some others, it has been shown that solid insulation may have a corona inception voltage, let's say, of 400 V. As time goes on, as it is cured in vacuum, that may rise and then fall off to below the 400-V level again.

I feel that the degradation will increase with time and that your corona pulses will also be increased.

Therefore, I think it should be on any pulse that comes along, in my own personal opinion.

Reynolds: Well, I agree that it will be excellent if we could detect that point reliably. But, really, I think the best you can do under most circumstances is to say we are increasing the voltage across the specimen at some known rate and we are looking for corona inception.

You, somehow, have to make a judgment about when that inception has occurred.

Now, you can have somebody sitting there looking for a pulse to occur. Our experience is that he will not pick it up as quickly as a piece of logic will say, "I've seen five corona pulses," because that happens very quickly; in other words, I think you are getting a better result with the five successive half cycles because that is quicker than the operator will do it. Now, you can cut this down to three if you like.

It may be in some critical areas, and perhaps yours will be one, you want to cut it down a little bit. However, if you cut it as low as one, then it will provide a false alarm.

Dunbar: My other comment was on the magnitude. Let us state that in a connector, when you are designing in terms of connectors to get up in the neighborhood in space at all pressures to 6-7 kV, you have many difficulties. In addition, however, the corona pulses, even at these very high voltages, initial spike voltages, are so minute you can barely see them. Therefore, I have often wondered about the detection device here on the magnitudes. What is your cutoff, in magnitude?

Reynolds: Well, it depends. What can a good system detect for you? Well, ~0.03 pC is about the sensitivity for specimens of relatively low capacitance. Under idealized circumstances, with everything tuned up, you get a little bit lower than that, maybe 0.01 pC. Then you could achieve good reliability.

Question: What is the frequency of these five cycles over which you integrate?

Reynolds: Whatever frequency the supply voltage is: 60 cycles, normally.

Holbrook: What happens under dc conditions where occasionally you have a system that has a high-insulation resistance and takes quite a bit of time for the capacitive discharge to occur?

Reynolds: Then this sort of clock-operated logic wouldn't apply in dc systems. For the rest of the detection system, in fact, we do use exactly the same detection system.

Normally, in cases where we are examining dc corona, it has been our practice, and I know the practice of quite a number of people working in this field, that you simply record peak voltages on a chart recorder. Then you are stuck going through it and finding out what happened afterwards, which isn't nearly such a neat technique as you can use with ac.

Holbrook: You say that the wave form that you display with your detector may be different than the actual wave form of the pulse occurring in the area of discharge.

My question is: how can you determine what the original pulse shape might be, and, secondly, how would you suggest applying the pulse shape that you have seen in your detector in developing a model for postulating mechanisms for breakdown?

Reynolds: Well, the only thing we do know is the volt-second area, and this is the only thing you ever know. I have never seen one suggested that would actually tell you the wave form that occurred across the void, because it is a very fast-rising pulse. Further, there is no way of getting it out from that void and into your detector without modifying it. So, I thing this is one of the fundamental problems in connection with corona research.

We don't really know what the wave shape looks like, and except under certain very idealized conditions, you can't find out. In practical systems you can't find out, so this is the weakness in just looking at the peak voltage and the wave shape of the pulse. But the system that I am talking about at least has the advantage that it is calibrated in charge, and that is a fundamental measurement. If you measure peak voltage, it is not really fundamental to anything. It may be a good way of detecting the corona inceptions that occur, but that's really all it does for you. It doesn't tell you about magnitude unless you have done some very elaborate work about the network between you and the site of the corona.

Question: There were some measurements taken by Bailey that were reprinted in *Electrical Insulation*, by, I guess, an insulation sub-committee of the IEEE last year where he did take some measurements with a sampling oscilloscope and constructed what was apparently the true corona pulse.

Reynolds: Yes. I've seen that. However, he had some very closely controlled conditions.

August: Why can't you have a corona pulse in some translucent system and just photodetect the output. You can get nanosecond rise time, even faster than nanosecond rise times, and there are scopes that will display even faster than that.

Discussion (contd)

Reynolds: Yes, I agree. That's a perfectly feasible thing to do, I think. The only thing I would say about that is that you usually care about corona in something like a transformer or a piece of cable, and you don't have this transparent condition that you need.

Dunbar: One of the other things to look for in the detection of the wave shape is the fact that the wave shape does change for different types, whether you're in clear gas straight gas, or in an insulation gas, or likewise if you had certain composites of insulation. This makes your one detector system a little bit edgy, I believe.

Reynolds: I can't agree that it makes it edgy at all. What it measures is charge. It always does that, repeatedly, irrespective of the wave shape.

Now, unless you know a great deal about the whole system, that's about all you can get out of it. But, charge is what you care about. As a matter of fact, I recall, Mr. Dunbar, you mentioned in your paper just the fundamental thing like the impedance of the power supply. It makes an enormous difference in the amplitude of the voltage, whereas it won't make any difference to the charge. The charge is something fundamental you can measure.

References

1. Progress Report of Study Committee No. 2 (H. V. Cables), CIGRE 1969 Meeting, Paper 21-01, p. 35.
2. Eager G. S., Jr., and Bahder, G., "Discharge Detection in Extruded Polyethylene Insulated Power Cables," *IEEE Transactions on Power Apparatus and Systems,* Vol. PAS-86, pp. 10–34, Jan. 1967.
3. Eager, G. S., Bahder, G., Silver, D. A., "Corona Detection Experience in Commercial Production of Power Cables with Extruded Insulation," *IEEE Transaction* Paper 68 TP-15-PWR.
4. Eager, G. S., Bahder, G., Suarez, R., Heinrich, O. X., "Identification and Control of Electrical Noise in Routine Reel Corona Detection of Power Cables," *IEEE Transaction* Paper 69 TP-100-PWR.
5. ASTM D1868-67T, Tentative Method for Detection & Measurement of Corona Pulses in Evaluation of Insulation Systems.
6. Kreuger, F. H., *Discharge Detection in High Voltage Equipment,* American Elsevier Publishing Co., Inc., New York, 1965.

N70-32300

DC Voltage Breakdown Processes and External Detection Techniques

R. E. Heuser
Goddard Space Flight Center
Greenbelt, Maryland

I. Introduction

A persistent problem affecting spacecraft is the electrical breakdown of the gas environment. A gas breakdown can cause a number of unwanted events from spurious rf signals and disruption of sensitive circuits, to complete destruction of circuits and experiments. A good example would be a breakdown near the surface of a photomultiplier tube. A report by K. R. Mercy (Ref. 1) surveys spacecraft voltage problems from 1961–1967.

The first part of this report will show that space flight introduces a variable not normally encountered when dealing with voltage breakdown on earth. It will show that the breakdown voltage is not just a function of the distance between electrodes, but a function of the product of electrode spacing and pressure. For uniform fields this is described by Paschen's law. This is an important fact to consider since at atmospheric pressure one can prevent a breakdown simply by increasing the electrode spacing. In a spacecraft, however, changing the electrode spacing will not change the breakdown voltage; the breakdown will occur at a different pressure, but with the same pressure-electrode spacing product. A discussion of Townsend's ionization coefficient α and γ and the similarity principle will be used to show that the breakdown voltage is a function of pressure times electrode spacing.

A. Townsend's First Coefficient, α

After an electron has traveled a free path, i.e. a collisionless path λ in the direction of the field E, the energy gained is given by $Ee\lambda$. If $Ee\lambda > eV_i$, where e is the electron charge and V_i is the ionizing potential of the gas, the electron will have enough energy to ionize the gas. The chance that an electron will ionize is then governed by the probability of occurrence of free paths of length λ, which are equal to or greater than λ_i, where

$$\lambda_i = V_i/E$$

The number of electrons, n, that have free paths greater than λ_i is

$$n = n_0 \exp \frac{-\lambda_i}{\lambda_m} = n_0 \exp \left(\frac{-V_i/E}{\lambda_m} \right)$$

where n_o = number of electrons starting out on free paths

$$\lambda_m = \text{mean free path.}$$

The number of ionizing collisions per unit length of path per electron α is equal to the number of free paths multiplied by the chance that the free path is greater than ionizing length λ_i and can be written as

$$\alpha = \frac{1}{\lambda_m} \exp\left(\frac{-V_i/E}{\lambda_m}\right)$$

however, λ_m is inversely proportional to the pressure p,

$$\lambda_m \, \alpha \, \frac{1}{p} = \frac{1}{Ap}$$

where A = a constant of proportionality

$$\frac{\alpha}{p} = A \exp\left(\frac{-V_i Ap}{E}\right) = A \exp\left(\frac{-Bp}{E}\right) = f\left(\frac{E}{p}\right) = f\left(\frac{V}{pd}\right)$$

for an applied voltage V across plane parallel electrodes separated a distance d.

B. Townsend's Second Coefficient, γ

Let n equal the number of electrons reaching the anode/s; n_0 be the number of electrons released by the cathode by external means, i.e., cosmic rays, UV, etc.; n_- be the number of electrons released by the cathode positive ion bombardment; and γ equal the number of electrons released from the cathode per incident positive ion.

Then

$$n = (n_o + n_+) \exp(\alpha d)$$

$$n_+ = \gamma \left[n - (n_o + n_+)\right]$$

$$n = n_o \frac{\exp(\alpha d)}{1 - \gamma \left[\exp(\alpha d) - 1\right]}$$

$$i = i_0 \frac{\exp(\alpha d)}{1 - \gamma \left[\exp(\alpha d) - 1\right]}$$

In addition, γ is seen to be a function of E/p.

C. Similarity Principle

Two discharges can be said to be similar if for equal voltages they have equal current densities, irrespective of their dimensions. Consider Townsend discharges with equal values of current i_o and having electrode spacings d_1 and $d_2 = ad_1$, where a is some constant. The requirement of equal currents means that

$$\alpha_1 d_1 = \alpha_2 d_2$$

$$\alpha_2 = \alpha_1/a$$

Further, V is the same for both

$$E_2 = E_1/a$$

Now, if the pressures are such that

$$p_2 = p_1/a$$

$$\frac{\alpha_2}{p_2} = \frac{\alpha_1/a}{p_1/a} = \frac{\alpha}{p}$$

In other words, α/p is an invariant quantity. Similarly,

$$\frac{E_2}{p_2} = \frac{E_1/a}{p_1/a} = \frac{E}{p}$$

D. Paschen's Law

Now, recall the Townsend current equation

$$i = i_0 \frac{\exp(\alpha d)}{1 - \gamma \left[\exp(\alpha d) - 1\right]}$$

The condition for the discharge to be self-sustaining is

$$1 - \gamma \left[\exp(\alpha d) - 1\right] = 0$$

$$1 - \gamma \exp(\alpha d) + \gamma = 0$$

$$\gamma \exp(\alpha d) = 1 + \gamma$$

$$\gamma \exp(\alpha d) = 1 \qquad \text{For } \gamma \ll 1$$

The $\gamma \exp(\alpha d)$ is the number of secondary electrons emitted by $\exp(\alpha d)$ positive ions, or one more than the number of ions due to one primary electron. This produces a self-sustaining discharge.

Let

$$\alpha/p = \phi(V_B/pd)$$

$$\gamma = \psi(E/p)$$

$$E = V/d$$

then

$$\psi(V_B/pd)\exp[pd\phi(V/pd)] = 1$$

Thus, the breakdown voltage V depends only on the product of gas pressure and electrode spacing. This has been done here for uniform fields, but the principle of breakdown voltage being a function of pressure times electrode spacing can also be applied to nonuniform fields.

II. Experimentation

Two methods of detecting a voltage breakdown have been investigated so far. These are the single probe and the photomultiplier tube.

A. The Test Setup

The test setup is shown in Fig. 1. The electrodes consisted of two polished stainless steel disks having 4-in. diam. The back of each disk has a threaded stud-like protrusion for mounting purposes; this stud was also tapped to permit attachment of the high voltage and ground leads. Each electrode was screwed into a piece of 0.25-in. Teflon which made up part of the structure that kept the electrodes parallel. The electrical connections came through the back of the piece of Teflon into the stud, and were wrapped with Teflon tape. The Teflon mounting plate, and wrapping with Teflon tape, were used to ensure that the discharge was confined to the space between the electrodes. The Teflon supports were set on a polystyrene base. The base had a slot down the middle, while the bottoms of the Teflon supports were T-shaped to fit the slot. The supports had oval slits cut in the bottom, through which it was possible to put nylon screws to hold the supports in place. The base had tapped holes to accommodate the screws. The whole setup was isolated from the bell jar bottom and collar by putting it on a polystyrene platform with Teflon legs. There is no significance to the fact that different materials were used, except that they were the most readily available insulators.

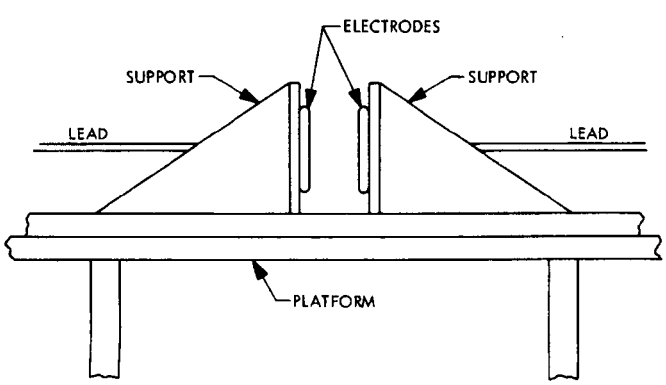

Fig. 1. Test setup

B. The Single Probe

The single probe, shown in Fig. 2, consisted of a piece of single-strand wire that had 3.18 cm of insulation stripped off one end. Wire braid was put around the length of the wire, and this was covered with shrink tubing.

The purpose of the wire braid was to reduce the pick-up of ambient noise. The wire went through a BNC feed-through on the bell-jar collar, with the shield being grounded to the collar, and the current was read on a Hewlett-Packard 425A micro-microammeter. It should be pointed out that there was substantial noise pick-up without the shield. The position of the probe with respect to the electrodes is shown in Fig. 3.

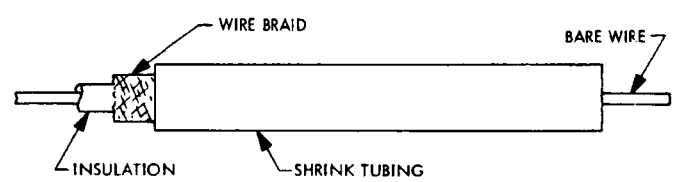

Fig. 2. Single probe

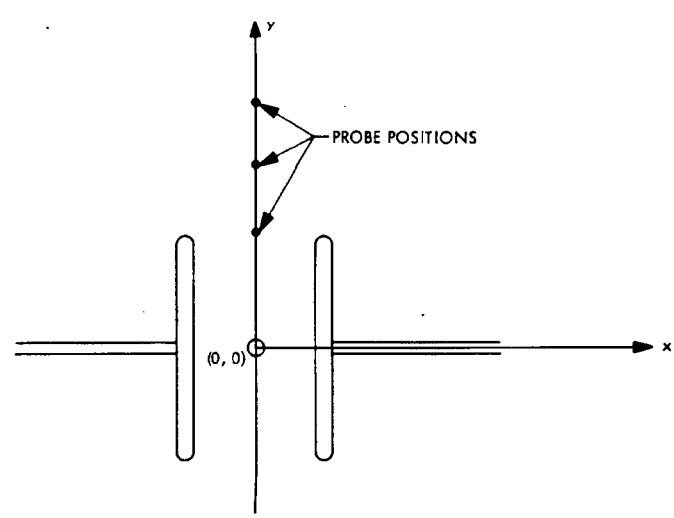

Fig. 3. Probe positions

If we attach a coordinate system to the drawing, as shown, the probe in the drawing is at $x = 0$, $y = 2$ in. For a given y-position, the probe was put in different x-positions, but the data presented in this paper is for the position $x = 0$. Later, when I speak of moving the probe further from the electrodes, it will mean keeping the x-coordinate constant and equal to zero, and increasing the y-coordinate in the positive y-direction.

C. The Photomultiplier Tube

There were several problems to be overcome before the photomultiplier could be used as a discharge detector. We first started using an EMR 541D, and this worked fine at 30 μm. As the pressure was raised, however, the output of the tube indicated that a discharge was taking place at the tube itself. We thought the most logical place for the breakdown was at the tube face, as we had been very careful in insulating and shielding the input leads. So, we tried putting a very fine mesh screen in front of the face of the tube. This helped, but did not eliminate the problem. Next we mounted the tube inside a minibox, Fig. 4(a), and put the fine mesh screen over the opening in the box; however, we still experienced breakdown problems. Finally, we made a collar from aluminum foil that ran from the tube to the screen, about 0.25 in. This seemed to close all the field lines, and the breakdown problem was eliminated.

Although this eliminated the breakdown problem, it was an unwieldy piece of equipment that would not be suitable for use in a test chamber. We next had a vacuum-tight aluminum container fabricated, Fig. 4(b), that would hold a phototube and a power supply for the tube. In this way we could keep all the high-voltage leads at ambient pressure, with only the 15-V leads for the power supply and the signal lead coming out of the container. This system worked well, but it was rather heavy; for tests of long duration we did not know how long the container would remain pressurized. Next, we took an RCA 1P21 phototube, a high-voltage power supply, and the three leads; i.e., 15-V and signal leads, and potted them in GE615 potting compound. The GE615 is a clear RTV-type compound. We could see if any breakdown took place inside the potting compound. Again we had trouble with breakdown around the face of the tube. This time we solved the problem by covering the top of the tube with aluminum foil, with a slit cut in the foil to admit light, and attached the foil to ground. I imagine that a metallic film deposited on the glass would achieve the same end, although we did not try it.

D. The Single Probe Results

The single probe consists of a piece of bare, single strand wire which is usually biased with some voltage and acts as a collector of charged particles. The probe used in the accompanying graphs was 3.18-cm long. It was found that for our purposes a positively biased probe was more sensitive. At the same time, a probe at ground potential tended to distort the field less. In Fig. 5 the probe was at +30 V, while in Fig. 6 the probe was at ground potential. In both cases, the probe acted as a collector of electrons. It was noticed in the data, Fig. 5, that the farther the probe was placed from the discharge, the more particles it captured. This seemed incongruous,

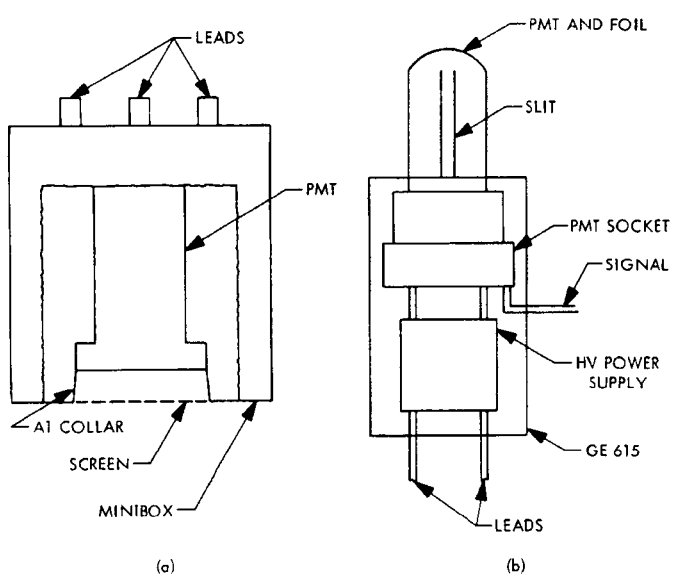

Fig. 4. Photomultiplier-tube configurations

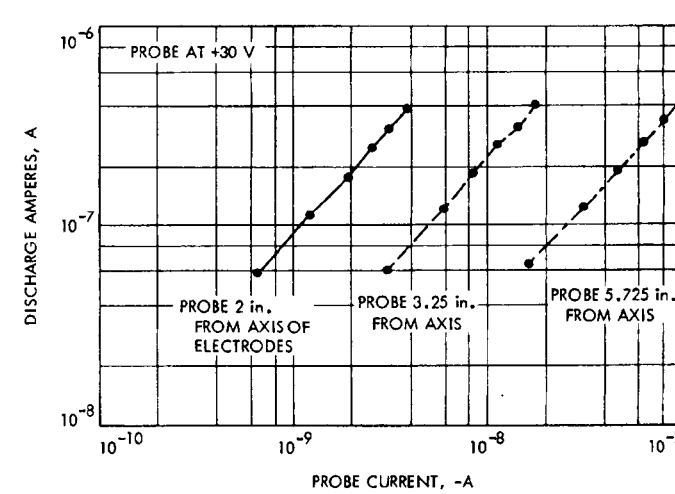

Fig. 5. Probe response at various distances from discharge

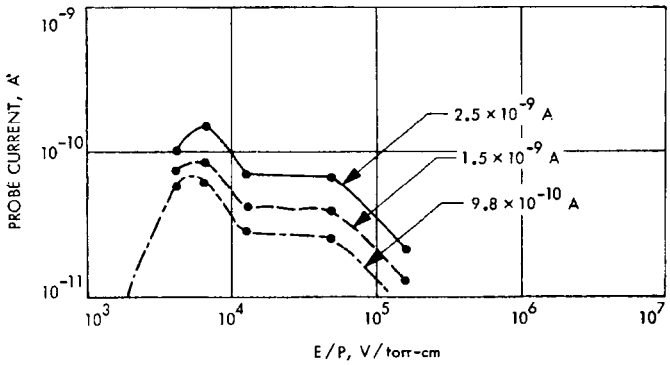

Fig. 6. Probe output vs E/P for constant discharge current

since the electron and ion densities are higher as you get closer to the discharge. However, consider the effective capture cross section of the probe:

$$2LR\,(1 + P/K)$$

where L is the length of the probe, R is the radius of the probe, P is the potential energy, and K is the kinetic energy. Now K is proportional to mg^2, where m is the mass and g is the asymptotic approach velocity. Therefore, if g increases, P/K decreases; if g decreases, P/K increases. Since electron velocities decrease with distance from the electrodes, P/K increases, and the effective capture cross section also increases. The algebraic sign of P/K depends on whether P is an attractive $(+)$ or a repulsive $(-)$ potential. There will be a point beyond which the density will be so low that the probe will capture fewer particles despite its increased capture ability.

Figure 6 shows the relation between probe output and E/P for the probe setup, as shown above. Recall that E/P is an invariant quantity for similar discharges, and that E/P is related to the energy of the electron. The sensitivity of the probe is different for different discharge currents, but curves of constant discharge current show a parallel behavior. In other words, the probe is most sensitive at a particular value of E/P, regardless of discharge current. It should be noted that for this study the sensitivity of the probe is defined with respect to change in E/P. This is because a change in E/P will change the input to the probe, even if the discharge current is constant.

E. The Photomultiplier Tube Results

The second instrument used to detect a voltage breakdown was the photomultiplier tube (PMT). We used two tubes, an EMI 6256S and an RCA 1P21, both of which are sensitive in the visible region. The photons which activate the tube are produced by radiative recombination, bremsstrahlung, and the return of excited atoms to the ground state, to name a few.

In Fig. 7, the EMI 6256S tube output vs E/P is plotted. It was thought that the response of the tube could be explained from this data in terms of the Townsend coefficients α and γ. However, no suitable relationship has been found which can be used to explain the tube's operation. It should be noted that the tube output vs E/P curve follows the profile of a curve of $(\log \alpha) + \gamma$ vs E/P as shown in Fig. 8. This data comes from Brown (Ref. 3), but it is not represented in this form. It is empirical data, and not derived. We have not been able to connect this relationship with the discharge characteristics, however. The data can be used to determine the current of a

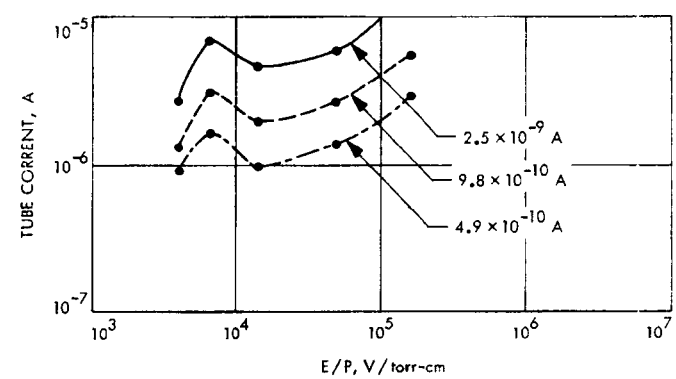

Fig. 7. Phototube output vs E/P for constant current

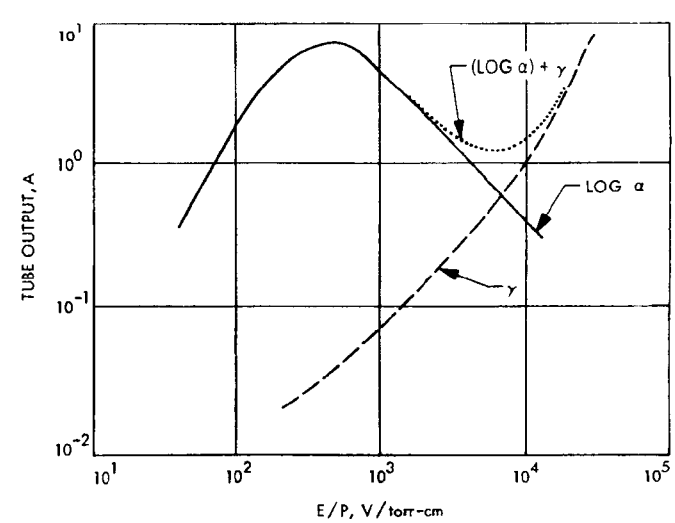

Fig. 8. Alpha and gamma vs E/P

discharge, since E/P and tube output are measurable quantities.

Another useful representation of the data is to plot tube output vs discharge current at specific pressures, as shown in Fig. 9. This data was taken with the RCA 1P21 tube. Since we know the voltage at which the equipment is operating, since we can compute the pressure in a spacecraft compartment by techniques discussed in Ref. 4, and since we will have evaluated the response of the tube to a discharge current at constant pressures, we can then determine the power loss in systems that have been instrumented with photomultiplier tube corona/voltage breakdown detectors.

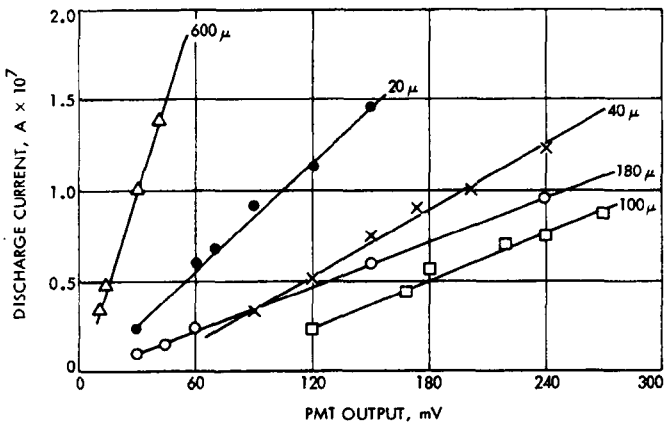

Fig. 9. PMT output vs discharge current for constant pressures

III. Summary

We have determined that for a particular pressure, the photomultiplier tube can detect a smaller discharge current. At 30×10^{-3} torr, the tube can detect 10^{-11} A, and the probe can detect 10^{-9} A. At pressures above 400 μm the probe becomes useless, unless the discharge is extremely violent.

IV. Conclusion

Both the PMT and the single probe are good detectors of a discharge under the condition that it is visible to them. Other work will be done to investigate the current level sensor and voltage pulse detector circuits.

Discussion

August: One problem about using photo tubes as detectors that is always bothersome is the fact that before you get an actual ionization, you can get excitation of your molecules, whatever you are using, which will give you light output without necessarily having any ionization. So, I think the whole problem of very low-level detection really has to be examined a lot more thoroughly.

I think about the only way you can get around this is maybe to put selective filters in your photomultiplier, which will accept certain excitation levels and eliminate others, so you can discriminate against them.

Heuser: We didn't use the photo tube alone; we had an external monitoring system. On the ground side of our circuit we ran it through a resistor and digital voltmeter. A breakdown would correspond to a reading on the digital voltmeter and the coinciding output of the photomultiplier tube. This is why I say we had certain currents. I did not notice that we had excitations.

August: This depends on your photomultiplier characteristics, too. In general, I approve of the idea of the photomultiplier. Even if you are at field strengths where you are apt to get excitation radiation, that you are at a dangerous region, and even if you don't get any ionization you should be worried at that point.

Question: The shape of some of your curves, I think your explanation of why you are getting the uptrend again in, let's say, multiplier output, to very high E/P values is because of the gamma process. But, you are also probably high enough so that you should be worrying about direct photo ionization in there, too. This might explain some of your results of your direct photomultiplier output, and probably at the highest pressures you are getting sufficient absorption of ionization radiation. This will be very high frequency, and will probably not be detected by your photomultiplier which, in turn, could be giving peculiar effects in your photomultiplier output.

References

1. Mercy, K. R., *Survey of Voltage Breakdown/Corona Problems Associated with Space Programs 1961–1967*, NASA TEP-101. National Aeronautics and Space Administration, Goddard Space Flight Center, Greenbelt, Md., 1967.

2. Druyvesteyn, M. J., and Penning, F. M., *Review of Modern Physics*, p. 99. J. Wiley & Sons, N. J., 1940.

3. Brown, S. C., *Basic Data of Plasma Physics*, p. 238. MIT Press, Cambridge, Mass., 1959.

4. Scialdone, J., *Dynamic Pressure of a Volume with Various Orifices and Outgassing Materials*, NASA TMX-327-67-574, National Aeronautics and Space Administration, Goddard Space Flight Center, Greenbelt, Md., Oct. 1967.

PRECEDING PAGE BLANK NOT FILMED.

N70-32302

Testing of High-Voltage Spacecraft Systems in a Simulated Ionospheric Plasma

D. R. Burrowbridge
Goddard Space Flight Center
Greenbelt, Maryland

To test high-voltage systems adequately, one must consider the interaction between the charged particles of the ionosphere and the system's high electric fields. Failures and malfunctions in orbit have occurred which were possibly due to an interaction with the plasma (Ref. 1). The ionospheric plasma can be thought of as a low-level discharge. Its effects on high-voltage systems will include leakage currents, RF attenuation, large sheaths, inducement of outgassing, and possible catastrophic discharging. Figure 1 shows the variation of charged particle density vs height in the ionosphere. Note the large day-to-night variation and the range of densities.

These charged particle densities produce an ion flux on the order of 10^{11} ions/s-cm^2 as the result of the relative motion between the ions and spacecraft. The electron mobility is such that there is no directed flux. The laboratory simulation is produced by creating a low-level discharge with an electron gun, Fig. 2. The gun is made of a nude ionization gauge, wired so that an electron beam is created. This beam produces ionization between two parallel plates in the ion source, as shown in Fig. 3. An electric field in this region polarizes the plasma so that the ions are accelerated through the screen into the test volume. The remaining screens prevent high-energy electrons from the beam from entering the test volume. This ion beam is neutralized by electrons scattering and diffusing around the edges of the ion source. Figures 4 and 5 show typical energy profiles of the ions and elec-

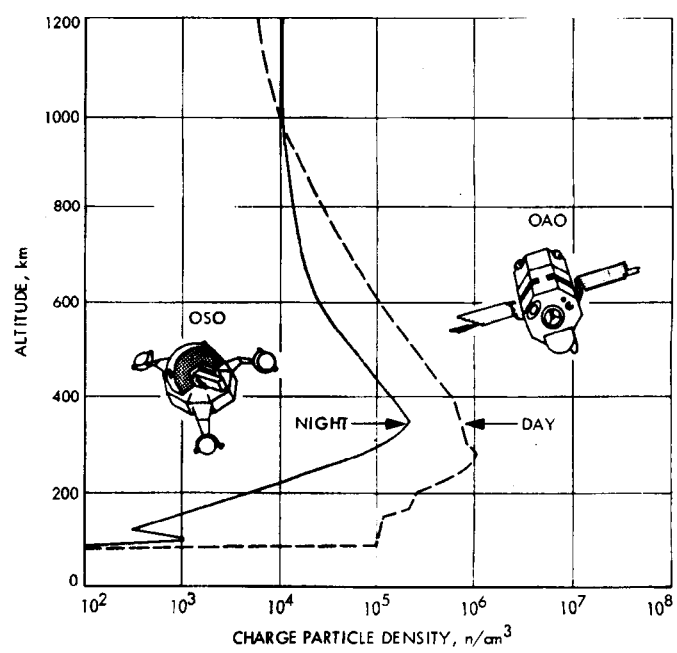

Fig. 1. Ionospheric density variation

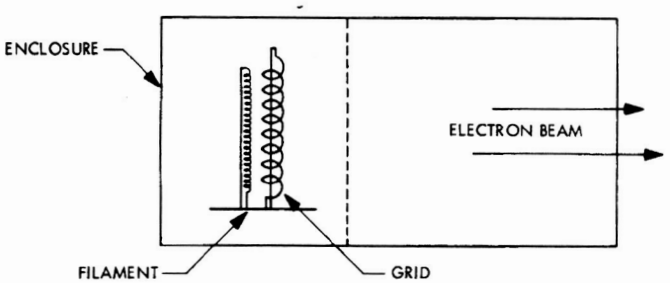

Fig. 2. Electron source

trons in the test volume. The ion energy can be varied from 2–30 eV, with an energy spread of 1 to 6 eV. The electrons have a 6-eV thermal velocity distribution. Figure 6 helps to visualize the spatial variations of the simulated ionosphere. The ion flux decreases to one-half its maximum value from the cylinder axis to the edges. The flux also decreases away from the source so that the flux of the back of the cylinder is about half its value at the front. Fluxes are measured with the retarding potential analyzer (RPA) (Fig. 7).

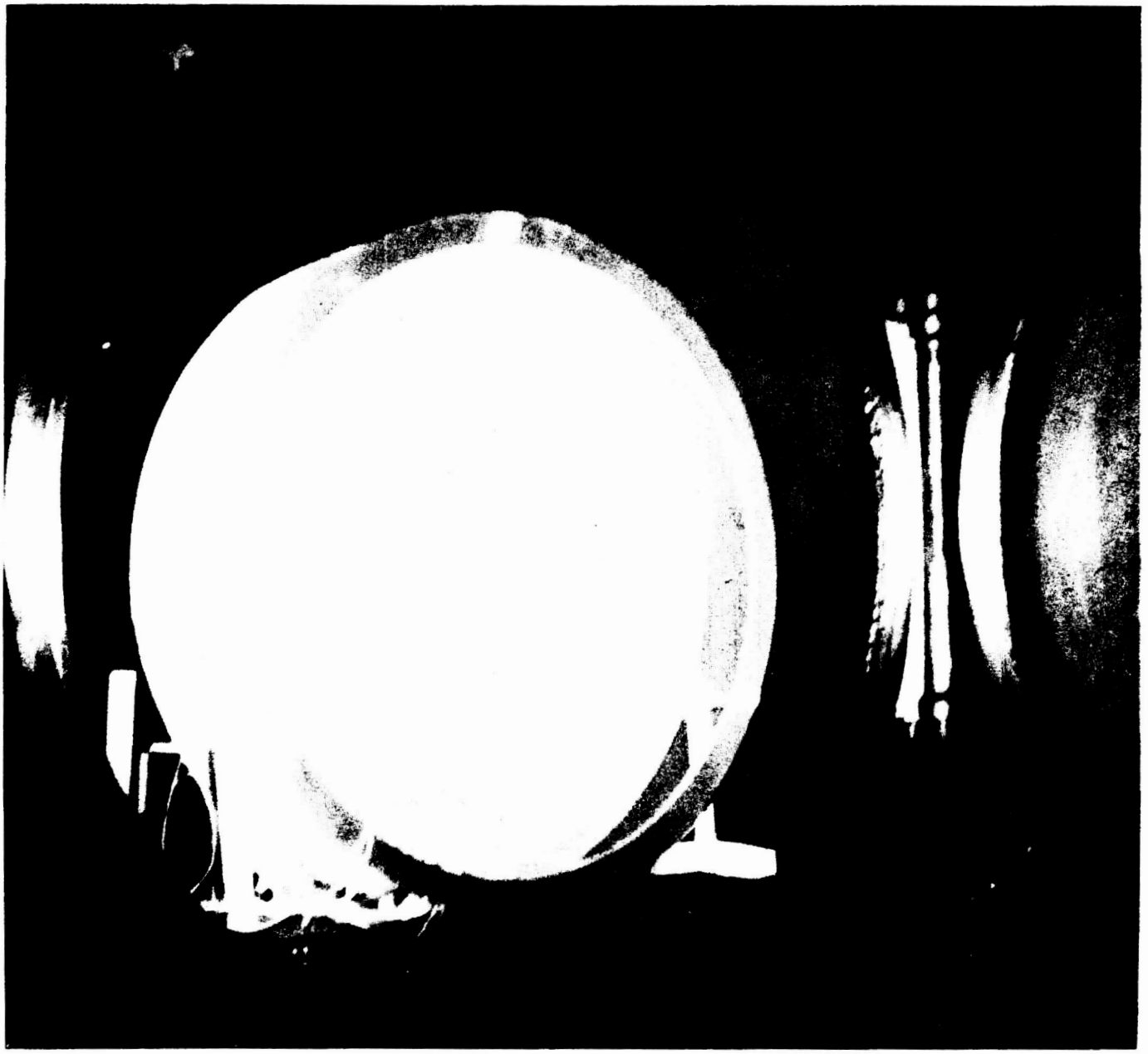

Fig. 3. Electron gun

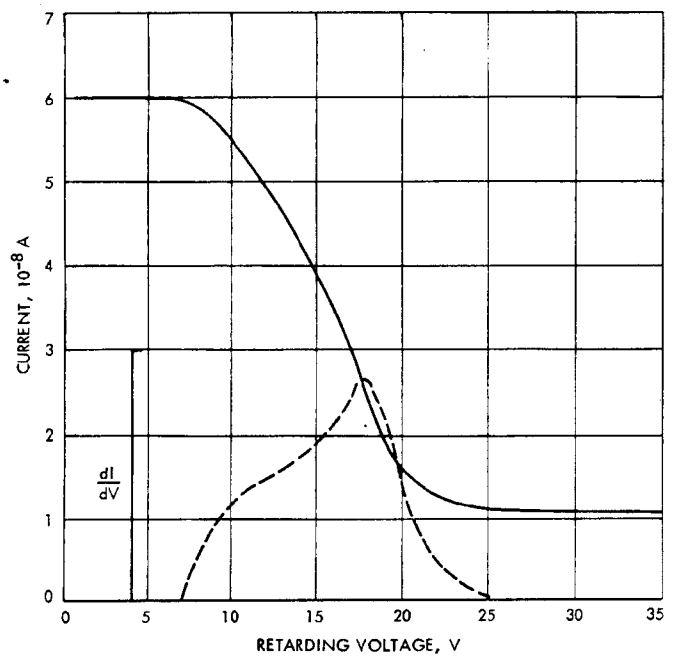

Fig. 4. Ion-energy distribution

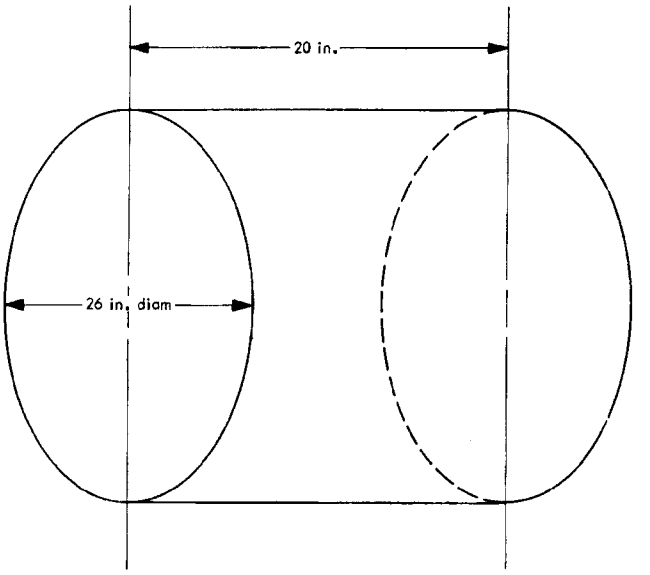

Fig. 6. Spatial variations in simulated ionosphere

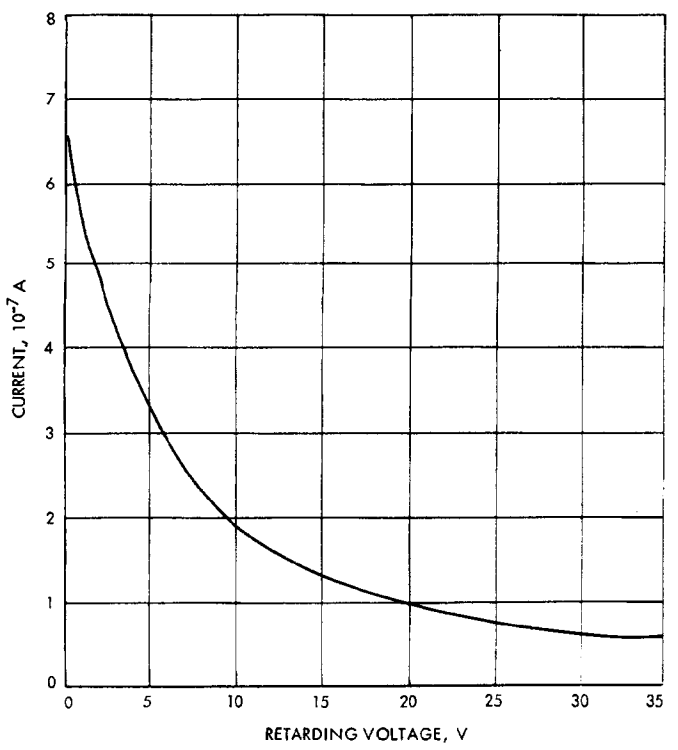

Fig. 5. Electron-energy distribution

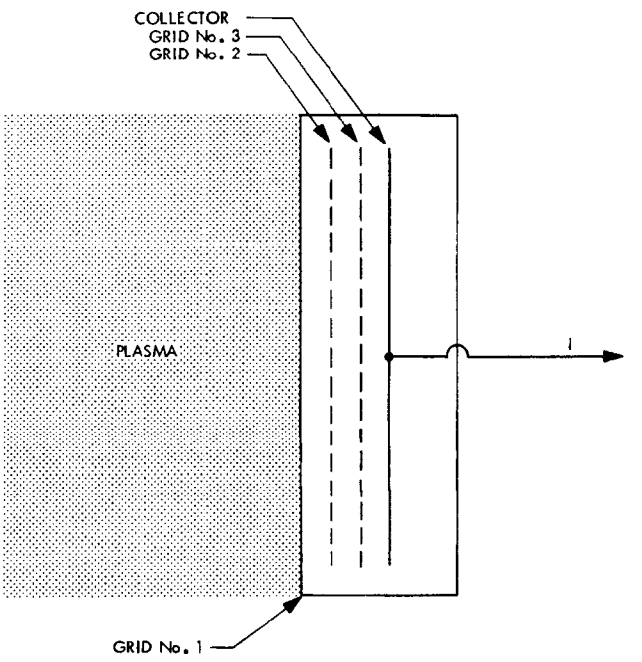

Fig. 7. Retarding potential analyzer

The simulated ionosphere is characterized by an ion beam whose flux density duplicates that experienced in orbit. The electron density of the simulation is of the same order as that in orbit, but the electron temperature is about one order of magnitude larger. Ion species are not duplicated, N_2^+ and N^+ in the laboratory vs 0^+,N^+ and H^+ in orbit; and, pressure is not duplicated, 10^{-5} torr

vs 10^{-8} torr, or less. The system is continually being upgraded to improve the simulation.

To date, tests have been performed on eight experiments for three different spacecraft.* The test item is typically an optical detector, high-voltage power supply, and current amplifier. Figure 8 shows the test setup for a plasma test of the Harvard College Observatory spectroheliograph experiment for the *Orbiting Solar Observatory*. The best test results are obtained when prototype instrumentation is used so that actual effects can be determined as opposed to mock-ups and simulated detectors. One type of system has shown itself to be particularly sensitive to the plasma. This system features an open cathode photomultiplier and cannot distinguish between incoming photons or charged particles. Figure 9 is the amplifier output from such a system. The detector is being excited by ions, not photons. In this case, the output produced by ions is sufficient to mask the measurement for which the experiment was intended. This type of experiment requires ion traps to exclude the plasma from the region of the detector.

Extensive studies were made on the ion trap design for the Goddard Experiment Package (GEP) for the *Orbiting Astronomical Observatory* (*OAO*). Modification of the light baffle was examined as a means for effectively eliminating ions from the detector region. Figure 10 shows the modified light baffle used in the study. In the GEP, light enters the open end of the light baffle from a Cassegrain system that has an aperture of approximately 38 in. The stops of the light baffle prevent scattered light from entering the detector region represented by the RPA. The modification consisted of adding ring electrodes to the stops. A study was made to determine the attenuation of the ion beam as related to the potential on the electrodes and their location. Figures 11 and 12 show the equipotential lines produced by two different electrode configurations (Ref. 3). The second one produces the highest potential in the baffle and also produced the greatest attenuation of the ion beam. Figure 13 is a plot of transmitted ion current as a function of the voltage on electrode B for ion beams with mean energies of 2 and 5 eV.

**Orbiting Astronomical Observatory (Startracker),* Wisconsin Experiment Package, Smithsonian Astrophysical Observatory Celescope, Goddard Experiment Package ion trap, Princeton Experiment Package spectrometer; *Orbiting Solar Observatory,* Harvard College Observatory Spectroheliograph for *OSO-II, OSO-IV,* and *OSO-G; Applications Technology Satellite,* Multicolor Spin Scan Camera.

The input current density corresponded to approximately 3×10^{-8} A total current so that the net ion flux was reduced 1000 times. Figure 14 shows the electron attenuation as a function of the voltage on electrode B. This is reduced from a total current of 6×10^{-7} A, or by 30 times. This test gives the amount of attenuation that can be expected for the ion trap. However, the high-energy tail of the ion distribution and the high-electron energy do introduce some uncertainty; however, the test provides more information than the electrolytic plots as to the attenuation for marginal potentials.

The influence of the plasma on high-voltage breakdown was evidenced in a test on the *HCO–OSO* experiment. During this test, a plasma exposure at an elevated pressure 10^{-3} torr, and an ion flux of 5×10^{11} ions/cm^2-s, which corresponds to an orbital ion density of approximately 10^6 particles/cm^3, produced arcing in the high-voltage system. These arcing conditions were not duplicated in a plasma-free environment until a pressure of 10^{-2} torr was reached. This indicates that the presence of the plasma produces an effective pressure which is higher than the actual pressure. It would not be unreasonable to assume that this effect is operative at lower pressures, in which case a plasma environment could induce breakdown when the pressure was "too low" to sustain it.

To summarize, interactions between electrical systems and a simulated ionospheric plasma have been observed. These interactions can explain some malfunctions and failures observed in orbiting spacecraft. In light of these observations one should test high-voltage systems to a charged-particle environment so that their susceptibility can be determined and, if necessary, be corrected.

The author wishes to express his gratitude to the efforts of D. A. Huguenin in obtaining the electrolytic tank plots. The cooperation and assistance of the experimenters and Goddard Space Flight Center personnel in the performance of these tests has been greatly appreciated.

Discussion

August: Your ion energies weren't too high, but I was wondering why you didn't use a 3-grid analyzer to take care of any secondary electrons that you might kick off your collector? You were varying your second grid negative so that, that would have collected any secondaries.

Burrowbridge: When I look at the ions, I generally hook it up a bit different than as I described. I keep a positive bias on the collector.

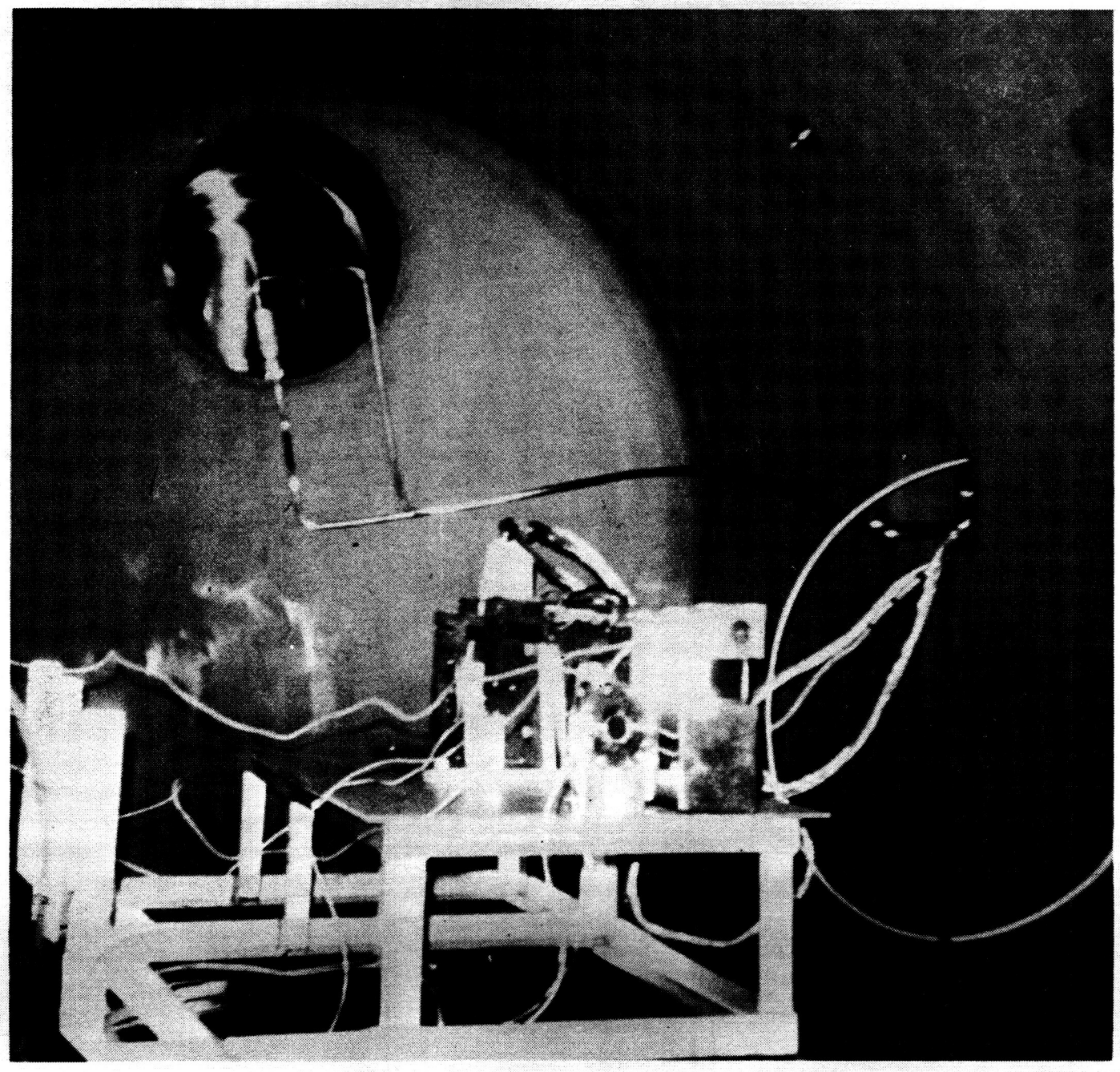

Fig. 8. Spectroheliograph experiment test setup

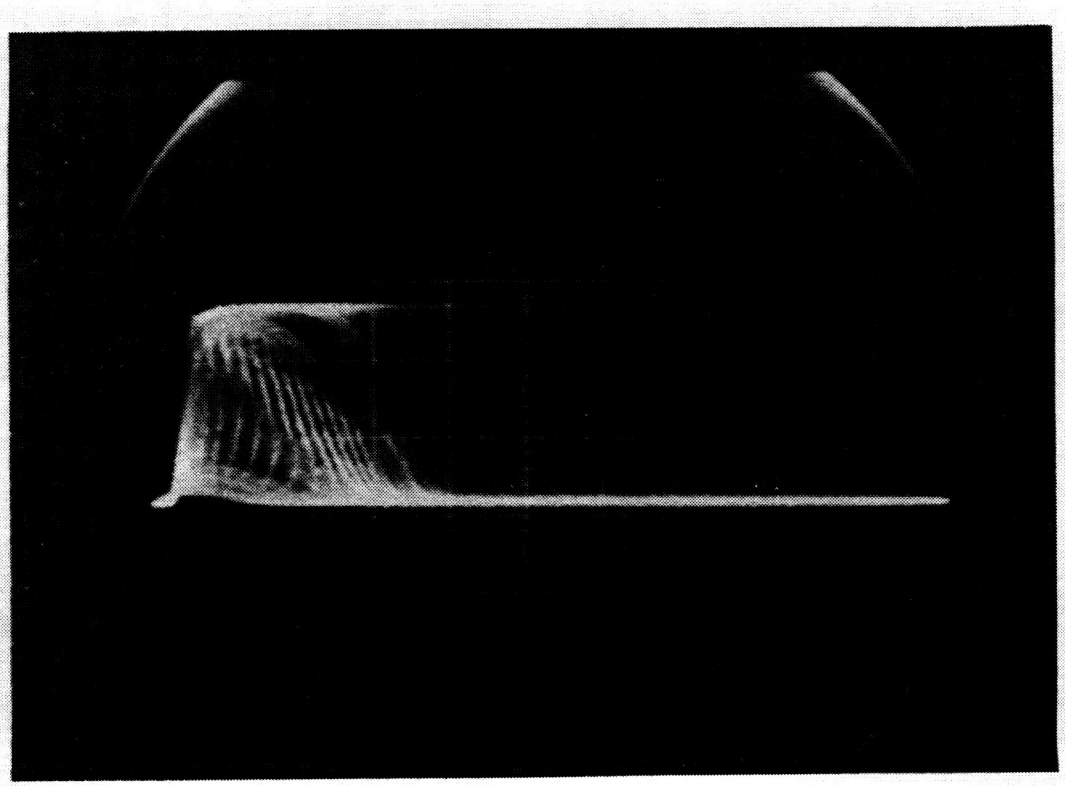

Fig. 9. Plasma effect PMT

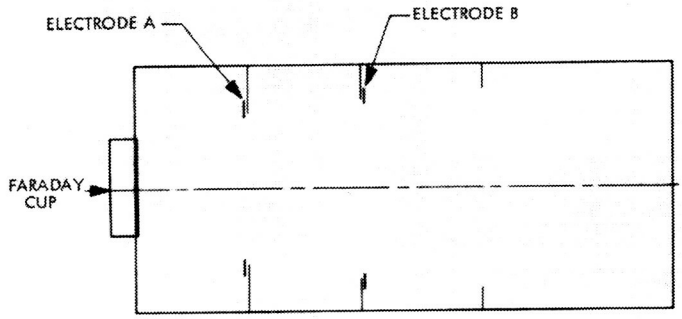

Fig. 10. Modified GEP light baffle

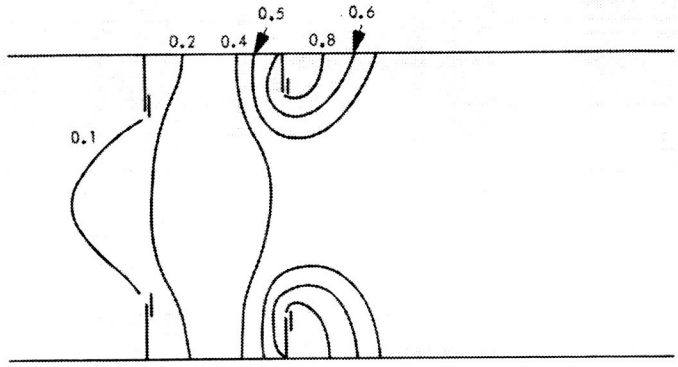

Fig. 11. Equipotential line plot

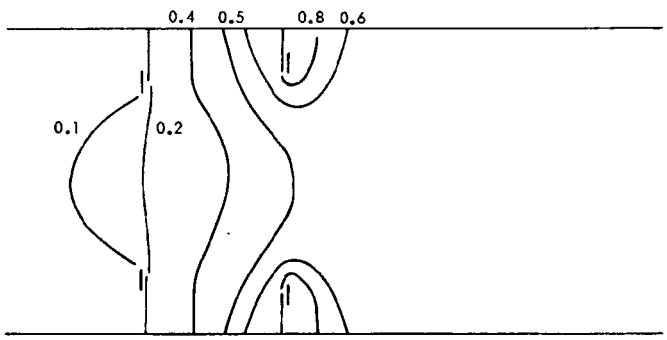

Fig. 12. Equipotential line plot, optimum configuration

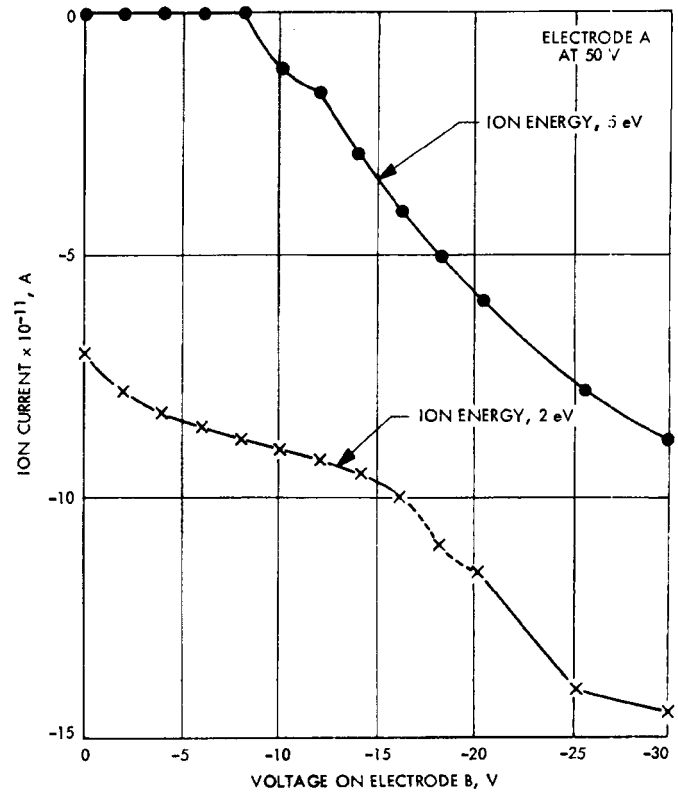

Fig. 13. Current vs electrode voltage

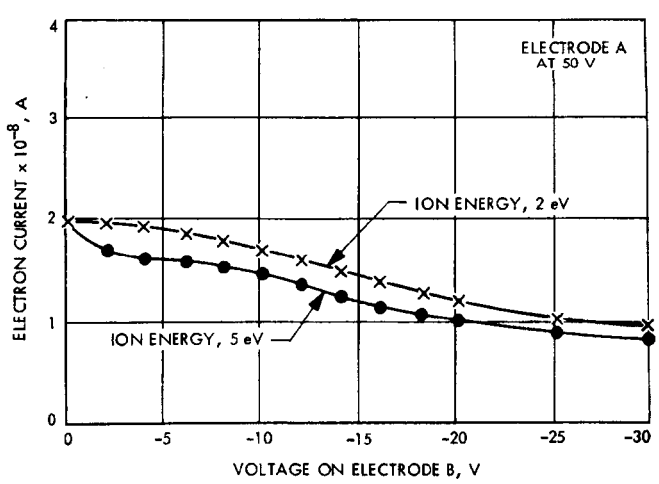

Fig. 14. Current vs B-electrode voltage

References

1. Street, H. L., et al., *High Voltage Breakdown Problems in Scientific Satellites*, X-300-66-41. National Aeronautics and Space Administration, Goddard Space Flight Center, Greenbelt, Md., 1966.

2. Burrowbridge, D. R., *A Technique for Simulating the Ionospheric Plasma*, X-325-68-172. National Aeronautics and Space Administration, Goddard Space Flight Center, Greenbelt, Md., 1968.

3. Einstein, P. A., "Factors Limiting the Accuracy of the Electrolytic Plotting Tanks," *Brit. J. Appl. Phys.*, Vol. 2, No. 49, Feb. 1951.

N70-32302

Rocket-Exhaust Initiation of Conduction in Connectors at Altitude

R. W. Ellison
Martin Marietta Corporation
Denver Division
Denver, Colorado

I. Introduction

The initiation of destruct circuits has been reported at staging of several spacecraft boosters. The exhaust plume of retrorockets has been invoked to explain conduction in 28–36-V circuits.

Tests in altitude chambers with pressure cartridges designed to simulate the exhaust of retrorockets are reported. Conduction between connector pins exposed to these exhausts was observed; it was serendipitously discovered that conduction from the pressure cartridge to the target connector was even more likely than conduction between adjacent pins.

The need for definitive experimental investigation of the values of electron concentration sufficient to initiate conduction in connectors will be emphasized.

Figure 1 shows a *Titan IIIC* equipped with a staging camera and three of its photographs. Figure 2 shows the staging of the solid rocket motors as viewed from the ground.

During the launch of Vehicle 4 from the Air Force Eastern Test Range (AFETR) on October 15, 1965, three flight anomalies, not critical to the mission, occurred on Stage II within seconds after it was separated from Stage III:

(1) All Stage II pressure measurements reflected zero counts for 400 ms starting 1.5 s after separation (1.3–1.7).

(2) Disturbances were noted in the Stage II instrumentation power supply (IPS) bus at approximately 2.39 and 2.45 s after staging.

(3) Loss of Stage II RF 2.5 s after staging.

Table 1 is a more exact statement of the anomalies attending Stage II separation from Stage III.

The first problem was identified as having occurred at different times on two other *Titan III* flights. In these cases the pressure measurements all went to zero counts.

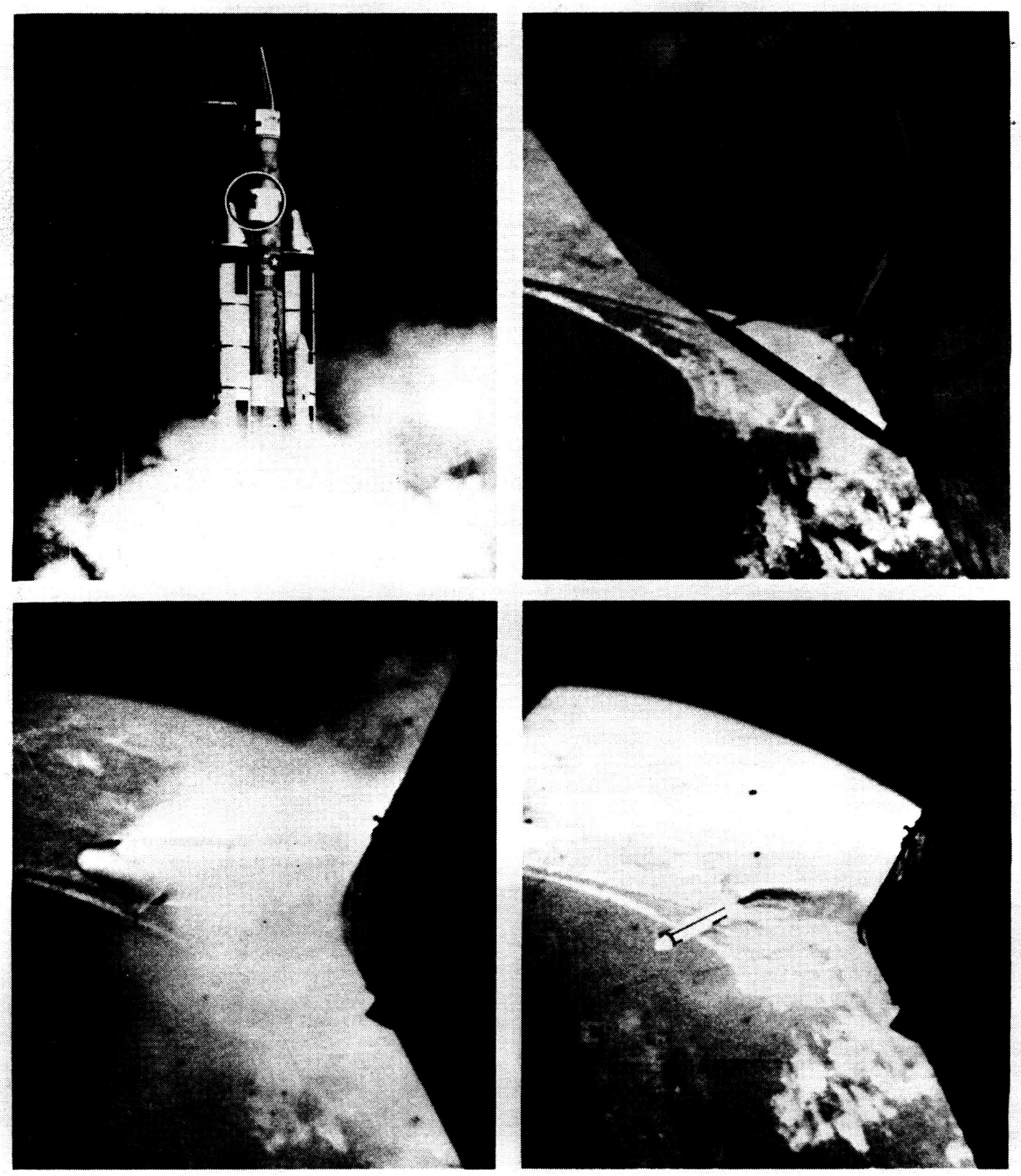

Fig. 1. *Titan IIIC* equipped with staging camera and sample photographs

Table 1. Anomalies attending Stage II separation from Stage III, *Titan IIIC-SLV4*

	Event	Time, s
	Bolt blow	0.000
1.	Pressure transducers to 0 counts	1.3–1.7
2.	First IPS short	2.444–2.455
	Second IPS short	2.507–2.514
3.	Loss of PCM carrier	2.516
	Shock on transtage	2.524
	Loss of SSB carrier	2.528
Retrorocket burnout: 2.40–2.50 s.		

There is no physical phenomenon that would explain the pressure behavior, so it was concluded that this phenomenon is associated with the instrumentation. Further analysis determined that by loss of the single-point ground on the transtage it was possible for Stage II to generate a difference in potential of 3.5 V between the instrumentation 10-V power supply and the encoder reference. When the voltage exceeds 3.5 V, the common mode voltage exceeds that of the 8.4-voltage encoder reference causing a reversal of polarity on the pressure measurements, providing an indication of zero counts. It is believed that this difference in potential is generated by negative static charges on the missile structure due to retrorocket firing. Similar problems have been noted in the *Agena* program.

II. Stage II Telemetry Loss

Even though the IPS bus voltage measurement did not reflect shorts or disturbances by playing out the PCM serial train and the envelope of the single side band, it was determined that the voltage transients of 11 and 7 ms occurred at the times indicated. Since both positive and negative IPS busses are carried through the staging connector on adjacent pins, it is conceivable that these shorts may have occurred due to ionized gas from the retrorockets breaking down the gap between pins. A second possibility is a destruct which caused IPS bus shorting. The loss of Stage II telemetry that occurred approximately 2.46 s after separation was the loss of RF carrier. It was first concluded that this loss of RF may have been due to damage to the telemetry antennas in Compartment 2A. However, in the subsequent investigation, it appeared that the single-side-band RF output failed 12 ms after the loss of PCM RF carrier. This would indicate that the loss of telemetry was due to damage in Compartment 2B rather than 2A, because the RF outputs of these two systems are multiplexed in that compartment and have a common RF cable to the antennas in Compartment 2A.

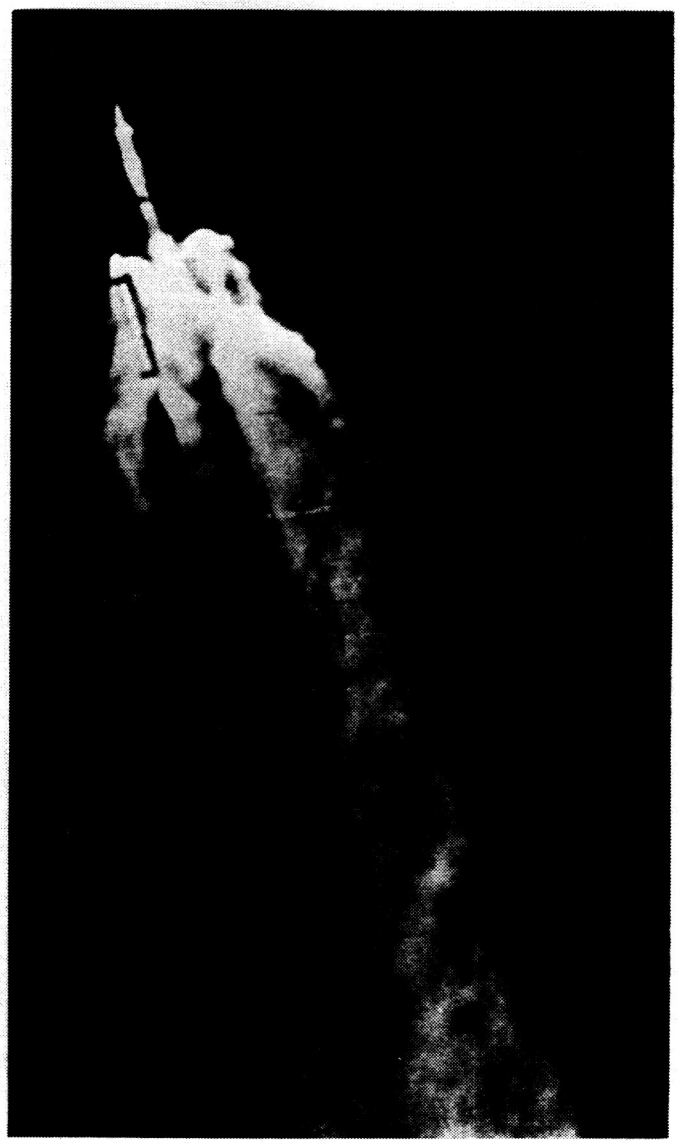

Fig. 2. Solid rocket motors staging

III. Transtage Shock

It has been concluded that a pressure front disturbed the transtage 2.528 s after staging. The guidance accelerometer, airframe accelerometer, and engine motion all indicated a symmetrical load application. This would rule out a piece of debris that might have impacted on the transtage.

It is believed that the pressure front was due to the release of gas from the Stage II oxidizer tank. Only two causes for this could be envisioned:

(1) Failure of the oxidizer dome was due to continued combustion of fuel ice.

(2) Failure of the oxidizer dome was due to inadvertent destruct of Stage II.

The first cause appears unlikely because the oxidizer is dissipated rapidly and cannot be collected in the form of oxidizer ice. This, then, would require a collection of fuel ice in the immediate area of the oxidizer leak and continued combustion to raise the dome temperature in excess of 500°F in 2.5 s. Another reason this cause of failure appears unlikely is the timing of the telemetry loss. It appears that the PCM carrier loss was 12 ms earlier than the single-side-band carrier. If the dome were to break loose, the only direct cause of loss of telemetry would be the loss of telemetry antennas and coax located directly above the dome. In this case, however, both sources of RF would be interrupted simultaneously. It is also evident from the above table that the single-side-band link was still in operation at the time of the transtage shock.

The second cause of failure appears to be the most likely because the single-side-band and PCM transmitters, as well as the multiplexer for the RF outputs, are in Compartment 2B. Therefore, the data in Table 1 indicate that the disturbance started in Compartment 2B rather than 2A. Exact correlation of time of the destruct system triggering is difficult. Our estimate would be 2.497 to 2.500; however, this does not include the time required to rupture the oxidizer dome sufficiently to generate the large pressure front. Therefore, it is inconclusive whether the first IPS short was caused by activation of the destruct system or the result of electrical disturbances. Consideration was given to identification of the destruct system trigger. Possible causes are:

(1) Ionization at retrorocket shutdown which caused arcing between two adjacent pins in the staging connector.

(2) Physical contamination of the staging connector pins.

(3) Static charge buildup which caused destruct circuitry failure.

The detailed evidence and analysis that led to the conclusion that this pressure measurements anomaly was created by electrostatic induction of voltages between grounded parts and the IPS are contained in Appendix A.

The other four anomalies have been ascribed to conduction in the Stage III/II disconnect being initiated by retrorocket exhaust. The evidence and analysis that indicate this explanation for IPS shorts, for the shock felt by transtage, and the loss of PCM carrier 12 ms before loss of the SSB carrier became impressive when one phenomenon suffices to explain all four of these observed events. The details of this matter are given in Appendix B.

High-voltage breakdown (in the absence of simulated exhaust) was measured at altitudes; Table 2 presents the results obtained with the circuit shown. No electrical activity was observed below 360 V; 420 V were required to initiate corona and 460 V were required for breakdown.

It is not known what values would be found when a connection had been contaminated by an SPR exhaust. Figure 3 is the appearance of the connector halves after one exposure to the exhaust of a standard pressure cartridge fired at altitude of 150,000 ft in the chamber shown in Fig. 4.

Table 3 with the circuit shown is the result of tests using a pressure cartridge in the chamber. The oscillo-

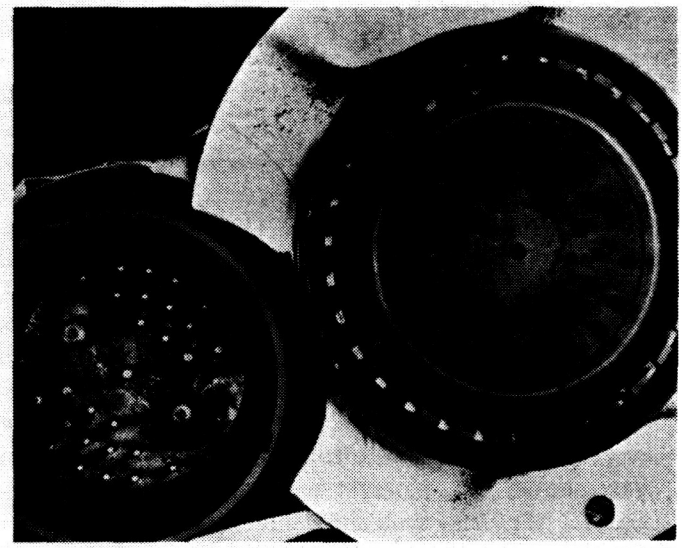

Fig. 3. Connector halves after exposure

Table 2. High-voltage breakdown

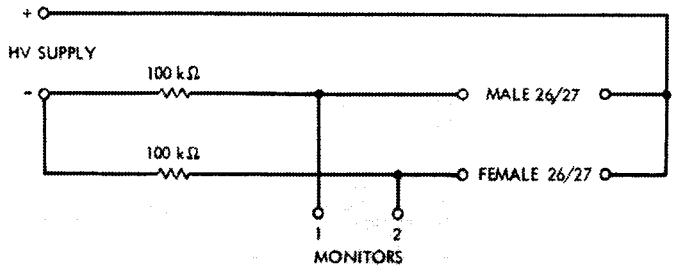

Test No.	Male	Female	Test chamber altitude, ft	Breakdown voltage, V	Extinguish voltage, V	Pin combination	Corona threshold
1	X		165,000	460		26/27	
2		X	155,000	700		16/27	
2		X	155,000	550	450	16/27	
3		X	160,000	560	420	26/27	
4	X		178,000	460	360	26/27	
5	X	X	176,000			26/27	420

graph connections monitor the current, if any, when the cartridge is fired. A change to 110 Vac for convenience in firing the pressure cartridges had no apparent effect on the measurements which indicated that the plasma did initiate conduction.

A third series of altitude tests was undertaken to determine if currents, once initiated, would approach the values of 1.4 A by the electrical circuit parameters. Values from 0.4 to 5.0 A were observed in tests where conduction was initiated; the extreme variability of initiation is seen in the results of Table 4.

A. Test No. 10

At this point, a connection was made between the low side of the output of the dc supply and power ground. Note both the low side of the ac firing circuit and the case of the pressure cartridge are tied to power ground. High-level current pulses at a 60-Hz rate were recorded. The data here indicated the possibility of ac currents flowing from the cartridge to the connector pins through the gaseous plume created by cartridge ignition.

B. Test No. 11

Transient currents were again recorded.

C. Test No. 12A

The connection between the dc supply and power ground was removed. No transient current was recorded.

C. Test No. 13

With the dc supply off, and the power ground connection made again, the transient currents were again present in the data. This test confirmed the fact that the currents recorded were not leakage currents.

D. Test No. 14

The distance between pins 26 and 27 was modified to be 1/32 in. Transient currents were recorded with no steady state current present with dc supply on.

E. Test No. 15

For this test, only the monitor resistor was installed in the high side of the dc supply output. Transient currents were again recorded.

Additional current monitoring channels were added for Tests 16 and 17 to assure that all currents could be identified as cartridge-to-test connector or contact-to-contact currents involving only the connector. The results

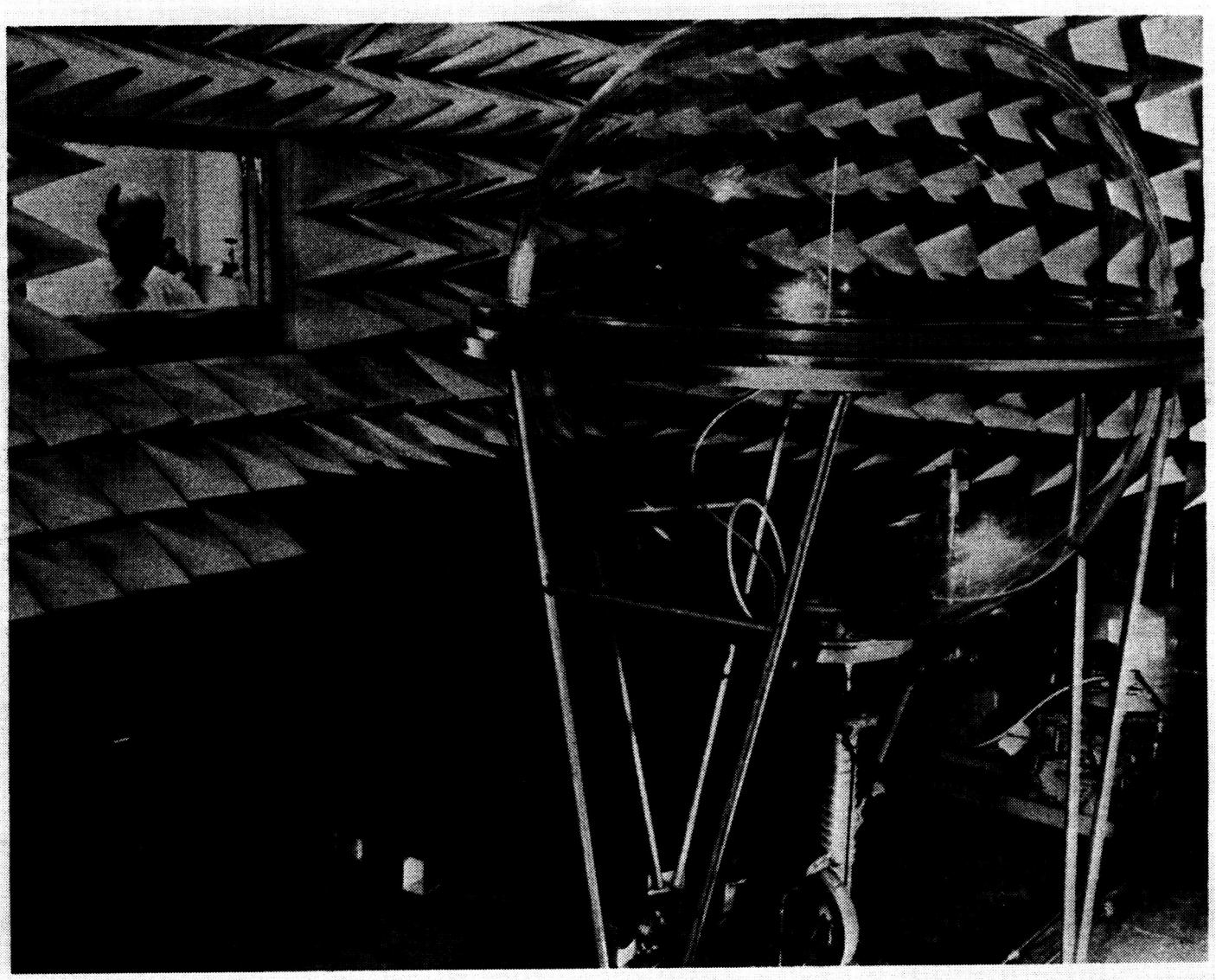

Fig. 4. Altitude chamber

Table 3. Pressure cartridge tests 1–4

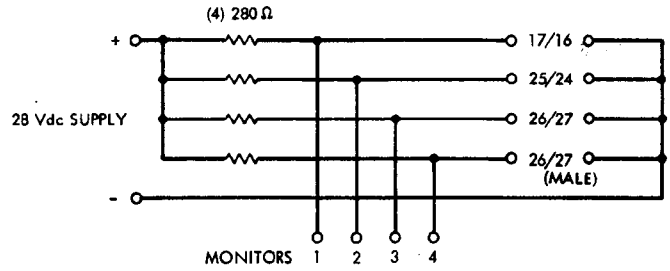

Test No.	Male only	Female only	Both	Pin combination	Separation distance,[a] in.	Test chamber altitude, ft	Firing circuit voltage	Current measured, mA
1			X		0.5	165,000	34 Vdc	None
1A			X	24/25F	0.5	175,000	34 Vdc	12
1A			X	26/27F	0.5	175,000	34 Vdc	4
1A			X	26/27M	0.5	175,000	34 Vdc	2.5
2			X	16/17F	0.5	172,000	34 Vdc	4
2			X	24/25F	0.5	172,000	34 Vdc	4
3			X	16/17F	0.5	165,000	34 Vdc	8
3			X	24/25F	0.5	172,000	34 Vdc	8
4			X	24/25F	0.5	165,000	110 Vac	4

[a]Between pressure cartridge and connector face.

are given in Table 5; the dominant currents were indeed from the cartridge to the connector.

For the last series of tests, the case of the standard pressure cartridge was insulated from ground and the connection which had existed from the firing circuit to ground was also eliminated. No currents over 1 A were observed as had been the case when grounds provided a path for firing circuit plume currents to return from the connector. Currents of 0.4 and 0.5 A were recorded with more connectors; when plume conducted currents were permitted by return through grounds, female connectors were found to be as susceptible to plume initiated conduction as were male connectors. There is not much difference between male and female connectors when the ground return path is precluded (Table 6 and Fig. 5).

IV. Summary

These laboratory tests suggest that exhausts may connect separating stages preventing exorbitant static voltage differences until separation exceeds the plume capabilities; data from Von Hippel and von Engel* on the other hand indicate that flames necessarily create a few volts of potential difference by the long-known calorelectric effect. There will normally be a voltage of 2 to 10 V between separating stages, if there are connections between stages during initial separation by retros or engines. The currents produced in staging lanyards and in staging cables may very well warrant consideration, especially if ordnance or sensitive digital circuits are crossing between stages during separation.

Staging phenomena and anomalies are especially important in studies intended to prevent failures by erudite and imaginative scrutiny of anomalies and minor disturbances occurring during flight and test programs.

*von Engel, A., "Electric Discharges and Excited Species," in *The Molecular Designing of Materials and Devices*, Chapt. 18. Edited by A. von Hippel. MIT Press, Cambridge, Mass., 1965.

Table 4. Pressure cartridge tests 5–14

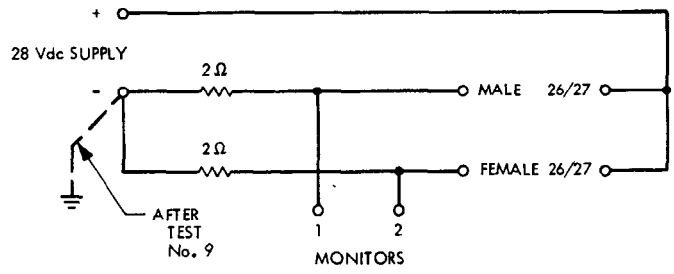

Test No.	Male only	Female only	Both	Pin combination	Separation distance,[a] in.	Test chamber altitude, ft	Firing circuit voltage, Vac	Current measured, A
5	X				2	165,000	110	None
6	X			26/27	2	165,000	110	None
7	X			26/27	0.5	165,000	110	1.15
8	X			26/27	0.5	160,000	110	0.51
9	X			26/27	0.5	130,000	110	0.4
10	X			26/27	3	177,000	110	5
11	X			26/27	3	165,000	110	2.15
12A	X			26/27	3	165,000	110	None
13	X			26/27	3	165,000	110	3.6
14	X			26/27	3	140,000	110	3.1

[a]Between pressure cartridge and connector face.

Table 5. Pressure cartridge tests 16 and 17

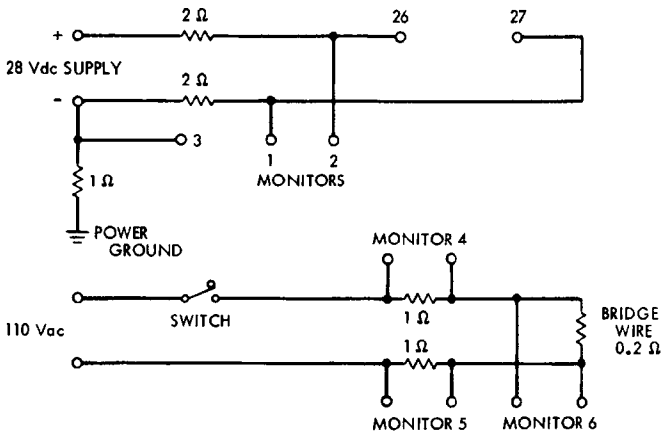

Test No.	Male only	Female only	Both	Pin combination	Separation distance,[a] in.	Test chamber altitude, ft	Firing circuit voltage, Vac	Current measured, A
15	X			26/27	3	165,000	110	7.85
16	X			26/27	3	165,000	110	1.5
17	X			26/27	3	170,000	110	3.5

[a]Between pressure cartridge and connector face.

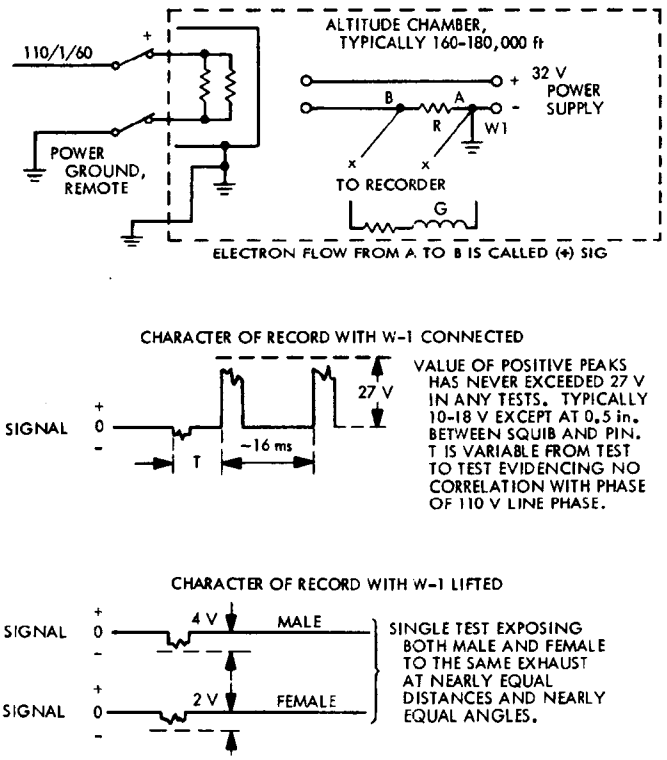

Fig. 5. Test arrangement and results

Table 6. Pressure cartridge tests 18–22

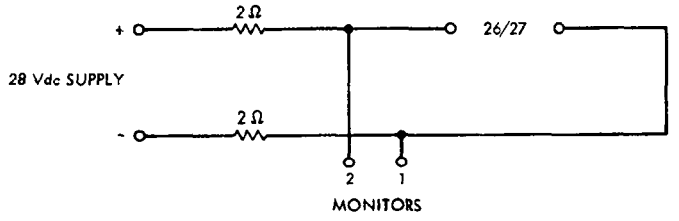

Test No.	Male only	Female only	Both	Pin combination	Separation distance,[a] in.	Test chamber altitude, ft	Firing circuit voltage, Vdc	Current measured, A
18	X			26/27	0.5	165,000	34	0.4
19	X			26/27	0.5	165,000	34	0.5
20		X		26/27	0.5	165,000	34	None
21		X		26/27	0.5	165,000	34	None
22		X		26/27	1.0	165,000	34	None

[a]Between pressure cartridge and connector face.

Appendix A

Stage II Pressure Measurements Dropout

I. History

Beginning at approximately 1731:49.6, data from the Stage II PCM telemetry indicated that all pressure channels were reading zero counts, which corresponds to a binary word of 00000000. This reading corresponds to a differential input voltage of −0.80 mV. Other relative conversions are:

$$0.00\,\text{mV} = 5 \text{ counts } (00000101)$$

$$+\,40.0\,\text{mV} = 255 \text{ counts } (11111111)$$

II. Analysis

A survey of pressure conditions aboard the vehicle showed that the negative input signals could not have been produced by the transducers without failures, and this seems unlikely.

It is also not reasonable to believe that the excitation power could have caused such a condition, since none of the other measurements powered by this supply showed any similar reaction. The RF transmitter, of course, can be eliminated since it has no effect of this type on data encoding.

The only logical item remaining is the PCM encoder and an examination of this item alone also fails to show any component or function common to pressure channels alone. The unique situation, which is the only condition unique to pressure channels alone, is the magnitude of dc common mode voltage existing on the signal leads that go into the encoder. A tabulation of the existing common mode on all channels connected to the Stage II encoder is shown below:

Type of measurements	DC normal common mode voltage, Vdc
Actuator travels	0.0
Reservoir level	0.0
Temperature: thermocouples	0.0
Temperature: bridges	0.18
Voltages	0.0
Pressures	4.75

Figure A-1 is a simple representation of a PCM encoder signal input and the related circuits. Under normal conditions the top line from the transducer to the encoder is positive with respect to the bottom line. This voltage is measured by the encoder so long as the top line is between −0.8 and +40 mV with respect to the bottom line. As can be seen from the circuit, the common mode voltage exists because of the voltage divider bridge circuit. Common mode voltage is not measured by the encoder under normal conditions and does not harm the encoder in any way unless it becomes excessive. To protect the encoder from excessive common mode two back-biased diodes are connected to the positive input line. These diodes are back-biased by a positive 8.2-V and a negative 6.2-V power supply. This network limits the common mode on the top line to between +8.3 and −6.3 Vdc. The voltage on the bottom line is limited between +8.4 and −6.4 Vdc. The difference in limiting voltage on the two lines is caused by the IR drop in the diodes across the two lines.

If a negative common mode voltage existed to cause conduction between the negative power supply and the signal lines, a positive differential signal of about 100 mV

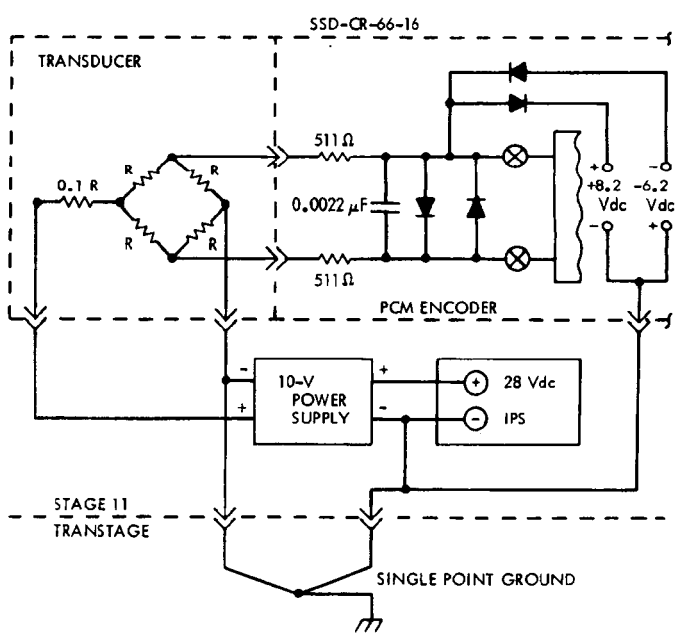

Fig. A-1. PCM encoder signal and power circuit interconnections

would be generated. This would cause the encoder to read full scale since it exceeds 40 mV, which is full scale. This condition did not exist in our case, but if we hypothesize a positive common-mode signal large enough to cause conduction, a negative differential signal of about 100 mV will exist. This condition will cause the encoder to read 0, which is the condition encountered.

The difference between the required 8.3 and 8.4 V required to cause conduction and the normal common mode of 4.75 V is the additional voltage required to cause this phenomena. This voltage could be 8.40 = 4.75 = +3.65 Vdc. This voltage would also be limited to this value by the conducting diodes and, thus, could never affect the signal circuits, which have significantly less than 4.75 V of common mode. This can be shown by adding the 3.65 V of induced common mode to the existing 0.18 to total less than 4 V and never affect the signal circuit.

An examination of the connections between the signal and power circuits will show that the 10-V excitation power supply circuit is completely isolated from the 28-V IPS circuit after Stage II/transtage separation. This creates a capacitor that has the plates coupled together with a diode. The simplified diagram, Fig. A-2, shows the condition that exists before and after the back-biased diode breaks down. It should also be pointed out that all the circuits of interest are isolated from the airframe at this time.

Additional components, in the form of parallel plate capacitors to the previous circuit, lead to the reason for the potential difference buildup between the IPS and 10-V systems.

The IPS and 10-V systems closely simulate capacitor plates referenced to each other and to the airframe as shown in Fig. A-3. This condition has been demonstrated to exist.

If a charge were to accumulate on the airframe during the time that the IPS and 10-V systems were isolated,

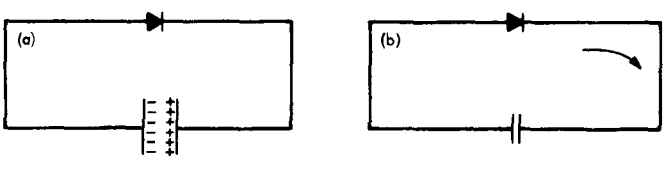

Fig. A-2. Back-biased diode

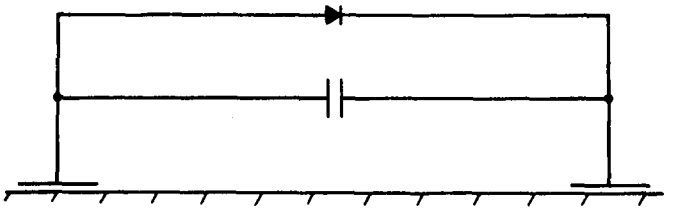

Fig. A-3. Capacitor-plate relationship

electrostatic induction would establish the opposite charge on the IPS and 10-V systems, but not necessarily of the same magnitude on each. The charge induced on each would be directly proportional to the capacitance between that system and the airframe as shown below:

$$Q_{IPS} = C_{IPS/AF} V_{IPS/AF}, \qquad Q_{10V} = C_{10V/AF} V_{10V/AF}$$

where Q is the charge in coulombs, C is the capacitance in farads, V equals voltage in volts, and AF represents the air frame.

It is the difference between Q_{IPS} and Q_{10V} that will determine the potential difference between the IPS and 10-V system. It is this potential difference, when added to the existing common-mode potential, that causes the back-biased diode to conduct and pressure channels to go to 0 counts. The voltage is determined by:

$$Q_{IPS} - Q_{10V} = C_{IPS/10V} V$$

$$V = 3.65 \text{ V}$$

$$\text{Assume } C_{IPS/10V} = 0.01 \times 10^{-6} \text{ F}$$

$$Q_{IPS} - Q_{10V} = 0.01 \times 10^{-6} \times 3.65$$

$$= 0.0365 \times 10^{-6} \text{ C}$$

III. Cause

A charge buildup of this magnitude on the skin of the vehicle is easily realized from the transtage ACS engine-flame impingement and from Stage II retrorocket impingement. This phenomena has been proven to exist in similar cases and in much greater magnitudes than required to create this condition.

The conclusion of this study is that electrostatic induction created a potential difference between the IPS and 10-V systems to overcome the back-biased diodes that protect the PCM encoder and created a negative signal on the encoder signal leads. This occurred on the channels requiring the least addition of common mode voltage, which just happened to be the pressure-measuring channels.

Appendix B

Stage II Telemetry Loss

I. History

There appeared to be a severe transient on the IPS bus. Data from the PCM encoder at 1731:50.539 appears very questionable, so other means were used to analyze the problem.

At 1731:50.539 the PCM encoder output decayed almost linearly to zero during 4 ms and remained at zero for about 5 ms. The recovery required about 2 ms, when a transmitter center-frequency shift of about 25 Hz appeared. The pulse train was nearly normal following this transient, and the transmitter drifted back to its original frequency, indicating that the transmitter felt the transient but in much smaller amount than the encoder. At 1731:50.602 another condition almost identical to the first occurred. The duration of this transient was shorter (7 ms) than the first, but had the same characteristics and results. Three ms later telemetry ceased abruptly.

A reproduction of the SSB/FM data also showed that some unusual circumstances were present during these same periods. The results are not as clear on the SSB data, but obviously some power transients were present. The SSB unit became very unstable at low power levels and became oscillatory over a range of about 12–18 V. A complete dropout of the SSB did occur during the same periods that the PCM dropped to zero. In addition, the SSB became very unstable following the first transients, but recovered and was almost normal prior to the second transient. The response of the SSB was considerably slower than the response of the PCM, thus explaining the reason for the slower recovery from the transients.

Laboratory tests indicate that the IPS voltage dropped to 8–10 Vdc during each of the transients experienced. This value is difficult to define, but characteristics of the digital logic support the conclusion that the IPS did not drop to zero and did drop below 12 V. The SSB unit supports the conclusion that the IPS did drop below 10 V. From the information gained from studying the curves of these two units, and considering the time period involved, it is concluded that 8–10 V is a reasonable estimate.

At 1731:50.612, the PCM telemetry link failed abruptly. At 1731:50.624, the SSB telemetry link failed abruptly. Both failures were characterized by an abrupt disappearance of RF signal. At the time RF energy disappeared, modulation in the form of both PCM and SSB were present.

II. Analysis

A. IPS Bus Short Circuit

The reason for the short circuits on the IPS bus is not clear but several possibilities exist. A possibility that was investigated and proven reasonable is the arcover of pins in the staging connector (Stage II/transtage) that carry the IPS power forward. This is the only possibility that has been strongly supported by test data and substantiated to a reasonable degree.

Another possibility is that the connector could have fallen back onto a supporting bracket corner and shorted the two pins. This possibility is very remote because of the cable stiffness that holds the cable.

If a fire were present in Compartment 2A, 2B, or 2C a short circuit could have been created by the insulation burning off the IPS wires.

If an arcover were to occur between the IPS positive and the airframe, a short transient would be generated. This condition would clear itself very rapidly and would have to recur for the second transient to occur. The arcover would result from the electrostatic induction previously mentioned. This possibility is not as strong as the first because it is not expected that the transient would be as large as the one that occurred.

There are two telemetry links of Stage II with associated modulation systems, power sources, etc. The antennas for these two links are in Compartment 2A, fed by a cable that carries the signals from Compartment 2B. Signals from both transmitters are combined by an RF multiplexer into one cable in Compartment 2B, and exist on a common conductor from that point to radiation. Between the transmitter and the RF multiplexer, the two transmitter signals are on separate cables. These two cables are routed along the instrumentation truss for 5 and 9 ft, respectively, and are exposed to mechanical disturbances in the vicinity.

Both failures are characteristic of open-circuited RF output circuits, and the fact that modulation still exists at the time of failure denies dc power loss as a reason for the failures. If the dc power source had failed, modulation would have disappeared before the RF signal disappeared, so dc power failure can be ruled out even though two IPS transients occurred prior to this time.

A possible cause of the failures, investigated and proven unlikely, is the activation of the power supply control relay in the transmitters. When energized, this relay removes B+ voltage from the power amplifier and would cause an abrupt loss of RF energy. It is also possible that the two transmitter control relays actuated at a different time. This was one of the first modes of failure suspected and tested. The tests, which were conducted in the Instrumentation Development Laboratory of Martin Marietta's Denver Division, prove that a transient three times the duration of those that occurred in flight will not trigger the control relays. The longer the IPS is off, the stronger the possibility that the relays would actuate when power is reapplied. The test duration firmly rules out the possibility of this type of RF failure.

The only other type of failure that could cause this series of events is physical destruction of either the transmitters or the cables that connect the transmitters to the RF multiplexer. The latter seems more likely, but either could have occurred had the destruct charges in Compartment 2B been ignited at this time. The cables are routed a few inches from one charge and are exposed to direct view from the position of the charge. This type of destruction cannot be verified but could have caused the type of failure that occurred.

B. Rocket Exhaust Electrical Effects

The rocket exhaust plume at altitudes above 120 km is hemispherical in shape in unimpeded expansion. Three retrorockets are located, exit nozzle forward, 28 ft aft of the Stage II/transtage interface. The presence of Stage II suggests that this interface is submerged in flame at all points around its circumference. The merged flame sheet can be envisioned to spill over the forward ring frame of Stage II and possibly to introduce flame and ionization inside the Stage II forward staging splice section.

Tests were conducted to determine if the flame might possibly initiate the Stage II destruct system. This possibility is based on the contact arrangement in staging disconnect half L3AP3. The command receiver destruct circuit is found on a pin 26 adjacent to a pin 27 connected to the positive terminal of the destruct battery. A momentary current between these pins could initiate the destruct explosives. The second destruct explosive connects to pin 25.

This connector has a cable length and is chuted so that it is intentionally deflected to swing out at staging to face toward the retrorocket exhaust.

The purpose of the tests was to determine if any of several flame conditions could initiate the current required for destruct. The investigation included:

(1) Burning of the connector seal to a conductive mass; the seal is made of silicone foam rubber and appears unable to withstand temperatures above 200–300°F even for periods of seconds.

(2) Ejecting of partially burned propellant fragments at retrorocket shutdown, bridging the pins.

(3) Triggering a static discharge, accumulated on the capacitance between wiring and airframe, discharging in the area of the pins.

The test arrangements were chosen to create worse conditions than probably existed during flight. The conclusions drawn from the test results are only the possibility and not the probability that one of these conditions was involved in the flight failure.

The test used a simulation of the ordnance destruct circuit on Stage II. The simplified network is shown in Fig. B-1. The circuit consists of a current-limiting 2-Ω resistor, ordnance bridge wire, and a −30 Vdc source connected to pins 26 and 27 of L3AP3. The total distributed resistance in the wires is 0.3 Ω.

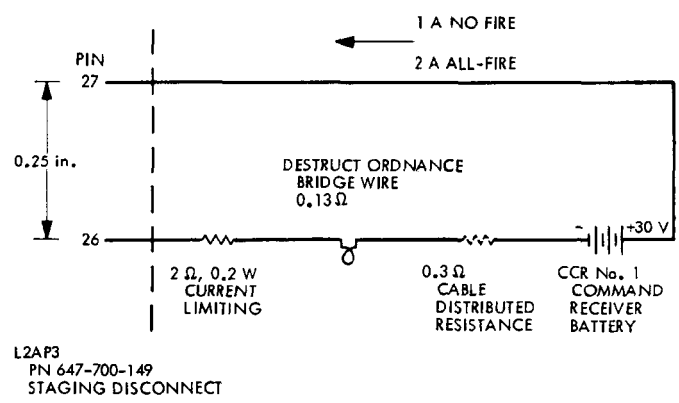

Fig. B-1. Stage II ordnance destruct circuit

The test setup is shown in Fig. B-2. The staging disconnect plug and pressure cartridge were evaluated to a simulated altitude between 120,000 and 180,000 ft. The distributed resistance was not simulated. The destruct initiator simulator was used. It has the same 0.13-Ω resistance as the bridge wire. The fixed resistor was used for the instrumentation voltage if a complete circuit is achieved during tests. The pressure cartridge firing pulse was also monitored on the Visicorder paper trace.

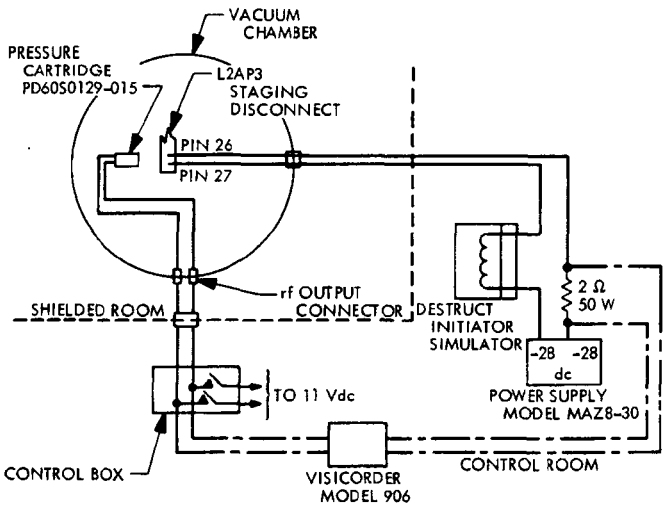

Fig. B-2. Test setup

The test consisted of firing the pressure cartridge to create a hot-gas environment for the plug pins. The voltage across the resistor was monitored to determine the circuit current transient in magnitude and duration. The dc power supply was varied during successive tests.

The test results are shown in Table B-1.

Table B-1. Rocket exhaust electrical effects test results

Run	Supply voltage, Vdc	Maximum current, A	Duration, ms	Configuration	
				Distribution, in.	Angle, deg
1	28	11.2	3	0.5	0
2	28	13	2.3	0.5	0
3	34	8	5	6.5	0
4	34	5.3	3	6.5	0
5	34	0	0	5.5	85
6	34	9.3	4.6	5.25	45
7	34	0	0	31	0

In Runs 5 and 7 the current duration was not sufficient to initiate the destruct simulator.

Discussion

August: I don't know whether you can describe what these are, but on your retrorocket firing or your stage separation, did you look to see what the probable ionization level of the gases was?

Ellison: We made some rough calculations of what the ionization should be at the distance of the Stage 3 from the retrorocket, which was about 25 ft at this altitude; we came up around 10^9–10^{10}, but the method of calculation is so gross that I don't think you can pinpoint it any more than 10^9–10^{11}.

It is probably in that range of electrons/cm^3, but this is very qualitative because it is flowing along the skin. The effects of the strip stream at 160,000 ft are highly questionable, so we don't have any great faith in these numbers. We think they are in that ball park, however.

August: People at our lab, Ed Vance and J. Nanevicz, have looked at some of these problems and, in particular, I guess we have looked at the charging on the forward rocket as a possible source of this breakdown.

But, I would like to make some general comments about problems that we have had with low-voltage breakdown.

Those who have made measurements with, let's say, planar probes in plasmas at pressures as low as 10^{-3} torr, for example, with a reasonable plasma density of 10^6–10^8 electrons/cm^3 often notice what are called scintillation discharges with relatively low voltages. This is due to a charge built up on an insulating film on the probe; for example, copper oxide film on copper electrodes or aluminum oxide films. So, it is to be expected in general that these thin film things can give you discharges with relatively low voltages, such as, 10–20 V, perhaps.

I once looked into the problem of antenna breakdown in a rocket exhaust in which a number of possible mechanisms were considered. One possibility was direct pressurized due to the exhaust; another was ionization in the hot exhaust gases. I concluded that neither of these was the appropriate answer for that particular situation, but the igniter used for that was a very high burning igniter, something like 3,000°C. For the duration of the time it was burning it gave sufficient ionization so that this was a probable cause rather than the lower flame temperatures where the gas density rises.

Ellison: You may not be aware of it, but this was discussed with Nanevicz and Ed Vance and people at the time. In addition, it was suggested that we look at some of these phenomena represented by a Lockheed problem on *Agena* that was written up by Dr. Varney and Dr. Abbott from Lockheed at the previous workshop.

PRECEDING PAGE BLANK NOT FILMED.

N70-32303

High-Voltage Breakdown in an *OSO-IV* Pointed Experiment

N. L. Hazen, M. C. E. Huber, and E. M. Reeves
Harvard College Observatory
Harvard University
Cambridge, Mass.

I. Introduction

The second of a series of experiments prepared by the Harvard Observatory for the *Orbiting Solar Observatory* (*OSO*) program was launched aboard *OSO-IV* on October 18, 1967. After five weeks of highly successful scientific operation (Ref. 1), a failure occurred in the high-voltage subsystem associated with the primary detector; the instrument was permanently disabled.

Our experience on a previous *OSO* and the early stages of development of this particular instrument were reported at the last workshop on high-voltage breakdown at the Jet Propulsion Laboratory (Ref. 2), so that it seemed pertinent to make this follow-on report about the effectiveness of the measures described at that time for avoiding high-voltage problems. This paper describes the instrument, its test background, and the nature of the failure that occurred in orbit. In addition, certain recommendations will be made based on the experience described.

It should be noted that although the technology invested in the equipment described is several years old, this will always be the case with recent flight experiments. This is due to the fact that several years are required for design and development. Similarly, the developments reported at this workshop and the recommendations made in this paper will not be fully exploited until some time in the future.

II. Instrument Description

The Harvard Observatory instrument consists basically of a scanning spectrometer placed at the focus of a single-element reflecting telescope.

The exterior of the instrument is shown in Fig. 1. It is approximately $4 \times 8 \times 42$ in. in size, weighs approximately 40 lb, and is housed in polished gold covers for proper radiative thermal properties.

The wavelength region covered by the instrument, 300–1400 Å, explains the simplicity of the optics shown in Fig. 2. Optical efficiencies are so poor as to prevent the use of anything except the simplest of reflective optics. There are no optically transmitting materials for these wavelengths and, hence, no windows or protective envelopes can be used around sensitive elements.

Radiation from the sun (see Fig. 2) enters an aperture and falls on a spherical telescope mirror which focuses

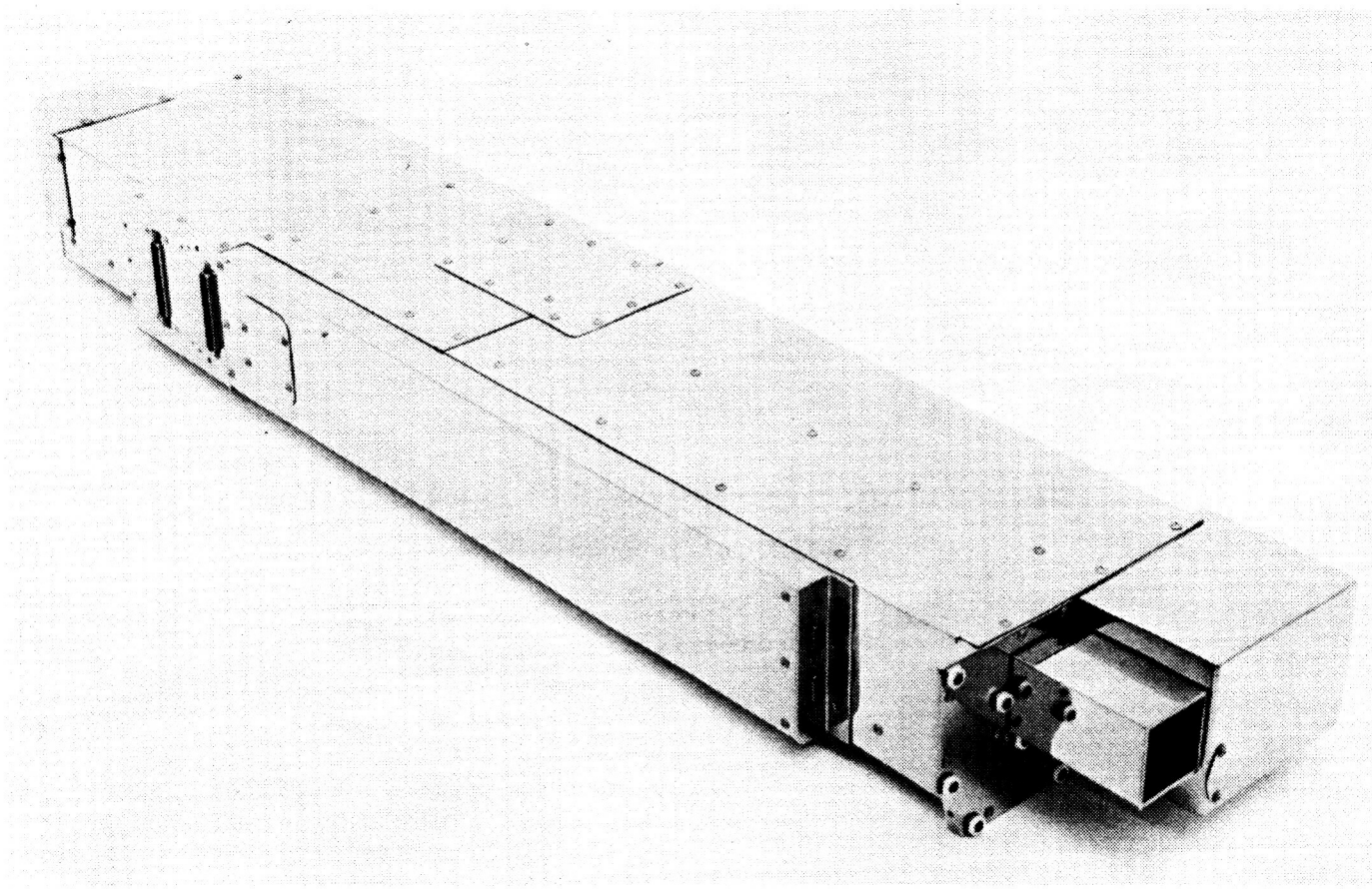

Fig. 1. OSO-IV instrument outside appearance

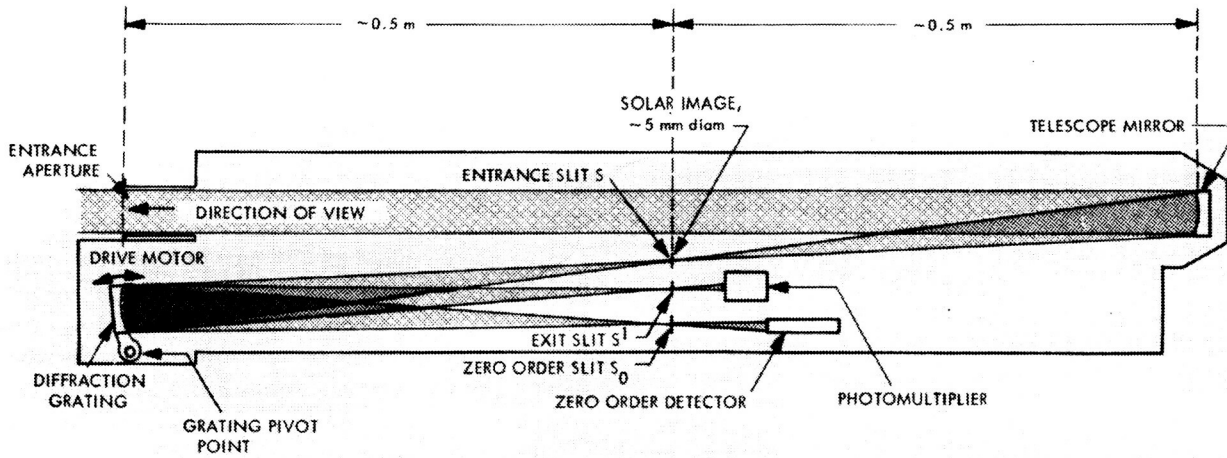

Fig. 2. Instrument optical layout

an image of the solar disk into the plane of the spectrometer entrance slit. The small dimensions of the entrance slit, approximately 150 microns on a side, act as a field stop and admit the radiation from 1′ of the solar disk. This radiation passes into the spectrometer and is diffracted by an original concave grating ruled in gold. The emission line spectrum typical of this wavelength region is scanned by rotation of the grating, bringing successive parts of the spectrum to the exit slit. The combined slits produce a resolution or band pass of approximately 3 Å. The photon flux through the exit slit is sensed by a windowless photomultiplier operating with grounded cathode. In addition, a white light sensor behind a third slit serves as an angular reference during wavelength scan by detecting the zero order radiation reflected from the grating.

The electronic system, shown in Fig. 3, can be separated into three main subsystems. At the top is the command and digital control subsystem. A digital control network (wavelength selector) receives commands and basic spacecraft timing pulses and, in turn, produces the remaining timing signals required by the instrument. It also controls the wavelength scanning system consisting of a pulse shaper, stepping motor, and mechanical

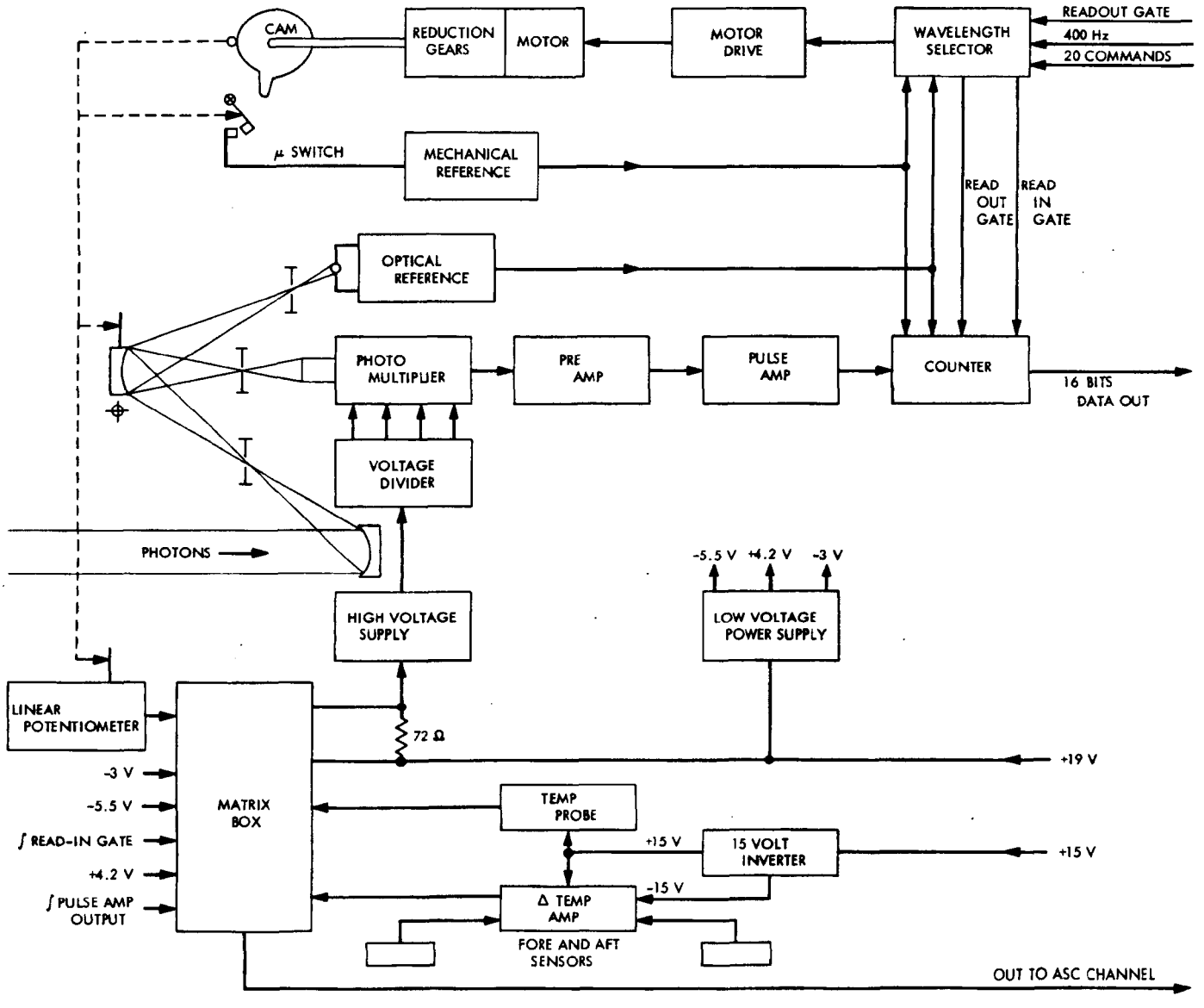

Fig. 3. Electronics block diagram

drive. The power distribution and housekeeping data subsystems, shown at the bottom of the illustration, consist of two low-voltage power supplies, the matrix or junction box, and various sensors.

The ultraviolet (UV) detection and primary data subsystems, shown in the center of Fig. 3, consist of a high-voltage power supply (HVPS), temperature-compensated voltage divider, photomultiplier, pulse preamplifier and amplifier, and finally the 16-bit binary counter/shift register. The photomultiplier is a crossed-field magnetic electron multiplier (Refs. 3 and 4) produced by the Bendix Corporation. It has a tungsten photo-cathode (insensitive to near UV and visible light), continuous resistive dynode and field strips, and external magnetic field structure. It requires a high voltage of 1750 V for proper operation and has no protective envelope.

The actual instrument configuration, with the external covers removed, is shown in Fig. 4. Note particularly the HVPS, the UV detector assembly, and the connectors and cable which join them.

The instrument acquires ultraviolet data in two fundamental forms as shown in Fig. 5. At the bottom is a typical wavelength scan of a small central region of the solar disk from 300–1400 Å with approximately 3 Å resolution. By commanding the wavelength scan system to place the band-pass on any emission line, and by activating the spatial (i.e., azimuth and elevation) raster system of the spacecraft, one can acquire spectroheliograms (images in particular wavelengths) of the sun which when reconstructed by suitable data reduction techniques take the pictorial form shown on the upper part of Fig. 5.

III. Development and Test Background

As a result of the *OSO-II* experience, reported previously (Ref. 2), effort was devoted to developing and testing the *OSO-IV* instrument in order to avoid the high-voltage breakdown problems suffered before.

The instrument was designed at the Harvard Observatory but constructed in hybrid fashion. Some of the modules were developed and built by subcontractors, others were developed at Harvard and fabricated by vendors, and still other parts were fabricated at Harvard. Instrument final assembly, integration, and test were done at Harvard. Critical subassembly and all final assembly were done in Federal Class 100 clean facilities.

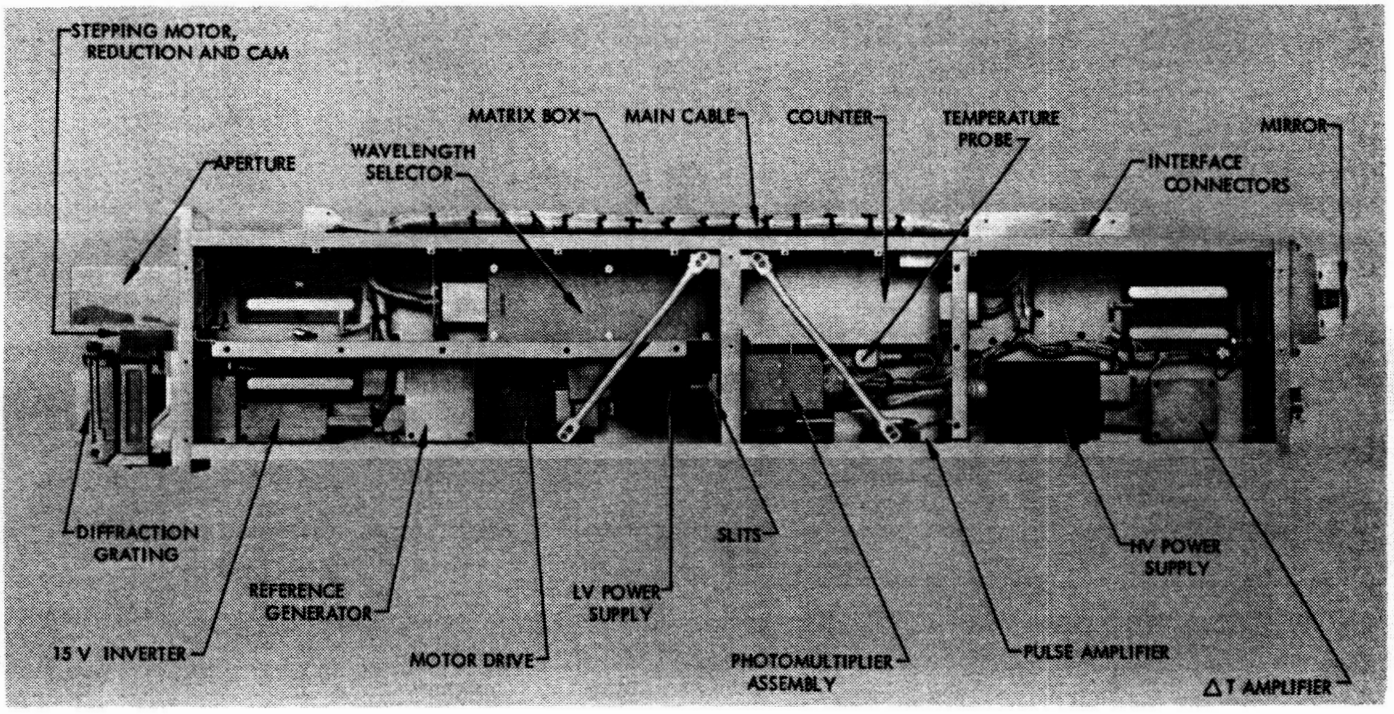

Fig. 4. Instrument interior

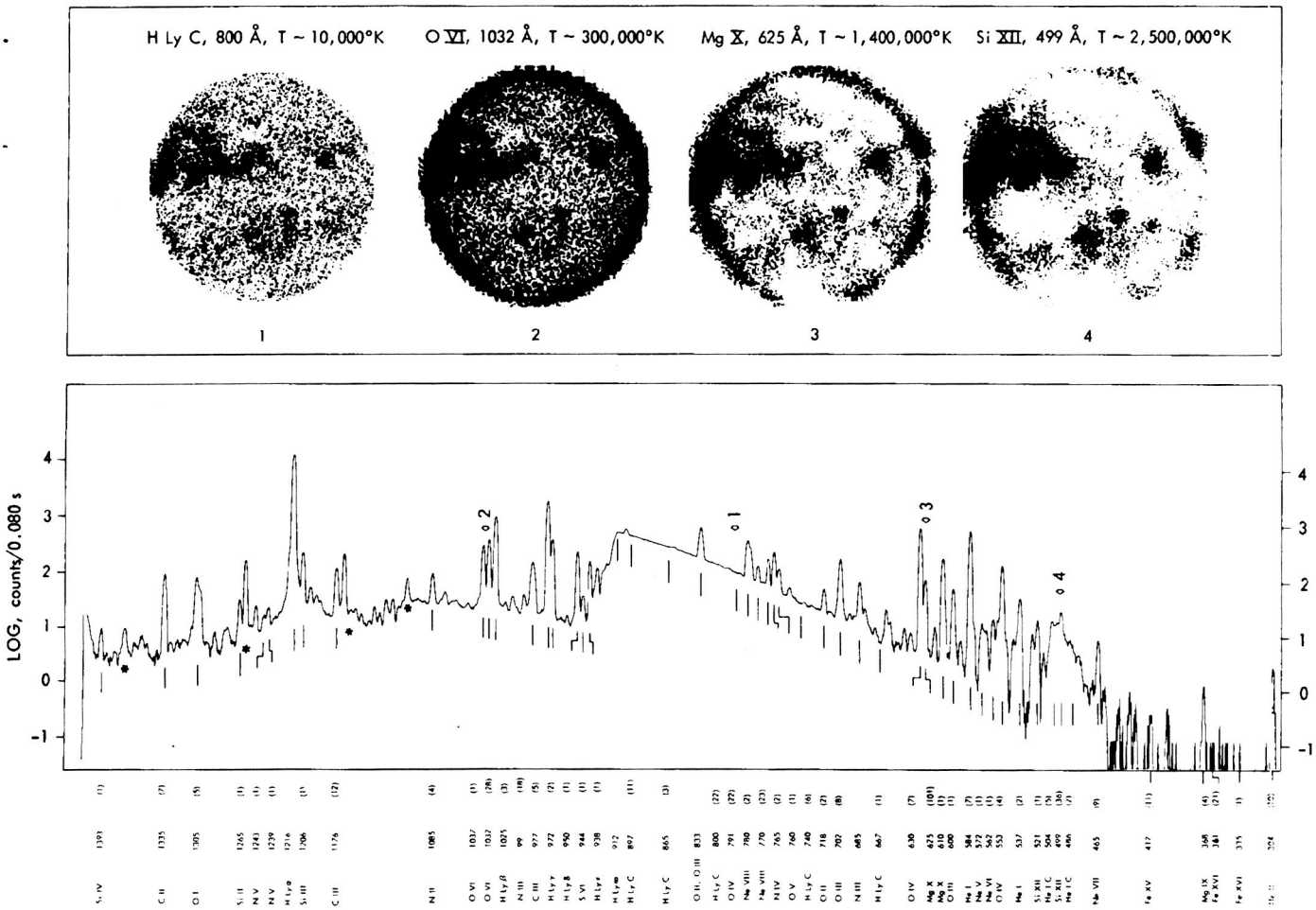

Fig. 5. Basic data summary

Extraordinary precautions were taken in design, with materials selection, and electronics piece-part usage. Elaborate qualification and aging procedures were used on electronic parts, and instrument handling was carefully controlled to prevent contamination. The instrument design was reviewed critically by several independent groups to ensure that design defects had been substantially eliminated.

After completion of the various model instruments, all normal qualification and acceptance tests required by the Goddard Space Flight Center (GSFC) were performed, including exposure to temperature extremes, thermal vacuum, vibration, acceleration, and others. In addition, however, as a result of our *OSO-II* experience a number of special tests were performed on the prototype and flight models. These explored two general areas: (1) the immunity of the system to external influences such as extreme temperature, vacuum, and plasma environments, and (2) the ability of the system to withstand (at least for many hours) conditions of high-voltage breakdown without disabling damage.

Insensitivity to combined temperature-vacuum conditions was tested on a number of occasions. In addition to the normal thermal vacuum qualification and acceptance tests (approximately 15 and 9 days, respectively, in temperatures ranging between −10 and +40°C, and vacuums between 10^{-5} to 10^{-9} torr), the UV detector subassembly and the entire instrument were subjected to hundreds of hours of vacuum and thermal vacuum exposure in the course of normal calibration activities. After delivery, the instrument also underwent thermal vacuum exposure as part of the normal spacecraft acceptance tests. These tests were thought to be more than adequate to demonstrate immunity to vacuum conditions.

The prototype instrument was also tested to investigate how orbital plasma affected the performance of the instrument (Ref. 5). These tests were made at GSFC in a facility generally similar to that illustrated in Fig. 6. This testing facility is described more completely in another paper (Ref. 6) presented at this Workshop.

Simulated plasma densities were varied between 10^4 and 10^6 particles/cm^2. The instrument was subjected to these conditions while operating fully and observing an ultraviolet source. The conclusions from the tests were that simulated orbital plasma did not induce any high-voltage discharge during the operation of the experiment, nor did it produce any undue interaction with the detection system. Additional exploratory tests performed in more sensitive, i.e., non-flight, configurations produced only moderate interactions.

Two principal types of tests were performed to establish the degree of immunity to high-voltage breakdown conditions in the vicinity of the experiment. The first was a series of corona tests performed on the complete fully operating instrument and separately on the HVPS. With the operating instrument within a vacuum test chamber, the pressure would be systematically varied between 0.01 and 0.20 torr. This would invariably induce spontaneous corona within various parts of the high-voltage detection system because of the open construction mentioned earlier. It was our goal to make the instrument immune to damage even though these conditions were not expected to be encountered in orbit. After the correction of several design deficiencies, this immunity appeared to be achieved, as demonstrated by many hours of continuous exposure in the laboratory.

The second type of test involved establishing the degree of immunity of the instrument to transients received from external sources along the various input-output lines. This was accomplished by introducing ½ mJ transients of 100 V initial amplitude, produced by a capacitor discharge, on each of the input and output lines of the instrument. Again, such testing produced no apparent damage.

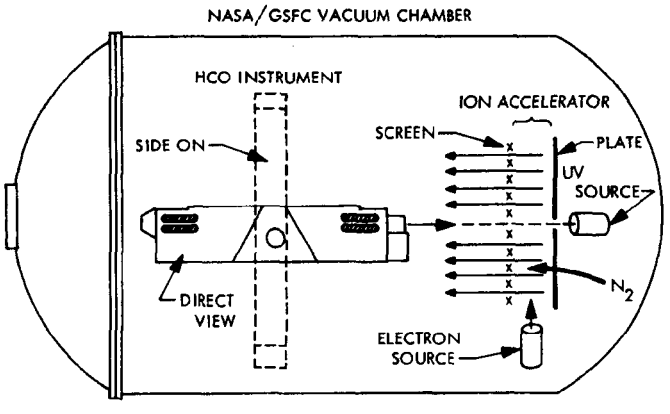

Fig. 6. Plasma test arrangement

As a result of these tests, we were confident at the time of launch that the instrument was immune to the hostile factors of the immediate environment and to any possible brief high-voltage breakdowns within itself.

IV. Failure Analysis

The instrument failure occurred after approximately five weeks of useful service. The topography of the spacecraft orbits associated with the failure analysis is shown in Fig. 7. A *Quick-Look* hardline data link had been established between the Ft. Myers Satellite Tracking and Data Acquisition Net (STADAN) station and GSFC, and also between GSFC and the Harvard Observatory, to allow near-real-time data coverage from those orbits that passed over the Ft. Myers station. Only Ft. Myers had this capability. As illustrated, the failure occurred during orbit No. 637 on November 29, shortly after the last daily pass within range of the Ft. Myers station. The failure was, therefore, not observed for corrective action until 16 h later during orbit No. 646, the first pass the following day at Ft. Myers. The play-back data for the critical orbits around the point of failure, subsequently obtained from the Johannesburg and Santiago stations, showed a clear record of the events preceding and following the failure. Data analyses and laboratory studies were performed in considerable detail and the results are available in a Harvard Observatory report (Ref. 7). For the purposes of this paper we will, therefore, present enough data to depict what most probably occurred, without the considerable substantiating evidence that is available.

The principal data characteristics of this failure were (1) unusually high primary current readings from the HVPS, (2) noise in the main digital system, and (3) interaction with the mechanical reference (MR) circuitry which activates a status bit in the Pulse Code Modulation (PCM) data word and serves as a wavelength scan reference.

The data for the 50 min contiguous to the time of failure are presented in summary form in Fig. 8. The basic time interval is 30.72 s, which represents one cycle of the analog housekeeping data subcommutator and,

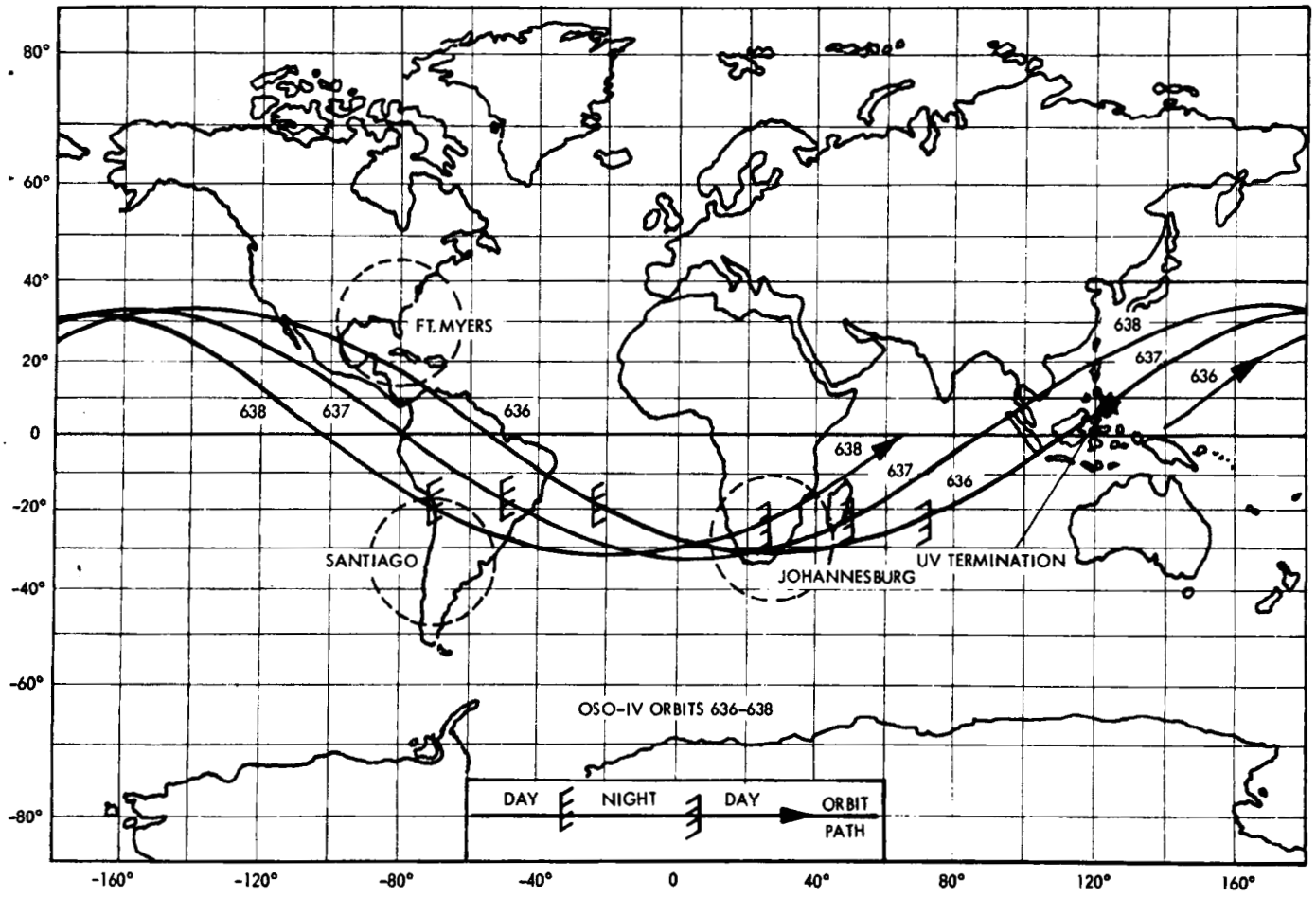

Fig. 7. Orbital geography at failure

hence, one sample at the HV primary current. This is also the equivalent of 192 Harvard data words in the PCM system. The characteristics of normal operation of the instrument can be observed at the left of the illsutration. At the top, the high-voltage current is between 9 and 11 mA with modes fluctuations. A second plot shows the MR status bit recurring at regular infrequent intervals in an expected manner. The remaining two somewhat complementary presentations of the main data output reflect normal data and the fluctuations expected from the geometry of raster picture operation (time to complete one raster picture equals 5.12 min).

An abrupt change can be seen at the time of failure. The high-voltage primary current immediately achieves the current-limited value and is interpreted as resulting from an excessive load on the power supply.

The primary data can be shown to have no statistical correlation with the previous ultraviolet data; this is interpreted as a loss of high voltage to the detector. The third characteristic is the frequent and random triggering of the mechanical reference circuitry. The combined presence of these three characteristics has been designated as Mode I.

At the far right of Fig. 8, a different set of characteristics can be observed. The high-voltage primary current is still high but apparently fluctuating randomly. The primary data system is uniformly quiet, and there is no unusual interaction remaining with the mechanical reference circuitry. These characteristics have been designated collectively as Mode II. One can observe in the first 35 min after failure several occasions of transition between Mode I and Mode II. The existence of these transitions is further demonstrated by a careful analysis of the complete data.

Fortunately for the analysis, both a prototype and a spare flight instrument were available for test; they

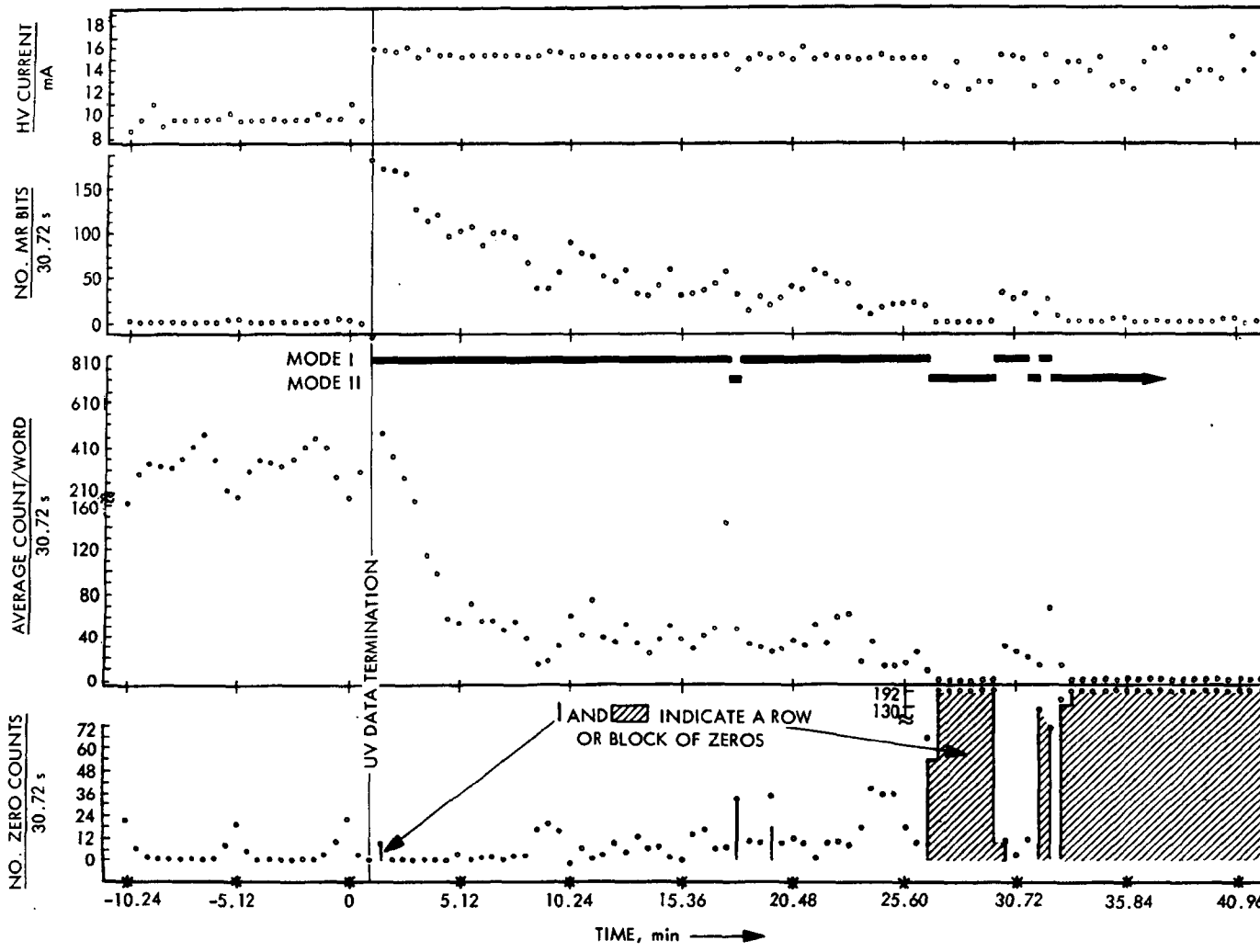

Fig. 8. Data summary: orbit No. 637

allowed very accurate simulation of the various presumed mechanisms of failure.

Careful system and data analysis determined that the counter and pulse amplifying system were operating satisfactorily and, therefore, were not the source of the noise in the main data system or of the mechanical reference interactions.

Laboratory tests were continued and showed that although high-voltage breakdown to a variety of places could produce the data noise and high current, only high-voltage breakdown to the primary ground return could additionally produce the spurious mechanical reference indications and, therefore, the Mode I condition. This was shown to result from the close physical proximity of the primary return wire and the mechanical reference circuit input line within the matrix or junction box (see Fig. 9).

The identification of Mode II is more difficult. When the presumed breakdown path was reduced to a short circuit to the primary, the noise and mechanical reference interaction disappeared, but the current remained high and stable. Further testing demonstrated that the additional Mode II characteristic (i.e., oscillation of the supply primary) was present only when the capacitor C1 was open-circuited, and the effective resistance on the secondary was low or zero. When the effective resistance was high, Mode I characteristics were still present even though capacitor C1 was open.

Capacitor C1 is a 35-V tantalum capacitor which has been shown in the laboratory to become open-circuited

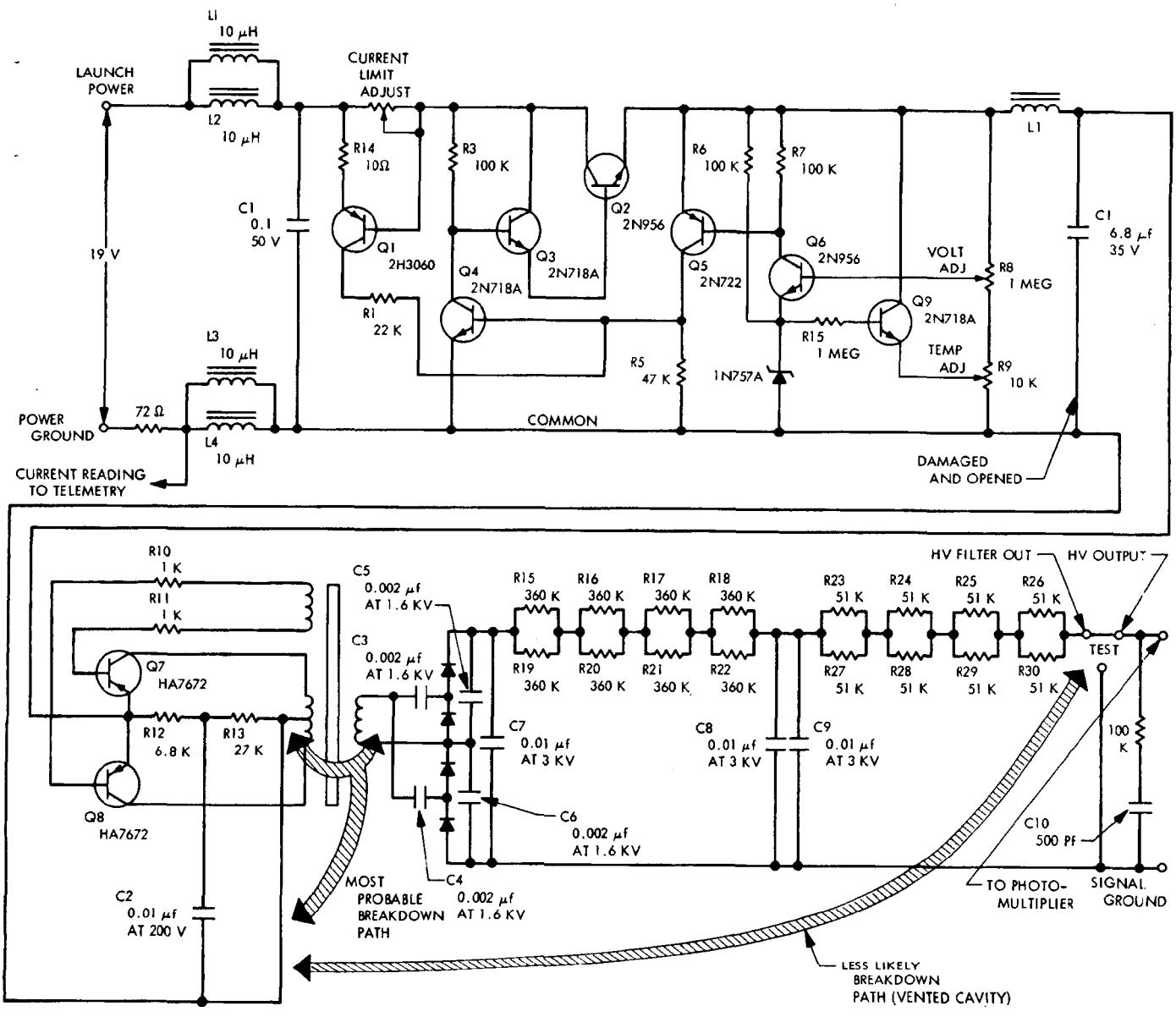

Fig. 9. Schematic: high-voltage power supply

at very modest voltages, especially in the inverted polarity.

The high voltage is close to the primary ground return in two principal places, both within the high-voltage power supply, illustrated in Fig. 10. One of these places is within the transformer module and the other is a point where a pin servicing the high-voltage enable plug and a copper printed-circuit conductor are closely adjacent. This second potential breakdown path is thought to be improbable because it is impeded by a physical separation and a conformal epoxy coating on the printed circuit board.

The remaining potential breakdown area is the transformer illustrated in Fig. 11. It consists of an aluminum core box wrapped in Teflon tape overlayed with the primary winding. This is again wrapped with Teflon and the secondary applied. The finished transformer is finally wrapped in Teflon tape and then conformally coated with General Electric RTV-11 silicon rubber at atmospheric pressure. As reported by the manufacturer, the transformer is assembled into a module, and the entire module is encapsulated with Armstrong C-7 epoxy after having been degassed at a pressure of approximately 20 torr. The module is released to atmospheric

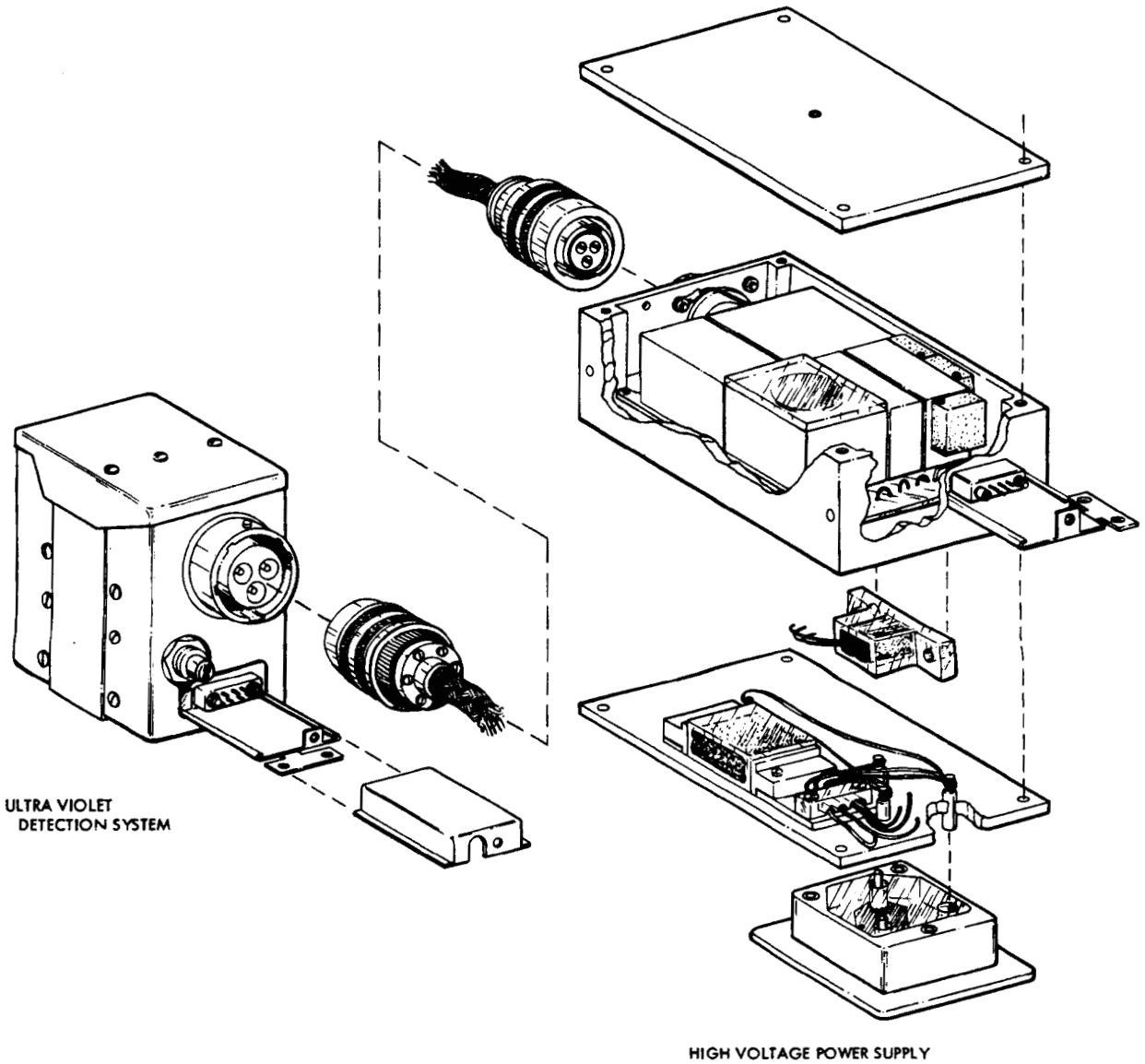

Fig. 10. Exploded view: high-voltage power supply

pressure prior to curing. From elementary pressure-volume relationships, one can show that the gas (namely, air) trapped within the transformer by virtue of the RTV seal was at a pressure of 20 torr if no penetration of the encapsulant occurred, or at some higher pressure if penetration did occur.

With the information available, we can reconstruct the probable failure mechanisms of orbit No. 637.

Following the launch of the instrument, the air trapped within the transformer by the manufacturing process gradually leaked or diffused out of the module until its pressure reached a value favorable to high-voltage breakdown between the leads or windings of the primary and secondary.

Such breakdown then occurred, producing the Mode I condition as well as large transients on the primary return line. These transients, aggravated by the presence of the inductor and series resistor in that leg, caused the capacitor C1 to open. As the breakdown condition continued, interaction developed with the materials of the transformer, which reduced the resistance paths, first intermittently, then more permanently, eventually producing the Mode II condition.

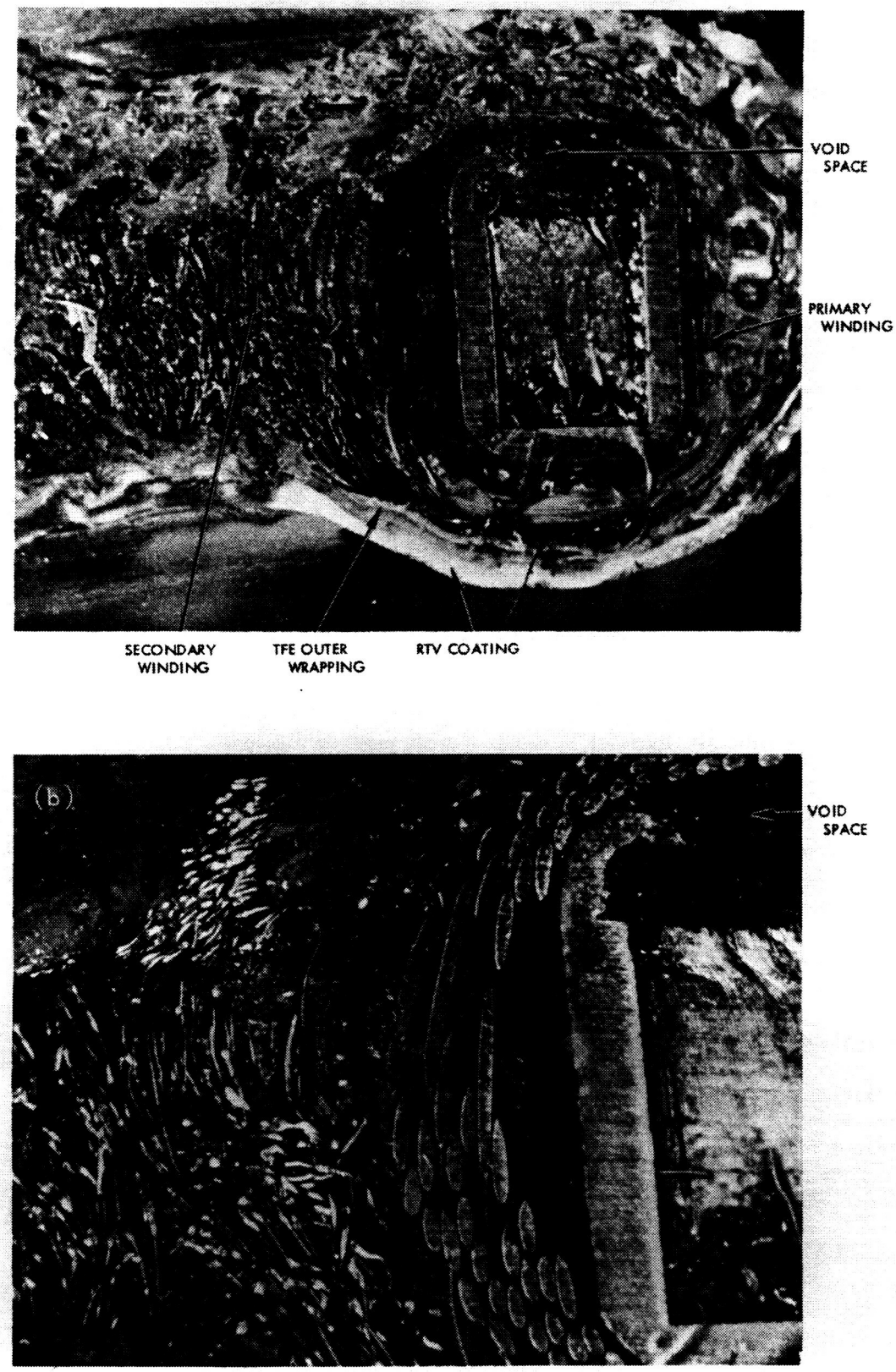

Fig. 11. Photomicrograph: high-voltage transformer section

A number of other possible related factors were brought into the analysis and considered. These included unusual variations in the instrument temperature, the observed passages through the South Atlantic Anomaly which resulted in data system noise, the occurrence of solar flares in the period before failure, and the observation of a variety of anomalies in spacecraft performance. All of these have been studied and none have been shown to have any bearing on the observed failure.

V. Recommendations

In view of the specific experience with the *OSO-IV* experiment, we have formulated recommendations for future flight instruments. The *OSO-G1* program, will use spare flight instrument from *OSO-IV* with a few modifications to improve its scientific capabilities. Obviously, the problems in the high-voltage section have to be prevented from recurring; that they have been prevented has to be proved by meaningful testing. Our recommendations now are:

First, the manufacturing techniques used in the transformer section must be improved. This has been done in cooperation with Transformer Electronics Company (TEC) of Boulder, Colorado. The goals were to avoid high-electric fields by proper winding and to encapsulate the transformer thoroughly. Mr. Byers of TEC has discussed the methods employed in these areas in a paper presented at this Workshop (Ref. 8).

For further confidence we ordered supplies of similar capability from Electro-Mechanical Research of Princeton, New Jersey, whose units stem from a well-developed design. Ideally, the power supply with the best prelaunch performance record would be flown, but it appears now that only one will be available in time.

Second, we recommend qualification and acceptance tests which go beyond even the extra testing requirements imposed on our *OSO-IV* instrument, such as plasma, corona, and spike tests. Besides these and the conventional vibration and thermal-vacuum tests, there appears to be a definite need for extended vacuum exposure of high-voltage equipment. By this we mean tests at orbital pressures for full desired lifetimes. Preferably, the entire instrument should successfully pass a vacuum exposure test for the period of the mission. This, however, is prohibitive in most missions for several reasons, including the resulting delay of the launch and the financial aspects of lengthening the schedule. The increased obsolescence of an experiment due to the time required to perform such tests is also significant. Nevertheless, high-vacuum life tests for qualification of high-voltage equipment, performed on a statistically meaningful sample, should be required. Flight units should be tested for unit acceptance by an operational vacuum exposure for the minimum desired lifetime.

Third, we recommend the use of an overload-sensitive circuit that protects the instrument by turning off the high-voltage power supply immediately in case of overload. This will probably prevent irreversible damage that would occur to the electronics during prolonged operation under faulty conditions. As shown in Fig. 12, the load (i.e., the input current) is sensed across a 10Ω resistance in the +19-V input line. The nominal voltage drop across this resistor is approximately 0.17 V and is, therefore, insignificant.

The trip point is specified as an rms load 50% above nominal for a time exceeding 100 ms. This load level is, of course, below the level corresponding to the current-limited operation of the power supply. In addition, short transients which may be induced from outside the experiment will not turn off the high-voltage supply because they are excluded by the time delay. The status of the overload protection is transmitted by telemetry. A most important aspect is the capability to override the sensing circuit and, thus, keep the instrument from being disabled by a malfunction in a safety device.

Lastly, we recommend a carefully developed progressive turn-on plan in orbit. Time should be taken to follow a systematic approach, starting with a check-out of low-voltage systems and, after an appropriate outgassing period, short periods of high-voltage turn-on. The periods of high-voltage exercise are lengthened until acceptable permanent operation has been established. A *Quick-Look* capability is indispensable for this work. On *OSO-IV*, high voltage was turned on the first time for 5 s after approximately 140 h in orbit (i.e., after nearly 6 days).

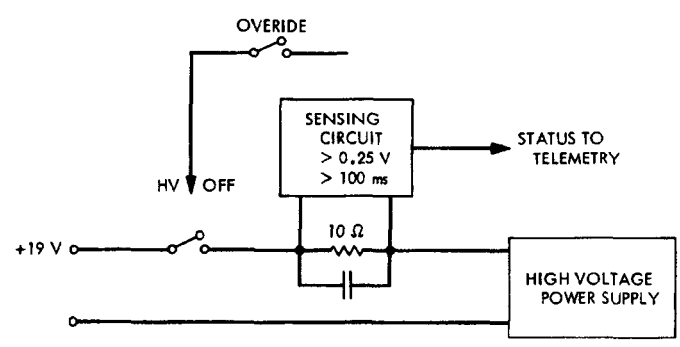

Fig. 12. Overload protection circuit, block diagram

By synchronizing this 5-s period so that it included a telemetry reading of the HVPS input current, we obtained enough data to establish the perfect performance of the entire detection system. Since the data were received in real time, we could evaluate them immediately and progress more rapidly. The overload protection in *OSO-G1* should take care of some of the concern about in *OSO-IV*, namely irreversible damage in case of a breakdown. Nonetheless, we will follow a similar turn-on schedule again as a matter of sound practice.

VI. Conclusion

As long as instruments such as ours continue to require open high-voltage systems for detection, there will continue to be a critical concern about high-voltage breakdown. We have described our most recent experiences and the additional precautions to be exercised on the next flight. Eventually, through such experience, and through exchange of information in Workshops such as this, the handling of high voltage exposed to vacuum may become a routine matter.

The *OSO-G1* instrument described earlier was completed and flown in August 1969 as part of the sixth *OSO*. The high-voltage system recommended in this paper has performed faultlessly since that time, contributing to the outstanding performance of the instrument in returning scientific data. The power supplies flown were by Electro-Mechanical Research, as mentioned earlier.

VII. Acknowledgments

The work described in this paper was performed under NASA Contracts NAS4-184 and NAS5-9274 from the Goddard Space Flight Center. We would also like to acknowledge the contributions of the Harvard Observatory engineering group, notably Messrs. Chevrier, Diamond, Dower, Gramer, and Rechavi.

Discussion

Bunker: Did I see a connector on that high-voltage power supply?

Hazen: Yes, you did. We had connectors on both ends. Because of the open nature of our detector, the connection to it is a rather difficult proposition. On an earlier instrument we had used solder techniques and considered them rather unsuccessful.

In any case, it is a tenuous business and you have to go from a high-voltage supply to a detector. At some point there has to be a connection. In this experiment we tried connectors and, in our opinion, they worked out successfully. We tested them rather exhaustively. We expended considerable care venting them to assure that they didn't trap gas. I think, judging from our experience, that those particular connectors and that particular application didn't cause problems. It is a risky business, though.

Bunker: That wasn't the cause of your breakdown?

Hazen: No, and I think from the nature of the data we can conclusively show that it did not occur at the connector.

Reynolds: What was the high voltage?

Hazen: This supply was operated at 1750 Vdc; other voltages were generated in the voltage divider network, but that is not of concern here.

Hunkle: I would just like to comment that we had a failure very similar to yours with a 1640-V power supply using an image dissector tube in *Axe III*.

We discovered the problem while the camera was in the satellite down on the launch pad in a similar system. We determined that the critical pressure point, when reached, would remain in that area. It was a gas leak. I believe that the camera failed on about the 45th day. We immediately turned the camera off and waited for, I think, three or four weeks. We had run many tests in our chamber at Fort Wayne and determined about a 80:20 percent ratio. That is, if it failed 80 days, we would leave it off for the full 100 days. When we shut it off and turned it back on, it worked fine.

Hazen: It certainly appears both in this failure and, incidentally, in the one reported in the last workshop that irreversible damage might well have been prevented by immediate off-switching and that, of course, is what we propose to do.

Forsberg: It appears that in all the experiences that I have had in talking with people about breakdown, no one has yet actually simulated a corona condition in the laboratory in the way of simulation to evaluate their breakdown circuitry or their corona protection circuitry. Would you comment on that?

Hazen: We have, as a matter of fact. The spacecraft manufacturer has developed the overload protection circuit for us and we have tried it at their plant; it worked well. We have not tried it in simulated breakdown conditions. We have also simulated breakdown conditions in our own lab without using that circuit. The

Discussion (contd)

combination of those two experiences leads us to be quite confident that one will make the other operate.

Forsberg: Will you comment on the type of simulation that you used in your laboratory? The thing I am trying to get at, is that in all of my experience nobody has actually come out with some kind of corona source or corona simulator to represent the noise.

Hazen: Well, the simulator I have in mind is an actual X-flight, high-voltage power supply which broke down in a vacuum chamber.

Forsberg: But, wouldn't this simply be an arc that you would be presenting to your circuit?

Hazen: It would be a random sample of a typical experience.

Forsberg: I see. Do you feel that would be adequate?

Hazen: Yes.

Benden: Have you considered enclosing your high-voltage power supply in a metal box and pressurizing it?

Hazen: I think it is certainly a valid concept. Unfortunately from the nature of our business at some point we have to bring the high voltage into an open system.

Benden: That's true.

Hazen: One concept, and I think a valid one, as valid as any other, is to enclose and hermetically seal a power supply and at some hermetically-sealed output terminal make the transition to an open construction. We are not planning to use it on this next flight, but I think it is a valid concept.

References

1. Goldberg, L., Noyes, R. W., and Parkinson, W. H., "Ultraviolet Solar Images from Space," *Science*, Vol. 162, No. 95, 1968.
2. Reeves, E. M., "High Voltage Effects in Satellite-Borne Spectrometers," in *Proceedings of the Workshop on Voltage Breakdown in Electronic Equipment at Low Air Pressures*, Technical Memorandum 33-280. Jet Propulsion Laboratory, Pasadena, Calif., Dec. 1966.
3. Heroux, L., "Photoelectron Counting in the Extreme Ultraviolet," *Applied Optics*, Vol. 7, p. 2351, 1968.
4. Macar, P. J., Rechavi, J., Huber, M. C. E., and Reeves, E. M., "Solar-Blind Photoelectric Detection Systems for Satellite Applications," *Applied Optics*, Vol. 9, pp. 581–593, Mar. 1970. Also available as Report No. TR9, Harvard College Observatory, Jul. 1969.
5. Diamond, S. M., *A Simulated Orbital Plasma Test of the HCO OSO-IV UV Spectrometer*, HCO Solar Satellite Project Technical Report No. 8. Harvard College Observatory, Harvard University, Cambridge, Mass., May 1969.
6. Burrowbridge, D. R., "Testing of High-Voltage Spacecraft Systems in a Simulated Ionosphere Plasma," in *Proceedings of the Second Workshop on Voltage Breakdown in Electronic Equipment at Low Air Pressure*, Technical Memorandum 33-447. Jet Propulsion Laboratory, Pasadena, Calif., June 1970.
7. Dower, R., Hazen, N., Rechavi, J., *Harvard College OSO-IV Pointed Experiment—An Analysis of the Malfunction During Orbit No. 637*, HCO Solar Satellite Project Technical Report No. 7, Harvard College Observatory, Harvard University, Cambridge, Mass., Feb. 1969.
8. Byers, H. C., "Design Considerations for Corona-Free High-Voltage Transformers," in *Proceedings of the Second Workshop on Voltage Breakdown in Electronic Equipment at Low Air Pressure*, Technical Memorandum 33-447. Jet Propulsion Laboratory, Pasadena, Calif., June 1970.

N70-32304

The Prevention of Electrical Breakdown in Spacecraft

F. W. Paul and D. Burrowbridge
Goddard Space Flight Center
Greenbelt, Maryland

Our presentation is a description of a manual still in print titled, *A Manual for the Prevention of Electrical Breakdown in Spacecraft*. The manual provides guidance, based on actual experience, making it possible for the designers and fabricators of high-voltage equipment for space applications to avoid failures caused by electrical breakdown. The document is divided into seven major subject areas, as follows:

1. Phenomena associated with electrical breakdown.
2. Design principles.
3. Design and fabrication practices.
4. Test considerations.
5. Specifications.
6. Design review check list.
7. Bibliography.

The material was compiled from the literature listed in the bibliography and from conferences with experienced personnel at the Goddard Space Flight Center, Ames Research Center, Jet Propulsion Laboratory, and the University of Chicago.

In the first section, the prebreakdown phenomena in gases goes into gases as insulators, how gases become conducting, Townsend's first coefficient, Townsend's second coefficient, gaseous ions, and space charge.

The breakdown phenomena in gases goes into Paschen's Law, the breakdown in homogeneous fields, time lags for breakdown, direct-current discharge types, and breakdown in alternating fields.

The phenomena part of this manual deals primarily with gas breakdown. As has been pointed out in this meeting, this is where the major difficulty lies.

Figure 1 is an example of some of the basic information provided. This curve, which you have seen before turned the other way, relates discharge type as a function of the supplied voltage and current in the discharge. There is only one region, to the right of the glow, where the gaseous discharge obeys Ohm's law; this is the area in which problems are created.

A curve showing the region where multipacting will occur as a function of applied electric field and the frequency is shown in Fig. 2. A curve is also shown where the harmonic regions occur.

Figure 3 is a copy of a table which summarizes the breakdown phenomena, that is, whether it occurs in gas, liquid, or solid, and the mechanism, time effects, etc.

A very brief summary is also provided informing the reader of some of the terms and sources for additional information, and topics.

Figure 4 is a reproduction of a representative table which enumerates the dielectric strength in arc resistance for selected insulation materials suitable for molding, extrusion, or casting. A table listing the dielectric strengths of various gases is also in the manual. This information is taken from the literature, and the appropriate references are provided.

A type of connector we prefer, is shown in Fig. 5. This connector is used in one of the Goddard Space Flight Center systems to connect 5 kV from the high-voltage power supply to the detector. In this case, the connector is just a mechanical connection; it has no voids, outgassing, or other connectors for it to jump to, and has no pins. This type of connector has been used with good success.

The first page of a conformal coating procedure, supplied to us by the University of Chicago, is shown in Fig. 6. It provides an example of the detail required in procedures of this sort in order to get good results. You cannot really leave such problems to the discretion of technicians. It is necessary, therefore, to go into this detail to get the reliability and quality required.

The first page of a Jet Propulsion Laboratory specification for *Mariner '69* is shown in Fig. 7. Provided by Earl Bunker, it shows the detail required. Included in this specification is a detection circuit; unfortunately it is not as up to date as the one Bunker presented yesterday. A great deal of care must be taken to make sure that you get the product that you are buying and one that will work for you.

There is really no original information in here. It has been compiled for the application of space hardware and is a collection of valid information conveniently packaged into one document.

I would appreciate any comments you have on the preprinted versions provided to you; there are typographical errors, but these will be corrected. Any suggestions for improvements would be appreciated; we would also be grateful if you would tell us of any errors you might find.

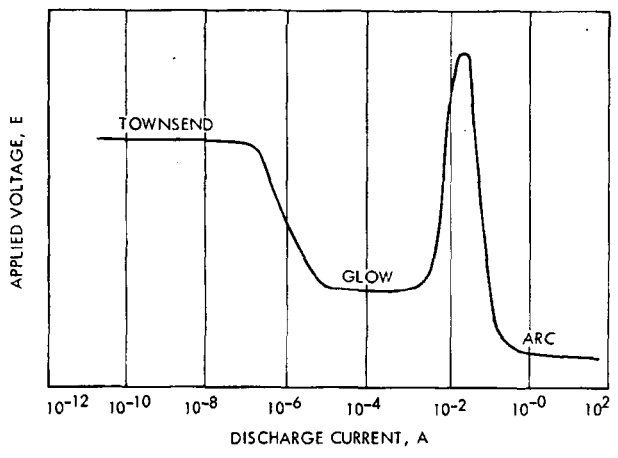

Fig. 1. Applied voltage vs current for a typical gas discharge

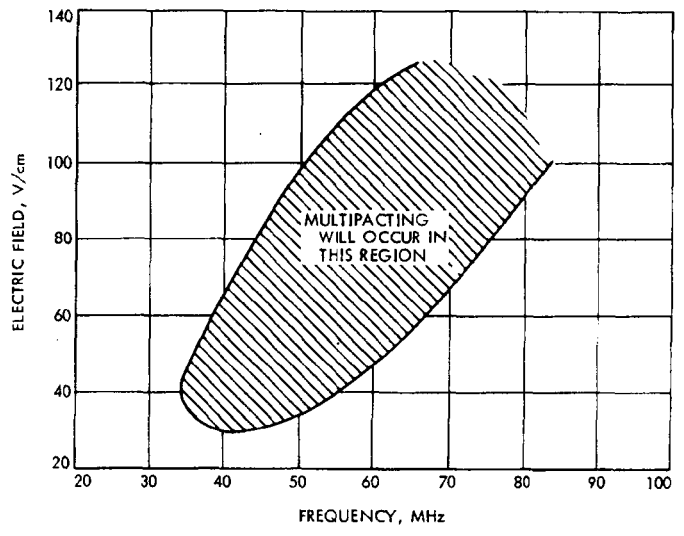

Fig. 2. The values of electric field and frequency for which multipacting may occur

Table 1

Generalizations of Breakdown in Gases, Liquids and Solids.

	GAS	LIQUID	SOLID
1. BREAKDOWN PHENOMENA			
Mechanisms of Breakdown:	Townsend mechanism satisfactory for threshold in non-electronegative gases; $\gamma(e^{\alpha\delta}-1) = 1$. Townsend mechanism may be modified to include electronegative gases. Space-charge distortion may lead to other mechanisms: e.g., streamers. Field emission may occur at high pressures.	Definitely involves field emission: may involve electron avalanche formation. Other mechanisms may involve thermal breakdown, bubble formation, suspended particles, and electrochemical degradation.	Electronic breakdown as exemplified by the Seitz, Von Hippel, and Frohlich theories. Other mechanisms include thermal breakdown, breakdown by associated gas discharges, electromechanical and electrochemical breakdown.
Time Effects: A. Statistical Time Lags	Decreased by irradiation or by field emission when it occurs (high pressures).	None due to lack of initiatory electrons because of field emission. May occur for some other reason.	
B. Formative Time Lags	At very low overvoltages (> 1 percent), long time lags of the order of several ion transit times are observed, at least up to atmospheric pressure (10^2-10^3 μ sec); hence, Townsend mechanism is adequate at small overvoltages. At higher overvoltages, streamers probably occur with consequent short time lags.	Longest observed formative times are shorter than ion transit times for electronic mechanisms. For ordinary thermal breakdown, time lags are much longer (minutes or days) and depend on overvoltage, heat conduction and ambient temperatures.	Probably like liquids, with the additional possibility of fixed voids, very long time lags due to degradation by discharges (up to years) may occur.
2. VARIABLES INVOLVED IN BREAKDOWN			
Density (proportional to reciprocal of mean free path):	Townsend mechanism predicts Paschen's Law; space charge deformation and field emission (high pressures) cause deviations from Paschen's Law.	Cannot conveniently change mean free path by pressure change as in gases; however, by analogy with gases, similar effects complicated by field emission might be expected.	Probably like liquids.
Electrode Spacings, δ:	See Paschen's Law above: Townsend mechanism predicts a decrease in E_b with increasing $P\delta$: however, refer to electronegative gases below.	Same as for gases if avalanche mechanism: often confused with area affect for curved electrodes. If suspended matter or	E_b increases for mica at small thicknesses (10^{-5} cm). Dependence on δ difficult to detect at usual larger thicknesses. E_b varies

Fig. 3. Facsimile reproduction of a part of Table 1

Table 2

Dielectric Strength and Arc Resistance for Selected Insulation Materials Suitable for Molding, Extrusion or Casting.

Material	Arc Resistance (seconds)	Dielectric Strength (volts per mil)
Acetal resin copolymer	240	500-2100
Acrylic resins	no tracks	400-500
Acylonitrile Butadiene-Styrene	70-80	350-400
Alkyd molding compound	175-235	300-350
Cellulose acetate	50-310	230-265
Cellulose acetate butyrate	unknown	250-400
Ethyl cellulose	60-80	800
Diallyl phthalates	105-140	350-400
Epoxies	120-300	300-500
Fluorinated ethylene and propylene (copolymer)	>300	500-600
Mica—glass bonded	240-300	350-400
Neoprene	unknown	300
Nylons with glass fibers	0-150	400-550
Phenolic molding compound—unfilled	tracks	300-400
Phenolic molding compound with glass fibers	0.4 to 150	140-370
Phenylene oxide resins	unknown	500
Phenylene oxide resins with glass fibers	120	1020
Polychlor otrifluoroethylene	>360	530
Polyethylene, irradiated	unknown	2500
Polyolefin	unknown	1300
Polypropylene with glass fibers	75	300-475

Fig. 4. Facsimile reproduction of Table 2

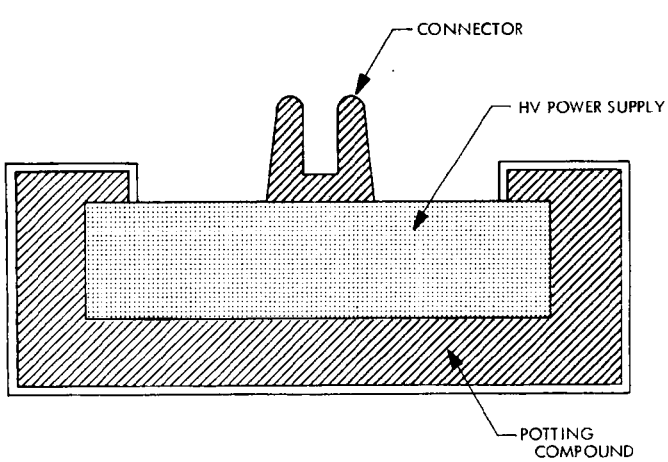

Fig. 5. Direct-contact 15-kV assembly

Conformal Coating Procedures

An interesting and valuable example of the procedures followed by laboratories most consistently successful in avoiding electrical breakdown failures is offered by the following specification prepared and used by the Laboratory for Astrophysics and Space Research of the University of Chicago. One should note the detail with which the procedure needs to be described to insure that the persons using this outline are informed of all the precautions that must be taken.

CONFORMAL COATING PROCEDURES

I. PREPARATION

1. Inspect module, board, stick, etc. to insure all condensers, resistors, wires, etc. are firmly supported or touching a firm supporting structure in order that conformal coating will secure them firmly into place.

2. Be certain that inspection code or marks are on material to be conformal coated.

II. PROCEDURE

1. Wash the unit in a fresh bath of isopropanol alcohol. A used or unused tray should be used to wash the unit, with positive assurance that the tray is not contaminated with any other foreign materials of any kind should be made.

2. The unit should be washed for no less than one hour and no more than two hours.

3. The unit should be agitated frequently in order to flush away dislodged particles. In some cases, the use of a small brush may be necessary to assure proper cleaning of spots of contaminated areas. In all cases, the brush should be one which has not been used for any other type of cleaning.

Fig. 6. Facsimile reproduction of a procedure

1. SCOPE

1.1 Scope. This document covers the design requirements for providing High Voltage Protection for Mariner Mars 1969 Flight Equipment.

1.2 Description. The High Voltage Protection requirements delineated herein are to be applied to packaging and testing of electronic equipment operating within a specified voltage range. Voltage breakdown considerations not included in this document are as follows:

a. Voltage breakdown in cavities or wave guides in vacuum due to secondary emission (multipacting) or other effects.

b. Conduction (Townsend) current between two electrodes of the order of 10^{-8} ampere or less due to the existence of free electrons in the gap.

High voltage protection requirements are applied to equipment design to assure that electronic equipment employing high voltages will survive an intentional or inadvertent turn-on and operate without damage while in the critical air pressure region or the vacuum of space.

2. APPLICABLE DOCUMENTS

2.1 The following documents, of the exact issue shown, form a part of this design requirement to the extent specified herein.

SPECIFICATIONS

Jet Propulsion Laboratory

FS500441 B	Soldering Process, Mariner Mars 1969 Spacecraft, General Specification for
*FS500450	Transformers and Inductors, Electronic Packaging, General Specification for

Military

MIL-T-27B	Transformers and Inductors (Audio, Power, and High Power), General Specification for

REQUIREMENTS

Jet Propulsion Laboratory

M69-3-220 1 November 1966	Functional Requirement, Electronic Packaging
*M69-220-1	Design Requirement, Mariner Mars 1969 Flight Equipment, Electronic Packaging
M69-220-5A 3 May 1967	Design Requirement, Planer Packaging, Mariner Mars 1969 Spacecraft

STANDARD

Military

MIL-STD-202C	Military Standard, Test Methods for Electronic and Electrical Component Parts

PROJECT DOCUMENT

Jet Propulsion Laboratory

PD 87 13 October 1966	Mariner Mars 1969 Parts Control Document

*Not released as of the release date of this design requirement.

Fig. 7. Facsimile reproduction of a *Mariner '69* specification

Discussion

Perkins: I think you should be complimented on getting this data collected and put in one place because it is really very useful.

There is one section that I would think would be highly desirable to eliminate completely because it is misleading, and that is the table of the dielectric strength of materials. Over a period of many years I have had more trouble with people who use such data for design than you can imagine. Those data that are quoted are short-time dielectric strengths. Even those values are not necessarily correct because when you start looking at the literature you will find that one piece of data will have 3 mils, another will have 0.25 in., another will have maybe an inch. You will find that with any given material the dielectric strength value that you determine is a function of the thickness of the material. It is also a function of the size and geometry of the electrodes, humidity, temperature, and the disposition of the operator who ran the test.

Now, the reason these data are misleading is that you can never operate an insulation at voltages even closely approximating the short-time dielectric strength. If you will plot a voltage-time curve, which means the life that you can get for an insulation for a particular electrode geometry, and show life versus a given stress, you will find that many of these things will have ultimate stresses, where corona can exist, only on the order of 50 to 100 V/mil or else they will fail miserably and rarely can you run above 400 V/mil in the absence of corona. Now, this applies to alternating current. With dc, you can go up probably to 2,000.

I would say that the best thing to do if you want to talk about dielectric strength is to go down your list and eliminate those figures and say excellent, good, and lousy.

The same thing applies to the table on tracking resistance. Those data were apparently obtained from the ASTM-D-495 test for the most part. Now that is a test in ASTM we have been trying to throw out because you can get absolutely and completely misleading data from it. You can take one material and vary the electrode shape, which is permissible under the test, and prove the material to have 5 s or 200 s on certain types of materials.

A good tracking test, unfortunately, does not exist; that is why the thing has managed to stay.

Again, I think you should be specific, and say that this is that test, that it is questionable, and that the performance of the material should be evaluated in terms of the use for which it is intended.

Burrowbridge: Thank you. Again, a lot of this material is simply compiled information, and I agree with you, you know, that this data comes under standard tests. But, if somebody is designing a system and he has 2,000 V, he doesn't know whether this puts him on a good, excellent, or poor table. I will concede that this information can be questioned, but perhaps somebody like du Pont can get this other type of information out.

Perkins: I have tried. The trouble is the person who is selling insulation likes to quote short-term dielectric strength figures because it sounds like a good selling point. It is absolutely of no value to the designer, but if you can say that a material will stand 3,000 V/mil, the salesman can go ahead and beat the table and be enthusiastic about the good material he is offering, whereas, in practice, he may not be able to run it over 20 or 50 V/mil.

August: One problem I think you might want to bring up is that occasionally a lot of these dielectrics are operated rather close to their high-temperature limits and there isn't too much data available on how the dielectric constant changes. If you are stressing something pretty hard, however, and are operating it at a pretty high temperature, you can rapidly lose your effectiveness. I think that needs to be included in your manual, too.

Burrowbridge: Well, again the main gist of this thing has been toward the gas breakdown and I won't presume to tell the materials people where to go to get the good materials.

Dunbar: Along with Mr. Perkins' comments, there are curves and data taken of two types. One is temperature: dielectric strength vs time, which for a limited number of materials shows us the limited number of materials that could be added. There also is another significant curve, or group of curves, which he brings up, which are temperature-dependent. They show the temperature dependence on dielectric strength. When adding these two functions together it helps to give you an overall view. This gives Teflon, I think, in the neighborhood of 22 V/mil to be on the safe side.

If you add a corona field due to a gas discharge, it will knock it down to about 5 V/mil.

Burrowbridge: Where are these curves available?

Dunbar: They are, I think, in the 1968 EI. I can't remember the name of the author, McMahan, I believe, EI, of IEEE. He has a curve on degradation, I believe.

Perkins: The original authors were McMahan and Perkins.

Burrowbridge: Are the data valid?

Perkins: They had better be.

Goldlust: Perhaps we are making too much of this point, but I will have to concur with Mr. Perkins because his company has got me into a lot of trouble by listing Kapton as 7,000 V/mil. This is for a half-mil film.

There is one other point that I wish to note. These short-term tests very critically depend on how fast the voltage is initially raised. I am at a disadvantage in not having read your manual, but I hope that in all cases where a voltage is listed, for the help of the designer and for me, personally, that you will list whether it is RMS 60 Hz, or 400 Hz, or whether it is dc.

Burrowbridge: Well, this information was taken from the encyclopedia issue of insulation and is referenced as such.

Goldlust: For the sake of clarity, I think that throughout the manual when a voltage is listed, unless it is expressly understood that we are working with dc, I think it should be indicated as such, or ac peak, or RMS.

Cardwell: I am interested in this insulation problem, not from a sine wave or dc standpoint but from a square wave standpoint. Most of the power conditioning work we perform is done with a switching mode, and it is very difficult to find. Perhaps you can advise us where we can find insulation data on square wave or pulse applications.

Perkins: Well, I can tell you that it is very hard to come by. I first ran into it on pulsed cables during World War II. We found that the only way to get satisfactory results at that time was to run life tests on the materials, but we could correlate them with the corona starting level. In other words, if at the peak voltage of the pulse we did not have corona on the corresponding 60 Hz or 400 Hz ac, we did not get into trouble with failures. That is about all the information that I have.

Cardwell: I think you will find that that is generally true except for pulses that are becoming more and more popular in high-energy physics work where you are talking about nanosecond pulses. Then I think we have other problems.

Benden: I am at a disadvantage, too. I haven't read the report and I don't know really whether this should fit in here, but I feel that in the design for corona problems the designer should be aware of the noise that can be generated from a systems standpoint, signal-to-noise is what I am really saying. This might not be appropriate in this report, but people should be aware of it.

Burrowbridge: We pointed to the problem, but we didn't go into the details of it.

Ellison: I wanted to make a comment. I really think you need some footnotes added to the section on gas breakdown which will provide more exhaustive references and, at least, more recent treatments of some of the gas breakdown phenomena. I strongly suggest von Hippel's *Molecular Engineering Series;* two books which document very briefly the failure of Paschen's Law with many gases and at high distances. Otherwise people are going to be misled, I believe, into thinking that this might be the Gospel truth and that Paschen's law says thus; of course, you all know that the general problem with Paschen's law is that it actually fails with some gases.

Two such references added in a footnote would seem sufficient.

Burrowbridge: In most cases, I point out that it is only good for parallel plates and, as you know, it is not that much in use.

Ellison: It isn't only good for parallel plates, but what I am saying is insert a footnote or a precautionary word. The other point that needs to be emphasized even more is that even though you can live with corona and noise, the noise on other systems can't stand it.

Burrowbridge: This is pointed out.

Heuser: A very small point, but several people have talked about polyolefin insulators. I was under the impression that polyolefin was a generic term for polyethylene and polypropylene, and I was wondering if people are using the same term to mean different types of insulators?

Perkins: I am not sure that I know exactly what you are talking about there. The term polyolefin means a chemical series which includes polyethylene, polypropylene and things that have copolymers. The cross-linked ones, too, come under the same category. In addition, there are, of course, modifications besides the olefins; e.g., the ethylenediaminocetate copolymers. All of these are lumped under the general term polyolefins.

Heuser: That is my point. People are given data for polyolefin insulators and there is a difference in the different polyolefins, and I think you had some numbers for polyolefin in the manual.

Discussion (contd)

Burrowbridge: Possibly.

Perkins: Yes, the dielectric constant can vary over a fair limit, not too large, but over a reasonable limit simply because the density varies. You can manufacture polyolefins from roughly 0.8 density, or specific gravity, up to over unity. Of course, the dielectric constant of something like this essentially varies directly as the density, the number of atoms/cm^3, is a rough measure of the dielectric constant. Therefore, things like that can vary a fair amount and other characteristics can vary substantially.

Benden: I would like to clarify the noise comment I made. I am concerned not so much from an EMI standpoint, but from conducted noise, within the unit itself, modulation, and this kind of effect. I am divorcing this comment from catastrophic failure. That is the way I want to clarify it.

Burrowbridge: Thank you.

August: I would like to make a comment on that, too. As you may know, SRI does a fair amount of corona discharge work on aircraft where they charge up and want to get rid of it. This is primarily a noise problem.

But, sometimes I think we look at all these breakdown problems and decide that if we have a breakdown, this is it. We have had it. I am just wondering to what extent we can live with some of these breakdown problems, such as corona, for example, and let something deliberately corona. In some cases we may not get much noise from it. We may be able to deliberately induce corona in parts where the corona is not a problem and keep other parts from going into corona. Maybe this doesn't belong in a design manual, but I think this is something that we could talk about.

PRECEDING PAGE BLANK NOT FILMED.

N70-32305

The Influence of Gas Velocity on the Breakdown Potential of Argon, Helium, and Nitrogen

J. A. Gardner
Jet Propulsion Laboratory
California Institute of Technology
Pasadena, California

An experimental investigation was performed to determine the influence of gas velocity and pressure on the electrical breakdown potential of argon, helium, and nitrogen between parallel plate electrodes and with concentric electrodes. This type of information is useful for two reasons: (1) for starting or devices that depend on an electrical discharge such as an MHD or magnetoplasmadynamic arcs, and (2) for evaluating characteristics of electrical components or equipment which might be exposed or immersed in a gaseous flow field.

A photograph of the general apparatus used in these sets of experiments is provided in Fig. 1. A 6-ported glass test fixture with a pair of parallel electrodes enclosed inside was used for gas discharge containment and generation. The gas stream flowed from left to right. The positive pole is the top electrode and the negative pole is at the bottom.

A schematic representation of the details of the actual discharge region is shown in Fig. 2. The electrodes were constructed of copper and installed downstream of a lucite nozzle. They were 1-in. squares, 0.5-in. thick, and were separated by a distance of 0.5 in. The exit of the nozzle was 0.5-in. high and 2-in. wide. The gas entered the space between the electrodes at approximately room temperature.

The high-voltage d-c power supply, used to supply the potential to the electrodes to initiate breakdown, consisted of a primary controlled transformer, a full-wave rectifier, and two 4-μF capacitors for filtering.

The experimental procedure consisted of first setting the desired gas flow conditions, including velocity and pressure, and then increasing the output voltage of the

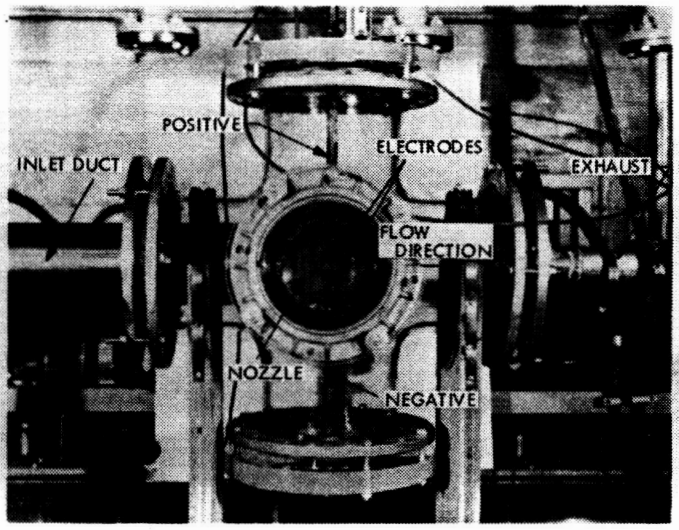

Fig. 1. Experimental apparatus

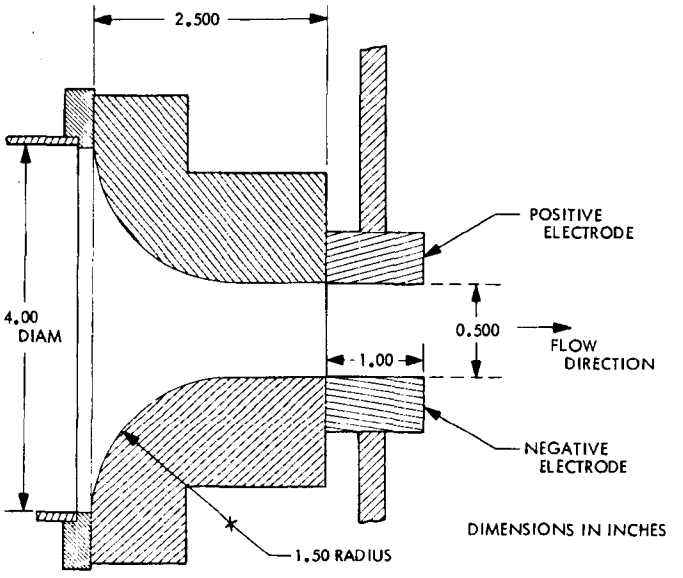

Fig. 2. Two-dimensional subsonic nozzle and parallel flat-plate electrode configuration

high-voltage d-c supply until the onset of breakdown was achieved or observed on the oscilloscope. The oscilloscope used a 10,000:1 precision voltage divider and the image was recorded on film.

Figure 3 shows some data taken to show the influence of velocity and pressure on the breakdown voltage for argon between the parallel electrodes. The data given are for three pressure ranges: 200 torr, 100 torr, and 50 torr. The 200-torr case, for example, shows a decrease in breakdown of approximately 3600 V. After the onset of a velocity, at ~100 ft/s, the breakdown potential drops to approximately 1800 V; corresponding situations exist for the other pressure regions.

Breakdown potentials for helium are a function of gas velocity, electrode spacing, and pressure. The results for He for constant electrode spacing are shown in Fig. 4. These results were obtained over gas velocity ranges of from 0 to 525 ft/s and at a pressure range of from 50 to 400 torr.

The breakdown potential for helium at all pressures tested was significantly below that for a stagnant gas, even for comparatively low velocities; furthermore, once this reduction occurred, an increase in the gas velocity had a smaller effect. In fact, after the initial decrease in breakdown potential had taken place, the potential breakdown point had a tendency to level off at roughly 50–80% below that measured for the stagnation conditions. A comparison of these results with the argon case is shown in Fig. 5 which illustrates the 100-mm case for argon in the upper region and helium in the lower region. Of course, the static case is what would be expected from the Paschen curves and the relative positions of the curves follow through with the effect of velocity. The argon data do remain at least within the ranges tested above the helium data at all times.

The nitrogen data, shown in Fig. 6, exhibited considerably more scatter. The very sudden decrease in the breakdown potential with the onset of a gas flow was not apparent as it was for the helium and argon.

There is, a slight reduction, perhaps 10% for the nitrogen, but it is not as large as that for the argon and helium.

Since the physical mechanism to describe the observed phenomenon of reduction of breakdown potential with a dynamic gas, i.e., for helium and argon, for example, is not yet known, the dependence of velocity, pressure, and gas species on the breakdown potential is also not very well understood.

We did some other testing in order to try to better understand this phenomenon. High-speed photographs were taken at the onset of breakdown realizing that the time scale of the breakdown phenomenon and the time scale for which these photographs would be taken would

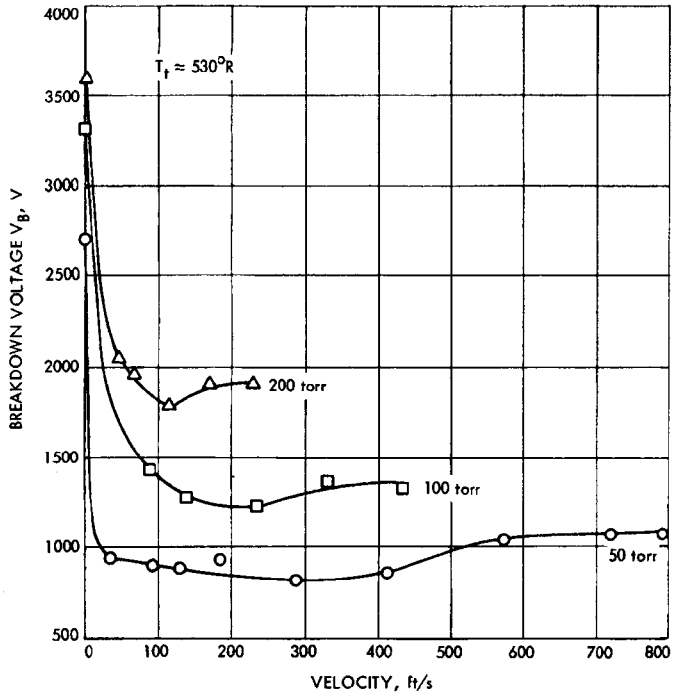

Fig. 3. Influence of velocity and pressure on breakdown potential for argon flow between parallel flat-plate electrodes

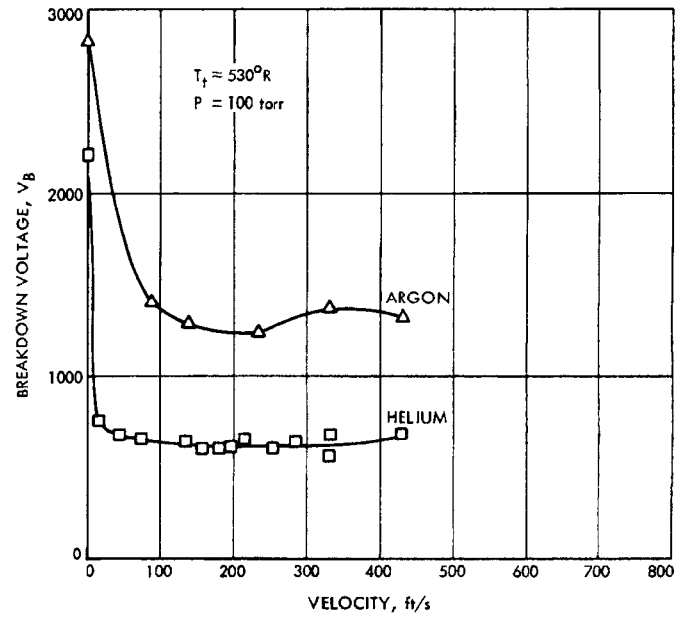

Fig. 5. A comparison between helium and argon at a pressure of 100 torr for flow between parallel flat-plate electrodes

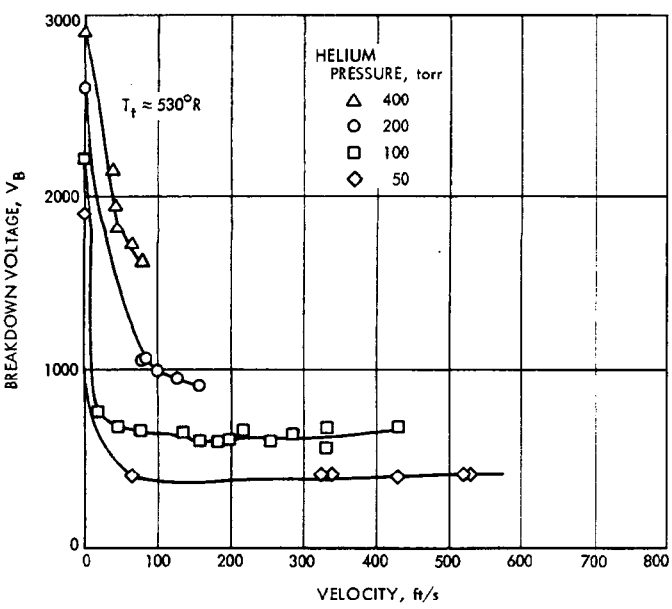

Fig. 4. Influence of velocity and pressure on breakdown potential for helium flow between parallel flat-plate electrodes

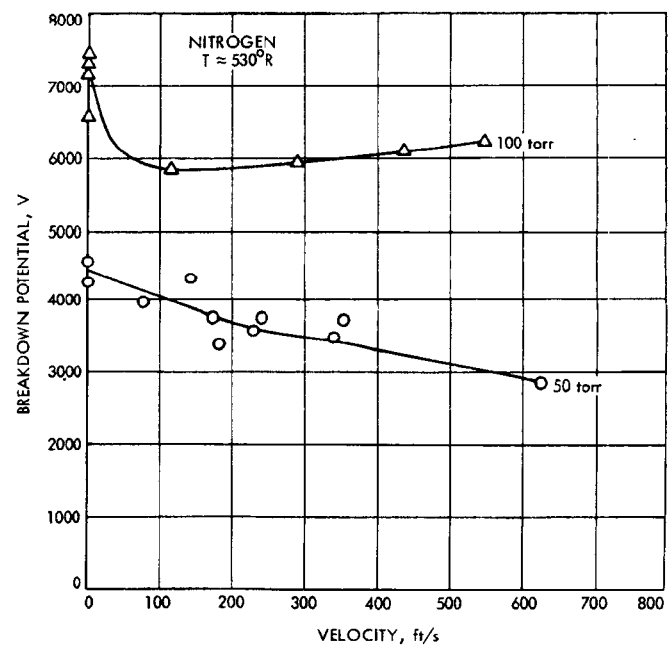

Fig. 6. Influence of velocity and pressure on the breakdown potential of nitrogen between parallel flat-plate electrodes

be considerably different. But Figure 7 shows what happens with the flow condition between the electrodes. The gas velocity in these pictures was calculated to be 127 ft/s. The velocity profile between the electrode region was measured with a pitot tube to determine that it was in fact uniform, which was the purpose of the convergent nozzle.

Frame 1 is the first that was taken on the high-speed film at 5500 frames/s where there is no visual glow between the electrode region. The second frame represents the first frame after the onset of visual image. From the indication of the second frame, you can see that the visual discharge appears roughly midway between the leading and the trailing edges of the electrodes. However, due to the frame speed, this does not necessarily represent the location of breakdown.

The velocity of the discharge column in the direction of the gas stream was calculated from the change in position of the discharge column; the discharge column changes between Frames 3 and 4. The velocity was determined to be roughly 115 ft/s. The calculations for the gas velocity from the flow parameters was determined to be 127 ft/s.

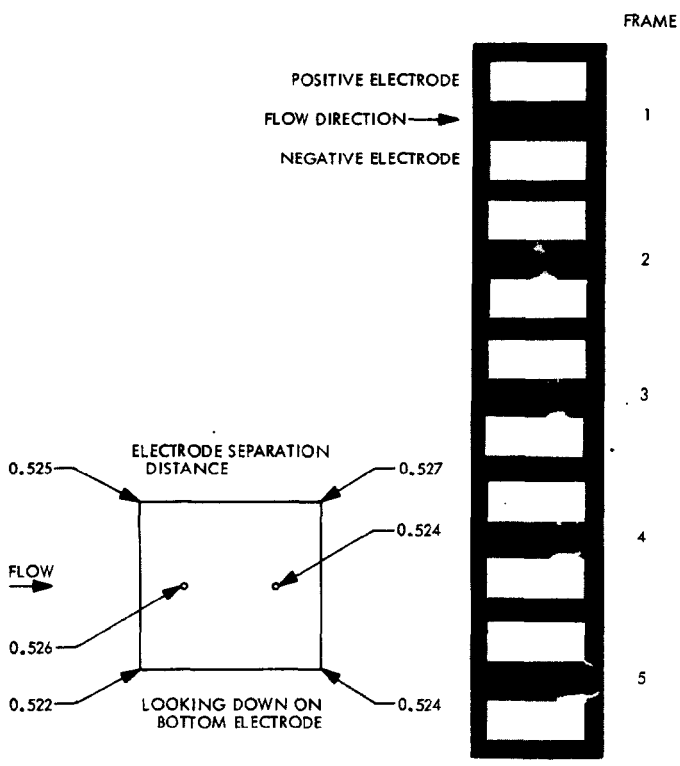

Fig. 7. High-speed photographs of the onset of breakdown and the movement of an argon plasma column in the flow direction: *electrode separation distances are also indicated*

If one makes the assumption that (1) the onset of breakdown occured between the first and second frames and the discharge moves downstream with the velocity of the gas, or the velocity at which you could calculate from the frame exposures, (2) that the illumination was sufficient to expose the film, and (3) that the discharge didn't actually occur at this point because of illumination problems, then you can calculate that the discharge column must have occurred roughly in the region of the first quarter of the electrode. Hence, it did not occur at the leading edge but somewhere between the leading edge and the first quarter electrode length downstream. Actual measurements of electrode spacing are also shown in Fig. 7.

Visual observations were made of the discharge through the 6-ported glass test fixture. The end on view, in other words, looking up into the flow region, did not make it appear that the discharge visually occurred along the edges of the electrode either. You might also notice that as the discharge proceeds downstream, the column is distorted from a vertical column and actually deforms into a U-shape, which can be seen in Frame 5.

For comparison of the measurements obtained with the parallel-plate electrodes, additional experiments were performed using an axisymmetric annular configuration similar to that used in a magnetoplasmadynamic arc. Both swirling and non-swirling flows were passed between the axisymmetric electrodes. The axisymmetric configuration is shown in Fig. 8. In this case, the anode is composed of copper. The tip of the cathode is thoriated tungsten. There is a lucite insulator placed between the positive and negative poles. The regions for radial and tangential injection to produce the swirl and nonswirl flow conditions are shown.

The axial nonswirling flow in the electrode region was accomplished by injecting the gas through a radial injector. The results for the axial flow with argon are shown in Fig. 9. This is a nonswirl case for pressure ranges of 200, 100, and 50 torr. This is an indication of the speed of sound using a temperature of 530°R. Again, a drop-off in the breakdown potential with an increase in velocity is apparent.

One thing must be remembered, the actual electrode separation distances are hard to determine at the site of

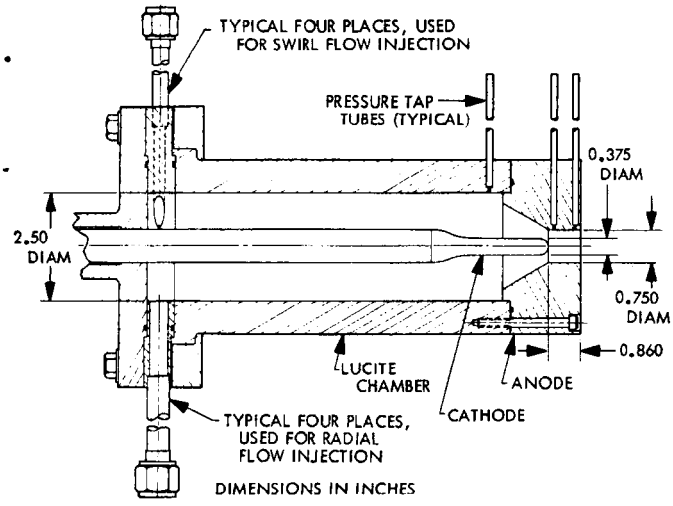

Fig. 8. Concentric electrode configuration

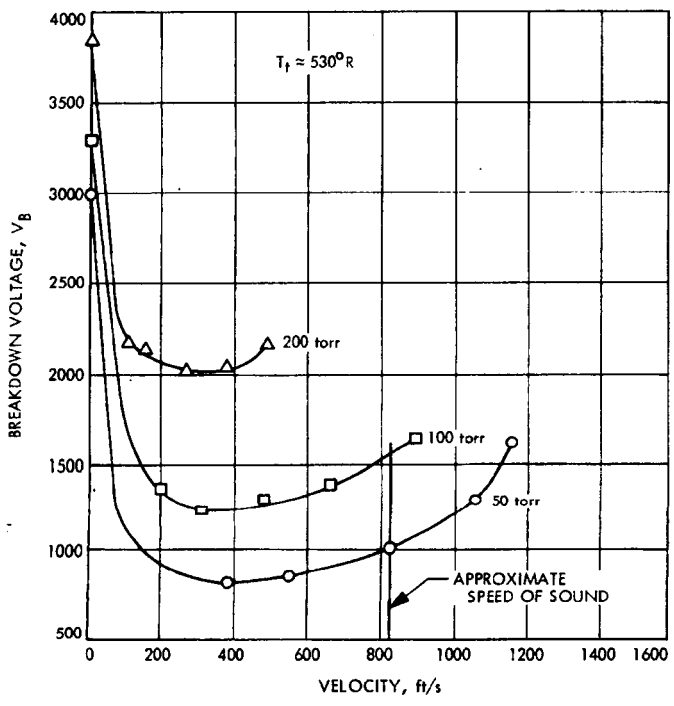

Fig. 9. Influence of velocity and pressure on breakdown potential for nonswirling argon flow between concentric electrodes

the actual discharge since (1) visual observations cannot be made from a cross-sectional point of view, and (2) the closest point of electrodes is unknown.

Experimental results with concentric electrodes using tangential injection, swirl case, with argon gas are shown

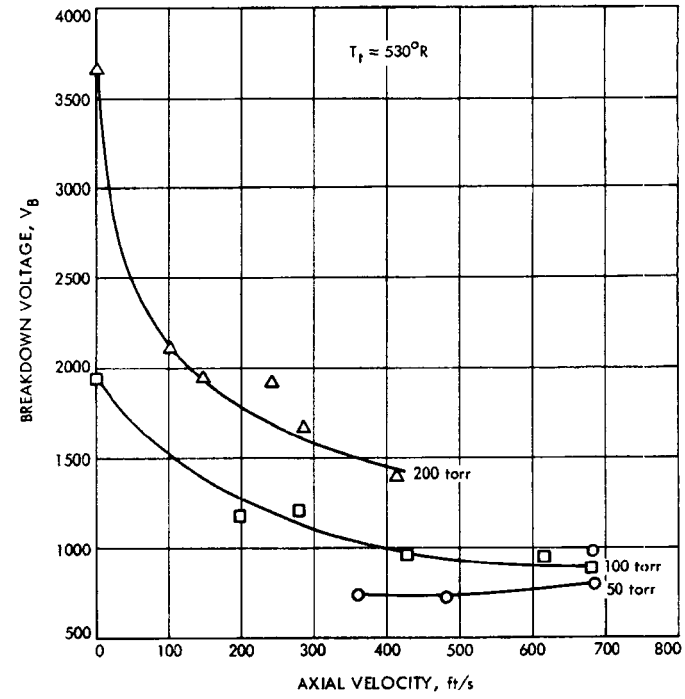

Fig. 10. Influence of velocity and pressure on breakdown potential for swirling argon flow between concentric electrodes

in Fig. 10. Curves for 200-, 100-, and 50-torr pressures are shown. Apparently, there was considerably more scatter with the swirling flow than with the nonswirling cases. The reason for this is not well understood.

In summary, a significant effect of gas velocity on the breakdown potential has been observed during experiments conducted with argon and helium flowing between parallel-plate electrodes. This reduction in breakdown potential was also observed with argon flowing between concentric electrodes as shown and observed with MPD arcs.

The nitrogen data did not indicate the sudden decrease in breakdown potential as with argon and helium.

For parallel-plate electrodes, the onset of breakdown appears to begin in the space between the electrode surfaces and not at the leading or the trailing edges of the electrodes.

After breakdown, the discharge column moves downstream to the trailing edge with the apparent velocity of the gas and deflects into a U-shaped configuration and remains attached to the trailing edges of the electrodes.

Discussion

Carruthers: In your experiments I was wondering whether you took into account the fact that at the constricted portion of the nozzle the pressure is lower when there is flow than when there is not flow for a given pressure in the upstream chamber. It appears that, at least in the nitrogen data, this pressure drop alone might account for the drop in voltage required to sustain the discharge, though it wouldn't explain the rare gas data.

I was wondering whether this pressure drop was taken into account and if you had ever plotted any of these curves against the actual pressure in the discharge region?

Gardner: Actually, that pressure that is plotted is the pressure within the discharge region. The pressure that is shown is the pressure that totally encloses the electrodes. The pressure drop due to the dynamic effect of the gas is extremely small. The pressure that we actually measure in the glass envelope of the electrodes is the same pressure that is the static pressure within the electrode region themselves. Further, we are talking about only lower regions of, say, 10 to several hundred feet per second. So certainly at the lower regions you don't expect that the dynamic effect of the gas really perturbs that pressure.

August: Would you care to comment on possible charging of the lucite due to flow over? This happens in a lot of systems and might give you higher stresses than you anticipated.

Gardner: This is a good point, and I think it is something we should look into.

He is referring to a possible charge development taking place on the lucite nozzle which is just upstream of the electrodes. We haven't done that. We have made some measurements, just recently. Another gentleman is working in this area, and he was concerned with preionization problems.

The effect you mentioned of having a buildup of charge may appear possible on the parallel-plate electrodes, but I don't think it would occur on the axisymmetric electrodes.

August: That happens all the time on metals in aircraft, for example, at subsonic speeds, just simply due to frictional flow.

Gardner: I don't deny, that there is a charge buildup on the electrodes. That would obviously take place on the concentric ones. But since there is no lucite nozzle, on the concentric electrodes, I don't think that phenomena would still be there. Where would the charge buildup take place if it is not, indeed, on the electrodes?

August: Well, in the axisymmetric case it probably wouldn't because the lucite is too far away, I think, to give you any added gap fields and not knowing details of your system, in each charge buildup, would not be increased in other than your high-voltage supply.

Gardner: Well, I am looking for a mechanism so I will take your comment with envy.

Bunker: I was wondering if you are using some kind of an ultraviolet source or illumination in the gap to provide free electrons to cause your voltage breakdown?

Gardner: No, we have no such sources and, as I mentioned, there is another gentleman that is looking for these kinds of things.

Bunker: Is there any corollary that could be drawn to this in the static case on dc. The voltage breakdown is much higher because the dielectric charges up and actually reduces the field gradient so you don't have a breakdown. Maybe this is what the gap is doing when it is static and when you are blowing it along. Maybe this effect may not take place and explain why it only breaks down at lower voltage. Just a comment.

N70-32306

Breakdown Studies for Possible Atmospheres on Mars and Venus

J. A. Gardner
Jet Propulsion Laboratory
California Institute of Technology
Pasadena, California

Experimental data of gaseous breakdown resulting from an applied electric field are presented for three component mixtures of gases which are in the range of individual concentrations believed to exist on the planets Mars and Venus. These experimental investigations were performed because of the future needs when scientific missions will be sent to the surfaces or to penetrate the atmospheres of these planets.

The important parameters in a study of this nature are the breakdown potential and the product of gas pressure and electrode separation distance. These parameters are sufficient to generate the well-known Paschen curves.

In this investigation, the applied voltages ranged from 0–7,000 V and the product of pressure and electrode separation ranged from 2–400 torr-cm.

Both the atmospheres of Mars and Venus are believed to contain mixtures of nitrogen, carbon dioxide and argon. In light of certain recent data the argon is somewhat questionable; however, the fractions of these various constituents are believed to be considerably different for the two planets.

The geometry for the electrical discharge tube used in these experiments is shown in Fig. 1. The tube consisted of two ultra-high purity copper, 1-in. diam disks, separated by roughly 5 cm, or 1.9 in. The disks are ultra-high purity copper mounted on 1/16-in. tungsten rods which pass through the glass envelope that surrounds the electrodes. One disk was the negative electrode and the other the positive electrode.

The two surfaces were flat within approximately 0.001 in. and were paralleled to within 0.001 in. as measured from the disk centers. The high-voltage d-c power supply was identical to that in the preceeding paper and was a primary controlled transformer used in conjunction with a full-wave rectifier and 4μF capacitors for filtering.

The concentrations of the constituents selected for the atmosphere of Mars consisted of 86.63% N_2, 11.21% CO_2, and 2.16% Ar. The mixture for the atmosphere of Venus consisted of 86% CO_2, 9% N_2, and 4% Ar. These figures reflect greater accuracies than present knowledge permits; the accuracies of these concentrations are not to imply that we understand the constituents of the

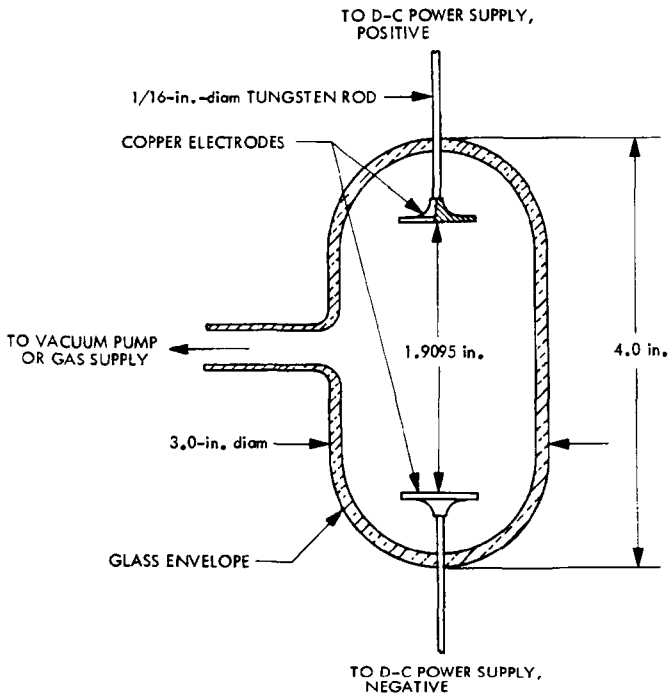

Fig. 1. Electrode configuration

planets, but represent the accuracies of the analysis that was made of the gas prior to these tests.

To perform the tests, the discharge tube was first evacuated to a minimum pressure of 10 microns and refilled with the test gas several times. After the final purge, the pressure in the test gas was selected and monitored by an aneroid pressure gauge. Once the desired pressure was obtained, the voltage of the d-c supply was increased until the onset of breakdown.

A typical voltage time curve for these experiments is shown in Fig. 2. This is a manually-controlled ramp and it was found that experimental results were fairly insensitive over the range in which the increase in voltage as a function of time could be controlled. Two breakdown points, which were superimposed on Polaroid film, are shown in Fig. 2.

The Paschen curves for the gas mixtures of Mars is shown in Fig. 3. In order to give you a reference, measurements were made of spectroscopically pure argon. The curve for ultra-high purity nitrogen is also shown. The curve for air was taken from some of Penning's* work. The bold line represents the atmosphere of Mars for these concentrations.

Data for the atmosphere of Venus are presented in Fig. 4 again with data for spectroscopically-pure argon, ultra-high purity nitrogen, and air. However, the data for air was not secured by use of copper electrodes; steel electrodes were used.

If you superimpose the two plots in Fig. 4, i.e., the atmosphere of Venus and the atmosphere of Mars, they appear quite similar, and do not deviate substantially from that of air. It is difficult to say what the true Paschen curve would be for the atmosphere of the planets because the overriding factor for making predictions is most likely highly dominated by the percentage and composition of the minor constituents.

To show some of this effect, Fig. 5 is presented; it shows some other work performed at the Jet Propulsion Laboratory related to binary gas mixtures and their breakdown potentials.

Figure 5 shows data that were taken for mixtures of nitrogen and helium. These data were taken because of the possibility of problems with helium leak testing of some spacecraft components. The lowest curve is for spectroscopically pure helium, the top curve represents extra-high purity nitrogen, and the curves in between represent various degrees of mixtures of 10% He and N_2, 50% He and N_2, and 90% He and N_2.

Note that Fig. 5 is on a log plot, but the difference between a 10% N_2 in a pure He environment, or, as stated here, 90% He and 10% N_2, causes you to lose approximately a third of the distance between the two pure cases. So a minor constituent can have an important effect. There is also the Penning effect to consider in which the actual breakdown potential is significantly below either one of the two gases.

Although the data for the planets appear similar to the nitrogen data, it should be noted that a slight amount of impurity of an unknown minor constituent could affect the actual breakdown potential considerably.

Therefore, in summary, until better information is available on the actual composition of the atmospheres of the near planets, the results shown here should be considered as only a possible case of what might be expected and you should design for cases that may be considerably different.

*Druyvesteyn, M. J., and Penning, F. M., "The Mechanism of Electrical Discharges in Gases at Low Pressure," *Rev. Mod. Phys.*, Vol. 12, p. 87, 1940.

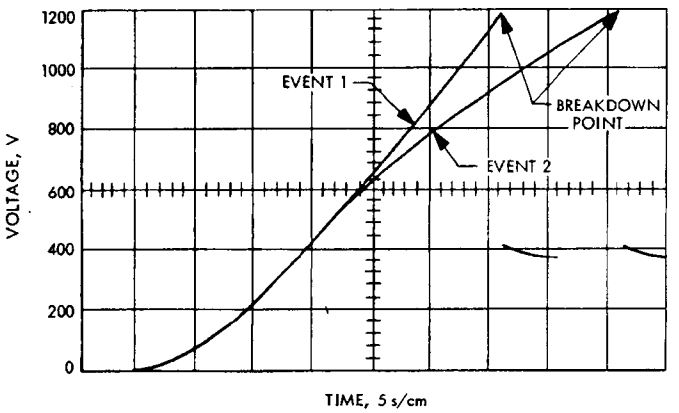

Fig. 2. Typical voltage-time curve with breakdown points indicated

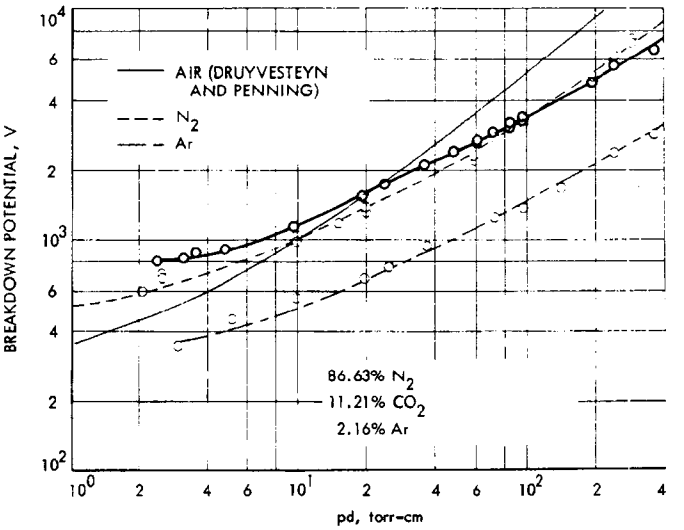

Fig. 3. DC potential breakdown curve for a possible Martian atmosphere

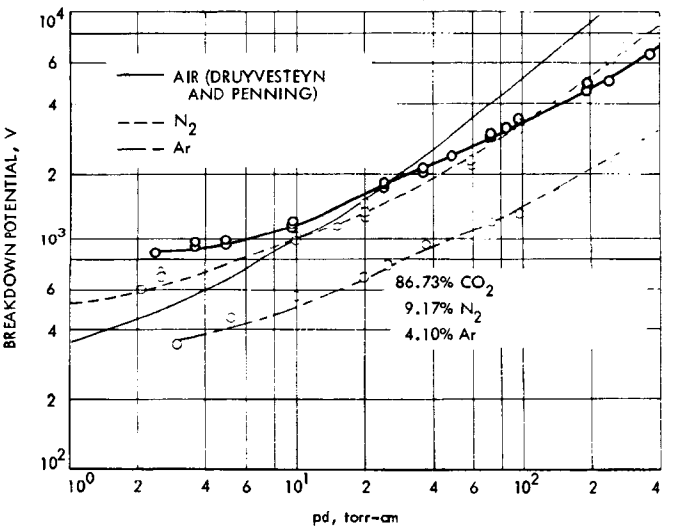

Fig. 4. DC potential breakdown curve for a possible Venusian atmosphere

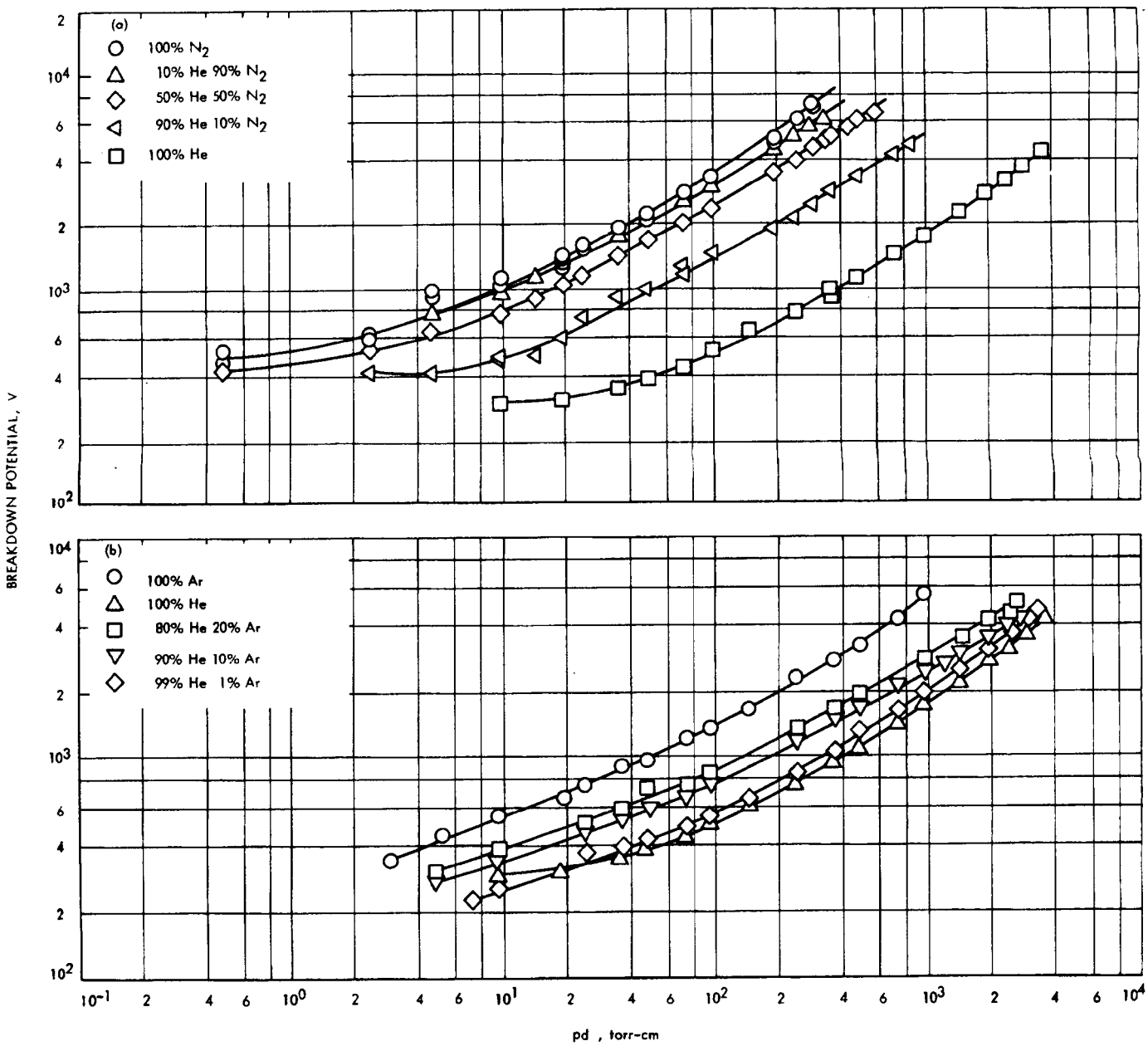

Fig. 5. DC potential breakdown curves for mixtures of nitrogen-helium and argon-helium showing the affect of gas mixtures in the absence of the Penning effect

Discussion

Ellison: Did you allow any particular amount of time to deabsorb the gases that have been in your cell?

You said you took it down to 10 microns for a while, and I didn't know whether you took any other measures to get the electrode surfaces clean of residual gas or not.

Gardner: Oh, yes. We would run a whole set of data first, just to clean the electrodes out. The system you saw was actually part of an ultra-high purity gas-mixing system constructed for other reasons, and so it was extremely tight. We could have evacuated down to about 10^{-8}.

Ellison: You did clean up that way, though?

Gardner: Yes.

Dunbar: On these tests, did you by chance take just a very small quantity of helium in your nitrogen to see if there was a definite effect that way?

Gardner: No. In fact, I could make a comment on that. Truly, if one wanted to do an adequate job of determining what the breakdown potentials would be for a planet, one should do a complete parametric study.

The problem is, I think, if you look at the data that are available for the near planets, that the numbers of gases that you get through this parametric study are very large and the concentrations change from day to day. So, I think if you wanted a job that would last forever, this would be a good one.

Actually, the way these compositions came about as a colleague of mine at the Jet Propulsion Laboratory, Dr. Robert Rhein, is doing work in combustion studies for determining the possibility of having some kind of motorized vehicle, or what have you, on one of the near planets, This study just happened to come about because he took the time to have samples, a Mars sample and a Venus sample, of atmospheres made up. Since I was doing some breakdown work in a different area but still dealing with mixtures, I went ahead and ran these samples. However. I had not made a parametric study for that reason.

Carruthers: A comment on the atmosphere of Mars. Since there is no oxygen in the atmosphere, the very intense Lyman-alpha radiation from the sun can penetrate the surface because there is a window in the CO_2 absorption at that wavelength. Therefore, if you operate electronic equipment during the daytime, you have to take into account this very strong UV flux which can release protoelectrons from metallic surfaces.

Gardner: I think one other point that should be brought out is, as we all know, the pressure ranges that are postulated for Mars, for example, I think the latest one is in the neighborhood of 8 mbar, and for the planet Venus it is in the order of 200 atm. So, don't extrapolate these curves too far.

Dunbar: Occasionally a person will make an electronic component for assembly. In one part of the component he may use a trace element of helium, say 10%, with nitrogen, and then he subcontracts another component in which argon is used and attaches it to the first one. Could you comment on any difficulties which might arise from such design practices?

Gardner: I think that certainly the effect of helium on any components that are run in atmospheric conditions will be certainly detrimental.

We had some problems, I guess it was with *Ranger VII*, in which the final stages of the transmitter were pressurized. They were backfilled with nitrogen. We had an apparent failure that occurred within the final stages of the transmitter. It was postulated that because of the backfilling done with helium for helium-leak checking, the residuals could still be there when we pressurized with nitrogen.

So, I think one should be careful when using helium. Helium, of course, is much worse than argon, from the standpoint of the Paschen curves. But, I am sure that there may be other gases or mixtures of gases that could be even worse.

PRECEDING PAGE BLANK NOT FILMED.

N70-22507

RF Voltage Breakdown in Coaxial Transmission Lines

R. Woo
Jet Propulsion Laboratory
California Institute of Technology
Pasadena, California

With increasing RF power requirements for space missions, RF voltage breakdown has received considerable attention. Of particular interest is the coaxial transmission line configuration, since it is often encountered in the RF system. When pressure is sufficiently low that the mean free path is longer than the inner-to-outer conductor separation distance d, multipacting can occur. Multipacting breakdown in the coaxial line geometry has been investigated previously (Refs. 1 and 2). As pressure is increased, the mean free path is shortened. When the mean free path becomes shorter than the separation distance, the principal electron production mechanism is no longer secondary electron emission, but ionization by electron collision. Breakdown that occurs under these conditions will be termed ionization breakdown. There have been studies of ionization breakdown in the coaxial line geometry, but these have generally been restricted in terms of experimental parameters and breakdown processes (Refs. 3–5). Moreover, these breakdown data have been displayed in rather complex and impractical schemes. We have obtained a large amount of breakdown data in air for the 50 Ω coaxial line geometry, and the data are summarized in a unified, concise, and practical plot.

Two experimental setups were used: (1) 10–150 MHz lumped circuit test set (Ref. 1), and (2) 150–800 MHz and 1700–2400 MHz transmission line test set (Ref. 2). Dry air was used and pressure was measured with a McLeod's gage. To minimize the effects of products of ionization of one breakdown measurement on subsequent breakdown measurements, the vacuum system was evacuated to less than 30 μ and new air introduced before each breakdown measurement. Reproducibility of the breakdown power readings was within $\pm 4\%$, and the accuracy of the readings was within $\pm 4\%$.

Figure 1 summarizes the data obtained; p is the pressure, f is the frequency of the applied field, and λ is the wavelength of the applied field. Multipacting breakdown data corresponding to the lower breakdown boundary and obtained previously have been included along

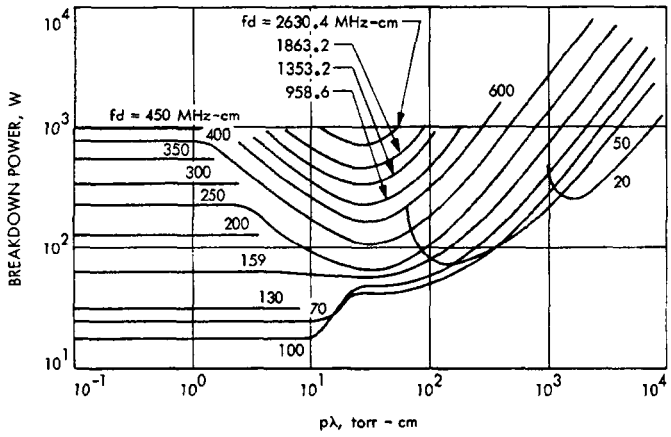

Fig. 1. Unified plot for RF voltage breakdown in 50-Ω coaxial transmission lines

with the ionization breakdown data. Brown and MacDonald (Ref. 6) showed that breakdown data can be represented by a three-dimensional surface using similarity parameters. Figure 1 essentially defines this surface. However, the similarity parameters of Fig. 1 are not the same as those used by Brown and MacDonald, but have been chosen for practical reasons. If a design engineer wishes to determine the breakdown behavior of a coaxial transmission line component at a particular frequency, he computes the corresponding *fd*. By referring to Fig. 1 he not only has breakdown power as a function of pressure, but also information on the effects of changing either frequency or line size.

The *fd*–*d*λ plane shown in Fig. 2 is very helpful in identifying the breakdown processes involved. The limits indicated are similar to those discussed by Brown and MacDonald (Refs. 6–8). Although they are in the form of lines they are meant to indicate transition rather than abrupt change. The mean free path limit separates the ionization and multipacting breakdown regions. For *fd* values less than the multipacting cutoff limit, multipacting will not occur.

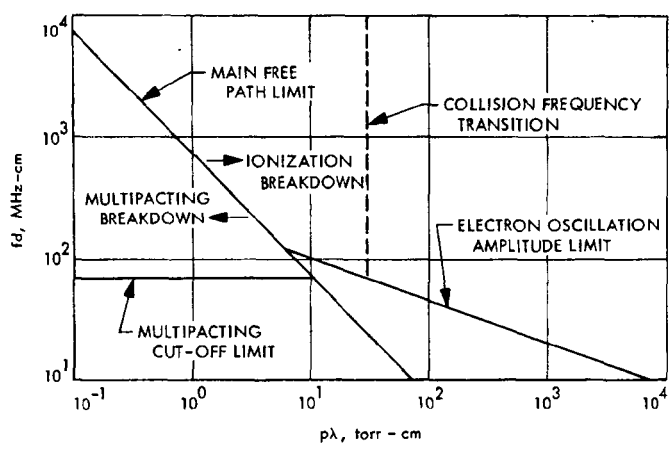

Fig. 2. The *fd*-*p*λ plane showing limits of breakdown processes

It is also convenient to use the similarity parameter *fd* in discussing the ionization breakdown region. When *fd* is greater than approximately 100 MHz-cm, frequency is sufficiently high and the separation distance sufficiently large that the electrons are not swept out of the discharge region. This is diffusion-controlled breakdown. The minimum breakdown power occurs at the collision frequency transition (pλ ~ 30 torr-cm). The electron neutral collision frequency and the applied frequency are approximately equal at the collision frequency transition, and energy transfer to the electrons from the field is maximum. When *fd* is less than 100 MHz-cm, the applied frequency is sufficiently low and the separation distance sufficiently short that the amplitude of oscillation of the electron cloud can approach and exceed the separation distance. The oscillation amplitude limit corresponds to the condition for which the amplitude of oscillation of the electron cloud is equal to the separation distance. At this limit, electrons are lost to the conductor surfaces, and the power required for breakdown rises rapidly. This behavior is illustrated in Fig. 1 for *fd* values of 50 and 20 MHz-cm. In the case of *fd* = 20 MHz-cm, another minimum is observed if pressure is further decreased. This additional minimum is present for smaller values of *fd* as well. This region has been studied by Gill and von Engel (Ref. 9) who attribute the additional minimum to the ions.

The scaling correspondence for ionization breakdown was checked between various sets of data. Frequency was changed as much as seven times. Scaling correspondence was within reproducibility of the data except for the region around *fd* = 100 MHz-cm between *p*λ values of 10 and 100 torr-cm. In this region the spread in the data was as much as 30 W and breakdown power increased with a decrease in separation distance when *fd* was held constant. This is to be expected since as discussed above this is a region of several transitions and breakdown is affected by surface conditions.

The minimum power-handling capability is of particular interest. Shown in Fig. 3 is breakdown power as a function of *fd* along the collision frequency transition. This gives the minima of the diffusion-controlled break-

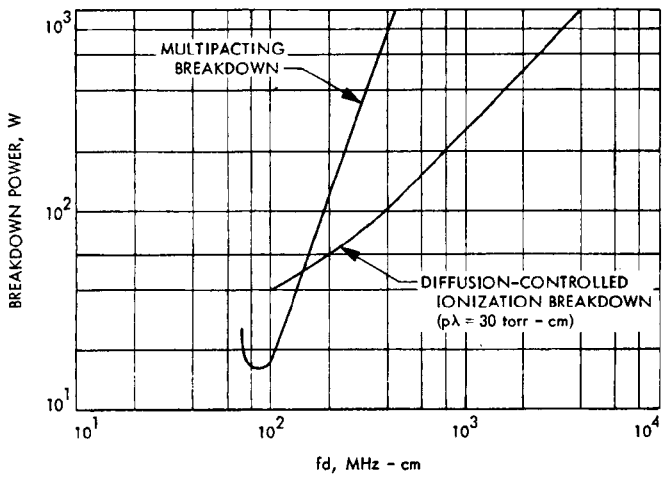

Fig. 3. Minimum power-handling capability in terms of *fd*

down curves. The multipacting data are also included for comparison. When *fd* is less than 145 MHz-cm, the ionization breakdown power level is higher than the multipacting breakdown power level; the reverse is true when *fd* is greater than 145 MHz-cm.

It should be emphasized that the data of Fig. 1 correspond to a perfectly matched transmission line. If mismatches in the line exist, the breakdown power level must be correspondingly derated. The scheme of data presentation in Fig. 1 can be used for configurations other than the 50 Ω coaxial line. Similar curves can also be obtained for gases other than air.

I should like to express my gratitude to G. Voyles of the Jet Propulsion Laboratory for his efforts in obtaining the experimental data.

Discussion

Woo: I just remembered that there is an important point I forgot to make. With reference to the curves that I showed you for RF, you can also see what happens as you gradually decrease frequency as you go from microwave into the audio regions, because you can extend it.

Furthermore, you can extrapolate on the high pressure side and come up with curves good at atmospheric pressures for the coaxial transmission line geometry. We have done that.

August: I think that was very good, and the information is presented in, I think, a rather useful way for design engineers. The only point I would like to comment on is, and this is not a criticism, but I think you have to emphasize other things besides just plain mismatch.

First off, there are essentially universal curves for computing what the breakdown levels are from which you basically get your design curves, so that in cases where you run into odd geometries at coaxial connectors or at windows or other things, I think you have to get off these things and go to the universal curves from which you derive these.

However, I am glad you emphasized the aspect of mismatch. One thing you have to worry about besides mismatch is that you can essentially derate those curves by 6 dB and double the field at 100% mismatch. This will establish a minimum level. This is fine except perhaps where you are feeding through a transmitter, where you have very high reactive fields which are in excess of double the level you would assume on the transmission line from power transmission aspects. This also applies to irises or other obstructions where you have high reactive fields, which you can't get by, let's say, by doubling the assumed voltage level on the transmission line. In those cases you have to get off these things and go back to the universal curves.

I guess you assumed either copper or aluminum for establishing your multipacting curves and variation with respect to the ionization curves. This would usually be true for most things so that these curves are usable.

Again, in design manuals I think you need to emphasize the point that if you get off these things, you better be careful, because you can shift the multipacting level up and down in relation to the minimum of ionization.

One further thing that I think is sometimes ignored in putting these things together in systems is that the ionization levels and also the multipacting levels are affected by stray magnetic fields that you may get from other components, so that if you have these close to your transmission lines you better do something else.

Woo: Those are good comments. You were talking about irises and things like that. This is basically for the coaxial transmission line geometry. In relation to space missions, most of the lines are very well matched, so this study applies to those conditions.

August: The important thing there is that I think we have usually found that our problems tend to be right at the window feed through, from whatever your transmission line transmitter is in a coaxial line or in a wave guide system, because then you have the reactive field. Even if you are well matched, you always have reactive fields.

There again, you perhaps have to take the diffusion losses to, let's say, supports for the coaxial line or for the wave guide, whatever it may be.

Woo: This transmission line is just one part of the whole system.

Young: On your coaxial transmission lines, have you performed any shielding effect tests or RF leakage tests at sea level and at the

Discussion (contd)

critical air pressure, for comparative purposes? If so, what were your observations?

Woo: Are you talking about the microwave transmission line system setup?

Young: I am more interested in the typical coaxial transmission lines.

Woo: I see. Well, the lines are terminated and there is no leakage in the system.

Are you asking if when you hook up the transmission line components is there any leakage?

Young: You would normally have some leakage.

Woo: I see. No, we didn't measure that. I don't think there was much leakage because it was a pretty tight system. Are you asking us because of safety hazards or –

Young: Suppose you have standing waves, for example, on lines have been known to cause certain voltage breakdown problems. In a number of papers that have been presented, there have been remarks of a sudden increase in the VSWR under certain conditions. I believe this is probably brought about by a change in the characteristic impedance of the line. You are suddenly no longer terminated in the characteristic impedance in the line; therefore, you get an increase in the VSWR which can cause breakdown.

Woo: Well, we just tested for the initiating conditions. As soon as it breaks down we turn it off. When the breakdown does occur, the power is reflected; we have a circulator and it dumps the power into a dummy load.

Young: I guess your tests are not typical shielding effectiveness tests.

Woo: No, I guess not.

August: One more comment about the multipacting breakdown. We put out these curves and we do this design information mostly because we are concerned that if we do get a breakdown it might ruin the characteristics of the system. I think it is important to point out that under many conditions, multipacting is not a really significant parameter in that you can allow a system to multipact and you may lose a little power, assuming that you have outgassed it and taken care of all the transient problems that develop, and you can allow a system to multipact, so that the multipacting limits that you show are merely for onset and not necessarily where the system is being damaged particularly by the multipacting.

References

1. Woo, R., "Multipacting Discharges Between Coaxial Electrodes," *J. Appl. Phys.*, Vol. 39, pp. 1528–1533, February 1968.
2. Woo, R., "Multipacting Breakdown in Coaxial Transmission Lines," *Proc. IEEE (Letters)*, Vol. 56, pp. 776–777, April 1968.
3. Herlin, M. A., and Brown, S. C., "Electrical Breakdown of a Gas Between Coaxial Cylinders at Microwave Frequencies," *Phys. Rev.*, Vol. 74, pp. 910–913, October 1948.
4. Gould, L., *Handbook on Breakdown of Air in Waveguide Systems*, Microwave Associates, Burlington, Mass., April 1956.
5. Francis, G., *Ionization Phenomena in Gases*, Butterworth's Scientific Publications, London, 1960.
6. Brown, S. C., and MacDonald, A. D., "Limits for the Diffusion Theory of High Frequency Gas Discharge Breakdown," *Phys. Rev.*, Vol. 76, pp. 1629–1633, December 1949.
7. MacDonald, A. D., *Microwave Breakdown in Gases*, John Wiley and Sons, New York, 1966.
8. Brown, S. C., *Handbuch der Physik*, Vol. 22, pp. 531–575. Edited by S. Flugge, Springer-Verlag, Berlin, 1956.
9. Gill, E. W. B., and von Engel, A., "Starting Potentials of Electrodeless Discharges," *Proc. Roy. Soc. London*, A192, pp. 107–124, April 1949.

N70-32308

Reduction of Gas-Discharge Breakdown Thresholds in the Ionosphere Due to Multipacting

G. August and J. B. Chown
Stanford Research Institute
Stanford University
Stanford, California

The subject of our presentation is multipacting, particularly those areas which present serious problems. We have already had several discussions of multipacting.

We ran into multipactor problems several years ago while running tests on high-power values, in which we experienced arcs which were evidently caused by multipacting.

As Mr. Woo suggested, the Jet Propulsion Laboratory had experienced problems in the *Ranger* program; the Hughes Aircraft Company also encountered failure in components which was attributed to multipacting.

Yesterday, I discussed a *Nike-Cajun* flight in which multipactor presented evident anomalous breakdown which evidently appeared to be gas breakdown.

Up until several years ago, people weren't too much worried about multipactor problems. For example, Hughes had made some measurements that indicated that multipactor was unlikely to cause much power absorption in the systems in which it occurred. Usually, on antennas and other structures where you multipact, the change in VSWR of the system is small enough that not too much concern is expressed.

It was generally felt that multipactor was much more of a nuisance problem than a hazard. In general, I agree with this thesis except that I think you have to state that it applies only to steady-state multipactor conditions and probably at relatively low frequencies, i.e., under several hundred megahertz.

My feeling is that particularly at the beginning of multipacting, which I will call the transient, and even at relatively low frequencies, you can experience severe problem in power-absorption, VSWR, or gas discharge.

When you get up to very high frequencies, even the long-term steady-state multipacting may result in substantial power absorption.

I have been asked to define multipacting and to briefly explain it. Rather than get involved with theory, we shall limit this presentation to the difficulties we have

experienced and to our test results. Furthermore, I will try to give you a capsule summary of multipacting and present a reasonably coherent picture of what we are exploring.

A multipactor discharge is basically a resonance phenomenon, as shown in Fig. 1. If you introduce an electron onto an RF field and go through the equations, you will find it will make an excursion as described in Fig. 1.

If two electrodes are spaced in a parallel electrode configuration, for example, separated by distance d, then an electron will just go up to one, and a half cycle later it will come back to the next one.

If this gap is shortened incrementally, then the electrons will impact on the electrodes. Given the appropriate electric field, you can make the impact energy sufficiently large so that it will kick off a secondary electron, which will then enter the discharge and sustain it. Basically, then, it is an electron resonance.

The discharge is sustained by secondary emission. This is in contrast to the usual gas breakdown where the electrons cause ionization of gas atoms, which then sustain the discharge. Ionization also occurs here, but this is basically an electron discharge. The electron energies are sufficient to ionize most gas atoms, so you will get some positive ions trapped in the discharge, but they are a secondary aspect of the discharge.

Going through the equations of the simple theory, one finds a breakdown voltage given by the equation in Fig. 1.

Now, this is very simple theory. It is necessary to incorporate the initial energy of the secondary electron

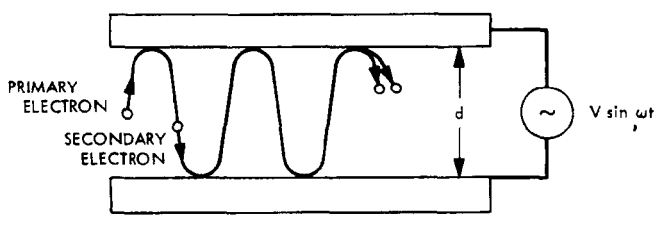

APPROXIMATE OPERATING CONDITION:

$$d = 2 \times \text{rf EXCURSION} = 2\,\frac{eE}{m\omega^2}$$

$$V = Ed = 2\pi^2\,\frac{m}{e}\,(fd)^2$$

Fig. 1. Multipactor discharge: electron resonance in an RF field, with discharge sustained by secondary emission

as it comes off the surface. Then, the starting phase must be incorporated, and you find that the actual operating breakdown voltage is given by about a factor of π lower, so this is an over-estimate by about a factor of π.

Since we are operating with secondary emission, we must be concerned about surface conditions, and the surface conditions obviously depend on contaminants; i.e., how you treated the surface. Furthermore, one great difficulty with multipacting is these things change with time, because you are making gas ions. Some of them get impacted on the surface and they change surface chemistry.

These are difficult problems. All we know is that multipactor surfaces change with time. Eventually, you see little heat-ring surface discolorations. Table 1 shows some of the characteristics of a multipactor discharge.

Table 1. Multipactor discharge characteristics

Cause	Result
Energy source	An RF electric field
Electron source	Secondary emission
Operating conditions	$mfp > d$ $\tau = N/f$ $\gamma > 1$ ($u > 20$ to 200)
Discharge state	Electron cloud, $n < n_c$
Starting conditions	At fd = 70–150 MHz-cm Vb = 30–50 V rms
Pressure dependence	Vb independent, n is dependent on ions, collisions

One of the essentials is that the mean free path of the electrons must be larger than interelectrode spacing. The secondary emission is greater than unity. Typical starting conditions are listed at the bottom. Generally, in this range you find that the starting voltage is fairly flat and is about 30 to 50 V RMS peak, as shown in Fig. 2.

Contrast this to 250 to 350 V minimum dc breakdown voltage for dc discharges at the minimum of the Paschen curve.

The discharge starting voltage is pressure independent; however, the electron density in the discharge depends on pressure, because the ionization is pressure dependent. These ions are trapped and partially neutralize the space charge cloud.

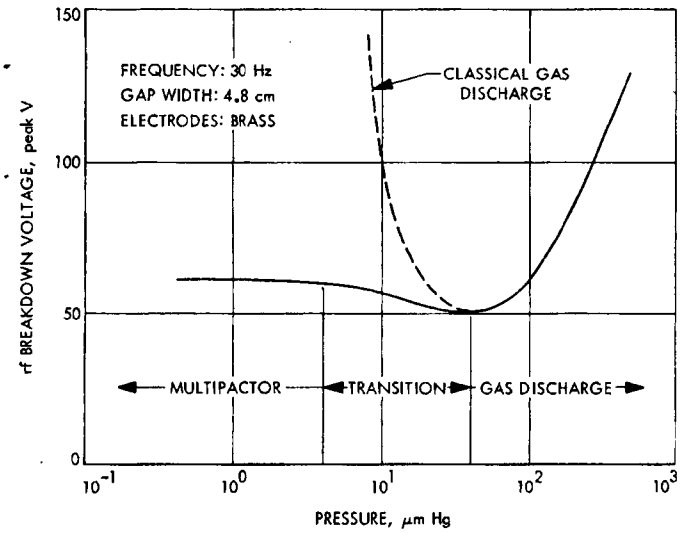

Fig. 2. Peak volts and RF breakdown voltage vs pressure

In Fig. 2, we have RF breakdown voltage and peak volts versus pressure for a fixed spacing and frequency. This is fundamental mode operation. Now, I won't go into too much detail because Mr. Woo has already commented on the subject this morning.

Incidentally, with reference to Fig. 1, I should mention that it is possible to get multipactor operation between parallel electrodes or coaxial electrodes in higher-order modes in which the electron basically crosses the gap in an odd number of half cycles (where odd is one, three, five, and so on). Fundamental mode operation is shown in Fig. 1.

In Fig. 2, the important thing is that the level at which multipacting begins can shift up or down depending on the gap, frequency, and the material. Thus, this is just a sort of arbitrary level for this particular system. The multipactor level may be lower, or it may be much higher.

The foregoing discussion summarized multipacting in general. Now, I would like to discuss some of the initial characteristics of multipacting since these present the most problems. In particular, let us consider the electron densities that you get in a discharge, and the heating that can result.

Data taken some time ago are shown in Fig. 3. Multipacting occurs between parallel elecrodes, which have holes drilled through one electrode, behind which is a

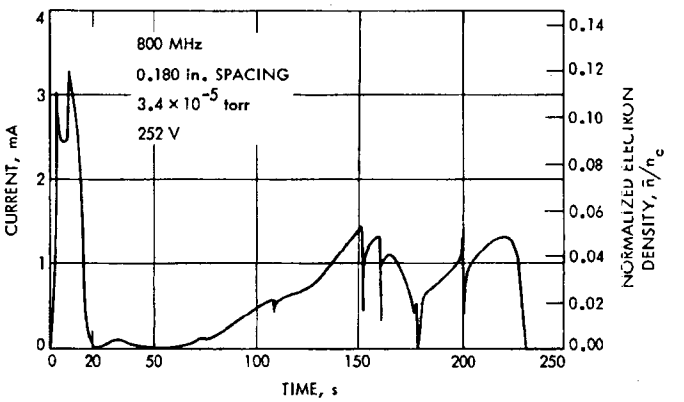

Fig. 3. Electron density variation with time at 800 MHz

Faraday collector to sample the electron current and infer the electron density.

This particular frequency is fairly high; operation is actually in first higher mode operation, and were somewhat overvolted. The starting voltage was probably ~ 140 V. The data were plotted both in direct current collected in the cup, and on the right side of Fig. 3, in a normalized electron density given by the average electron density divided by the critical density. Critical density is the density at which the plasma frequency is equal to the operating frequency. It is not expected that a critical density greater than unity would be realized.

The critical density for this particular frequency is 8×10^9 electrons/cm^3 so that peak current density values are roughly 10^9. The significant features are that high-electron densities are achieved and that they persist for relatively long periods of time; e.g., well over 2 min. Some of the fluctuations are due to the fact that the discharge wanders back and forth over the collecting electrodes. This is not particularly significant.

The data in Fig. 4 were taken at a lower frequency. Again, the data were plotted against current and normalized electron density.

In this case, the critical density, was 6.4×10^8. We were getting roughly one-eighth of that, that is, about 8×10^7 electrons at the peak, Fig. 4, and then it drops off to $\sim 6.5 \times 10^6$.

The significant information in Figs. 3 and 4 indicate that you can get electron densities within a range of from 10^6 to 10^9, and that they persist for long periods of time.

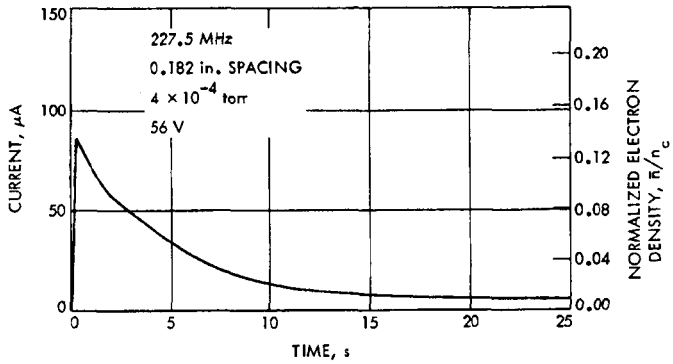

Fig. 4. Electron density variation with time at 227.5 MHz

We also made power loss measurements. From our strip transmission line, we could find how much power was being dissipated in the multipactor discharge. We found that for the case of Fig. 3, 1 mA gave power dissipation of about 1.3 W/cm^2. As a comparison, the same transmission line, if it were not multipacting, would be dissipating about 1/65 of that in ohmic losses on the surfaces. A copper transmission line was used. Multipacting, in that instance, was providing a heat load about 65 times larger than the ohmic losses.

As shown in Fig. 4, at a lower frequency we had a much lower current; ~100 μA peak compared to 1 mA in Fig. 3. Thus, we were getting only about one-tenth of the heating in that case.

The point is, as you drop down in frequency you tend to get smaller and smaller heating loads until they aren't much larger than the ohmic losses. However, at very high frequencies you can dissipate appreciable heat in the multipactor discharge. Naturally, the heat can provide substantial outgassing and other problems.

Now, I would like to switch to an application we made in which we ran into difficulties with multipacting.

We were provided an antenna, shown in Fig. 5, to test for gas-discharge breakdown. This happens to be a log periodic antenna, actually two cross-log periodic arrays. The elements were deployed from a channel so that the elements protrude from the channel. We call the two arrays A and B arrays. We found, to our dismay, that it multipacted; we hadn't expected it to multipact.

Figure 6 is a head-on view of one of the elements of the array. The view looks down on the cylindrical rod next to the top. The channel can be seen with some base blocks and feed lines and lines going to other parts of the array. Some elements of the array are at negative RF voltages while some are at positive. The shell is at zero voltage.

Now, I would like to digress for a moment and state that multipacting theory is still in the development stage. We know multipacting can occur between parallel electrodes and in coaxial lines. The geometry is such that the electrons move along the field lines.

We don't generally expect multipacting to occur in places where the field lines are fringing because then an electron need not follow a field line, so that it may not get into a resonance condition. Nevertheless, it has been found that multipacting sometimes occurs in these geometries. For example, in a re-entrant coaxial cavity, it was found that multipacting was occurring from the sides of the re-entrant post to the on the bottom, in the fringing field area. We found for the quadraloop antenna that we also experienced multipacting where we had fringing fields.

Figure 7 shows what the antenna looked like at the base; this will help to explain why we didn't feel it should multipact. A brass base block where our feed line came in was at positive RF voltage. This channel wall, is at ground potential. Field lines will go from the brass to the channel, but this gap is small. It is partially covered with dielectric fiber glass. We didn't feel there was too much chance of multipacting occurring in this area. Field lines coming out from the brass base block obviously go through the fiber glass to the channel and geometry did not look right for multipacting, except possibly in the 0.030 gap.

The spacing from the fiber glass to the channel wall was 0.25 in. We were testing the antenna at 160 MHz, about midrange, so that the frequency times spacing product was 100, which you might expect to result in some multipacting.

Another view of the base of this element is shown in Fig. 8. We had a fiber glass spacer to keep the positive RF voltage away from the channel ground enabling the feed to come in through the side.

Since we did experience multipacting, we immediately suspected the open area between the brass and the channel, shown in Fig. 7. We proceeded to pot this area, just using RTV, since this wasn't going to be potted for a space flight, but for a laboratory test. Therefore,

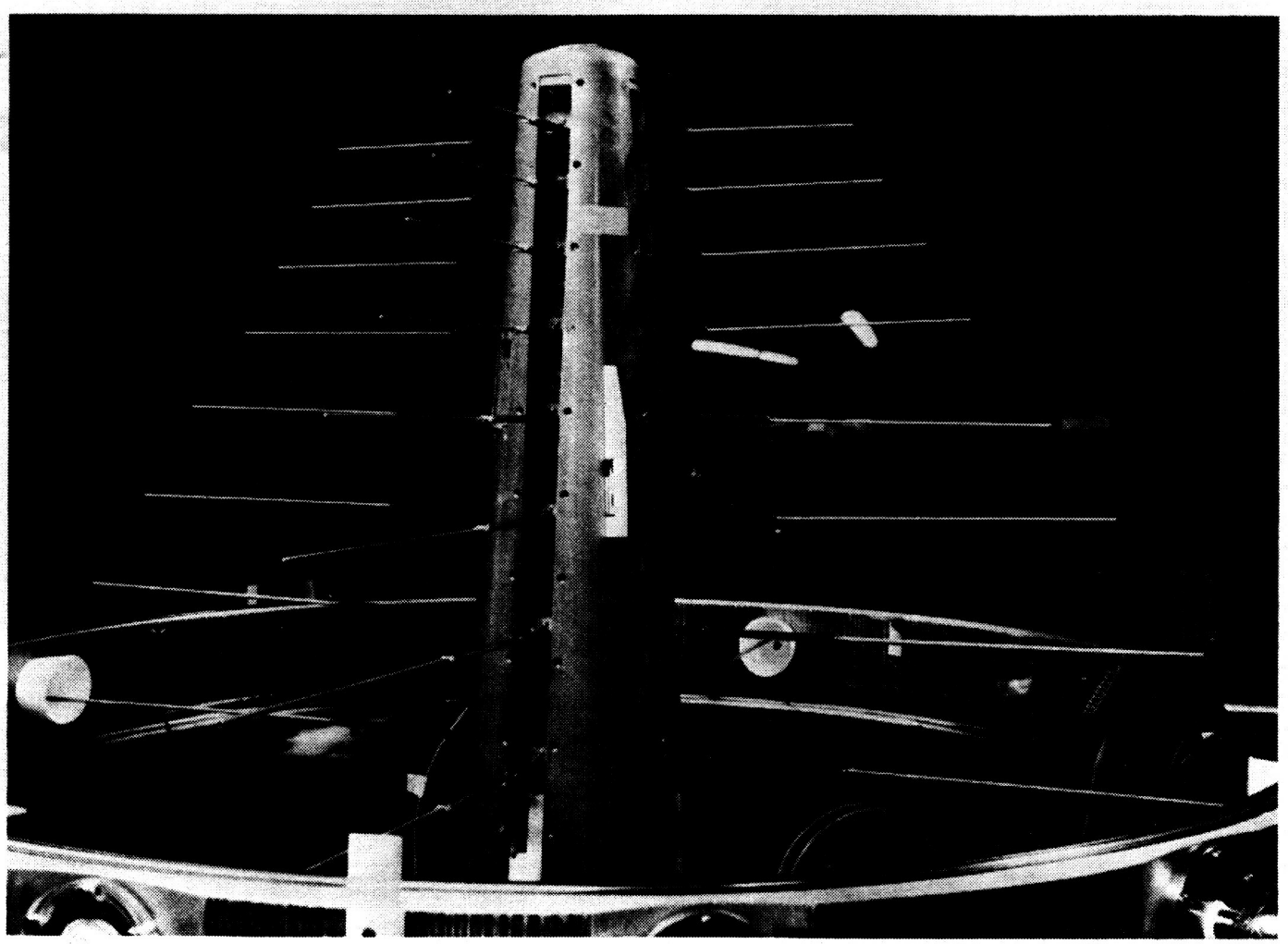

Fig. 5. Deployable log periodic antenna

we just potted enough to completely cover the area suspected to be multipacting. We potted up to the top of the brass block in Fig. 8.

It was found that we did not suppress multipacting. In fact, potting made it worse. This is one of the problems I would like to drive home to those who talk about potting open structure.

Generally, most dielectrics, i.e., most potting materials, will multipact at a lower voltage than bare metal. So, if you have large parallel surfaces exposed to RF fields, if they are potted, you may experience more problems than if they were metal.

Some of the possible multipactor conditions are listed in Table 2. One such condition is from one base block; i.e., the base block of one element over to the channel wall with this 0.25-in. spacing. We computed the voltage required to start it and, assuming that this voltage was on a matched 50-Ω strip transmission line, we were able to judge the amount of required power.

Obviously, if it were completely mismatched, it would take only a quarter of that power to start it. This matched power is fed to one element. It is a little difficult to determine the power for the entire log periodic array, but it is probably from two to six times that fed to one element.

Thus, you can generally estimate multipacting to occur at someplace in this range between one-half and six times the matched power listed.

The channel wall to channel wall distance also is listed in Table 2. The reason for this will be explained later.

Table 2. Possible multipactor conditions

BASE BLOCK TO CHANNEL WALL: d = 0.25 in., fd = 102 MHz-cm V_o = 30 V rms P matched = 18 W
CHANNEL WALL TO CHANNEL WALL: d = 1.25 in., fd = 510 MHz-cm (2nd mode) V_o = 200 V rms P matched = 800 W
BASE BLOCK TO BASE BLOCK: d AVERAGE = 2.5 in., fd = 1020 MHz-cm (4th mode) V_o = 350 V rms V element = 175 V P matched = 610 W

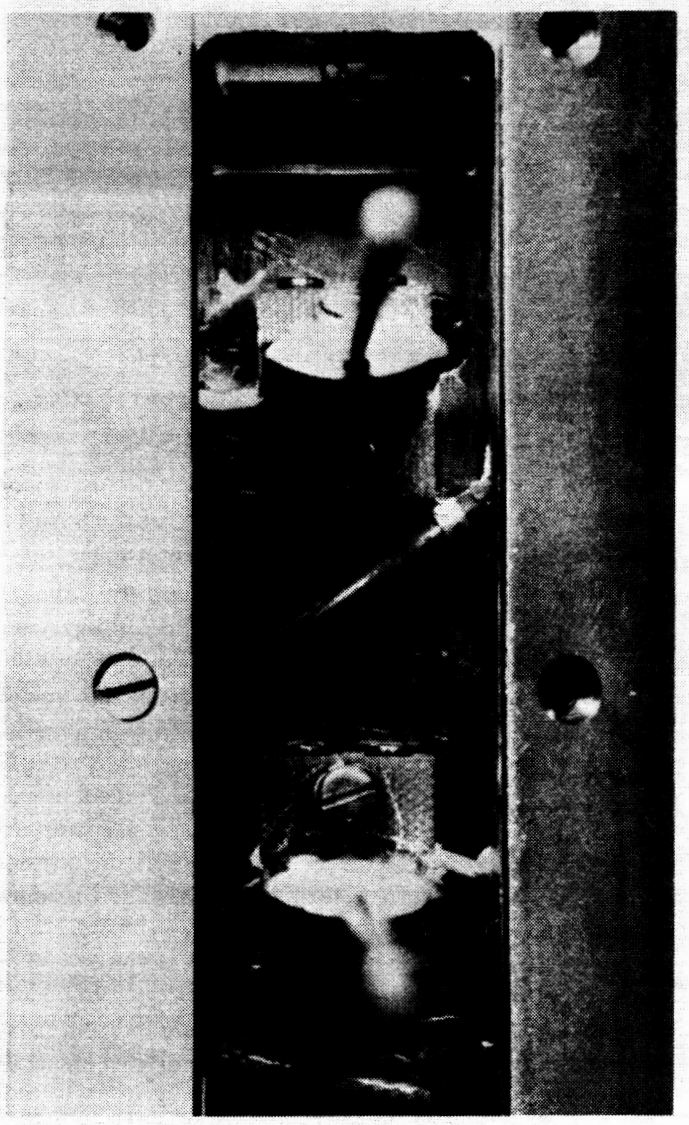

Fig. 6. Detail of feed and mounting block

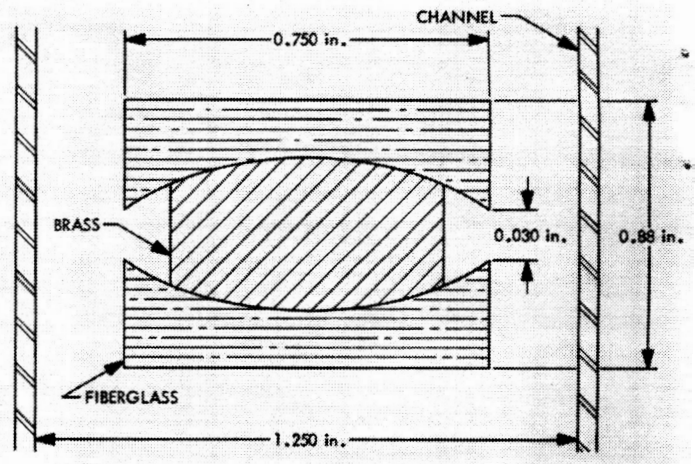

Fig. 7. Antenna base detail, plan view

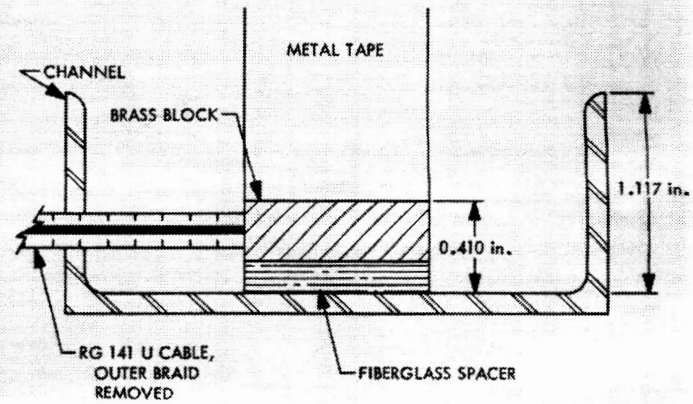

Fig. 8. Antenna base detail, side view

For this gap the Table lists the approximate level at which one might expect multipacting.

Normally, multipacting occurs between two electrodes; one at one RF voltage and one at the other RF voltage.

Both channel walls should be at a uniform RF voltage, so there is no reason to expect multipacting between channel walls. Nevertheless, we list this spacing in case multipacting did occur.

A third possible multipacting path is down the channel because adjacent elements; one is positive RF voltage, and the other is negative RF voltage. The spacing is variable, naturally, because it occurs in a log periodic array. We took an average spacing and judged that multipacting might occur in this mode.

Now, potting should have entirely eliminated multipacting of the first kind. Since multipacting continued

to occur after potting, the third kind of multipacting was occurring.

Later, we tested only a single monopole element where we couldn't possibly have adjacent elements to give us multipacting; we found we were still getting multipacting at rather high power levels, 400 to 500 W.

Evidently, we had, at least in part, contributing to the multipacting some peculiar mode which resulted in multipacting from channel wall to channel wall, at least initially. Probably, some of other factors were also operative in our long periodic array.

Now, let us turn to the breakdown data obtained for the log periodic array. In one of the arrays tested, we were interested in establishing the gas discharge line, as plotted in Fig. 9. We also checked the array at very low pressures; the power source was limited to a 200-W source which we drove on occasion up to 600 W.

We expected, by extrapolating, to get something like 4-kW power-handling capability at 10^{-3} torr, which is about 300 kft. We then proceeded to make low-pressure tests below 10^{-3} torr.

Figure 10 shows the results plotted both vs pressure and vs an altitude scale, which is approximately correct. We got multipacting at very low pressures at about 200 W. Both our B antennas and our A antennas gave us essentially identical results, so we were definitely getting multipacting below 10^{-3} torr at about 140–180 W.

When we took a fresh antenna, that is, one that had been setting in atmosphere for a few days, pumped it down to pressures in this range, and applied power, we found we were getting a gas-discharge breakdown along the upper sloping line. Again, this line is reasonably good, because we had two antennas. Not all of the points are shown, but instead of getting breakdown at about 4 kW, at 10^{-3} torr, it occurred at about 135 W.

The data are given, using an ambient plasma. We found multipacting occurred even without an ambient plasma. In addition, we experienced multipactor-initiated breakdown without an ambient plasma. Thus, the ambient plasma was simply helping to sustain the multipactor, but it wasn't vital to this process.

The important thing is that we lowered our breakdown from ~4 kW to ~35 W.

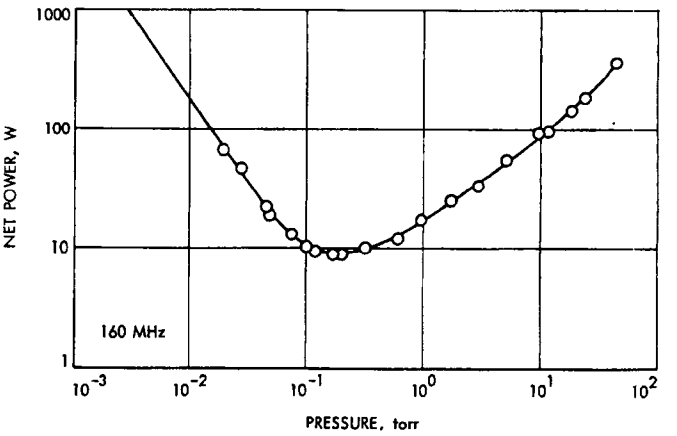

Fig. 9. Gas-discharge breakdown, antenna B, potted

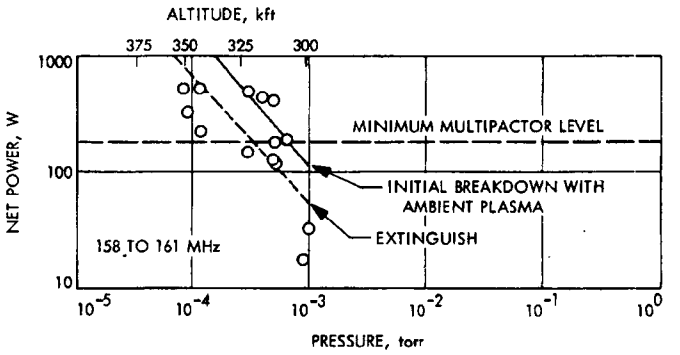

Fig. 10. Low-pressure breakdown, antenna B, potted

That is quite a few dB, quite a few dB derating that a multipactor discharge may give you. We also checked the extinguish value after we had gone into a gas discharge to see where it was. This should be at the approximate level of ambipolar diffusion breakdown, given a high-density plasma.

The data in Fig. 10 were for a potted antenna. We also unpotted it and checked. Figure 11 shows, basically, the same results. Potting didn't seem to make too much difference.

A composite picture of our results, gas breakdown curve, extinguish curve at much higher pressures, our multipactor-induced breakdown and extinguish level curve are shown in Fig. 12. As you can see from the ambipolar diffusion curve, we expected a ~10 dB change in breakdown level. Thus, if you are operating in a plasma of sufficiently high density, your gas breakdown will drop from the upper curve in the figure to the lower curve.

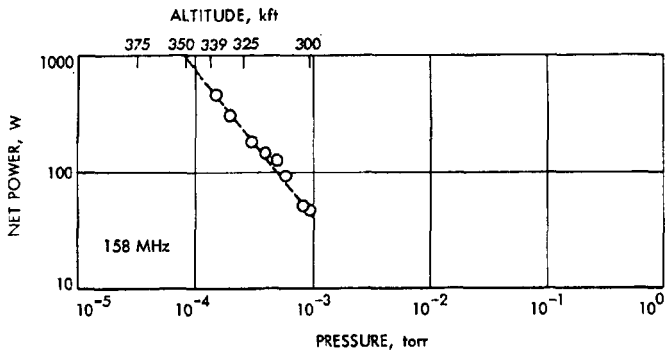

Fig. 11. Low-pressure extinguish curve, antenna B, unpotted

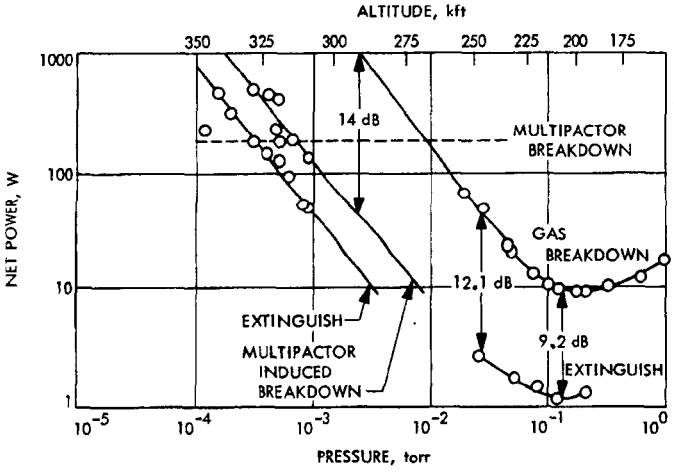

Fig. 12. Breakdown and extinguish powers for log periodic array at 160 MHz

However, we experienced a derating of 14–16 dB at about 10^{-3} torr, where we dropped from ~4 kW breaking level to ~135 W when the multipactor discharge triggered a gas discharge.

Now, one question I would like to answer before anybody asks me is how do I know this is a multipactor-induced discharge?

If you stay at any given pressure and repeatedly cause breakdown, you will find your breakdown level keeps moving up. For our case, it eventually moved up to the limits of our power supply, 500 or 600 W, as we gradually cleaned the surface.

This sort of behavior is characteristic of a surface phenomenon. It is not characteristic of a gas discharge which will repeat consistently at the one pressure, assuming you haven't changed gas constituents. We didn't do this because we were bleeding in air and constantly getting a fresh supply.

This is definitely a multipactor-triggered discharge. Therefore, it is very hard to get reliable data because surface conditions keep changing. You condition the surface. You can't guarantee on the next trial that your surface conditions were the same as on the previous trial. Therefore, we don't have a great many data points, but we are reasonably confident of the ones we do have.

As to an explanation for why this happened: two curves were shown in Figs. 3 and 4 of electron density in the initial phases of the multipactor discharge. We got densities of 10^6–10^9 electrons/cm^3, depending upon operating conditions, frequency, amount of overvoltage, etc. Such densities are much larger than those in the ionosphere; e.g., 10^4–10^5 electrons/cm^3. In fact, the densities are large enough for the particular antenna to permit an ambipolar diffusion discharge.

You might, therefore, expect multipacting to furnish enough electrons to enable a transition into an ambipolar diffusion discharge, in which case you would expect a lowering of 10 dB. After all, we can't extrapolate these things too far, so 14 dB is not far from 10 dB.

One other factor not mentioned, of great significance in multipactor discharge, is that on any electrode surfaces or dielectric surfaces, when you start multipacting you have a layer or monolayer of adsorbed gas molecules. Now, you are impacting electrons and kicking off secondaries, but these impacting electrons are also kicking off the gas atoms. It is a good way of cleaning up the surface. If you make calculations and take, for example, a 100-MHz discharge with, let's say, 10^7 electrons/cm^3, you will find that on a typical surface a monolayer will be about 10^{15} electrons/cm^2. Thus, a discharge of 10^7 electrons/cm^3 could be expected to clean off all the gas molecules in about 1 s.

Therefore, in 1 s you would expect all the gas to escape. If this gas is trapped in a ~1-cm gap, the pressure will rise from wherever you are starting, which may be a hard vacuum, up to about 100 microns.

At least a good deal of what is occurring in the very low pressure breakdown is due to suddenly raising the gas pressure locally, shifting along the breakdown curve

of Fig. 12 toward the minimum, and thereby lowering the threshold.

We haven't completely separated out both phenomena. I think probably the most significant thing is the gas coming off the surface. The reason I say this is that a multipactor should continuously give a certain amount of electrons at the base of the elements. If that is the dominant feature, we would expect to consistently repeat breakdown along the multipactor curve.

The fact that the breakdown level increases on each succeeding trial tells us that the gas is probably very important. If we remain at this pressure for a long period and try it again we shall find the breakdown threshold returns toward the initial curve. Thus, the gas effects and electron density effects are interacting; they aren't completely separated.

We also tried to cure the multipactor, i.e., prevent its occurrence. We tried potting, which didn't work. One of the standard techniques for increasing antenna breakdown threshold is to bias the elements. In effect, you can drive the electrons away, so that you don't start discharge; you increase the diffusion. This was attempted with an ambient plasma and resulted in a peculiar occurrence. We lowered the breakdown threshold even below this multipactor-induced curve, and this is possible if you have enough electrons. You may start a gas discharge with a dc discharge as well, and unfortunately, to get good effects with bias, you have to run bias voltages almost as high as your RF voltages. Bias, therefore, didn't buy us anything in this instance.

One point I would like to make before concluding is that we still don't know everything about multipacting, for example, about the power that we can dissipate. We still don't know all the geometry that will support multipacting. Some of this is still on a trial-and-error basis.

Discussion

Scannapieco: What kind of surfaces minimize the multipacting effect?

August: As far as space flight applications are concerned, I think no surface will minimize it. In vacuum tubes, you can use titanium layers which are very carefully deposited and which will not multipact. In real systems exposed to air and humidity, you build up surface layers and oxides which prevent this. You can try applying carbon black coatings which will tend to minimize multipacting. Unfortunately, if these things break down, you have a worse problem on your hands than if you started with a bare surface.

Scannapieco: Did you look at any flame-sprayed material?

August: No, we haven't. The people at Hughes have, however. The basic problem is that most of these things have oxide layers on them. You can't get rid of these things until you break them down in a hard vacuum.

Yorksie: Do you have any theory that might explain why potting does increase the multipacting phenomenon?

August: Dielectrics multipact easier. If you look at the secondary emission coefficients, the secondary emission coefficient crosses unity at a lower electron impact energy than on bare metals. Typically for dielectrics, it is down as low as 15 V, more commonly about 30 V; in fact, if you take something like bare copper, and most bare metals, the energy at which this crosses unity is about 200 eV. Actual copper has an oxide layer, and actual aluminum has an Al_2O_3 layer. These things multipact at levels characteristic of dielectrics.

Reynolds: Presumably, you are basically looking for a dense material that maintains its characteristics. Is that correct?

August: For potting, you mean?

Reynolds: Well, for the surface.

August: Well, I don't know that it necessarily has to be dense. All you want is something that tends not to multipact; that is, has secondary emission coefficient which is fairly low or doesn't cross unity.

Unfortunately, most of the measurements made on secondary emission coefficients have been made by physicists who have gotten into pure vacuums, baked out the surface, and cleaned off the oxide layers. These aren't representative of space flight situations. Contaminants do a lot of damage in multipacting. Our experience is that even finger greases will multipact substantially.

PRECEDING PAGE BLANK NOT FILMED.

N70-32309

The Effects of Outgassing Materials on Voltage Breakdown

J. F. Scannapieco
General Electric Company
Valley Forge, Pennsylvania

We will start by reviewing some of the basic equations which regulate outgassing and show their dependency on temperature and thickness. Then we will draw an analogy between mass transfer or outgassing and radiant heat transfer, and show how we utilize a computer program initially written for radiant heat transfer to determine the condensation rate caused by mass transfer.

The input requirement for this, instead of the normal thermal input, would be what we call design data. This describes what design data are, how they are obtained, and shows how this aids in obtaining the quantitative analysis of the system to establish the pressure as a function of time and a condensate on the surface in the system as a function of time.

At the end of my talk we shall consider a hypothetical black box having several simplifications in order to provide a simpler illustration.

The effects of outgassing are broken into two major categories, which aren't really separable. They are condensation and corona discharge; the latter includes arcover and multipacting, an associated phenomenon occurring at lower pressures.

I think the group gathered here can say it knows these have been encountered both in test and in flight, and is probably why we are gathered here.

The condensation effects are changes in optical properties on the surfaces on which the condensates would condense. This is a surface effect.

Electrical properties which are present, differ from corona discharge and arcover. These are conductivity and leakage current between electrodes. Condensation, which would or may ultimately be liberated by multipacting, causing a high-gas-pressure liberation, could return you to a corona discharge region. Chemical properties would also be surface. Chemical reactions, which may not be the right terminology, would include diffusion and actual chemical reactions. These, in turn, would be bulk effects in addition to surface effects.

The classical Langmuir equation is

$$W = kP\sqrt{\frac{M}{T}}$$

and is not considered in this analysis; as is well known, it is intended for ideal materials.

If you have a real engineering material, it is not too useful other than to show the dependence of sublimation on the various parameters.

Here we show that it is directly proportional to vapor pressure P and directly proportional to the square root of the molecular weight. This inverse dependence on temperature T isn't actually so. If you consider the dependence of vapor pressure in the Clausius Clapeyron equation

$$\log_{10} P = a - b/T + cT + d \log_{10} T$$

the vapor pressure is shown to be exponential with temperature and is the overriding factor. Thus, it is shown that the sublimation rate is exponentially dependent on temperature.

Fick's law is

$$dm = -ae^{-Q/RT} \frac{dc}{dx} A\, dt$$

where dm is the amount of sublimable fragment crossing a plane perpendicular to the direction of diffusion, dc/dx is the concentration gradient of the sublimable fragments in the direction of diffusion, A is the area of the planes across which diffusion occurs, dt is the time during which the diffusion occurs, a is a constant of the diffusing fragment in the material, Q is the activation energy, R is the universal gas constant, T is absolute temperature in °K, and the term $-ae^{-Q/RT}$ is the diffusion coefficient as is frequently expressed as D. It shows that the diffusion rate is also dependent on temperature. This is the biggest difference, really, between ideal material and engineering material; it is not just one substance. It is made of a conglomerate or a mixture, and will produce fractionating or diffusion. Depending on the thickness and temperature, diffusion could and usually does become a limiting factor in sublimation, not just the vapor pressure of the material.

The radiant heat transfer equation is

$$Q_{j-i} = \sigma F_{j-i} A_j (T_j^4 - T_i^4)$$

where F_{j-i} is the radiant-interchange factor.

The parameter we make the most use of in this analogy is the radiant interchange factor. What this establishes is the view factor for one surface in a system to the other surfaces, and it can be treated to consider reflectance from various surfaces, if you program the computer right, to give you what will ultimately come to one surface from another.

The correlation of radiant to mass, or particle, flux is

$$\Sigma_i\, \sigma(T_j^4 - T_i^4) \rightarrow W_j$$

$$\alpha_i \rightarrow s_i$$

An analogy can be drawn between the absorptance of the surface and thermal properties to the sticking factor, or accommodation coefficient, for sublimation and condensation phenomena.

We end up with a mass transfer

$$w_{j-i} = W_j A_j F_{j-i}$$

where w_{j-i} is the rate of sublimation or, as in this case, the condensation on surface i due to surface j. Further, w_j is the rate of sublimation in mass per unit area per unit time. The A_j is the area from which it is coming, and F is the configuration factor which we established from the geometric inputs in our computer program.

We can then sum the effects of all the surfaces in the system on surface i, which is the next equation

$$w_i = \sum_{j=1}^{n} W_j A_j F_{j-i}$$

This is the total condensate now on surface i due to all the sublimation that is occurring. To know this, of course, we have to have the right input data.

Part of the input data that is required is shown in Fig. 1. The y axis indicates the rate of weight loss, or weight loss, depending on whether you want to differentiate this later to use it or not. The x axis is duration in time; it is a log scale with the lowest temperature shown at the left. As you go up in temperature, the curves would look approximately as shown in Fig. 1. This isn't for any specific material; it is just a general curve.

Recalling the Clausius Clapeyron equation, once you have this for three different temperatures, you can use the first three terms which are the most dominant and establish the sublimation rate of your material as a

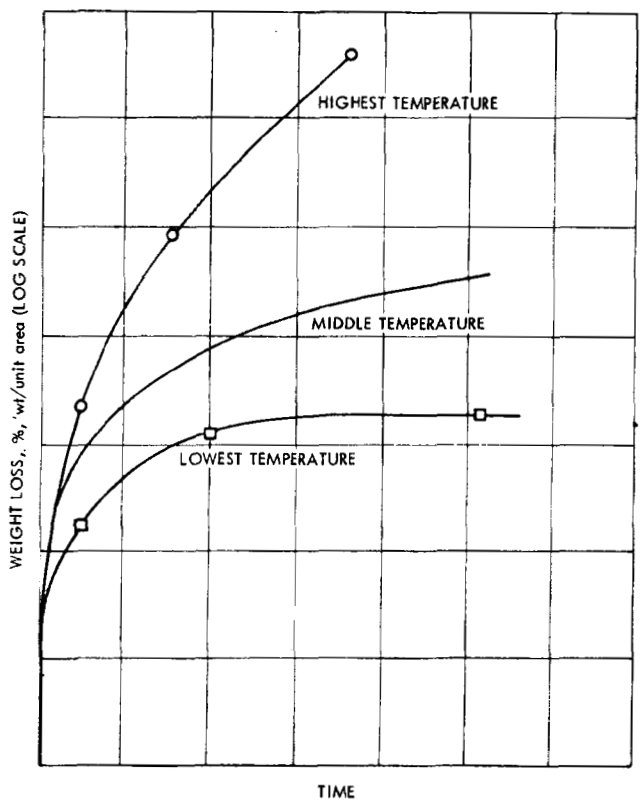

Fig. 1. Typical continuous weight loss dependence on temperature

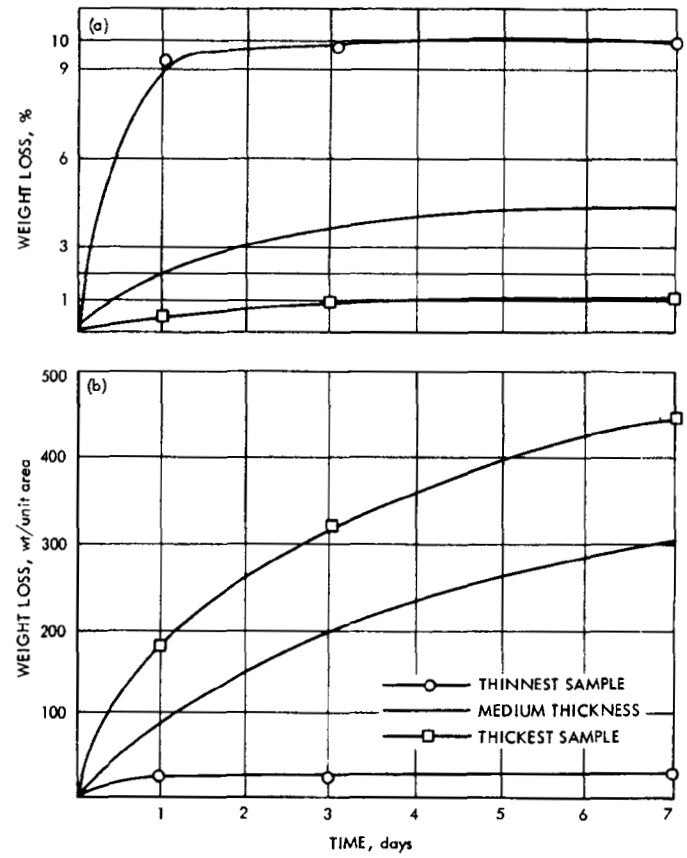

Fig. 2. Typical continuous total weight loss dependence on sample thickness

function of temperature at any temperature, based on three data points.

Now we have our material characterized as outgassing rate as a function of temperature, at any temperature.

Figure 2 shows some actual bulk weight loss which will be explained. For the time being, however, let us consider this sublimation rate now as a function of thickness. The weight loss, shown in Fig. 2(a), with the square points identify the curve for the thickest sample. The medium-sized sample is in the middle; the upper curve represents the thinnest sample. As a function of loss per unit area, Fig. 2(b), the thickest sample, will actually have the highest loss per unit area because it has not become diffusion limited.

A lot of the smaller fragments that are depleted on the thinner sample are still coming out.

If we have the data like this, we can perform a linear interpolation and establish the effect of thickness on sublimation rate. Defining sublimation dependency on these two parameters, then gives us what I call design data.

Regardless of the thickness of the material, the temperature it is at, or the temperature of the condensing surface, we know the properties of the sublimate that is coming off. To initiate it, condensation should be treated, except for its thickening factor, the same as sublimation. The same equations determine whether it occurs or not.

Total weight loss or total outgassing, which is what we have been talking about up to now, is shown in Fig. 3. This can logically and easily be broken into two separate types of weight loss: One of which is termed bulk, and the other gas weight loss. The gas weight loss goes up and goes straight across, because it is a short-term type.

The gas weight loss is the gasses and the moisture absorbed in the material and on its surface. The bulk weight loss is simply everything else and is composed,

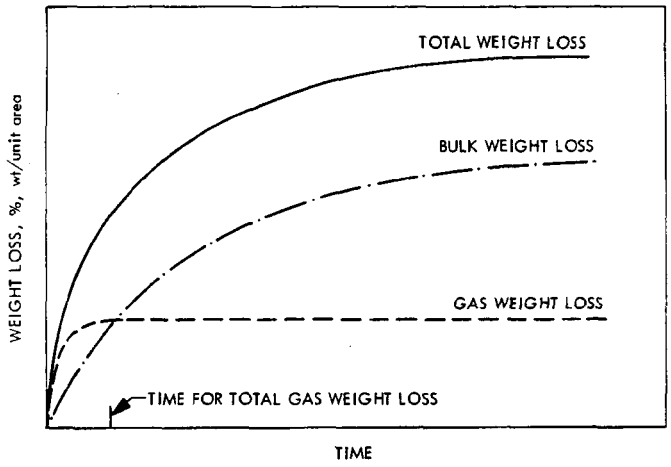

Fig. 3. Typical continuous total, gas, and bulk weight loss curves

in a real material, especially organics, of various additives for flame retardant, radiation resistance, processing aids, excess catalyst, and similar items.

In the hypothetical black box case, we will use a number of simplifications, partially because of the data I have available.

I don't have design data on any material in a complete manner. We have parts of design data for many materials, but they are not complete on any of them. Because of this, I picked a simplification of having an isothermal box at 155°F.

The data obtained from our facility are shown in Fig. 4. Actually, nine sets of this type of data, or at least seven, are required, if certain assumptions are reliable; to obtain design data.

The y axis shows both weight loss in percent and as a function of area versus time. This is *in situ* data; in other words, this is the change in weight measured right in the balance system in the vacuum system as a function of time.

This particular material is a 3-M black velvet paint and work is performed at 155°F.

To get design data now, you would have two other temperatures and thicknesses. For paint, the thickness parameter really drops out, because from a practical point of view when you paint a surface you only need a certain thickness, and you are after that minimum thickness giving you the properties you are after (whatever they may be, optical, protective, etc.).

So for a paint or other material which may have similar applications, where they are only used in one thickness; all you have to do is determine the temperature.

The schematic of our present facility is shown in Fig. 5. We have a Cahn microbalance with a suspended wire from which a sample can be hung. The sample is enclosed in a black box heater so it is radiatively heated; we also have a dummy sample in this same box with a thermocouple on it. The temperature is controlled by that thermocouple.

The box is designed so we get very little back scatter of the material offgas from the sample back to it before it can get outside this box. Once it gets outside the box, it will be condensed on the walls of the vacuum chamber at worst, or simply pumped out.

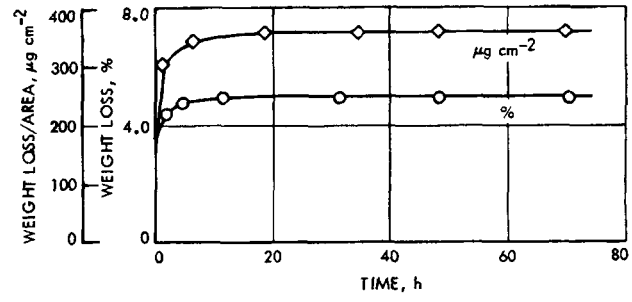

Fig. 4. 3M black velvet paint

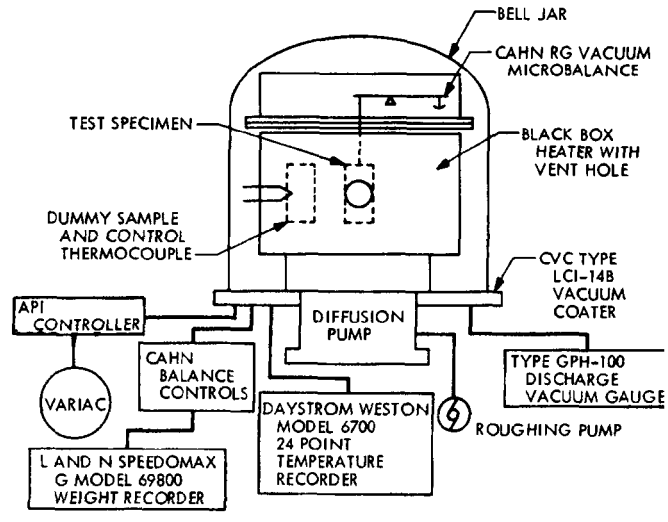

Fig. 5. Experimental configuration

Since our work is done at 155°F and the bell jar is maintained at 70°F, the difference in temperature acts as an efficient condenser system.

Figure 6 is a breakdown of the 3-M black velvet paint data shown in Fig. 4. The top curve is the total outgassing in weight per unit area. This can be broken down into gas weight loss and bulk weight loss. The way we established our bulk weight loss today was from before and after measurements. We stabilized the sample in a constant relative humidity and temperature chamber until it arrived at an equilibrium weight.

Then the sample was tested; after the test and passing through thermal vacuum, it went back into the same temperature environment. Then, we left it there and weighed it daily or weekly, depending on its rate of change, and established the new equilibrium weight.

A control sample was also maintained in this environment; however, it was not exposed to thermal vacuum.

Although I have a number of triangles defining the bulk weight loss, they are for purposes of illustration only as the last point is the only point we really have. The end point is firm; i.e., it was actually measured. The rest was filled in based on the shape of the total outgassing curve. That represents all of the real knowledge we have about the material.

This should actually and can actually be established from multiple weighings; i.e., taking samples for shorter time periods and plotting them. A much simpler, albeit more expensive method, is to perform mass spectrometric analyses continuously or repeatedly throughout the experiment. This would provide a basis for establishing the ratio of gas to bulk weight loss. At the present, the data format isn't suitable for analysis, at least not in the best form.

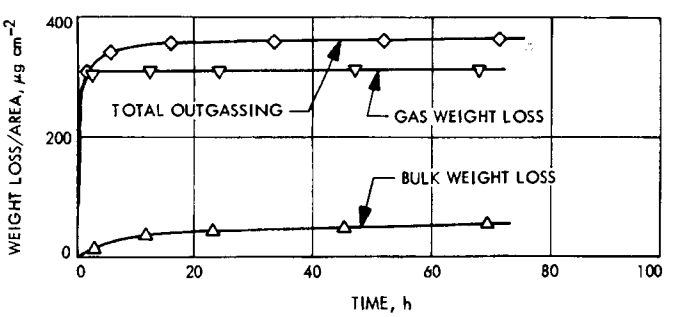

Fig. 6. Bulk and gas weight loss and outgassing for 3M black velvet paint

A much better form is presented in Fig. 7. It shows the rate of weight loss in $\mu g/cm^2/h$ for the 3-M black velvet paint. Actually, most equations are based on increments of seconds; however, this is the way my data are plotted. Actually, this is a differential of the curve in Fig. 6. The curve in Fig. 7 shows the bulk weight loss and the total outgassing as a function of time. The gas weight loss curve drops off quickly for a thin material such as paint.

Initially, the bulk loss is a couple orders of magnitude lower than the gas loss. Within a matter of a few hours, the reverse is essentially true. Gas loss is negligible, at least for the 3-M paint. I believe the 3-M black velvet paint had about a 5–6% weight loss for the test duration.

There were many paints that would look better if you just took them out and weighed them, but they would actually have a much higher bulk weight loss.

It turns out that the bulk weight loss percentage, if I recall, for 3-M black velvet, was on the order of a couple tenths of a percent, where the paints which would have ~3% weight loss; some may have ~2.8% bulk loss. Therefore, it is rather deceiving if you don't have the gas weight loss measurement. You could be misled as to the kind of material you select.

Figures 8–10 show measurements on various materials on which we have data and from which we will fabricate the hypothetical black box. The analysis will be performed on this black box, and it will show the pressure profile as a function of time.

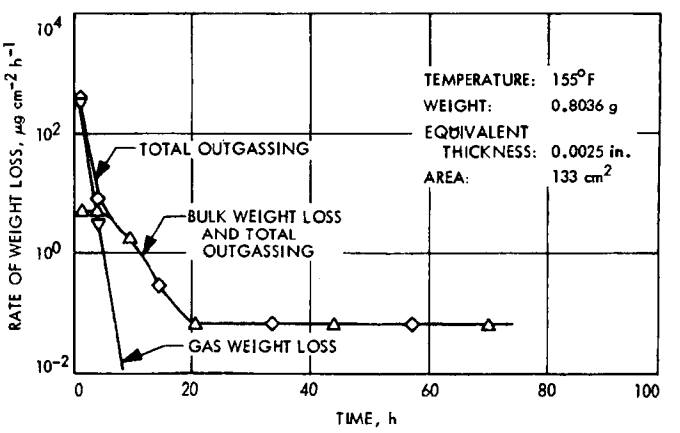

Fig. 7. 3M black velvet paint at 155°F

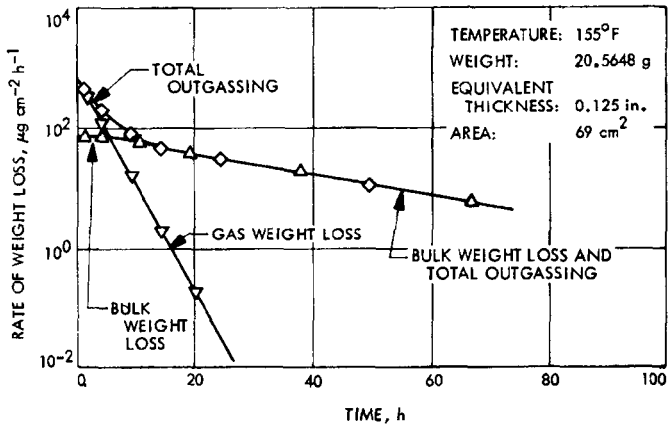

Fig. 8. PC-701 polyurethane

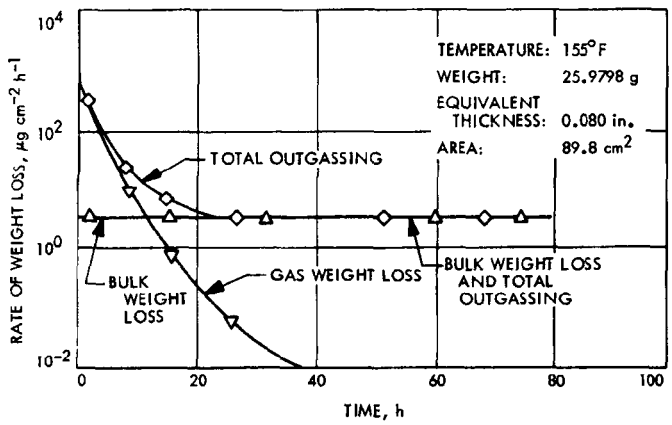

Fig. 9. Hysol H-9-3469-4190

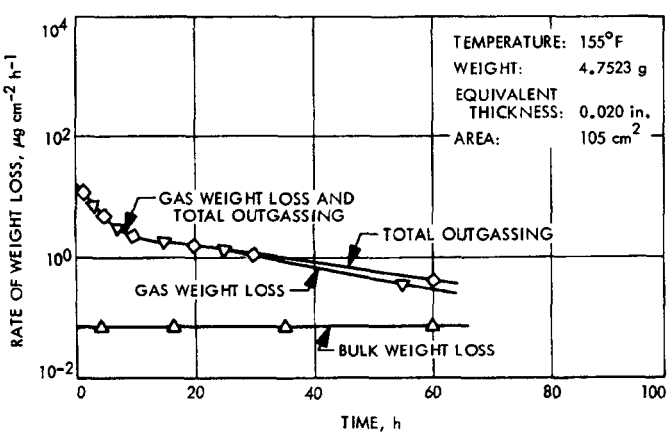

Fig. 10. Textolite 11-546

Figure 8 deals with polyurethane. All this work was performed at 155°F for a period of 75 h. The bulk weight loss is shown and, again, similar to the paint, the total weight loss after a rather short period of time is about a day. The gas weight loss is also shown. The bulk weight loss is again about an order of magnitude less than the total.

One thing I will note here, I have an equivalent thickness of an eighth of an inch. The actual sample thickness was about a quarter of an inch, but since, in application, polyurethane will normally be on a surface which would prevent outgassing from one side, essentially, we cut this thickness in half to get the equivalent use thickness.

An epoxy, Hysol, is considered in Fig. 9; it shows the total outgassing, and the same curves, essentially. The bulk weight loss is just about constant from the beginning. This means that you are, at the very onset, very diffusion-limited for the rate of weight loss. Total weight loss within a short period of time, about a day, becomes the predominant factor on weight loss. The gas weight loss falls off rapidly.

Figure 10 shows Textolite, which can be used for a circuit board application in a black box. Here we note just a little difference from what we have seen before. The gas weight loss, and the total outgassing are almost identical. The bulk weight loss is actually rather low compared to that, even over a period of several days; it has not become the dominating factor in weight loss.

I have arbitrarily designed the hypothetical black box. Its parameters are provided in Fig. 11. This black box is probably similar to some and dissimilar to others.

The 3-M paint covered ~1,000 cm² as did the polyurethane; the epoxy was ~250 cm², and the Textolite

CONFIGURATION:	LENGTH	= 12 in.
	WIDTH	= 6 in.
	DEPTH	= 2 in.
	VOLUME	~ 2300 cm³
	VENT AREA = VARIABLE	
COMPOSITION:	3M BLACK VELVET PAINT	= 10^3 cm²
	POLYURETHANE PC 701	= 10^3 cm²
	EPOXY HYSOL H9-3469-4190	= 2.5×10^2 cm²
	TEXTOLITE 11-546	
TEMPERATURE:	ISOTHERMAL AT 155°F	
	APPROXIMATIONS FOR HIGHER TEMPERATURES	

Fig. 11. Hypothetical black box

~1,000 cm³. These are the surface areas of the three materials and in the hypothetical black box.

We will treat it for an isothermal case at 155°F and give some idea on what approximations one might have for changes in temperature.

The constituents of the black box as a function of time, are shown in Fig. 12. The straight solid lines between data points is the important or dominating material for that type of weight loss, whether it is gas or bulk, and the broken lines indicate that the effect of the material is negligible.

So, if we look at this, we can see for the bulk weight loss primarily, the polyurethane will give us a pressure buildup in the system. Near the end, the Hysol, which we saw had a constant rate of weight loss, at least in the period of time with which we worked, will start to become important.

What I have used for a criterion for what is and what is not important for weight loss is to consider the maximum, and anything within one-quarter magnitude of that. Anything lower than that has been neglected and is shown in broken lines. Under 50 h, Hysol was more than one decade lower than the polyurethane. Therefore, it wouldn't have been important.

For the gas weight loss, you see something rather interesting and probably unexpected. In the beginning, the gas weight losses for the paint and Textolite were insignificant; i.e., during the first 5 h. Between 5 and 20 h, however, everything except the paint became important. The Textolite, therefore, became an important parameter.

After about 20 h, the gas weight loss is actually primarily dependent on the Textolite, which in the beginning wasn't important at all.

What this really shows, referring back to Fig. 10, is that it did have a rather drawn-out rate of weight loss for the gas load and rather high compared to the bulk weight loss.

The usefulness of such a curve, even though it might be rather confusing, is that in addition to summing these effects to arrive at a total gas load presented in the black box, it also shows what materials are causing the pressure buildup as a function of time within the system. Therefore, the curve can be useful to the redesign of the system if it becomes necessary. It can also serve to aid in determining how to extend its capabilities, and shows what materials are needed to start changing the surface area to replace, or what have you. A summation of the curve just mentioned and the curve in Fig. 13 shows the bulk weight loss and the gas weight loss in μg/h as a function of time. Based on this and ideal gas theory, we can establish the inputs of the box and its outputs, assuming a molecular flow through the orifice that is being vented from the box. One thing I want to point out is that by using an isothermal box one essentially neglects the pumping action you would get off a condensing surface inside the box, which in most hardware you would otherwise have. Thus, this bulk weight loss, although it shows rather high here, in most applications (where you would have colder temperatures than the sublimation temperature) a lot of this would be trapped off inside the black box and never really make it out, or at least make it out at a much reduced rate. It would

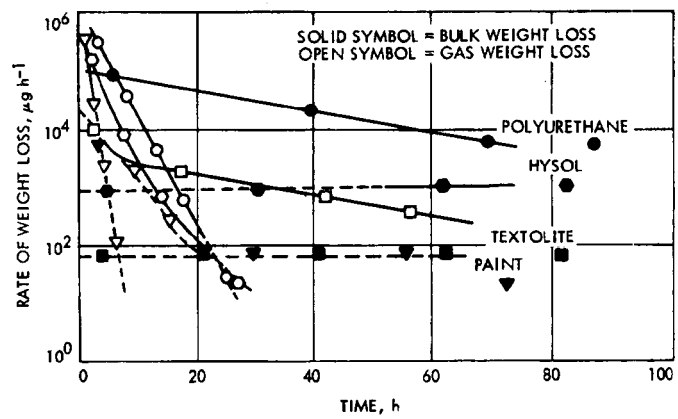

Fig. 12. Constituents of black box

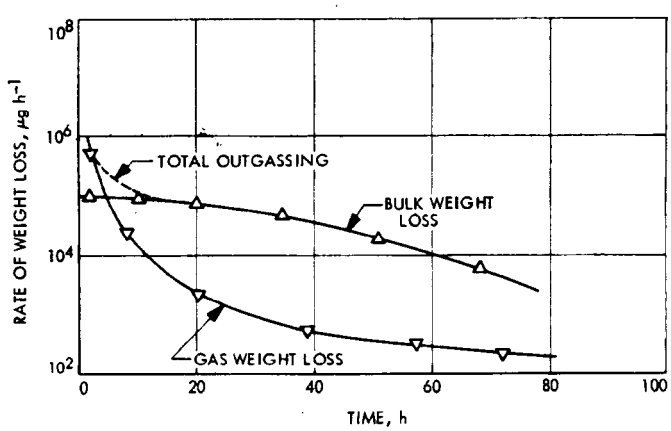

Fig. 13. Hypothetical black box rate of weight loss

normally come below the gas load, at least in the first few days.

The gas loss would probably be lower in many applications if you used a material other than Textolite, which you can see was the dominating factor from 10 h on. The gas weight loss curve might be expected to drop sharply if a material such as Textolite weren't in the system. The bulk weight loss would decrease for other reasons.

Figure 14 shows our actual results with the pressure profile now due to each of the constituents, the gas, and the bulk, as a function of time. The pressure in the box is indicated on the y axis in torr. A normal vented box is assumed if one weren't concerned with outgassing or simply was not aware of corona discharge or arc-over problems. The venting used to compute this was what would be a typical example resulting from the manner in which 2-way, 20-pin Cannon connectors are normally housed in electronic boxes. This would amount to an equivalent vent hole $y \sim 10\ \text{cm}^2$. By equivalent I mean that if you computed the impedance of the real geometry and then determined the equivalent simple hole geometry. Two of these would normally come out to $\sim 10\ \text{cm}^2$; this is the basis for these curves.

As you begin to expand the vent area, the curves drop proportionally. So this, as we could see in the beginning, is primarily dependent on the gas load and pressure.

After ~ 10 h in this application, both curves in Fig. 14 assume the same approximate importance and both represent approximately the total pressure. They are plotted on a log scale which explains their close proximity when added together.

I might mention a couple things about temperature. This has been assumed to be 155°F. As you go up every 90°F, you expect approximately an order of magnitude increase in the rate of weight loss. Therefore, the internal pressure would also increase proportionately. The same thing is true with the vent area.

If you open the vent area proportionally to this 10 cm² from which these were computed, since we are in a molecular flow region, the pressure would drop accordingly.

The computation to this point has been manual, and actually using a computer it is still rather simple to subtract out the condensed phases, which I haven't—having

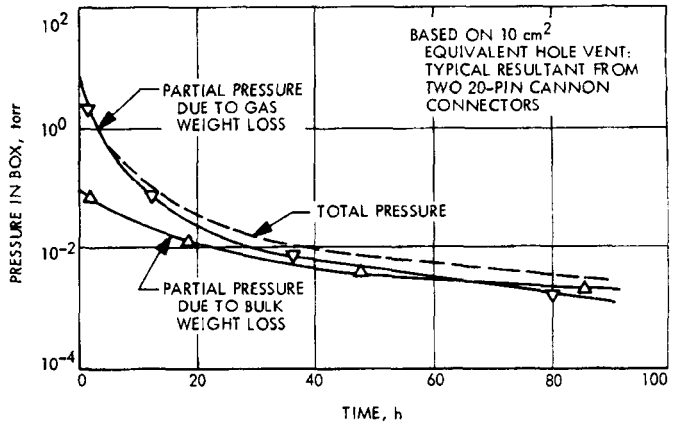

Fig. 14. Hypothetical black box average pressure

assumed an isothermal box. A more complex problem would be to consider variable temperatures inside your box, and their effect on the outgassing, and to consider variations in thickness in the materials inside the black box and their effect on outgassing.

Once you have this, depending on what theory you might hold and what your electronics is inside this, you could approximate what kind of a potential, electrode gas, etc., you could sustain without having a catastrophic failure or without creating sufficient corona to cause other problems later in other parts of the circuitry.

In conclusion, I would like to say there are analytical techniques to treat outgassing effects on space systems. The techniques to obtain the input data for these analytical procedures are available, and their system design in this way will be more reliable than using the technique which is presently used on many programs. That is, select a series of candidate materials, run a test and pick the best materials. I am not criticizing that technique; it is very practical. However, I ought to point out that we don't design any of the other areas of spacecraft in this manner. We don't do the mechanical, thermal, or electrical design based on this method of choosing certain parameters and saying, "We will pick the best. We won't worry if it will be sufficient. We just hope that what we pick will be sufficient."

As soon as you start getting into new areas, trying to become more sophisticated in your hardware, you will find problems if you don't approach it on a scientific basis. There is no reason why we can't do that today. Initially, it will probably appear that the data required for your input, the analysis, would be more expensive to perform

than a system design, but I think eventually it will be less costly. For one reason, you wouldn't be rerunning many materials on outgassing tests once you have your design data. This, essentially, would cover all the information you need about that material right up to the decomposition temperature, if this is about where your high-temperature test was run, and that's where it should be.

Discussion

Yorksie: You made a statement in conclusion that you don't have to do the experimental testing, you can use analytical techniques. I gather all your data is experimental data. Have you correlated this with your analytical techniques, and how does the correlation hold up?

Scannapieco: Well, are you talking about the input data, or the results?

Yorksie: The actual results.

Scannapieco: What I presented has been analytical. We have not run experiments to compare the two on this particular case.

We have in another system where we weren't considering real pressure buildup, but we were considering condensation effects. This was done in a nuclear space power system where we were concerned about condensation on the surface. That part of the analysis has been proven out in that case.

Yorksie: You did achieve good correlation?

Scannapieco: On the condensation rates, yes.

Carruthers: I would like to make a comment about the 3-M black paint, because we once made the mistake of painting the inside of a vacuum system with it. You showed in your slide that most of the outgassing is gas weight loss, and we find this to be true. Unfortunately, most of this gas weight loss is moisture. The vacuum system that we had, without the paint, would pump down to 10^{-6} torr in a couple of hours, and with the paint it would take a couple days to get down to 10^{-5}.

If the system was then let up to air for half an hour and pumped down again, it would take the exact same amount of time to pump down to 10^{-5} again. We knew that this was moisture because of the fact that when we put an extra cold trap in the vacuum system, filled with liquid nitrogen, it would pump down as fast as the system without the paint in it.

So this does show that the gas weight loss is a very important consideration, and it is something that comes right back when you let it up to moist air.

Scannapieco: In that application, definitely, but not in space. In space hardware this wouldn't be a problem. In the test chamber it could create problems, which also must be considered because all the hardware is tested in ground equipment first. The one thing that might save you there is, you probably have much less surface area of some hardware than you would of a shroud in a large vacuum chamber, so it is important.

Lagadinos: Would it be more convenient to express the weight loss in terms of the percentage of your sample? We have conducted a number of experiments, and we have analyzed a number of materials, both epoxies and various metal oxides. We have done it in terms of that. Have you considered that?

Scannapieco: Yes, actually we do reduce the data that way. The initial data that we get from our thermal vacuum balance, we reduce in percent as the function of time, and as weight as a function of surface area versus time.

As far as analytical techniques, percent is only important really to compare various temperatures. If you try and do a correlation on temperature, you don't plug these in a Clausius–Clapeyron equation versus time, but you plug them in versus percent loss. Essentially, this tells you that you are getting about the same constituents off as a function of percent loss, not as a function of time.

It is useful, in a sense, necessary, to come up with some of these curves that I have here, to have that data, but as far as actually plugging into the end equations that we used, it is not.

As far as choosing materials, I don't think it really matters whether you have it as a function of surface area or percent in many applications. I think the most important thing is to have the equivalent thickness about the same for the same applications. If you will recall, my figure showed the percent weight loss and per unit area both as a function of thickness.

We changed the percent weight loss in about 3 days. That was the bulk loss from 1–10% by changing the thickness from about 4 mils, I believe it was, to 0.25 in. This was an open sample.

In that particular test, percent weight loss, if you had a thin sample and a thick one, in which you were trying to compare two different materials, you would pick the thick one. If, however, you look at it as a function of surface area, you would have just the opposite effect. So it is important and useful, but, by itself, I don't think it is. It is one of the necessary pieces of information you need for the analysis.

Zaiden: Before you performed these tests, did you cure these materials at their recommended cure cycles?

Scannapieco: I don't know if they were recommended cure cycles. The materials were given to me by applications-type people who wanted to use them in a specific program; the way they were cured, or treated, or post treated, was the same as they were intended to perform in a vehicle.

As I recall, the paint was not post cured; it was a standard room-temperature cure that they would give 3-M black velvet, and I have that data if you would be interested. None of the other materials, to my knowledge, were treated.

Zaiden: Your first 20 h would be off if they didn't cure these properly.

Scannapieco: Yes, definitely, as far as the bulk loss is concerned. The gas loss shouldn't change much at all. I didn't mention some experiments we ran just to try to find out if some of these materials could be cleaned up.

Stern: We have three questions: (1) how did you differentiate between the gas loss and the bulk weight loss, (2) at what pressures did you run your tests, and (3) did you make any qualitative analysis on the outgassed materials and condensates that you collected?

Scannapieco: We didn't analyze any of the condensates or the off-gas products. This could have been done. We do it in other test systems, but in obtaining the data which I showed here, we did not. We have techniques where we not only measure the constituents of the condensate, but we measure the optical properties right *in situ*. So, in this particular case we did not. The operating pressure was at about an 8×10^{-5} to 5×10^{-6} torr range.

Once you define a specific test system you are working with, once you get below a certain pressure, such as the mean free path it is about the same as the characteristic dimensions of your system. The results shouldn't change, at least theoretically, and I think most people agree that will be the case. The important thing is to consider that you do not get a lot of backscatter from the test fixturing; in other words, once a particle has left your test sample, that you have on your thermal vacuum test, the probability of it returning to that sample should be very low.

What will really establish this is the geometry, the temperatures, and to some extent the pressures in the system. But, once you go below the mean free path, where the mean free path is about the same as the characteristic dimensions of the system, it doesn't matter; we were well below that. For an average Bell jar, of ~18 in. diam, it comes to about 10^{-4} torr.

You want to know how we broke up our curve into bulk and total gas. Well, the actual curve that we measured as a function of time *in situ* is the top curve, total outgassing. The only other measurement that we made is a before and after measurement.

What we do is, we take a sample and we put it in a container that has a constant relative humidity and temperature. In this same container, which is a glove box, there is an analytical balance. We weigh this on a daily or weekly basis as required, depending on its rate of change, until it comes into equilibrium. That is before the test.

After the thermal vacuum test, we put it back in the same environment and repeated the procedure. We get a new stabilized weight. By stabilized I mean there is virtually no change.

We also correct for small changes that would occur on this material against the control sample that we keep of the same material, same geometry, etc., put in at the same time, but never taken out of that control environment. So, we also normalize against that.

This gives us really just one point. The final bulk loss that I showed on the curves, at the point where we ended the thermal vacuum test. The way we interpolated the rest of the data on the curve was to look at the shape of the total weight loss curve, and knowing that the gas would diffuse out fairly fast, it was not too difficult to fill this in most cases.

You might think of the Textolite sample where this wouldn't be too true right offhand. If you recall that the total gas loss was very high, the bulk loss was very low, and even if you drew a straight line, you could do one of two things: draw a straight line from the origin to the final bulk point you have, which would give you one extreme, or draw straight up along your ordinate, then go parallel across at a zero rate of weight loss.

If you were anyplace in this region that these two extremes would represent, except for the first few hours, it wouldn't really make a lot of difference in drawing that particular curve, which is probably the most difficult to draw, where you have a high gas load.

Another thing is that this took a number of weeks to stabilize; probably months, if I looked up the data. Some of them take quite a while in post stabilization.

NASA — JPL — Coml., L.A., Calif.

TECHNICAL REPORT STANDARD TITLE PAGE

1. Report No. 33-447	2. Government Accession No.	3. Recipient's Catalog No.
4. Title and Subtitle PROCEEDINGS OF THE SECOND WORKSHOP ON VOLTAGE BREAKDOWN IN ELECTRONIC EQUIPMENT AT LOW AIR PRESSURE HELD AT THE JET PROPULSION LABORATORY, MARCH 5-7, 1969		5. Report Date June 30, 1970
		6. Performing Organization Code
7. Author(s) Edited by E. R. Bunker, Jr.		8. Performing Organization Report No.
9. Performing Organization Name and Address JET PROPULSION LABORATORY California Institute of Technology 4800 Oak Grove Drive Pasadena, California 91103		10. Work Unit No.
		11. Contract or Grant No. NAS 7-100
		13. Type of Report and Period Covered Technical Memorandum
12. Sponsoring Agency Name and Address NATIONAL AERONAUTICS AND SPACE ADMINISTRATION Washington, D.C. 20546		14. Sponsoring Agency Code
15. Supplementary Notes		

16. Abstract

Not applicable for this type of report.

17. Key Words (Selected by Author(s)) High Voltage Design and Testing Packaging and Cabling		18. Distribution Statement Unclassified -- Unlimited	
19. Security Classif. (of this report) Unclassified	20. Security Classif. (of this page) Unclassified	21. No. of Pages 212	22. Price

N70-32286 N70-32309

HOW TO FILL OUT THE TECHNICAL REPORT STANDARD TITLE PAGE

Make items 1, 4, 5, 9, 12, and 13 agree with the corresponding information on the report cover. Use all capital letters for title (item 4). Leave items 2, 6, and 14 blank. Complete the remaining items as follows:

3. Recipient's Catalog No. Reserved for use by report recipients.

7. Author(s). Include corresponding information from the report cover. In addition, list the affiliation of an author if it differs from that of the performing organization.

8. Performing Organization Report No. Insert if performing organization wishes to assign this number.

10. Work Unit No. Use the agency-wide code (for example, 923-50-10-06-72), which uniquely identifies the work unit under which the work was authorized. Non-NASA performing organizations will leave this blank.

11. Insert the number of the contract or grant under which the report was prepared.

15. Supplementary Notes. Enter information not included elsewhere but useful, such as: Prepared in cooperation with... Translation of (or by)... Presented at conference of... To be published in...

16. Abstract. Include a brief (not to exceed 200 words) factual summary of the most significant information contained in the report. If possible, the abstract of a classified report should be unclassified. If the report contains a significant bibliography or literature survey, mention it here.

17. Key Words. Insert terms or short phrases selected by the author that identify the principal subjects covered in the report, and that are sufficiently specific and precise to be used for cataloging.

18. Distribution Statement. Enter one of the authorized statements used to denote releasability to the public or a limitation on dissemination for reasons other than security of defense information. Authorized statements are "Unclassified—Unlimited," "U. S. Government and Contractors only," "U. S. Government Agencies only," and "NASA and NASA Contractors only."

19. Security Classification (of report). NOTE: Reports carrying a security classification will require additional markings giving security and downgrading information as specified by the Security Requirements Checklist and the DoD Industrial Security Manual (DoD 5220.22-M).

20. Security Classification (of this page). NOTE: Because this page may be used in preparing announcements, bibliographies, and data banks, it should be unclassified if possible. If a classification is required, indicate separately the classification of the title and the abstract by following these items with either "(U)" for unclassified, or "(C)" or "(S)" as applicable for classified items.

21. No. of Pages. Insert the number of pages.

22. Price. Insert the price set by the Clearinghouse for Federal Scientific and Technical Information or the Government Printing Office, if known.